Investigation of Novel Genetic Causes of Early Infantile Epileptic Encephalopathies Using Next Generation Sequencing and Zebrafish and Cellular Modelling

Devon Johnstone

This manuscript-based thesis is submitted as a partial fulfillment of the PhD program in Biochemistry with specialization in Human and Molecular Genetics

Department of Biochemistry, Microbiology and Immunology

Faculty of Medicine

University of Ottawa

Supervisor: Kym M. Boycott, MD/PhD

Abstract

Early infantile epileptic encephalopathies are a set of diseases characterized by poorly controlled or refractory seizures, contributing to, or in concert with, changes in cerebral function and neurodevelopment. Pathogenic genetic variants are a primary cause of these diseases, and many pathways have been implicated. This thesis focuses on the use of whole exome sequencing for the identification of genes implicated in three such diseases, and the use of *in vitro* and *in vivo* functional work to demonstrate pathogenicity. I identified variants in genes impacting the glycosylphosphatidylinositol (GPI) anchor biosynthesis pathway (*PIGP* and *PIGQ*) as well as confirmed the role of a novel gene associated with vitamin B6 dependent epilepsy (*PLPBP*), providing new mechanistic insights. I used flow cytometry to show that variants in *PIGP* and *PIGQ* impact the cell surface localization of GPI-anchored proteins, a group of important proteins on the cell surface. I used CRISPR/Cas 9 to create the first animal model of PLPHP deficiency in zebrafish, as well as provide the first evidence of mitochondrial localization of the protein and the impact of *PLPBP* mutations on neurotransmitters and the B6 vitamers. Treatment of *plpbp*$^{-/-}$ zebrafish larvae with pyridoxal phosphate, the active form of vitamin B6, improved survival and electrophysiological phenotypes. Finally, I characterize the phenotypic spectrum of patients with variants in each gene: 2 (*PIGP*), 7 (*PIGQ*) and 12 (*PLPBP*). Taken together, these findings reiterate the value of next generation sequencing for disease gene discovery, and further our understanding of the GPI-anchor and vitamin B6 pathways, facilitating future work in development of treatments for these devastating conditions.

Acknowledgements

First and foremost, I wish to thank all the patients and families who agreed to participate in the research studies published or submitted in this thesis. Without them, none of this would be possible, and they are what this is all about.

I am also eternally grateful to my supervisor, Dr. Kym Boycott. She took a chance on a fish biologist and gave me the opportunity to work in one of the most important rare disease research groups in the world, providing to me the opportunity to thrive. Although research is not without challenges, I have had an amazing time in this lab, and learned so much. Through this experience I feel that I have grown both as a person and a researcher, so thank you, Kym.

I am indebted to my thesis advisory committee members, Dr. Dennis Bulman, Dr. William Stanford, and Dr. Michael Schlossmacher. They contributed greatly to my academic development, and their guidance and feedback made my research stronger. The regular feedback I received from Dr. Bulman through exome rounds and lab meetings, kept me motivated and curious. I am also grateful to Dr. Schlossmacher for his efforts to start and support the MD/PhD program at the University of Ottawa, without which I would not be here.

I would also like to thank the lab members and collaborators I have worked with over these past years. Dr. David Dyment felt like a spiritual co-supervisor, and regularly checked in on me and gave me guidance throughout my training. I am thankful to Dr. Kristin Kernohan, who was a cornerstone for my success, she was always there to give advice, plan experiments, and critique my writing. I am grateful to Dr. Izabella Pena, with whom collaborating on zebrafish projects was an absolute joy, and I will always miss the positive energy she brought to the workplace day in and day out. To the rest of the members of the Boycott and Bulman

labs, both past and present, including Taila Hartley, Wendy Mears, Arran McBride, Yoko Ito, Chandree Beaulieu, Justin Wagner, Ruobing Zou, Meredith Gillespie and Samantha Rojas, thank you for your support and entertainment throughout the years!

The field of rare disease research is a small community, and I could not have been successful without the many great collaborators who have contributed to my research. There are too many to name individually, but I want to especially thank Dr. Philippe Campeau, Dr. Thi-Tuyet-Mai Nguyen, Dr. Marc Ekker and Dr. Clara van Karnebeek. It was a pleasure working with each of them, and they were instrumental to my success.

I also wish to thank my sources of funding. My research has been funded throughout the years by the Care4Rare Canada Consortium, which is funded by Genome Canada, CIHR, Ontario Genomics, the Ontario Research Fund, and the CHEO Foundation. My zebrafish work was supported by the Canadian Rare Diseases Models and Mechanisms Network, funded by CIHR. Lastly, I have been privileged to be personally funded by a Vanier Canada Graduate Scholarship.

Additionally, I want to thank my family and loved ones for their everlasting love and support throughout this long journey. They have shaped who I am as a person and keep me grounded and happy.

Finally, as I put the finishing touches on my thesis in the safety of my home in spring 2020, I want to thank and recognize all the front line workers whose efforts are helping keep us safe, healthy, and fed as we tackle the challenges of Covid-19.

Table of Contents

List of Abbreviations

3MT: 3-methoxytyramine

5-HIAA: 5-hydroxyindoleacetic acid

5-HTTP: 5-hydroxytrytpophan

α-AASA: α-aminoadipic semialdehyde

AADC: Aromatic l-amino acid decarboxylase

ADR: adrenaline

AED: anti-epileptic drug

ALP: alkaline phosphatase

AOX/DX: aldehyde oxidase (Mo cofactor)/β-NAD dehydrogenase

B6RD: (Vitamin) B6-responsive disorder

Cas9: CRISPR associated protein 9

CCDS: consensus coding sequence

CFM: cerebral function monitoring

CHO (Chinese hamster ovary

CRISPR: clustered regularly interspaced short palindromic repeats

CSF: cerebrospinal fluid

DBP: D site-binding protein

DD: developmental delay

DNA: deoxyribonucleic acid

DOPE: discrete optimized protein energy

dpf: days post-fertilization

DWI: diffusion weighted imaging

EEG: electroencephalogram

EIEE: early infantile epileptic encephalopathy

EIMFS: epilepsy of infancy with migrating focal seizures

EtNP: ethanolamine-phosphate.

FACS: fluorescence-activated cell sorting

FLAER: fluorescein-labeled proaerolysin

GA: Gestational age

GABA: γ-aminobutyric acid

GalNAc: N-acetylgalactosamine

GDD: global developmental delay

GFAP: glial fibrillary acidic protein

GlcN: glucosamine

GlcNAc: N-acetylglucosamine

GPI: glycophosphatidylinositol

GPI-AP: glycophosphatidylinositol-anchored protein

GTC: Generalized tonic-clonic

HC: Head circumference

HLF: hepatic leukemia factor

HMA-PAGE: heteroduplex melting assay polyacrylamide gel electrophoresis

HVA: 5-hydroxyindoleacetic acid

ID: intellectual delay

IGD: inherited GPI deficiencies

ILAE: international league against epilepsy

IP: intestinal phosphatases

LOF: loss of function

Man: mannose

MR: magnetic resonance

MRI: magnetic resonance imaging

MRS: magnetic resonance spectroscopy

mRNA: messenger ribonucleic acid

NAD: nicotinamide adenine dinucleotide

NGS: next generation sequencing

PA: 4-pyridoxic acid

PDA: patent ductus arteriosus

PDE: pyridoxine dependent epilepsy

PI: phosphatidylinositol

***PIGP*:** phosphatidylinositol glycan anchor biosynthesis protein, class P

***PIGQ*:** phosphatidylinositol glycan anchor biosynthesis protein, class Q

***PGAP*:** GPI-attachment to proteins

PFO: patent foramen ovale

PK: pyridoxal kinase

PL: pyridoxal

PLP: pyridoxal 5'-phosphate

PLPase: pyridoxal-phosphatase

PLPBP: PLP binding protein

PLPHP: PLP homeostasis protein

PM: pyridoxamine

PMP: pyridoxamine 5'-phosphate

PN: pyridoxine

PNG: pyridoxine 5'-β-D-glucoside

PNP: pyridoxine 5’-phosphate

PNPO: pyridoxamine 5’-phophate oxidase

PTZ: pentylenetetrazol

RNA: ribonucleic acid

T1: transporters (identity unknown),

TEF: thyrotrophic embryonic factor

TIM: typical triosephosphate isomerase

TNSALP: tissue non-specific alkaline phosphatase

U/S: ultrasound

VUS: variant up uncertain significance

WES: whole exome sequencing

WGS: whole genome sequencing

WT: Wild type

List of Figures

List of Tables

Chapter 1 General introduction

1.1 Rare disease

Rare genetic disease is defined as affecting fewer than 1 in 2000 Europeans, or less than 200 000 people in the United States. With over 20 000 genes in the human genome, collectively these diseases are common, impacting millions of patients and families globally (1-3). Though many genetic mutations are not compatible with life, with modern early genetic testing, treatments for some diseases are possible and more treatments are on the horizon (4). Regardless of whether a treatment is available, when a diagnosis remains elusive, patients and families are often subject to a 'diagnostic odyssey,' whereby a significant amount of time, stress, and human and financial resources are invested towards achieving a diagnosis. This places a burden on healthcare systems (5-7), and these families may experience years of consultant visits, imaging studies and invasive tests that may yield no definitive results (8). Thus, even in situations where a treatment neither exists nor is possible, simply having a firm diagnosis can provide clarity and improve patient experience and quality of care.

While approximately 50% of the estimated 7000 rare monogenic diseases were discovered by 2013, predictions of solving the remainder by this year unfortunately did not come to complete fruition (2). Therefore, there remains a substantial need for research to discover and validate novel genetic causes of disease, to improve diagnostic yield and use of healthcare resources, and hopefully pave the way for treatments in the future. This thesis focuses on the discovery and validation work for three genetic causes of early infantile epileptic encephalopathy.

1.2 Disease gene discovery

In the 20th century, the discovery of pathogenic variants causing Mendelian disease depended largely on techniques such as genome wide linkage mapping and Sanger sequencing (9), as well as other techniques such as karyotyping and comparative genomic hybridization (10). Though these technologies have been successful in discovering the causes of approximately 3000 genetic diseases including cystic fibrosis and sickle cell anemia (11, 12), their power is considered limited relative to next generation sequencing (NGS) for the discovery of many Mendelian disorders (9). Limitations such as low power and sensitivity when working with few cases and families, locus heterogeneity, reduced penetrance and diminished reproductive fitness, all impair the ability for these technologies to elucidate the cause of many rare diseases (9, 13). Furthermore, the use of traditional techniques for disease gene discovery can take years, with costs orders of magnitude higher than NGS (2, 9, 14).

1.2.1 Next-generation sequencing

Since the establishment of the original NGS technology platforms in 2005, they have revolutionized the study of human genetics (14). By using the principles of massively parallel sequencing, these technologies simultaneously sequence millions of short fragments of DNA, which are then computationally realigned and annotated for analysis, generally using an unbiased approach (9, 15). The use of NGS has greatly increased over the past decade for both research and clinical purposes, leading to reduced costs and significant gains in disease gene discovery, both for somatic and germline mutations (10).

There are several strategies that utilize NGS, and identification of germline mutations can include targeted panels, exome sequencing, whole genome sequencing (WGS), and mitochondrial DNA sequencing (10). In a clinical setting, targeted gene panels that include up to hundreds of genes with known association with the clinical phenotype, are generally used as a first line (10). However, if this testing fails to provide a diagnosis, then exome sequencing, often used on a research basis, is second line (16, 17), although exome sequencing as a first-line test is becoming increasingly common and WGS is becoming available in some jurisdictions (18).

While gene panels remain common, there are several benefits to using exome sequencing as an initial diagnostic platform, and the diagnostic yield of exome sequencing has been estimated to be 20-40% (19, 20). In fact, when compared with microarray-based comparative genomic hybridization (CGH), panel testing, and single gene testing, trio-exome sequencing (analysis of proband with both parents to help prioritize variants) was shown to have the highest diagnostic yield and cost-effectiveness (21, 22), facilitating the identification of causal variants in patients with genetic diseases (9).

An emerging trend in NGS is the ability to provide a diagnosis with increasingly rapid turnaround time. If a physician suspects that a diagnosis is potentially treatable, NGS can now be achieved within 2 weeks, and in one case, a non-resource limited center was able to perform whole genome sequencing and analysis within 48 hours (10, 23). In more resource limited centers, turnaround is on the order of months (24). These rapid turnaround times relative to other approaches can be crucial, as molecular diagnosis will potentially prompt not only potential treatment pathways, but also expedite specialty referrals, and provide psychosocial benefits to families (25).

1.2.2 Exome sequencing

Exome sequencing selectively sequences the ~1% of the genome that is protein coding, and has become a powerful method for disease gene identification (2). The general initial steps for exome sequencing, and NGS more broadly, are DNA extraction, quantification, library preparation, target enrichment, and sequencing. Then, in several bioinformatics stages, known as a pipeline, the data is realigned against a reference genome, quality controlled, and variants are annotated for analysis.

Researchers identify sequence variants in patients that are not, or are rarely found in control datasets such as in-house controls, the 1000 Genomes Project (26), the Exome Aggregation Consortium (ExAC) (27) and gnomAD (27), and are predicted to be pathogenic to the corresponding protein's function. Pathogenicity is predicted *in silico* using several tools that consider factors such as what type of variant is present, how tolerated different amino acid substitutions are, if the variant occurs in an important domain, and other factors (*e.g.* Polyphen-2 (28), SIFT (29)). Since each predictor is based on different underlying principles and assumptions, they are subject to their own biases and do not always agree. For this reason, Combined Annotation-Dependent Depletion (CADD) (30) is another tool used that takes multiple scores into account and attempts to provide a less biased prediction of variant pathogenicity. Variants/genes on the candidate list that are consistent with the inheritance pattern of the disease are evaluated for known association with disease(s), known function, and gene expression pattern. When candidate variants are identified, they are confirmed by Sanger sequencing as necessary. In summary, exome sequence has been a revolutionary diagnostic approach for patients with rare genetic diseases (2).

1.3 Epilepsy and early infantile epileptic encephalopathy

1.3.1 Epilepsy definition and history

Epilepsy was one of the earliest diseases to be recognized, with records dating as early as 4000 BC (31). It is a neurological disorder defined by recurring episodes of convulsions, sensory disturbance, and/or loss of consciousness caused by excessive or hypersynchronous activity in the brain (32, 33). Worldwide, it is estimated that between 4 and 10 individuals per 1000 are either living with, or being treated for, epilepsy with an individual lifetime risk of about 3% (31, 33-37). Among the neurological diseases, epilepsy has the second highest disease burden (behind stroke) in terms of years of potential life lost (38).

Clinically, the International League Against Epilepsy (ILAE) defines epilepsy as:

1. "At least two unprovoked (or reflex) seizures occurring more than 24 hours apart.
2. One unprovoked (or reflex) seizure and a probability of further seizures similar to the general recurrence risk (at least 60%) after two unprovoked seizures, occurring over the next 10 years;
3. Diagnosis of an epilepsy syndrome." (39)

Epilepsy is not one disease, but rather a large group of disorders that vary significantly in terms of clinical phenotype, etiology, treatment, and outcomes, and can be characterized by seizure types, age of onset, developmental status, co-morbid features, and etiology (40). More specifically, as per the 2017 ILAE classification of the epilepsies, diagnosis occurs at three levels. The first is the type of epileptic seizures, such as focal onset, generalized onset, and unknown onset. The second step is the diagnosis of epilepsy type, which includes focal epilepsy, generalized epilepsy, combined generalized and focal epilepsy, and an unknown

epilepsy group. At the third and final level are the epilepsy syndromes, whereby the diagnosis of a specific syndrome can be made (41).

1.3.2 Causes of epilepsy

The causes of epilepsy are numerous and heterogenous, including stroke, trauma, autoimmune, infection, hypoxia, and neoplasms (42). However, genetics has for a long time been recognised as a significant risk factor for epilepsy (43), with some estimates as high as 70-80% of cases of epilepsy have genetics as a major contributing factor (33, 34). Furthermore, it is estimated that first degree relatives of patients with generalized epilepsy have a 5-10x risk compared to the general public of developing epilepsy (44-46), and risk is significantly higher among monozygotic twins compared to dizygotic twins (47-50). The importance of genetic mutations on the incidence of epilepsy is increasingly being recognised, with some epilepsy gene panels including several hundred genes (51).

The genetic epilepsies are broadly divided in three major classes: genetic generalized epilepsies (GGE, formerly idiopathic epilepsy), focal epilepsies, and epileptic encephalopathies (EE), which are often considered the most severe (33). My thesis will focus on epileptic encephalopathies.

1.3.3 Epileptic encephalopathy

The epileptic encephalopathies are a heterogenous group of severe epilepsies that generally have an early age of onset, include several seizure types with frequent epileptiform activity on EEG, and the seizures are often refractory to medication and can lead to poor

neurodevelopmental outcome, or even death (52, 53). These conditions are frequently multi-systemic, with many additional devastating clinical features in addition to epilepsy. Widely recognised epileptic encephalopathies include early myoclonic encephalopathy, Ohtahara syndrome, West syndrome, Dravet syndrome, Myoclonic status in nonprogressive encephalopathies, Lennox-Gastaut syndrome, Landau-Kleffner syndrome, and Epilepsy with continuous spike-waves during slow-wave sleep (54). The most common epileptic encephalopathies are West syndrome, affecting 25-42/100 000 per year (55), and Dravet syndrome, which affects 1/22 000 (56, 57).

West syndrome was the first epileptic encephalopathy described in 1841 by Dr. W.J. West in a letter addressed to the editor of the Lancet, describing his own child with infantile spasms (58). However, it was not until the 1950s that the term 'epileptic encephalopathy' was first used in reference to West syndrome as well as Lennox-Gastaut syndrome (59). Soon after, it was used in reference to patients with language regression secondary to epilepsy (60) . These pioneers recognized that in certain diseases (such as West syndrome and Lennox-Gastaut Syndrome), the seizures and interictal epileptiform abnormalities could lead to progressive changes in cognitive and cerebral function (61). In the 1970s, Ohtahara *et al* were the first to describe early infantile epileptic encephalopathy (EIEE), whereby infantile spasms and EEG findings occurred before even three months of age (62). It was further recognized that these clinical phenotypes are not mutually exclusive, as Ohtahara syndrome can progress to West syndrome, and later to Lennox-Gastaut syndrome (63).

The ILAE provided their first formal definition of epileptic encephalopathy in 2001, as "a condition in which the epileptiform abnormalities themselves are believed to contribute to the progressive disturbance in cerebral function" (54). This definition, therefore, assumed that

the cognitive and developmental declines in patients with these conditions are a direct result of seizures. In contrast, however, it has long been recognized that children with intellectual disability are at an increased risk of developing epilepsy (64, 65). Thus, the most recent ILAE classification recognizes that in some conditions, (for example Dravet syndrome, whereby 80% of cases are caused by *SCN1A* mutations (66)), developmental delays may precede or be independent of seizure onset, and the ILAE introduced the broader term 'developmental and epileptic encephalopathies' (41). This document also recognized that single gene disorders can cause epileptic encephalopathy in some individuals, but in others the same gene can cause self-limited epilepsy, such as seen in *SCN1A, SCN2A, SLC2A1, KCNQ2, KNCA2 and CHD2 (41)*. In chapter 4, I describe the phenotypic spectrum associated with the vitamin B6 dependent epilepsy caused by mutations in *PLPBP*, showing phenotypes ranging from relatively benign and highly responsive to B6, to epileptic encephalopathy.

While epileptic encephalopathies can be caused by other factors such as hypoxia or ischemia, as with epilepsy in general, the cause is often genetic. To date, 97 genetic diseases have been categorized or associated with the term early infantile epileptic encephalopathy (12), though is it estimated this list is not yet complete as many patients remain without a molecular diagnosis. Though traditionally the diagnosis of EIEE was done on the basis of seizure semiology, EEG, and imaging studies, early molecular genetic testing can provide a diagnosis (67). Moreover, while the prognosis for children with EIEE is often poor, there are situations in which early diagnosis can prove invaluable. For example, rapid diagnosis can provide treatment options for patients with GLUT1 deficiency (68) and vitamin B6 dependent epilepsy (69), the latter of which responds very poorly to antiepileptic medications without vitamin B6, and a subtype of which I describe in Chapter 4. In another example, having a molecular

diagnosis of Dravet syndrome caused by mutations in *SCN1A*, can optimize disease management, where, for example, it is known that certain anti-seizure medications such as carbamazepine and vigabatrin will exacerbate seizures, but others such as topiramate can be beneficial (70), and even enable improved cognitive function (71, 72). Thus, early diagnosis and understanding disease pathophysiology can be critical for guiding informed therapy.

Despite there being over 20 different antiepileptic drugs, approximately 30% of epilepsy patients continue to have seizures (73, 74). Furthermore, while some epileptic encephalopathies can have adequate seizure control, other manifestations such as developmental delays may still be present. There is thus an urgent need to further study these conditions to understand their molecular underpinnings, disease mechanisms, and work towards the development of novel and repurposed therapies.

1.3.4 Disease pathways

There are numerous molecular pathways and mechanisms responsible for epileptic encephalopathies and other seizure disorders, including ion channels (75, 76), synaptic dysfunction (77), transporter defects (78, 79), impaired DNA repair (80-82), chromatin remodeling (83), transcriptional regulation (76), the mammalian target of rapamycin (mTOR) pathway (84), and inborn errors of metabolism (e.g. phenylketonuria) (53, 85). The mechanisms by which gene mutations cause disease phenotypes often remain poorly understood (53), however *in silico*, *in vitro*, and *in vivo* models are assisting in mapping disease pathways and identifying candidate genes (86, 87).

The inheritance of genetic variants causing epileptic encephalopathies is frequently *de novo* dominant, but recessive single-gene disorders, as is the case of the diseases featured in

Chapters 2-4, as well as somatic mosaicism, and rare cases of chromosomal anomalies (e.g. trisomy 21), can cause epileptic encephalopathy (53). More than one gene can cause the same electro-clinical syndrome, and one gene may cause phenotypic pleiotropy (53). For my thesis, I will focus on genes whose proteins are involved in two pathways: the GPI-anchor biosynthesis pathway, and vitamin B6 metabolism.

1.4 The GPI anchor

The glycophosphatidylinositol (GPI) anchor is a glycolipid which is responsible for anchoring hundreds of proteins to the cell surface (88), known as GPI-anchored proteins (GPI-APs). The GPI anchor is evolutionarily conserved, and is ubiquitous among eukaryotes, from fungi and protozoa to humans, and may be important for some archaea (89, 90). The GPI-APs serve many important functions, including acting as receptors, adhesion molecules, enzymes, transporters, and protease inhibitors (90). Ultimately, these functions are essential for embryogenesis (91), development (92), neurogenesis (93, 94), fertilization (95, 96), and the immune system (97).

1.4.1 The GPI anchor biosynthesis pathway

Crucial to the cell surfacing anchoring of GPI-APs is the proper biosynthesis, attachment to proteins and remodeling of the GPI anchor itself (Figure 1.1). This is a complex process, which requires proteins produced from at least 30 genes (90, 98). The process begins in endoplasmic reticulum, where at least 21 phosphatidylinositol glycan anchor biosynthesis (PIG) proteins catalyze the biosynthesis of the GPI precursor in at least 12 stepwise reactions (90, 99). Importantly, the first step of this process is mediated by the N-acetylglucosamine

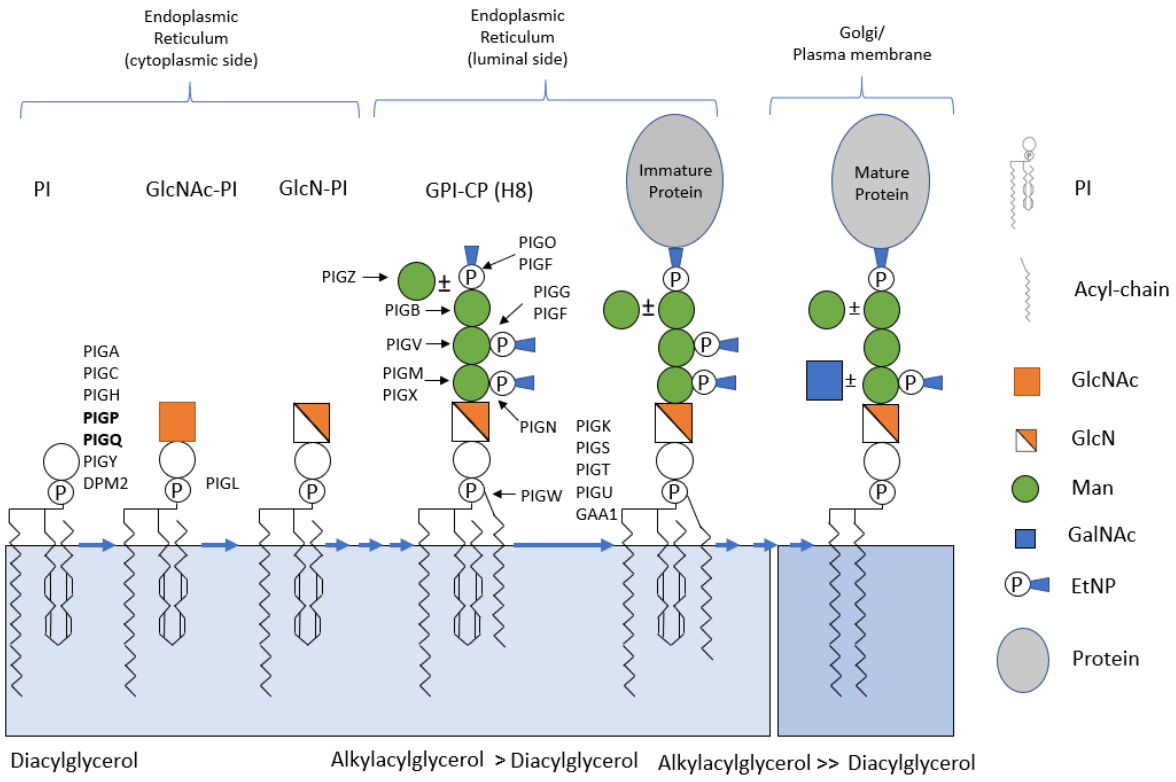
Endoplasmic Reticulum (cytoplasmic side)
Endoplasmic Reticulum (luminal side)
Golgi/ Plasma membrane
PI
GlcNAc-PI
GlcN-PI
GPI-CP (H8)
Immature Protein
Mature Protein
PIGA
PIGC
PIGH
PIGP
PIGQ
PIGY
DPM2
PIGL
PIGZ
PIGB
PIGV
PIGM
PIGX
PIGO
PIGF
PIGG
PIGF
PIGN
PIGW
PIGK
PIGS
PIGT
PIGU
GAA1
Diacylglycerol
Alkylacylglycerol > Diacylglycerol
Alkylacylglycerol >> Diacylglycerol
PI
Acyl-chain
GlcNAc
GlcN
Man
GalNAc
EtNP
Protein

Figure 1.1 Symplified biosynthesis and structure of the mammalian GPI anchor and associated GPI-APs.

The biosynthesis of the GPI anchor begins in the endoplasmic reticulum, in a multi-step pathway, starting with the transfer of GlcNAc to PI, a process which requires multiple proteins, including PIGP and PIGQ. Figure based on Fujita and Kinoshita (2012). Abbreviations: PI, phosphatidylinositol; GlcNAc, N-acetylglucosamine; GlcN, glucosamine; Man, mannose; GalNAc, N-acetylgalactosamine; EtNP, ethanolamine-phosphate.

transferase complex, a complex monoglycosyltransferase made from seven proteins (PIGA, PIGC, PIGH, PIGP, PIGQ, PIGY, and DPM2 (100-102). The GPI anchor is then transferred to proteins *en bloc* via the GPI transamidase complex consisting of PIGU, PIGT, PGAA1, PGS, and GP18 (103), and remodeling then occurs with the help of GPI-attachment to proteins (PGAP) proteins (90). The GPI anchor and GPI-APs are then sent to the Golgi by vesicles for further processing and ending with a mature GPI anchor in the cytoplasmic membrane at the cell surface, covalently attached to a GPI-AP at the C-terminus (90, 104).

1.4.2 Diseases involving the GPI anchor

The first disease recognized to be associated with defects in the GPI biosynthesis and remodeling pathway was paroxysmal nocturnal hemoglobinuria (PNH) (105). PNH is a rare blood disorder causing hemolysis due to defects in the complement system, particularly due to losses of the GPI-APs CD55 and CD59 on red blood cells (106). Takeda *et al* showed that that this disease is caused by somatic mutations in the X-linked gene *PIGA* (105), which is part of the complex in the first step catalyzing GPI biosynthesis.

Subsequently it was recognized that germline recessive mutations in the GPI anchor biosynthesis pathway could cause a new subclass of congenital disorders of glycosylation known as inherited GPI deficiencies (IGDs) (107). The first germline mutations affecting the GPI biosynthesis and remodeling pathway were identified in *PIGM*, leading to a propensity of venous thrombosis and seizures (108). Retroactively, however, it has been recognized that hyperphosphatemia with mental retardation syndrome (HPMRS, also known as Mabry syndrome), which was first recognized in the 1970s (109-111), is also caused by mutations in genes in this pathway (112), specifically *PIGV, PIGO, PIGW, PIGY*, PGAP2, and *PGAP3*.

Since the introduction of exome sequencing, there has been an explosion of discoveries of mutations in this pathway. To date, dysregulation of 22 genes in this pathway have been linked to diseases (107). To date, cases associated with each individual gene in this pathway are few, but collectively there are over 200 patients with diagnosed IGDs (104, 107). In all cases except *PIGA*, these diseases are inherited in an autosomal recessive manner.

There is broad clinical variability among this group of diseases, but commonly observed phenotypes include seizures (commonly refractory), developmental delays, hypotonia, and congenital malformations (104, 107). It is recognized that the broad clinical spectrum of these diseases is due to the range of molecular functions played by the GPI-APs (99).

These diseases are devastating to the patients and families, and often lead to poor quality of life and early death. Thus, there remains a significant need to continue to identify genetic variants causing diseases in this pathway, provide detailed phenotyping to characterize the clinical spectrum of the diseases, and investigate disease pathophysiology to ultimately inform optimal patient management in the near-term and development of therapies in the future. Moreover, genetic diagnosis and understanding of disease progression will help inform genetic counselling for affected families.

The genetics clinic at the Children's Hospital of Eastern Ontario sees patients and families with suspected genetic disease for diagnosis, management, and counselling. Three families presented with previously unknown neurodegenerative conditions, marked by refractory seizures and significant delays as well as congenital anomalies. Families that remain unsolved after standard-of-care investigation are offered participation in the Care4Rare research program (see Section 1.6). Thus, my objectives were to provide a molecular diagnosis

for each, which were mutations in *PIGP* and *PIGQ* in one and two families, respectively, and to provide functional evidence of causality and detailed phenotyping. Like PIGA, PIGP and PIGQ are also key members of the first step in GPI anchor biosynthesis; these discoveries are described in Chapters 2 and 3, respectively.

1.5 Vitamin B6 and epilepsy

Vitamin B6, also known as pyridoxine (PN), is essential for human survival. The metabolism of vitamin B6 is complex, and there are many subtypes, known as vitamers, however, only pyridoxal 5'-phosphate (PLP) is catalytically active.

PLP is a highly reactive aldehyde, and acts as a co-factor for more than 160 known enzymatic reactions, of which 70 are known to exist in humans (113). Given the high reactivity of PLP however, it is not stable in the environment, thus absorption of one of the non-phosphorylated vitamers is necessary, and a series of enzymatic reactions lead to the successful metabolism as B6 and conversion to PLP, to enable distribution of PLP across cells, the body, and the blood brain barrier (Figure 1.2).

For most individuals, vitamin B6 is plentiful in the diet, present in meat, fish, fruit and vegetables, and is produced by gut microbiota (114, 115). Unfortunately, genetic mutations that affect the enzymatic reactions required to interchange the multiple B6 vitamers, will also greatly increase the amount of B6 needed, and in such cases, diet and gut microbiota are insufficient, leading to disease.

Many biochemical and metabolic pathways depend on PLP, including amino acid and neurotransmitter metabolism, folate metabolism, 1-carbon metabolism, protein synthesis,

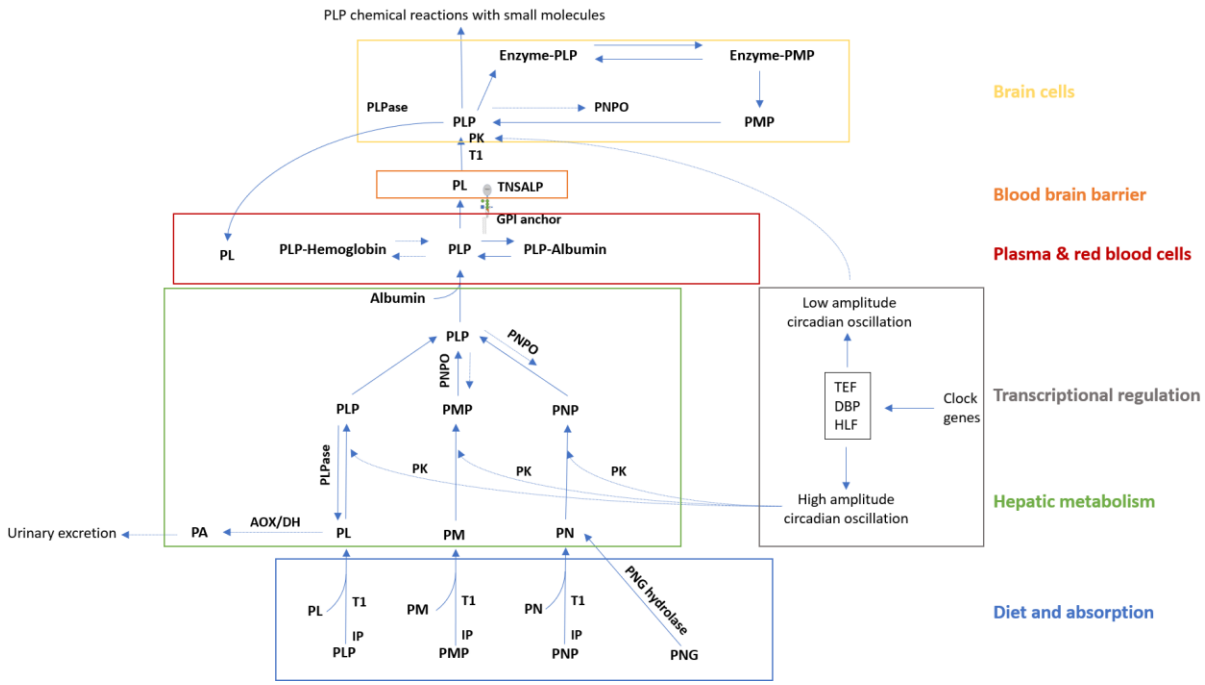
PLP chemical reactions with small molecules
Enzyme-PLP
Enzyme-PMP
PLPase
PNPO
PLP
PMP
PK
T1
PL
TNSALP
GPI anchor
PL
PLP-Hemoglobin
PLP
PLP-Albumin
Albumin
PLP
PNPO
PNPO
PLP
PMP
PNP
PLPase
PK
PK
PK
Urinary excretion
PA
AOX/DH
PL
PM
PN
PL
T1
IP
PLP
PM
T1
IP
PMP
PN
T1
IP
PNP
PNG hydrolase
PNG
Low amplitude circadian oscillation
TEF
DBP
HLF
Clock genes
High amplitude circadian oscillation
Brain cells
Blood brain barrier
Plasma & red blood cells
Transcriptional regulation
Hepatic metabolism
Diet and absorption

Figure 1.2 PLP synthesis and homeostasis pathways in mammalian central nervous system.

Multiple pathways and enzymes interconvert the various vitamin B6 ‘vitamers’ to enable the distribution of PLP, the active form of vitamin B6, to be transported across cell types, organs, and through the blood brain barrier. Figure adapted from Darin *et al* (2016). Abbreviations: AOX/DX, aldehyde oxidase (Mo cofactor)/β-NAD dehydrogenase; DBP, D site-binding protein; HLF, hepatic leukemia factor; IP, intestinal phosphatases; PK, pyridoxal kinase; PL, pyridoxal; PLP, pyridoxal 5’-phosphate; PLPase, pyridoxal-phosphatase, PM, pyridoxamine; PMP, pyridoxamine 5’-phosphate; PN, pyridoxine; PNG, pyridoxine 5’-β-D-glucoside; PNP, pyridoxine 5’-phosphate; PNPO, pyridoxamine 5’-phophate oxidase; T1, transporters (identity unknown), TEF, thyrotrophic embryonic factor; TNSALP, tissue non-specific alkaline phosphatase.

polyamine synthesis, carbohydrate and lipid metabolism, mitochondrial function, and erythropoiesis (115-118). The roles of PLP-dependent enzymes in neurotransmitter metabolism include the synthesis of the inhibitory transmitter γ-aminobutyric acid (GABA), thus it is not surprising that genetic mutations the affect the metabolism of PLP can lead to seizures, among other phenotypes.

Since PLP plays an important role in enzymatic activities, it is believed that local or global depletion of PLP leads to vitamin B6 responsive seizures (uniquely alleviated by high doses of PLP or its precursor pyridoxine (PN))(119). Epilepsies requiring B6 therapy are known as pyridoxine-dependent epilepsy (PDE)(120), and were first described by Hunt *et al* in 1954 (121). If untreated, PDE will potentially cause *status epilepticus* and death (122). Thus far, PDE-implicated mutations have been in genes involved in B6 vitamer metabolism (*e.g. PNPO* (123), *TNSALP* (124)), or in the accumulation of compounds that inactivate PLP (*e.g.* piperideine 6-carboxylate (P6C), *ALDH7A1*(125)). Additional genes involved in this pathway are likely also involved in human disease but have yet to be discovered. Furthermore, there are likely genes not yet associated with this pathway that are responsible for human disease.

1.5.1 *PLPBP* (formerly *PROSC*)

PROSC (proline synthetase co-transcribed homolog) is a gene found on chromosome 8 that belongs to the COG0325 family of proteins, which are ubiquitously expressed and highly conserved across evolution, suggesting an important function (126, 127). *PROSC* was first cloned and characterized by Ikegawa *et al* (127). Yeast and *E coli.* studies solved the crystal

structure and identified that COG0325 proteins have a PLP binding domain at the N-terminus (128), thus, a function related to vitamin B6 was suspected.

Previous experiments showed that the COG0325 proteins have no racemase activity (the catalysis of the inversion of stereochemistry) toward any of the 20 amino acids or their d-enantiomers, a function of the most structurally similar PLP-dependent enzymes (128, 129). This suggested that although COG0325 proteins likely interact with PLP, their true functions remained unknown. A study in *E coli.* deficient for the COG0325 protein YggS (*ΔYggS*) (128) showed an imbalance of keto acid and amino acid pools, which was attributed to the reduced availability of coenzyme A (CoA), an obligate cofactor for approximately 4% of known enzymatic activities (130). Additionally, another study associated *ΔYggS* with multiple cellular effects, including metabolism, and confirmed that YggS binds PLP (129).

While PLP is an essential enzymatic cofactor, excessive levels of PLP can also be problematic. PLP is a highly reactive aldehyde, and when in excess has the potential to interact with proteins and small molecules beyond its ~140 targeted apoenzymes. Thus, PLP concentrations need to be tightly controlled, and it was suggested that COG0325 proteins could play an important role in PLP homeostasis, though the mechanism has yet to be determined (129). The gene was renamed *PLPBP* (PLP binding protein) after the identification of variants in this gene whose seizures responded to vitamin B6 (131).

1.5.2 *PLPBP* and B6 responsive epilepsy

During the course of my thesis work on the identification of a homozygous variant in *PROSC* in a patient with EIEE and further characterization of this gene in zebrafish (see Chapter 4), Darin *et al* (131) and Plecko *et al* (132) reported that *PLPBP* is indeed associated

with early infantile epileptic encephalopathy. They first identified patients with *PLPBP* variants by screening patients whose seizures responded to vitamin B6 and did not have mutations in genes known to be associated with PDE (131). PLP treatment markedly improved outcomes, although all patients seemed to show a degree of developmental delay (131, 132). They identified missense, splicing and frameshift mutations, although no patients shared the same variant as our patient. The patients in their respective studies showed a high degree of phenotypic overlap with our patient, including early seizures, lactic acidosis, hypertonia, and acquired microcephaly. Some missense mutations were associated with a milder phenotype, with seizures controlled by B6 therapy and no developmental delays. Patients with frameshift or splicing mutations have acquired microcephaly and developmental delays even with treatment, and although they were PN and PLP responsive, the majority required adjunct therapy from other antiepileptic drugs. *PLPBP* therefore, has been established as a novel gene implicated in PDE.

Questions remained as to the exact pathophysiological mechanism and function of the protein. It was proposed that PLPHP (PLP homeostasis protein, the product of *PLPBP*) binds PLP and protects if from spontaneously reacting with other molecules, delivering it to the necessary apoenzymes and thus maintaining PLP homeostasis (131). This hypothesis highlights the complexity of this disease; in the absence of PLPHP, supplementation with B6 vitamers could increase PLP levels, but the PLPHP-free PLP would be free to react with molecules beyond the intended apoenzymes. Therefore, while vitamin B6 treatment may partially or fully alleviate seizures in these patients, they may show additional phenotypes, such as developmental delay, that might benefit from adjunct therapies.

Furthermore, given that diagnosed patients are maintained on vitamin B6 therapy, it is impossible to establish baseline measurements of biomarkers, such as the different B6

vitamers, which are important to understand the pathophysiology of the disease, or potentially identify biomarkers unique to the disease for the purposes of rapid diagnosis.

We also do not yet know the pathway(s) in which PLPHP deficiency causes seizures. In other pyridoxine dependent epilepsies, the seizures have been associated with reduced GABA (γ-Aminobutyric acid) synthesis (133, 134), since the enzyme glutamate decarboxylase (GAD), which synthesizes GABA from glutamate, is PLP-dependent. Since GABA is the most important inhibitory neurotransmitter in humans (and zebrafish), determining the degree to which PLPHP deficiency affects GABA levels will provide insights into how best to manage the disease, especially given that PLP treatment can itself be harmful (131). It must be considered however that PLPHP deficiency may lead to seizures through other mechanisms than the reduction of GABA levels.

Finally, the clinical presentation of the patient seen in Ottawa was suggestive of mitochondrial disease, and we subsequently became aware of several other unreported patients that have presented with a similar clinical and biochemical presentation. Determining if the PLPHP deficiency impacts mitochondrial function will provide important insight that could guide future work on therapeutics. Thus, my objectives were to provide a molecular diagnosis for the Ottawa family, provide detailed phenotyping of the new clinical cohort, provide functional evidence to implicate mitochondrial disease, and model this disease using zebrafish; these discoveries are described in Chapter 4.

1.6 Rare disease collaboration

The Care4Rare Canada Consortium is a national network established in 2010, and coordinated from CHEO Research Institute at the University of Ottawa, to discover the

molecular cause of unsolved rare genetic diseases. Patients and families with unsolved rare genetic disease are put forward for study and, if approved, are eligible for 'omic' approaches, including exome sequencing and functional studies using patient cells.

International collaboration is key to the identification of several unrelated individuals with similar phenotypes associated with mutations in the same gene - the current gold standard for novel disease gene discovery. Thus, global matchmaking is becoming more and more common place. Genes of interest are often shared via global databases (*e.g* Phenome Central (135), Gene Matcher (136), and Matchmaker Exchange (137)) to connect researchers that have an interest in the same gene. If there is a match, it is determined if the gene is associated with a similar phenotype in more than one patient, and large international collaborations are built to support novel gene discovery and clinical characterization of these new diseases.

In the absence of other patients, functional modeling using *in vitro* and/or animal models aid in assessing pathogenicity and therefore likelihood of disease causality. The Canadian Rare Diseases Models and Mechanisms (RDMM) Network was established to support the study of human disease genes and pathways in model organisms. Such studies help confirm variant pathogenicity, unravel the molecular mechanisms of rare disease, and enable the testing of novel therapies in the future (138).

1.7 Zebrafish as a model for epilepsy

Despite the explosion of disease gene discovery catalyzed by the use of next generation sequencing, there remains a gap in our understanding of the molecular underpinnings of many of these diseases (138). Although the discovery of disease genes is an important steppingstone and is hypothesis-generating, researchers must still turn towards the lab bench to investigate

the underlying mechanisms of disease pathogenesis. To that end, researchers make use not only of *in vitro* studies of patient cells, but also make use of growing abundance of model systems and organisms (138).

Zebrafish (*Danio* rerio) have been an important vertebrate model for genetics and human disease in recent decades. As a model system, zebrafish are relatively inexpensive to generate and maintain, have a short generation time (2-3 months), have large clutch sizes (and can breed weekly), are transparent during larval stages (particularly useful for studying development), and have a high degree of drug uptake (especially during larval stages) (139, 140). Zebrafish larvae also develop externally, and are readily accessible for using microscopy with reporter proteins (141). For the purposes of generating mutants, zebrafish are an ideal model system, and are readily amendable to gene manipulation via the CRISPR/Cas9 system (142) or antisense morpholinos (143).

Zebrafish are increasingly being utilized is epilepsy research, and behavioral tracking and electrophysiology experiments can be used (144). Several groups have shown seizure-like activity and drug responses in zebrafish with mutations in genes that reflect what is seen in patients with mutations in the human orthologs**.** For example, a zebrafish *scn1a* knockdown model showed seizure-like activity and was used to identify Clemizole as a possible new treatment for drug resistant Dravet syndrome (145). Another study then used the serotonin agonist fenfluramine in zebrafish as a candidate drug for this condition, validating the promising results of a prior clinical trial (146). Finally, Griffin *et al* (147) then identified further potential serotonin receptor agonists as possible treatments in zebrafish, and under a compassionate program, were even able to show a positive response of patients to clinically approved serotonin receptor agonists. As part of the Care4Rare team, I contributed to the development of a new method of genotyping zebrafish larvae (148), and helped characterize

the first zebrafish model of PDE, a knockout of *Aldh7a1* (149), which demonstrated that impaired lysine degradation with accumulation of PDE biomarkers, B6 deficiency, and low GABA levels in the *Aldh7a1*$^{-/-}$ larvae, may play a significant role in the seizure-like phenotype and PDE pathogenesis. Thus, zebrafish are a powerful model for the study of epilepsy genetics, and potentially for drug discovery.

1.8 Purpose

The overall objective of my thesis is to use next-generation sequencing tools and model systems to understand novel disease mechanisms associated with early infantile epileptic encephalopathy.

1.8.1 Rationale

Although seizures can be a function of numerous causes, such as brain trauma, chemical imbalances (e.g. sodium, glucose), infection, drugs, tumors, etc., a significant proportion of epilepsies are due to genetic mutations impacting important metabolic pathways. Severe early infantile epileptic encephalopathies (EIEEs), which further manifest into other phenotypes such as significant developmental delays and even death, are often resistant to current anti-epileptic therapies. In some cases, such as vitamin B6-responsive epilepsy, early identification of the cause can have profound impact on long-term outcomes. Furthermore, identification of genetic causes, even in the case of poorly treatable diseases, is instrumental in ending the "diagnostic odyssey," and understanding disease mechanisms may lead to future identification of therapies. To that end, my research is focused on the identification and characterization of rare genetic causes of EIEE and their mechanisms.

1.8.2 Hypotheses

The overarching hypothesis of this thesis is that dysregulation of important metabolic pathways will cause severe forms of early infantile epileptic encephalopathies (EIEE). More specifically that:

1. Additional genes causing EIEE remain to be discovered and their associated diseases characterized.
2. Mutations in *PIGP* and *PIGQ* will lead to impaired cell surface anchoring of GPI-APs.
3. *plpbp* null zebrafish will recapitulate features of the human disease, specifically seizures and early death, which will be improved by vitamin B6 therapy.
4. PLPHP localizes to the mitochondria.

1.8.3 Aims

1. Use exome sequencing to identify novel genes and variants implicated in early infantile epileptic encephalopathies.
2. Characterize the clinical presentation of novel or emerging EIEE and, where applicable, compare this presentation to patients with disease related to the same pathway.
3. Generate and characterize a knockout zebrafish model for *plpbp*.
4. Measure the effect of effects mutations associated with EIEE in humans and model organisms, including at the levels of mRNA, protein, flow cytometry of GPI-APs, metabolomics, electrophysiology, and behavior.

Chapter 2: Compound heterozygous mutations in the gene *PIGP* are associated with early infantile epileptic encephalopathy

Published in:

Johnstone DL, Nguyen TT, Murakami Y, Kernohan KD, Tetreault M, Goldsmith C, Doja A, Wagner JD, Huang L, Hartley T, St-Denis A, le Deist F, Majewski J, Bulman DE, Care4Rare Canada C, Kinoshita T, Dyment DA, Boycott KM, Campeau PM. 2017. **Compound heterozygous mutations in the gene PIGP are associated with early infantile epileptic encephalopathy**. *Hum Mol Genet* 26:1706-1715.

Permission for use from Oxford University Press:

2.1 Abstract

There are over 150 known human proteins which are tethered to the cell surface via glycosylphosphatidylinositol (GPI) anchors. These proteins play a variety of important roles in development, and particularly in neurogenesis. Not surprisingly, mutations in the GPI anchor biosynthesis and remodeling pathway cause a number of developmental disorders. This group of conditions has been termed inherited GPI deficiencies (IGDs), a subgroup of congenital disorders of glycosylation; they present with variable phenotypes, often including seizures, hypotonia and intellectual disability. Here, we report two siblings with compound heterozygous variants in the gene phosphatidylinositol glycan anchor biosynthesis, class P (*PIGP*) (NM_153681.2: c.74T>C;p.Met25Thr and c.456delA;p.Glu153AsnFs*34). *PIGP* encodes a subunit of the enzyme that catalyzes the first step of GPI anchor biosynthesis. Both children presented with early-onset refractory seizures, hypotonia, and profound global developmental delay, reminiscent of other IGD phenotypes. Functional studies with patient cells showed reduced *PIGP* mRNA levels, and an associated reduction of GPI-anchored cell surface proteins, which was rescued by exogenous expression of wild-type *PIGP*. This work associates mutations in the *PIGP* gene with a novel autosomal recessive IGD, and expands our knowledge of the role of *PIG* genes in human development.

2.2 Introduction

Glycosylphosphatidylinositol (GPI) is a glycolipid utilized by cells to anchor proteins to the cell surface. Addition of this posttranslational modification requires GPI biosynthesis via phosphatidylinositol glycan anchor biosynthesis (PIG) proteins, and remodelling via post GPI-attachment to proteins (PGAP) proteins (99). To date, more than 150 GPI-anchored proteins have been identified, and at least 27 known proteins are involved in the GPI anchor biosynthesis and modification process. GPI-anchored proteins (GPI-APs) have a variety of functions in the cell including, but not limited to, hydrolytic enzymes, adhesion molecules, receptors, protease inhibitors, and complement regulatory proteins (99, 150). Given these essential functions, it is not surprising that approximately half of the genes required for GPI anchor biosynthesis and remodelling have already been linked to disease, specifically *PIGA* (MIM 300868) (151-153), *PIGQ* (MIM 3008350) (154), *PIGC (MIM 601730)* (155), *PIGY (MIM 616809)* (156), *DPM2* (MIM 603564) (157), *PIGL* (MIM 280000) (158, 159), *PIGW* (MIM 616025) (160), *PIGM* (MIM 610293) (108), *PIGV* (MIM 239300) (112, 161-163), *PIGN* (MIM 614080) (164-169), *PIGO* (MIM 614749) (163, 170-172), *PIGG (MIM 616917)* (173), *PIGT* (MIM 615398) (174-176), *PGAP1* (MIM 611655) (177-179), *PGAP3* (MIM 615716) (180, 181), and *PGAP2* (MIM 614207) (182-184) (Supplementary Table 1). This group of disorders has been termed 'inherited GPI deficiencies' (IGDs) (99), and falls under the broader group of congenital disorders of glycosylation. Interestingly, all of these disorders are autosomal recessive or X-linked recessive (*PIGA*). IGD associated phenotypes often include seizures, intellectual disability, coarse facial features and hypotonia, but can also include microcephaly, hearing impairment, joint contractures, skin anomalies, congenital heart defects, urinary tract defects, skeletal anomalies and others (108, 112, 151-184).

Here we report a non-consanguineous family with a novel autosomal recessive disorder in two siblings characterized by early-onset refractory seizures, hypotonia, and profound global developmental delay. Whole exome sequencing identified compound heterozygous mutations in the gene phosphatidylinositol glycan anchor biosynthesis, class P (*PIGP*). Experiments in patient cells showed that these mutations result in defective PIGP function. Our findings add *PIGP* to the expanding list of GPI biosynthesis genes that when mutated cause rare genetic diseases.

2.3 Materials and methods

2.3.1 Patients

A family with two children presenting with neonatal onset seizures and hypotonia were evaluated by the genetics service at the Children's Hospital of Eastern Ontario. The parents gave informed consent to participate in the Care4Rare Canada research study, which was approved by the Children's Hospital of Eastern Ontario Research Ethics Board. In addition to clinical evaluation, blood and tissue samples were collected for DNA extraction and establishment of cell lines.

2.3.2 Whole-exome sequencing, and validation of identified variants

DNA from both affected siblings and the mother was extracted from whole blood. The Agilent SureSelect Clinical Research Exome kit was used to select for exonic DNA, and sequencing was performed on an Illumina HiSeq 2000. Alignment, variant calling, scoring and

annotation were performed as described in previous FORGE and Care4Rare projects (185). We compared variants to the 1000 genome phase 1 data set (April 2012 release) (186), the Exome Variant Server (http://evs.gs.washington.edu/EVS/), the ExAC server (27), and our in-house database (~2000 exomes previously sequenced at the McGill University and Génome Québec Innovation Centre). Variants were excluded if they were found at greater than 1% frequency in any database. Variants identified by whole-exome sequencing were validated by PCR amplification and sequenced using bi-directional Sanger sequencing. DNA from both parents was also Sanger sequenced. Primers: Met25Thr Fwd 5' CACCCCTTCTGTTGCGG 3' and Rev 5' CTTCCCTTGTCACTGAACGC 3'; Glu153AsnFs*34s Fwd 5'TGGGTCTCCATCAGACACAG 3' and Rev 5' AAATGCCTCTCTGGAGGAAC 3'. Due to allelic dropout of the Met25Thr variant in the mother, the primers Fwd 5' CCAGCCTGGGTGTCTGTATG 3' and Rev 5' AATCGCTCTTTCTGGCAATG 3' were used for Sanger sequencing her DNA.

2.3.3 Cell line establishment

A skin biopsy was taken from the affected male child to establish a fibroblast cell line. The cell line was established at the Centre for Applied Genomics (Toronto, Canada). Fibroblasts were maintained in HyClone DMEM media (GE Healthcare Life Sciences) supplemented with 10% fetal bovine serum, Penicillin-Streptomycin (SV30010, GE Healthcare Life Sciences), and 2mM L-glutamine (SH3003401, Thermo Scientific). Age-matched control cells lines were cultured in parallel.

2.3.4 Real-time PCR

Total RNA was extracted from patient and control cell lines using the RNeasy Mini Kit (QIAGEN), and cDNA was synthesized using the iScript kit (BioRad Laboratories) per the manufacturer protocols. Control reactions were run in parallel without reverse transcriptase. We amplified cDNA using gene-specific primers and iQ SYBR Green Supermix using the following conditions: an initial denaturing steps of 95°C for 3 minutes, followed by 39 cycles of 95°C for 10s, 55°C for 20s, 72°C for 30S, and a final melting curve generated in increments of 0.5°C per plate read, using a CFX96 Touch Real-time PCR Detection System (BioRad Laboratories). We quantified gene expression using the Ct method with CFX Manager software (BioRad Laboratories) and all data was corrected against GAPDH as an internal control. Primers: GAPDH Fwd 5' TGCACCACCAACTGCTTAGC 3' and Rev 5' GGCATGGACTGTGGTCATGAG 3'; PIGP Fwd 5' TTACCTCGTGTGGGCCTTTA 3' and Rev 5' ATGGATGGAGTCGAGTGGAG 3'. Experiments were repeated with 2 technical replicates.

2.3.5 Analysis by flow cytometry

Fresh blood samples from the affected male child and healthy controls were fixed with 10% formaldehyde, red blood cells were lysed in 0.1% Triton X-100, then the samples were stained with the GPI-AP markers: PE-anti human CD16 (BioLegend), FITC-mouse anti human CD55 and CD59 (BD Pharmingen), or FLAER-Alexa 448 Proaerolysin (Cedarlane) for 1 hour at room temperature. Non-specific binding was washed off before analyzing by a BD FACS Canto system (BD Biosciences). Granulocytes and lymphocytes were selected for

by size, and flow cytometry results were analyzed using FlowJo software. For analysis of unfixed granulocytes, the samples were stained for 20 minutes on ice and red blood cells were lysed in FACS Lysing Solution (BD Bioscience).

2.3.6 Functional analysis using PIGP deficient HAP1 cells

PIGP deficient HAP1 cells were generated by exon trapping mutagenesis (a gift from Dr. Morihisa Fujita, Jiangnan University, China) (187). We then cloned two h*PIGP* isoforms containing the 5'UTR using a Hep3B cDNA library, and ligated to generate C-terminal tagged wild-type and mutant pME *hPIGP* HA, generated by site-directed mutagenesis in isoforms 1 (NM_153681.2) and 2 (NM_153682.2). We also cloned hPIGP isoform 2 containing the 3'UTR from a Hep3B cDNA library and ligated to generate N-terminal tagged wild-type and mutant pME HA-hPIGP, strong promoter driven constructs, and pTK HA-hPIGP, weaker promoter driven constructs. The HAP1 cells were then transiently transfected with the various *PIGP* cDNAs (mutants or wild type) containing vectors, or an empty vector, by electroporation. Transfection efficiency was monitored by luciferase assay, and flow cytometry analysis was performed 2 days after transfection. For the analysis of protein expression, HEK293 cells were transiently transfected with various *PIGP* cDNAs and PIGP protein expression was analyzed by Western Blotting using an anti-HA antibody (Cell Signaling). Intensities of the bands were normalized with the loading control (GAPDH), and luciferase activities used for evaluating transfection efficiencies.

2.3.7 Phenotype rescue in patient fibroblasts

Patient fibroblasts were transduced with lentivirus expressing wild-type human *PIGP* cDNA NM_153682.2 (pReceiver-Lv105, Genecopoeia) and cultured in medium supplemented with puromycin as selection marker. The lentivirus-infected cells as well as untreated patient and control fibroblasts were then subjected to flow cytometry analysis using the markers FLAER-Alexa 448 (Cedarlane), FITC-anti human CD73, and PE-anti human CD87 (BioLegend).

2.4 Results

2.4.1 Patient descriptions

Two children with refractory epilepsy (Fig. 2.1A-C) were born to non-consanguineous parents of French-Irish ancestry; they have one healthy sister. The male proband (Fig. 2.1A,C) was born to a healthy G1P0 mother after an uncomplicated pregnancy. He was born after 41 weeks and 4 days, and weighed 4360 g (90-97th percentile). APGAR scores were 9 at both 1 and 5 minutes. He was admitted to the NICU after birth due to cyanosis and dyspnea associated with feeding. At 14 days of life, he started having seizures that comprised right-sided facial twitching. There were no structural lesions identified on MRI at the time. EEG showed abnormal frequent sharp waves from the bitemporal area with electrographic seizures from the right central region spreading to right temporal region areas.

Physical examination at 6 months of age showed his weight was 8.48 kg (50th percentile), height was 71.2 cm (90th percentile), and head circumference was 44.5 cm (75th percentile). By 3 years, 10 months of age, he weighed 12.15 kg (3rd percentile), was 98.2 cm

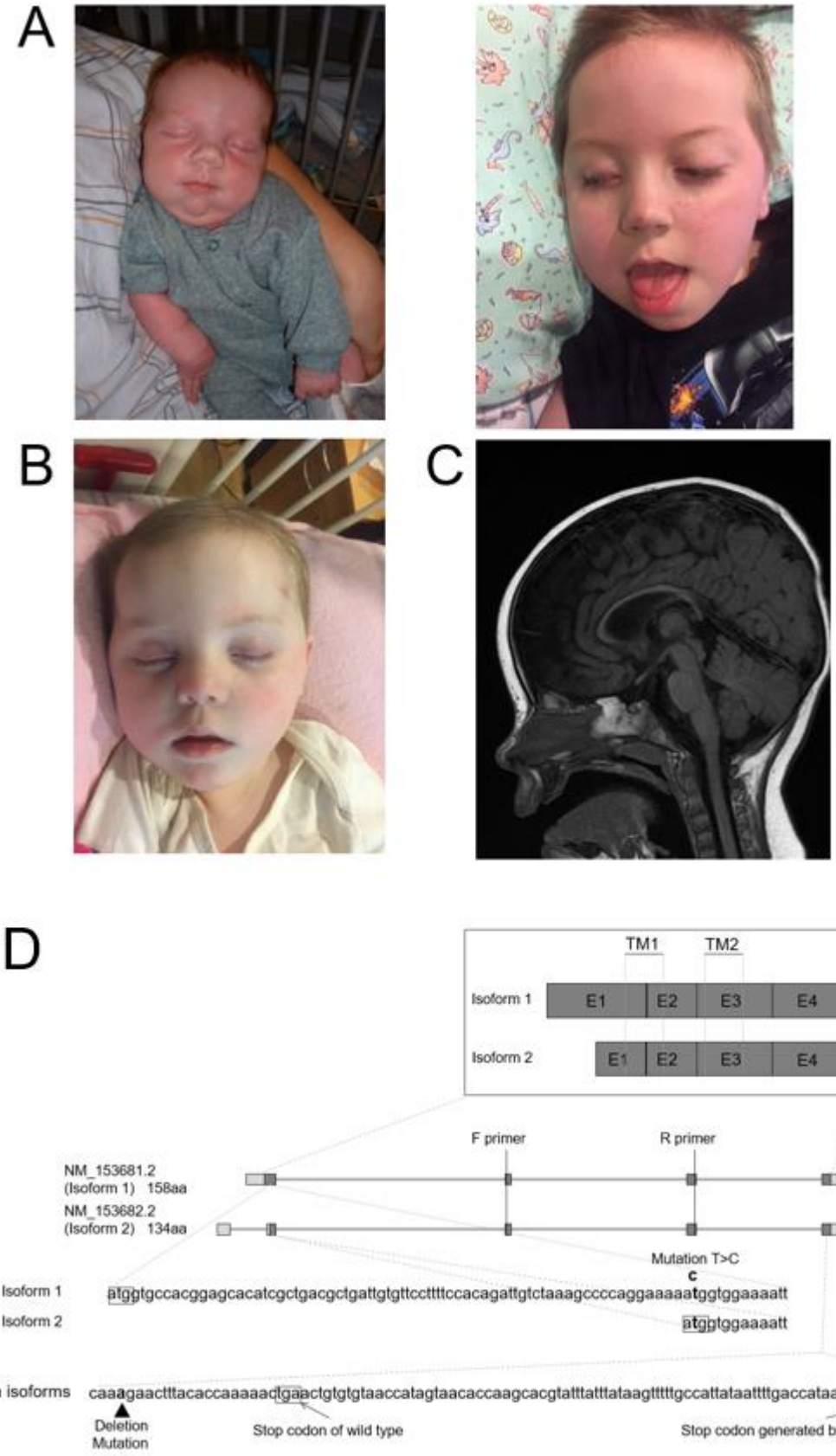
A
B
C
D
TM1
TM2
Isoform 1
E1
E2
E3
E4
Isoform 2
F primer
R primer
NM_153681.2
(Isoform 1) 158aa
NM_153682.2
(Isoform 2) 134aa
Mutation T>C
c
Isoform 1
atggtgccacggagcacatcgctgacgctgattgtgttcctttccacagattgtctaaagccccaggaaaaatggtggaaaatt
Isoform 2
atggtggaaaatt
Both isoforms
caaagaactttacaccaaaaactgaactgtgtgtaaccatagtaacaccaagcacgtatttatttataagtttttgccattataatttgaccataaattaatttga
Deletion
Mutation
Stop codon of wild type
Stop codon generated by frame shift

Figure 2.1: Clinical features of two children with compound heterozygous mutations in PIGP.

(A) Photographs of affected male child at 6 months and 9 years of age and (B) affected female child at 15 months of age showing sibling resemblance and hypotonic long facies. (C) MRI of male child at 5 years of age showing thin corpus callosum. (D) Mutations in PIGP localized on isoforms 1 and 2, which differ by 24 amino acids at the beginning of the first exon. The first mutation [Met25Thr (Isoform 1) or Met1Thr (Isoform 2)] leads to a missense or a loss of the start codon in each isoform, respectively. The second mutation, a deletion, causes a frameshift leading to a 34aa extension of the C-terminus. Inset shows the locations of the transmembrane domains (TM1 and TM2). Included are the location of the forward (F primer) and reverse (R primer) primers used for real-time PCR on cDNA.

in length (10-25th percentile), and his head circumference was 47.3 cm (less than 2nd percentile). He was noted to have cortical visual impairment. He had significant right-sided plagiocephaly (Fig. 2.1A) and held his lower limbs in abduction with contractures at the knees.

Repeat MRIs performed at 1 and 5 years of age showed a thin corpus callosum (Fig. 2.1C), with progressively increased T2 signal in the periventricular and subcortical white matter. His seizures persisted and were difficult to control. He never experienced infantile spasms. For example, at age 7 years, he was experiencing 12-25 seizures per day, each lasting 2-3 minutes. He has been trialed on phenobarbital, clonazepam, topiramate, vigabatrin, and levetiracetam in various doses and combinations. Since the introduction of levetiracetam at 8 years of age, in combination with clonazepam and phenobarbital, he has not had any reported seizures. An EEG at 9 years of age showed frequent multifocal epileptiform discharges and slow background activity for his age.

At his current age of 10 years, he has profound intellectual disability with little purposeful movements, no head control, and no vocalizations. He has profound central hypotonia with peripheral hypertonia, and hyperlaxity of the small and larger joints. He receives his nutrition by G-tube since age 8 years to manage recurrent aspirations.

The proband's younger sister (Fig. 2.1B) was born at 37 weeks gestation and weighed 3997 g (90-97th percentile). She started having complex partial seizures at 7 weeks of age, each seizure lasting several minutes and occurring 1-2 times daily. Seizures comprised eye twitching and apnea for 30-40 seconds. EEG at that time showed a poorly organized background with multifocal epileptiform discharges, and she was trialed on phenobarbital and topiramate. A brain MRI performed at 1.5 months of age found no structural abnormality. At 3 months of age she began having infantile spasms and EEG showed modified hypsarrhythmia.

She was started on vigabatrin which resulted in cessation of clinical spasms, but persistent modified hypsarrhythmia on EEG. Since then she has been trialed on gabapentin, valproic acid, levetiracetam, pyridoxine, pyridoxal-6-phosphate, folinic acid, and prednisolone, with no change in her modified hypsarrhythmia. Her seizures remained poorly controlled and at 17 months she was having 1-2 seizures a day. At approximately 2 years of age, she began having episodes of sustained eye deviation lasting hours which were non-epileptic and assumed to be episodes of oculogyric crises.

At 6 months, she weighed 6.76 kg (27^{th} percentile), was 66.1 cm in length (57^{th} percentile), and had a head circumference of 42 cm (45^{th} percentile); at 14 months her head circumference was essentially unchanged at 45.3 cm (46^{th} percentile). A G-tube was placed at 19 months to manage recurrent aspiration. She had no eye contract or tracking, and was diagnosed with a cortical visual impairment. She had low central muscle tone, with fisted hands and absent postural reflexes. She had positive clonus bilaterally, and an exam at 23 months noted 5-8 beats of clonus, as well as hyperreflexia (4+). She passed away at 26 months of age secondary to complications of her seizure disorder.

Investigations to identify the cause of this severe seizure disorder in this family included transferrin isoelectric focusing and enzyme testing (β-glucocerebrosidase, hexosaminidase A&B, β-galactosidase and arylsulfatase A), which were normal in the brother. Genetic tests for mutations in *ARX, STXBP1, MECP2* in the brother were normal, as was a microarray for chromosomal copy number variations. Plasma amino acids and urine organic acids were normal in both children. CSF neurotransmitter analysis in the sister revealed low homovanilic acid at 205 nmol/L (normal: 337-1299 nmol/L) and low 5-hydroxyindoleacetic acid at 195 nmol/L (normal: 208-1159 nmol/L). CSF neopterin and biopterin were within

normal limits. Liver function tests and alkaline phosphatase (ALP) were normal in both children.

Due to a lack of a molecular diagnosis for these siblings, the family was offered participation in the Care4Rare Canada research study to try to identify the cause of their rare disease using whole-exome sequencing.

2.4.2 Whole-exome sequencing identified compound heterozygous mutations in *PIGP*

To investigate the genetic cause of this clinical presentation, we performed whole-exome sequencing on genomic DNA from both affected children and their mother. Average coverage for the exomes was 144.68X for the male child, 121.59X for the female child, and 129.47X for their mother, with at least 96.7% of CCDS exons in each exome covered at 10X. Common variants [≥1% minor allele frequency in the 1000 Genomes project phase 1 data set (April 2012 release) (186), the Exome Variant Server (http://evs.gs.washington.edu/EVS/), the ExAC server (27) or ~2000 internal exomes] were excluded. An autosomal recessive mode of inheritance was suspected given the concordant phenotype in the siblings and lack of related family history. There were no homozygous rare variants shared by both affected children. After filtering for shared compound heterozygous mutations which were inherited and *in trans*, we identified a single gene, *PIGP;* both affected children carried maternally inherited NM_153681.2:c.74T>C (p.Met25Thr) and a second variant in trans, NM_153681.2c.456delA (p.Glu153Asnfs*34). Sanger sequencing confirmed the variants were present in both children, one inherited from each parent.

The c.74T>C (p.Met25Thr) *PIGP* variant occurs at a highly conserved residue (GERP 5.4, (188)) and was predicted to be deleterious by multiple *in silico* programs [CADD (30), Polyphen2 (189), SIFT (190), Mutation Taster (191), and Align GVGD (192, 193)]. This variant has been reported in the ExAC database (27) with very low frequency (2.47×10^{-5}). In the longest *PIGP* isoform 1 (NM_153681.2), this mutation causes a methionine to threonine missense change, though in isoform 2 (NM_153682.2), this variant leads to a loss of the start codon (p.Met1Thr) (Fig. 2.1D). The second variant [NM_153681.2:c.456DelA (p.Glu153Asnfs*34)] occurs in the final exon of all transcripts (Fig. 2.1D). Notably, only a handful of loss-of-function variants in *PIGP* have been observed in ExAC, all of which are considered rare and never seen in a homozygous state. Interestingly, mutations in other *g*enes whose proteins are in complex with *PIGP (PIGA, PIGC PIGQ, PIGY* and *DPM2*) have been identified as causative for similar phenotypes (151-157). Taken together, these findings indicate that the compound heterozygous variants in *PIGP* are likely the cause of this novel autosomal recessive condition and prompted us to further investigate the functional impact of these variants.

2.4.3 PIGP transcript levels are decreased in patient cells

We began by evaluating whether the mutations impacted *PIGP* mRNA levels by performing real-time PCR analysis on fibroblasts from the affected male child and age-matched controls (fibroblasts from the affected female child were not available). We found that fibroblasts from the affected child had reduced levels of *PIGP* mRNA (Fig. 2.2A). Western blot analysis of PIGP was attempted with four different antibodies; however, no antibodies specifically detected PIGP (data not shown). We conclude that patient cells have decreased levels of PIGP mRNA, and potentially protein.

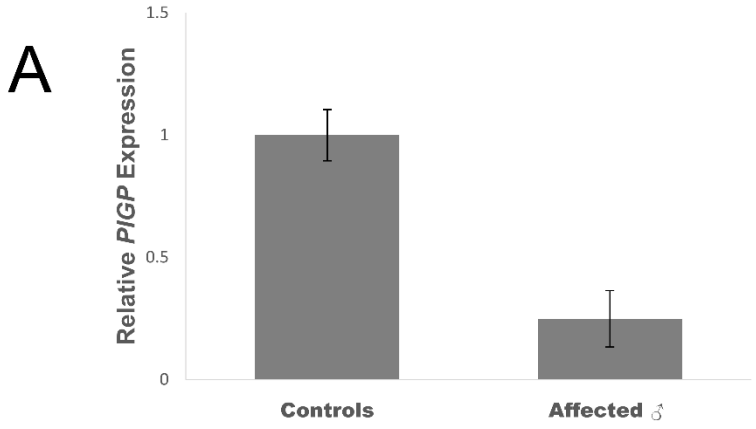
A
Relative PIGP Expression
1.5
1
0.5
0
Controls
Affected ♂

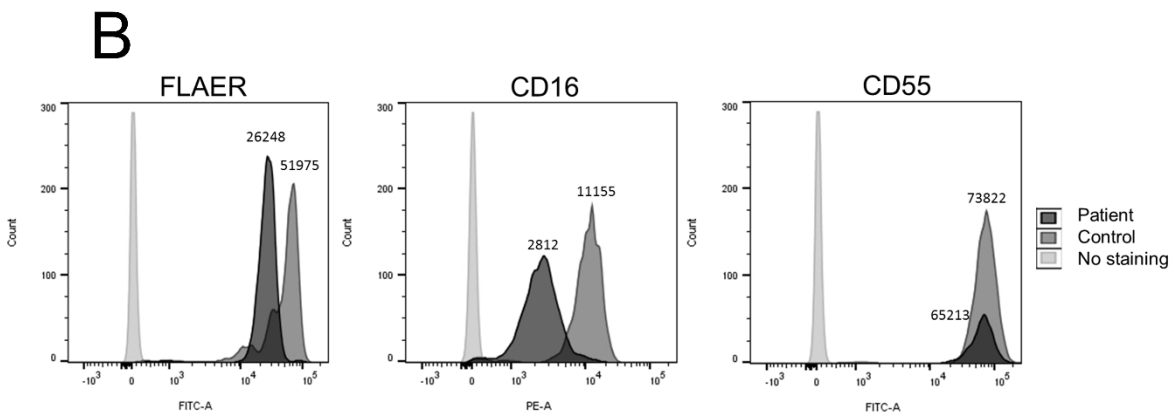
B
FLAER
CD16
CD55
26248
51975
11155
2812
73822
65213
Count
FITC-A
PE-A
Patient
Control
No staining

Figure 2.2: Impact of the *PIGP* mutations on patient cells.

(A) Real-time PCR on fibroblast cell extracts, showing that the affected male has reduced transcript levels of *PIGP*. Error bars represent standard error of the mean. GAPDH was used for normalization. (**B**) Flow cytometry analysis of granulocytes from fixed fresh blood of the affected male and control. Results show cell surface expression of fluorescently labeled proaerolysin 'FLAER', which binds directly to the GPI anchor, as well at expression of the GPI-APs CD16, and CD55 from triplicate experiments on fixed cells. Numbers above each histogram represent the mean fluorescence intensity (MFI).

2.4.4 Patient and *PIGP* deficient HAP1 cells showed reduced cell surface expression of GPI-anchored proteins, but artificially overexpressing wild type *PIGP* cDNA rescued this phenotype

PIGP is an integral component of the first reaction which commences GPI anchor biosynthesis, therefore, we next assessed whether the GPI-anchoring process was deficient in patient cells. To determine if patient cells had reduced cell surface expression of GPI-anchored proteins (GPI-APs), we stained fixed whole blood of patients and controls with fluorescent antibodies for GPI-APs (CD16, CD55, CD59), as well as with fluorescein-labeled proaerolysin 'FLAER' which binds to the GPI anchor itself, and performed flow cytometry to assess relative fluorescence (172). Analysis on granulocytes indicated that patient cells had reduced signal of CD16 (25% vs. controls) and FLAER (51% vs. controls) (Fig. 2.2B). We also analysed lymphocytes and repeated the experiments in live granulocytes from unfixed whole blood (Supplementary Fig. 2.1). We conclude that insufficient levels of PIGP and/or defective PIGP function in patient cells leads to reduced levels of GPI-anchored proteins at the cell surface.

To investigate the effects of each mutation on isoforms 1 and 2 independently, we performed the functional analysis of the mutant cDNAs using PIGP deficient cells made by exon trapping mutagenesis (187). We transiently transfected *PIGP* deficient HAP1 cells with either mutant or wild-type *PIGP* cDNA of two isoforms and analyzed the surface expression of GPI anchored proteins by flow cytometry. We found that the cells transfected with *PIGP*-Met25Thr isoform 1 (NM_153681.2) cDNA had reduced expression of CD55, CD59, and CD87 compared to cells transfected with wild-type cDNA (Fig. 2.3A), and that this difference was even more pronounced with *PIGP*-Met1Thr isoform 2 (NM_153682.2) cDNA (Fig. 2.3B),

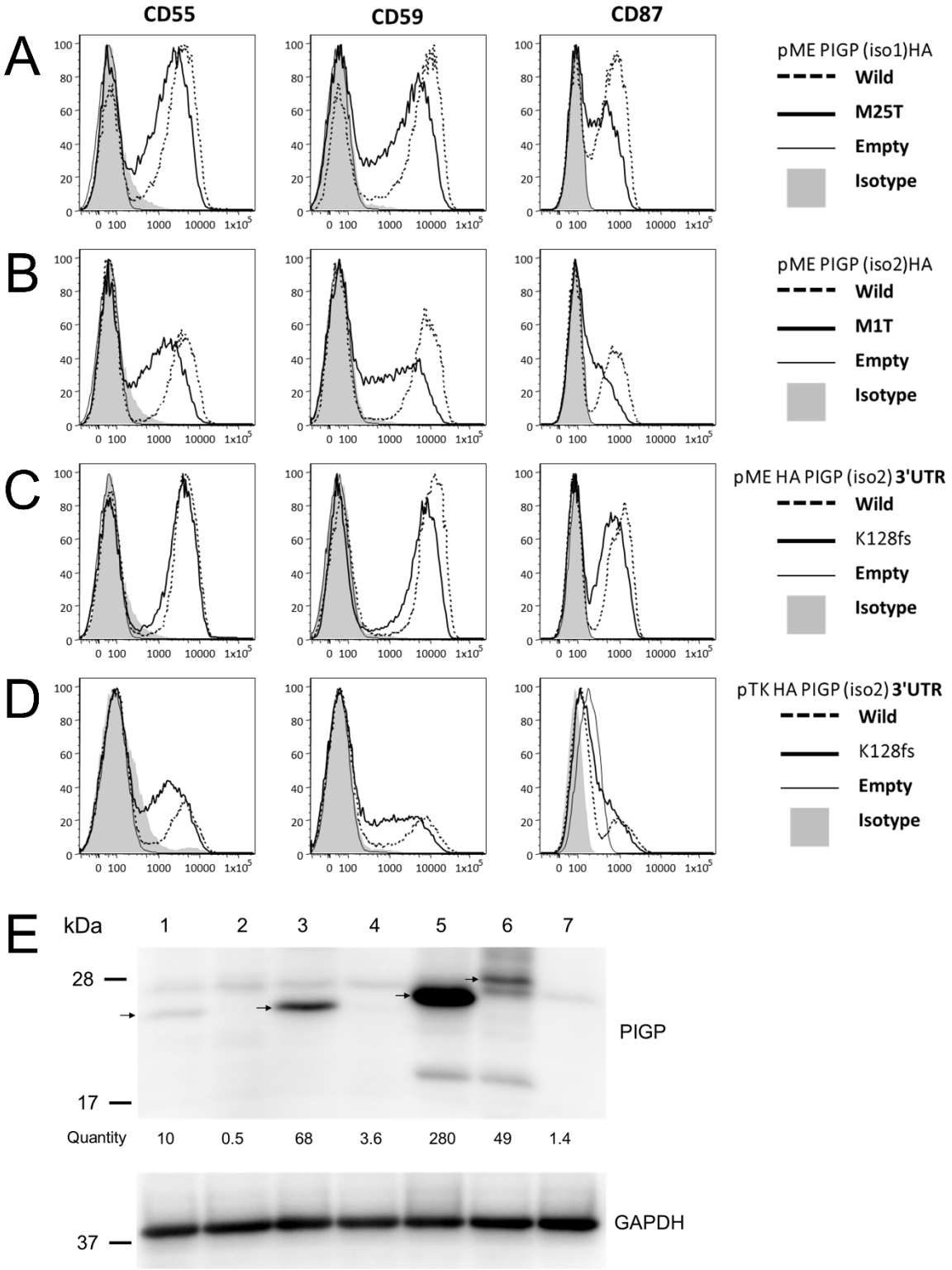
A
CD55
CD59
CD87
pME PIGP (iso1)HA
Wild
M25T
Empty
Isotype
B
pME PIGP (iso2)HA
Wild
M1T
Empty
Isotype
C
pME HA PIGP (iso2) 3'UTR
Wild
K128fs
Empty
Isotype
D
pTK HA PIGP (iso2) 3'UTR
Wild
K128fs
Empty
Isotype
E
kDa
1 2 3 4 5 6 7
28
17
PIGP
Quantity
10 0.5 68 3.6 280 49 1.4
37
GAPDH

Figure 2.3: Flow cytometry of *PIGP* deficient HAP1 cells.

Flow cytometry analysis of *PIGP* deficient HAP1 cells transfected with either wild type PIGP cDNA or mutant PIGP cDNA, analyzed as the expression of the GPI-APs CD55, CD59, and CD87. (A) The effect of c.T74C on the longest isoform (NM_153681.2), causing the variant p.Meth25Thr; (B) the effect of c.T2C on the dominant isoform (NM_153682.2) causing a loss of the start codon. The effect of the variant c.384delA on the dominant isoform (NM_153682.2), causing a frameshift and stop loss was analyzed using the strong promoter pME (C) as well as the weak promoter pTK (D). The effect of the first variant caused a stronger reduction of GPI-AP expression in isoform 2, however there was some residual activity despite the loss of the start codon. The effect of the second variant was stronger under the weak promoter (D) than the strong promoter (C). (E) Western blot on lysates from HEK293 cells transfected with various PIGP cDNAs or empty vector. Lanes 1 and 2 are isoform 1 (NM_153681.2) transfected with wild-type and Met25Thr PIGP cDNA, respectively. Lanes 3 and 4 are isoform 2 (NM_153682.2) transfected with wild-type and Met1Thr PIGP cDNA, respectively. Lanes 5 and 6 are isoform 2 (NM_153682.2) transfected with wild type and cDNA causing the frameshift mutation Glu129AsnFs*34, respectively. Lane 7 is empty vector. GAPDH (lower panel) was used as loading control. Lanes 1-4 had a C-terminus HA tag, whereas lanes 5 and 6 had an N-terminus HA tag, and HA antibody was used to identify PIGP, which is indicated by the arrows. There was non-specific background in all lanes at ~27kDa, the two smaller bands in lanes 5 and 6 are unknown. Isoform 2 (lane 3) was more strongly expressed than isoform 1 (lane 1). Both the Met25Thr and Met1Thr variants (lanes 2 and 4) decreased the expression of their respective isoforms. The Glu129AsnFs*34 mutation in isoform 2 also decreased PIGP expression but lead to an increase in protein size (lane 6), as expected. N-terminal HA tagged PIGP (lane 5) showed higher expression than C-terminal HA tagged PIGP (lane 3) of the same isoform.

but there seemed to be residual activity despite the loss of the start codon. Cells transfected with *PIGP*-Glu129AsnFs*34 cDNA from isoform 2 had slightly reduced levels of GPI-anchored proteins (Fig. 2.3C) as assessed by strong promoter driven constructs, and the reduction was more clear when driven by weaker promoter driven constructs, indicating that the frameshift mutation in the very C-terminal location also affected the PIGP activity (Fig. 2.3D). Western blot analysis using HA antibody on lysates from HEK293 cells transfected with mutant or wild-type HA-tagged *PIGP* cDNA showed that wild-type isoform 2 (Fig. 2.3E, lane 3) was found to be more highly expressed than wild-type isoform 1 (Fig. 2.3E, lane 1). However, the faint band detected in the wild type of isoform 1 was approximately the same band size as isoform 2, so it is possible that it was translated from the same methionine. Activity of wild type C-terminal tagged isoform 1 was lower than C-terminal tagged isoform 2 (Supplementary Figure 2.2), but neither the expression of PIGP-Met25Thr (isoform 1) nor PIGP-Met1Thr (isoform 2) produced a detectable amount of protein (Fig. 2.3E, lanes 2 and 4). The expression of *PIGP*- p.Glu129Asnfs*34 (NM_153682.2) in isoform 2 led to the expected increase in molecular weight of the protein (Fig. 2.3E, lane 6; wild-type in lane 5). These findings conclusively demonstrate that both patient mutations compromise PIGP function.

Finally, we wanted to see if we could rescue the deficiency in GPI-APs in patient cells. We transduced patient fibroblasts with a lentivirus overexpressing wild type *PIGP* isoform 2 cDNA (NM_153682.2) and repeated the flow cytometry assays for quantification of GPI-APs at the cell surface, comparing results with and without lentiviral rescue, and expressed relative to control fibroblasts. This resulted in increased detection of CD87, from 47% to 63% relative to control fibroblasts, and FLAER increased from 64% to 98% (Fig. 2.4).

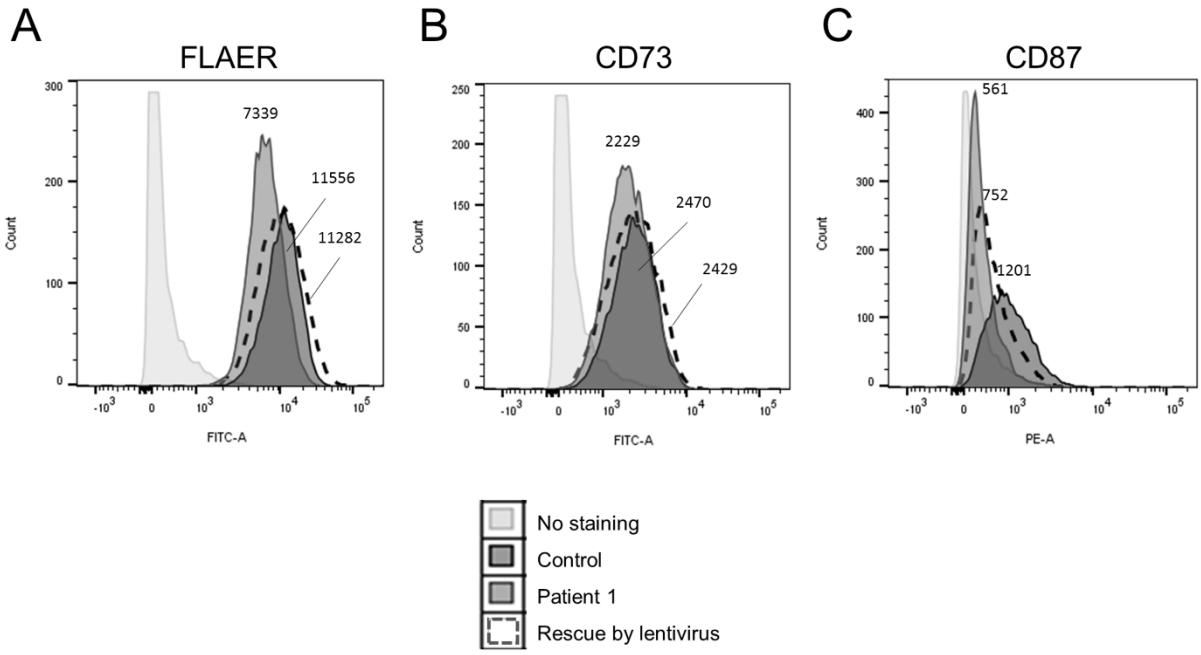
A
FLAER
7339
11556
11282
Count
FITC-A
B
CD73
2229
2470
2429
Count
FITC-A
C
CD87
561
752
1201
Count
PE-A
No staining
Control
Patient 1
Rescue by lentivirus

Figure 2.4: Flow cytometry analysis of patient, control, and rescued fibroblasts.

Labeled using fluorescently labeled proaerolysin 'FLAER' (**A**), CD73 (**B**), and CD87 (**C**). Fibroblasts from the affected male proband were compared with unaffected controls. Furthermore, patient cells were transduced with lentivirus overexpressing wild type *PIGP* cDNA (NM_153682.2),and were analyzed in parallel. The lentivirus restored FLAER on patient cell surface from 64 % to 98% (**A**), and CD87 from 47% to 63% (**C**). Numbers above each histogram represent the mean fluorescence intensity (MFI).

Taken together, our results show that patient cells have decreased levels of *PIGP* mRNA, and that expression of mutant *PIGP* cDNA in HEK293 cells produced a decreased amount of protein. Furthermore, both mutations have a deleterious effect on PIGP function, leading to decreased levels of GPI-APs at the cell surface. Taken together, we conclude that biallelic mutations in *PIGP* are the cause of this novel epilepsy syndrome.

2.5 Discussion

We have identified a novel autosomal recessive disorder characterized by early infantile epileptic encephalopathy, hypotonia, and profound global developmental delay. Both affected siblings carried compound heterozygous mutations in the gene *PIGP*. Molecular profiling of patient cells and an *in vitro* recapitulation system showed that these *PIGP* mutations adversely affect protein function, providing substantial support for causality of this syndrome. To our knowledge, this is the first report implicating *PIGP* in human disease.

It is worth nothing that in our findings, and those from other studies on IGDs, not all GPI-APs respond equally to disease-causing mutations, or to rescue experiments (e.g. Fig. 2.4). We have much to learn about the mechanistic specifics of this, however we must consider that following biosynthesis, there are many other processes involved in GPI trafficking and function. These are likely largely responsible in the differences in IGDs. Furthermore, the stability of different GPI-APs is also variable (194), and different cell types will show variable expression patterns of GPI-APs (195). For these reasons, it is important to use several different GPI-APs as biomarkers, and to test multiple cell types, with emphasis on granulocytes (195).

The IGDs are an increasingly recognised group of disorders. To date, all of these conditions are associated with seizures and developmental delay, which is consistent with the affected individuals reported here. Other findings, such as hypotonia, microcephaly and CNS abnormalities are also common, demonstrating the importance of this pathway for proper neurodevelopment. From IGDs characterized thus far, it appears that mutations in earlier steps of the pathway lead to degradation of precursor proteins which fail to become properly GPI-anchored, and this occurs through ER-associated degradation (177), while mutations in later steps can leave residual secretion of improperly GPI-anchored proteins such as ALP, which is released into the blood. The siblings reported here did not have elevated ALP levels. As PIGP is a member of the early pathway, this provides further support for this dichotomy. Overall, this novel condition bears remarkable resemblance to other IGDs.

Seizure control was difficult to achieve in these patients, though levetiracetam was effective in the male child. The levetiracetam responsiveness is interesting, as excessive levels of *PIGP* transcripts in brain tissue have been associated with levetiracetam resistance (196). This suggests that appropriate transcript or protein levels may play a role in the response to anticonvulsants. Levetiracetam binds to the synaptic vesicle protein SV2A, yet its exact mechanism(s) of action remain unknown, and there are no identified links to the GPI anchor. Further studies are needed to further investigate a link between PIGP and response to this medication.

Little is known about how dysfunction of *PIG* genes leads to the common IGD phenotypes. Given the vast number of GPI-APs, this question is incredibly complicated, but some insights exist. For example, homozygous or compound heterozygous mutations in *FOLR1,* a GPI-AP, have been associated with seizures refractory to antiepileptic therapy, as

well as intellectual deficiencies, and severe physical handicap (197). It is therefore logical to predict that compromising the FOLRI GPI anchor would also have similar effects. Another example is *CNTN2,* a GPI-AP involved in the organization of axonal subdomains at the nodes of Ranvier (198). Mutations in *CNTN2* have been associated with cortical myoclonic tremor and epilepsy (199). These are merely 2 of the 150+ GPI-APs which are likely disrupted in our patients and contribute to their clinical presentation. Broadening our knowledge of this pathway and the downstream effects of *PIG* and *PIGP* mutations is necessary to begin to elucidate the molecular pathogenesis of these disorders and investigate targeted treatment options.

In summary, we report a novel autosomal recessive disorder in a sibling pair affected by early-onset refractory seizures, hypotonia, and profound global developmental delay. Whole exome sequencing identified novel compound heterozygous mutations in the gene *PIGP*. Molecular findings showed that patient-derived cells have reduced levels of *PIGP* mRNA transcript, and expressing cDNA recapitulating the patients' mutations *in vitro* resulted in a reduced detection of PIGP protein compared with wild type cDNA. These mutations caused reduced expression of GPI-APs, which was rescued by providing wild type *PIGP* cDNA. These findings broaden our understanding of the disease pathogenesis of mutations occurring in the GPI anchor biosynthesis and remodeling pathway.

Chapter 2: Supplementary materials

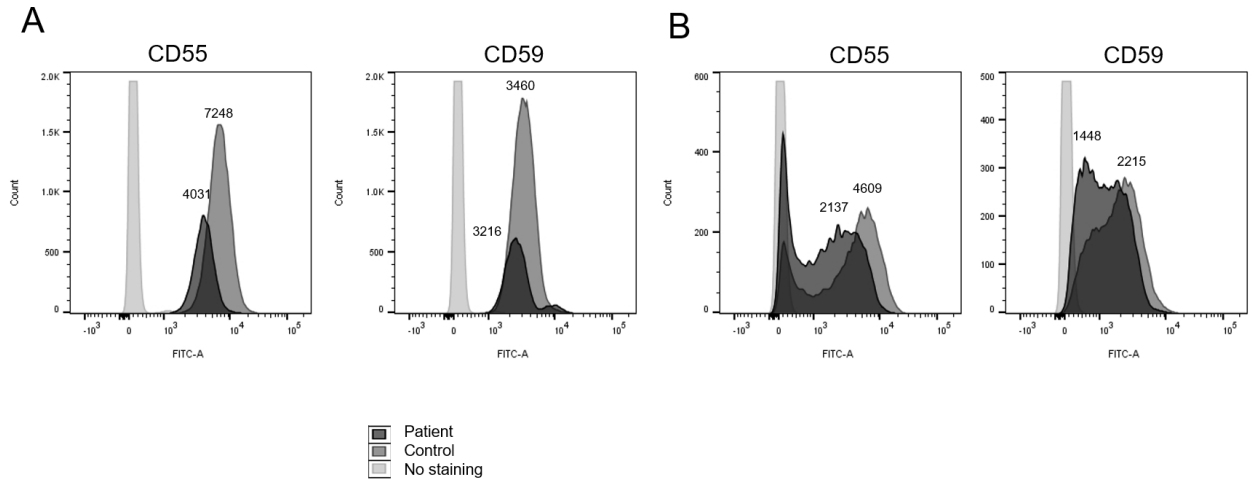

Supplementary Figure 2.1. Flow cytometry analysis of (A) live granulocytes.

Flow cytometry analysis of (A) live granulocytes from fresh blood of the affected male and control, (B) lymphocytes from fresh whole blood. Numbers above each histogram represent the mean fluorescence intensity (MFI). Note: lymphocytes are a mixed population of cells so that might influence the analysis and the comparison between the different experiments.

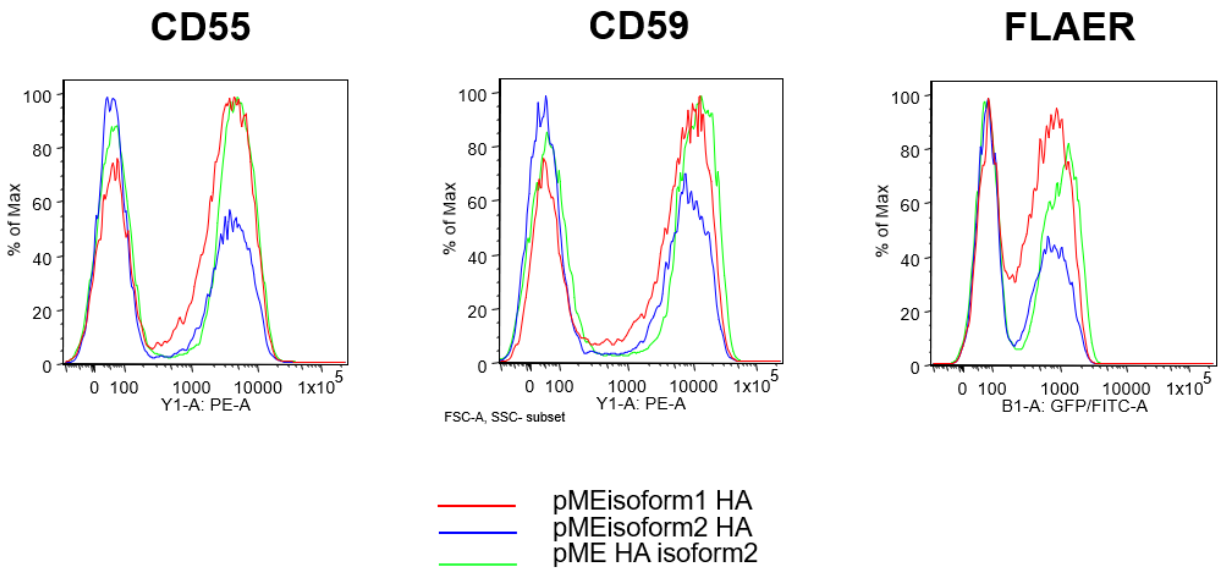
CD55
CD59
FLAER
% of Max
Y1-A: PE-A
FSC-A, SSC- subset
B1-A: GFP/FITC-A
pMEisoform1 HA
pMEisoform2 HA
pME HA isoform2

Supplementary Figure 2.2. Comparison of activity between isoforms 1 and 2, and between C-terminal and N-terminal tagged PIGP.

Activity of wild type C- terminal tagged isoform 1 was lower than C-terminal tagged isoform2, whereas there was no difference in activity between C-terminal and N-terminal HA- tagged isoform 2.

Supplementary Table 2.1: Summary of known IGD-associated genes and phenotypes.
Abbreviations: +(present), - (absent), AR (autosomal recessive), NA (not applicable), ND (not determined). Table adapted from Makrythanasis *et al* (2016) *(173)* and based on Kinoshita (2014) *(99)*.

Gene	*PIGA*	*PIGQ*	*PIGC*	*PIGP*	*PIGY*	*DPM2*	*PIGL*	*PIGW*	*PIGM*
References	3- 5	6	7	this publication	8	9	10, 11	12	13
GPI-biosynthesis step	1	1	1	1	1	1	2	4	6
IGD Mode of inheritance	X-linked (Xp22.2)	AR (16p13.3)	AR	AR (21q22.13)	AR (4q22.1)	AR (9q34. 11)	AR (17p11.2)	AR (17q12)	AR (1q23.2)
CLINICAL FEATURES									
Seizures	+	+	+	+	variable	+	+	+	+
DD or ID	+	+	+	+	variable	+	+	+	+
Hypotonia	+	+	ND	+	variable	+	+	+	-
Reduced head circumference	ND	ND	-	+	+	+	ND	ND	ND
Facial dysmorphism	variable	NA	-	+	+	+	+	+	-
Hearing impairment	+	NA	-	-	-	-	+	-	-
Joint contractures	+	+	ND	+	variable	+	ND	ND	ND
Skeletal anomalies	ND	ND	-	Short fingers	short fingers and small feet, proximal limb shortening, hip dysplasia	scoliosis	ND	ND	ND
Skin anomalies	variable	-	-	+	-	-	variable	-	-
Congenital heart defects	variable	-	ND	-	-	-	variable	-	-
Vesicoureteral reflex or anomalies in urinary tract	variable	-	ND	-	variable	-	variable	-	-
Anorectal anomalies	-	-	ND	-	-	-	-	-	-
CNS abnormalities in MRI	variable	+	-	+	variable	+	variable	+	-
Increased serum alkaline phosphatase	variable (mild)	-	-	-	variable (mild)	ND	variable	+	-
Decreased GPI-AP	+	variable	+	+	+	ND	+	+	+

Supplementary Table 2.1 continued

Gene	*PIGV*	*PIGN*	*PIGO*	*PIGG*	*PIGT*	*PGAP1*	*PGAP3*	*PGAP2*
References	14-17	18-23	17, 24-26	27	28-38	31-33	34, 35	36-38
GPI-biosynthesis step	7	8	10	11	12	13	16	17
Mode of inheritance	AR (1p36.11)	AR (18q21.33)	AR (9p13.3)	AR (4p16.3)	AR (20q13.12)	AR (2q33.1)	AR (17q12)	AR (11p15.4)
CLINICAL FEATURES								
Seizures	+	+	+	variable	+	variable	variable	variable
DD or ID	+	+	variable	+	+	+	+	+
Hypotonia	+	+	+	+	+	+	+	+
Reduced head circumference	ND	+	+	ND	+	+	+	ND
Facial dysmorphism	+	+	+	variable	+	-	+	variable
Hearing impairment	variable	-	variable	-	variable	-	-	variable
Joint contractures	ND	ND	ND	variable	ND	ND	ND	ND
Skeletal anomalies	hypoplastic terminal phalanges	ND	hypoplastic terminal phalanges	-	osteopenia, scoliosis, delayed bone age, short arms	ND	ND	+
Skin anomalies	-	-	-	-	-	-	-	-
Congenital heart defects	variable	variable	variable	-	variable	-	-	variable
Vesicoureteral reflex or anomalies in urinary tract	variable	variable	-	-	variable	-	-	variable
Anorectal anomalies	variable	variable	variable	-	variable	-	-	variable
CNS abnormalities in MRI	+	variable	variable	thin corpus callosum, cerebellar hypoplasia, cerebral atrophy	+	variable	variable	+
Increased serum alkaline phosphatase	+	-	+	-	- (hypophosphatasia)	-	+	+
Decreased GPI-AP	+	+	+	-	+	-	variable	+

Chapter 3: Early infantile epileptic encephalopathy due to biallelic pathogenic variants in *PIGQ*: Report of 7 new subjects and review of the literature

Published in:

Devon L. Johnstone, Thi Tuyet Mai Nguyen, Jessica Zambonin, Kristin D. Kernohan, Anik St-Denis, Nissan V. Baratang, Taila Hartley, Michael T. Geraghty, Julie Richer, Jacek Majewski, Eric Bareke, Andrea Guerin, Manuela Pendziwiat, Loren D.M. Pena, Hilde M.H. Braakman, Karen W. Gripp, Andrew C. Edmondson, Miao He, Rebecca C. Spillmann, Erik A. Eklund, Allan Bayat, Undiagnosed Diseases Network, Care4Rare Canada Consortium, Hugh J. McMillan, Kym M. Boycott, Philippe M. Campeau. 2020. **Early infantile epileptic encephalopathy due to biallelic pathogenic variants in *PIGQ*: Report of 7 new subjects and review of the literature**. *JIMD*. doi: 10.1002/jimd.12278. Online ahead of print.

3.1 Abstract

We investigated seven children from six families to expand the phenotypic spectrum associated with a rare early infantile epileptic encephalopathy caused by biallelic pathogenic variants in the phosphatidylinositol glycan anchor biosynthesis class Q (*PIGQ*) gene. The affected children were all identified by clinical or research exome sequencing. Clinical data, including EEGs and MRIs, was comprehensively reviewed and flow cytometry and transfection experiments were performed to investigate PIGQ function. Pathogenic biallelic *PIGQ* variants were associated with increased mortality. Epileptic seizures, axial hypotonia, developmental delay and multiple congenital anomalies were consistently observed. Seizure onset occurred between 2.5 months and 7 months of age and varied from treatable seizures to recurrent episodes of status epilepticus. Two affected individuals had midgut volvulus requiring surgical correction, and cardiac anomalies including arrythmias were observed. Flow cytometry using granulocytes and fibroblasts from affected individuals showed reduced expression of glycosylphosphatidylinositol (GPI)-anchored proteins. Transfection of wildtype *PIGQ* cDNA into patient fibroblasts rescued this phenotype. We expand the phenotypic spectrum of *PIGQ*-related disease and provide the first functional evidence in human cells of defective GPI-anchoring due to pathogenic variants in *PIGQ.*

3.2 Introduction

The GPI-anchor anchors more than 150 proteins to the cell surface (99). These GPI-anchored proteins (GPI-APs) play important roles in embryogenesis, cell signaling, immune response and neurogenesis (91, 93, 94, 104). Thirty-one different genes are involved in the biosynthesis of the GPI-anchor (200), of which 19 genes have been associated with human disease (201). Clinical features generally include global developmental delay (GDD), epileptic seizures, hypotonia, and congenital anomalies (104). The clinical spectrum is likely related to the various cellular functions of GPI-APs, which include adhesion molecules, complement regulatory proteins, hydrolytic enzymes, protease inhibitors and receptors (99, 150).

Phosphatidylinositol glycan anchor biosynthesis class Q (PIGQ) is a key co-enzyme in the N-acetylglucosamine transferase complex, the first step catalyzing the biosynthesis of the GPI-anchor (101, 202, 203), and is encoded by *PIGQ* (OMIM 605754) (204). To date, three patients with *PIGQ* variants have been described (154, 205, 206), however, for the first two patients, limited clinical information was published. Martin *et al* showed that *PIGQ*-deficient Chinese hamster ovary (CHO) cells transfected with human *PIGQ* cDNA lacking exon 3 did not restore surface expression of GPI-APs as well as wildtype (WT) (154), however functional data in human cells remained elusive. Recently, Starr *et al* (206) provided a detailed clinical description of a patient with compound heterozygous variants in *PIGQ*. Very little is known about the clinical and functional spectrum associated with *PIGQ* insufficiency.

Herein, we describe and expand the phenotypical and neurophysiological spectrum of PIGQ deficiency in seven affected individuals, and show reduced expression of GPI-APs in patient granulocytes and fibroblast cell lines, with reversibility using *PIGQ* cDNA.

3.3 Methods

3.3.1 Patient recruitment

Ethics approvals were obtained from the local institutional review boards and informed consent was obtained from patients´ legal guardians. Details of local ethics approvals are available in Supplemental Material. Collaboration was made possible using Matchmaker Exchange (136). Detailed clinical examinations, magnetic resonance imaging (MRIs) and electroencephalograms (EEGs) were collected for each subject. Here forth, we abbreviate each subject to "St" (St1, St2, etc.).

3.3.2 Exome sequencing

DNA was extracted from whole blood, purified and analyzed using an exome sequencing trio approach when both parents were available. All exomes were aligned to the human reference genome GRCh37/hg19. Detailed protocols for exome capture, sequencing, pipeline and analysis for each patient/family are available in Supplementary Methods. Primers for Sanger sequencing confirmation of variants are found in Supplementary Table 3.1.

3.3.3 Cell line establishment

For St3b, a skin biopsy was taken and sent to the Centre for Applied Genomics (Toronto, Canada), for establishment of a fibroblast cell line. A skin biopsy for St5 was similarly used for establishment of a fibroblast cell line at the Duke Cytogenetics Laboratory. A fibroblast cell line for St2 was established independently at the Children's Hospital of Philadelphia.

HyClone DMEM media (GE Healthcare Life Sciences) supplemented with 10% fetal bovine serum, penicillin-streptomycin (SV30010, GE Healthcare Life Sciences) and 2mM L-glutamine (SH30033401, Thermo Scientific), was used for cell-line maintenance.

3.3.4 Flow cytometry

Fresh blood samples from St4 and St5, as well as from healthy controls were stained with the GPI-AP markers: PE-conjugated anti human CD16 (BioLegend), FITC-conjugated mouse anti human CD55 and CD59 (BD Pharmingen), or Fluorescein-labelled proaerolysin (FLAER)-Alexa 448 (Cedarlane) for one hour on ice. Red blood cells were lysed in FACS Lysing Solution (BD Bioscience). Granulocytes from St1 as well as a control were stained with FLAER and analyzed by flow cytometry in a clinical lab.

For fibroblasts, cells were harvested at 80-90% confluency, stained with FLAER-Alexa 448, FITC-conjugated mouse anti human CD73 (BioLegend) or PE- conjugated mouse anti human CD109 (BioLegend) for one hour on ice in the incubation buffer containing 0.5% BSA, then fixed in 3.7% formaldehyde. For all assays, non-specific binding was washed off before analyzing by a BD FACSCanto II system (BD Biosciences) followed by FlowJo software analysis. Fibroblasts established from St2 and a control were stained with FITC-CD59 and analyzed by flow cytometry in an independent lab.

3.3.5 Rescue assays of GPI-APs on fibroblasts

Lentiviruses carrying a wildtype PIGQ-Lv105 (NM_004204.3) or an empty-Lv105 construct (GeneCopoeia) with the presence of packaging plasmids pMD2.G and psPAX2 (AddGene) were produced in HEK293T cells. Fibroblasts (established from St3b and St5) were transduced with the lentiviruses and selected by Puromycin resistance. Untransduced cells and control cells were subjected to flow cytometry analyses as described above for fibroblasts.

3.4 Results

We identified seven affected individuals with biallelic *PIGQ* variants from six unrelated families. The cohort comprised of five females and two males, from various ancestries. Detailed clinical summaries can be found in Supplementary Materials as well as Table 3.1 and Supplementary Table 3.2. EEG descriptions are found in Supplementary Table 3.3, and MRI findings are summarized in Supplementary Table 3.4.

3.4.1 Variants identified

We identified seven previously unreported *PIGQ* (NM_148920.2) variants predicted to be damaging and one previously identified variant (p.Y400del) (206). All were either in a homozygous or compound heterozygous state. The novel variants included two missense variants (p.G17R; p.G449R), a canonical splice site substitution (c.942+1G>A), an in-frame deletion (p.A377_S389del) and three frameshifts (p.Q527Afs*75, p.R538Afs*24 and p.G557Dfs*4) (Figure 3.1A). Variants identified in other genes are listed in the detailed clinical descriptions in Supplementary Materials but were excluded as disease-causing due to phenotype incompatibility, predicted benign pathogenicity, or mode of inheritance.

Table 3.1 Clinical features of seven new affected individuals from six families with biallelic variants in PIGQ, and review of the literature.
Abbreviations: DD (developmental delay), ID (intellectual delay), PDA (patent ductus arteriosus), PFO (patent foramen ovale), N/A (not applicable), U/S (ultrasound).

Subject ID/Source	St1	St2	St3a	St3b	St4	St5	St6
Variants & Inheritance (NM_148920.2)	Homozygous: c.1611del p.R538Afs*24	Maternal: c.1199_1201del p.Y400del Paternal: c.942+1G>A IVS4+1G>A	Maternal: c.1578_1579del p.Q527Afs*75 Paternal: c.1199_1201del p.Y400del	Maternal: c.1578_1579del p.Q527Afs*75 Paternal: c.1199_1201del p.Y400del	Maternal: c.1130_1168del p.A377_S389del Paternal: c.1345G>C p.G449R	Maternal: c.49G>A p.G17R Paternal: c.942+1G>A IVS4+1G>A	Homozygous: c.1670del p.G557Dfs*4
Gender	Female	Female	Female	Female	Female	Male	Male
Ancestry	Turkish	European/Puerto Rican	British Isles /French Canadian	British Isles/French Canadian	Lebanese/Iraqi	Mexican	Afghani
Current age	11y	6y6m	Deceased 2d	Deceased 5y	Deceased 9m	2y2m	Deceased 3y9m
Prenatal issues	-	Polyhydramnios	Prominent kidneys, premature rupture of membranes	-	Polyhydramnios, hepatomegaly, hydronephrosis	Dandy Walker malformation	-
Neonatal complications	-	Respiratory distress, hypoglycemia, failed newborn hearing screen in left ear.	Respiratory distress, renal and cardiac failure	Jaundice, secundum atrial ventricular defect detected after birth.	Respiratory distress	Respiratory distress, feeding difficulties, jaundice, PDA, PFO	Feeding difficulties, hypertonia
DD/ID	+	+	N/A	+	+	+	+
Seizure onset	6 months	7 months	N/A	Almost 4 months	7 months	6 months	2.5 months
Hypotonia	+	+	N/A	+	+	+	+
Abnormal movements	+	+	N/A	+	+	+	+
Facial dysmorphism	-	+	+	+	+	+	+
Cranial shape anomalies	-	+	-	-	+	+	+
Teeth anomalies	-	+	N/A	+	Too young	+	-
Skeletal anomalies	+	+	-	+	+	+	-
Joint contractures	+	-	-	+	+	-	-
Other dysmorphic features	+	-	+	-	+	-	-
Deafness	-	-	-	-	Mild left conductive	-	-
Ophthalmological anomalies	+	+	N/A	+	+	+	+.
Cardiac anomalies	-	+	+	+	+	+	+.
Genitourinary	+	-	+	No U/S done	+	+	+
Gastrointestinal issues	+	+	N/A	+	+	+	+
Serum alkaline phosphatase	Normal	Intermittently elevated	Not measured	Elevated	Elevated	Not measured	Normal

Subject ID/Source	Martin et al 2014(154)	Alazami et al 2015(205)	Starr et al 2018(206)
Variants & Inheritance (NM_148920.2)	Homozygous: c.690-2A>G	Homozygous: c.619C>T p.R207*	Maternal: c.968_969del p.L323Pfs*119 Paternal: c.1199_1201del p.Y400del
Gender	Male	N/A	Male
Ancestry	West African	N/A	N/A
Current age	Deceased 2y4m	N/A	Deceased 10m
Prenatal issues	-	N/A	Severe polyhydramnios requiring multiple amniocentesis fluid reduction procedures
Neonatal complications	At 4 weeks: cyanotic episodes with eye twitching, brief stiffening of upper body.	N/A	Feeding difficulties, trembling episodes
DD/ID	+	+	+
Seizure onset	4 weeks	N/A	7 months
Hypotonia	+	N/A	+
Abnormal movements	+	N/A	+
Facial dysmorphism	+	N/A	+
Cranial shape anomalies	-	N/A	+
Teeth anomalies	-	N/A	-
Skeletal anomalies	-	N/A	+
Joint contractures	-	N/A	N/A
Other dysmorphic features	+	N/A	+
Deafness	-	N/A	-
Ophthalmological anomalies	+	+	+
Cardiac anomalies	-	N/A	+
Genitourinary anomalies	-	N/A	+
Gastrointestinal issues	+	N/A	+
Serum alkaline phosphatase	N/A	N/A	Elevated

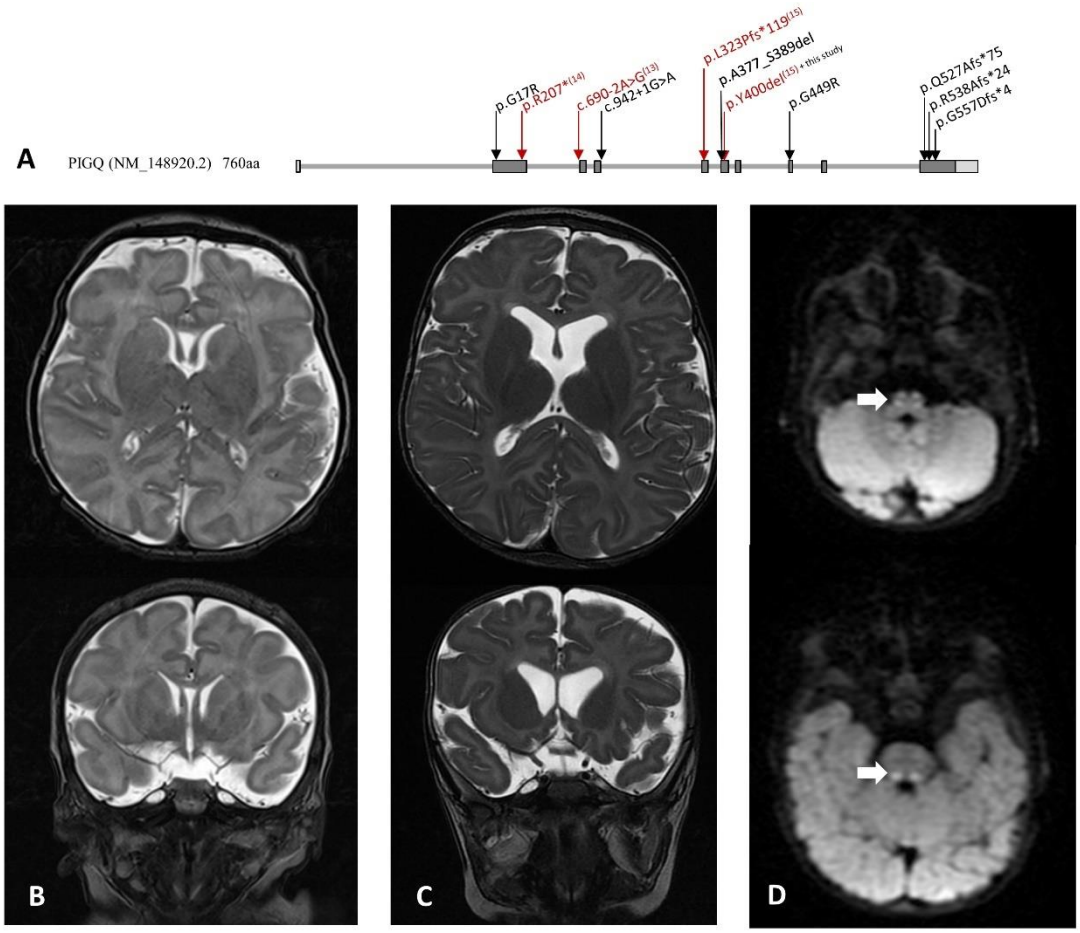
A
PIGQ (NM_148920.2) 760aa
p.G17R
p.R207*(14)
c.690-2A>G(13)
c.942+1G>A
p.L323Pfs*119(15)
p.A377_S389del
p.Y400del(15) + this study
p.G449R
p.Q527Afs*75
p.R538Afs*24
p.G557Dfs*4
B
C
D

Figure 3.1 Variants and imaging findings.

(A) Variants in *PIGQ* identified in this study localized on isoform 1 (NM_148920.2) of the gene. Variants reported in previous studies are in red with corresponding reference numbers in superscript. Brain MRI of subject 4 was performed at age 9 days (B) and 7 months (C). At each age, T2-weighted image sequences were performed with axial (top) and coronal (bottom) images shown. Brain MRI at 7 months showed progressive cortical volume loss with increased prominence of the lateral ventricles, consistent with loss of subcortical white matter volume compared to the prior study. Mild delay in myelination was apparent. (D) Diffusion weighted axial images identified restricted diffusion in the medial lemniscus tracts, bilaterally.

3.4.2 Phenotypic analysis

There was significant morbidity and mortality associated with biallelic *PIGQ* variants. Four of the seven patients died prematurely (St3a at 2 days of age, St3b at 5 years of age, St4 at 9 months of age, and St6 at 3 years and 9 months of age). A presumed affected older brother of St5 died a few hours after birth, but DNA was not collected so the relationship to the familial variants cannot be confirmed.

Abnormal prenatal findings included polyhydramnios (St2 and St4), prominent kidneys and premature rupture of membranes at 28 weeks (St3a), severe fetal hepatomegaly and hydronephrosis (St4) and enlarged lateral ventricles and hypoplastic cerebellar vermis suggestive of a Dandy Walker anomaly (St5). Neonatal complications were present in six patients, including respiratory distress (St2, St3a, St4, St5), jaundice (St3b, St5), heart failure (St3a), atrial ventricular defect (St3b), patent ductus arteriosus and patent foramen ovale (St5), hypoglycemia (St2) and feeding difficulties with irritability and limb hypertonia of the extremities (St2). St3a passed away at 2 days of life secondary to cardiac and renal failure.

Age at onset of epileptic seizures in the remaining six patients ranged from 2.5 to 7 months of age. Seizure types included focal tonic seizures (St1, St2 and St6, evolving to focal status epilepticus for St2 and St6), bilateral tonic-clonic (St2, St4, St5, St6) evolving to status epilepticus (St4, St6), myoclonic jerks (St3b, St5), epileptic spasms (St4), absence seizures (St1) and migrating focal seizures (St6) (Supplementary Table 3.2). Seizure outcome ranged from partially controlled with occasional breakthroughs with illness (St1, St2), to recurrent status epilepticus (St4, St6), daily focal seizures (St6) or daily clustered myoclonic jerks (St5). Seizures often clustered (St1, St3b, St5). Notably, St3b was seizure-free from four months

until age two years, but thereafter had seizures in cycles that would progressively worsen and taper off, with seizure-free periods of 7-12 days (Supplementary Table 3.2).

All six patients had a severe to profound GDD. Axial hypotonia was observed in all patients (Table 3.1, Supplementary Table 3.2). Appendicular hypotonia was observed in St2 and St5, whereas appendicular hypertonia was observed in the remaining patients. Severe head lag was observed in St2, St5 and St6. Stereotypic movements, opisthotonos, hyperkinetic movements, or random non-epileptic jerks were present in all patients (Supplementary Table 3.2).

Visual problems were diagnosed in all patients that survived the neonatal period. St3b, St4, St5 and St6 were diagnosed with cortical visual impairment. St1 had short fixation/tracking abilities, whereas an electroretinogram for St2 suggested impaired photoreceptor transmission in the retina. St4 had a mild unilateral conductive hearing deficit, whereas the other subjects had normal hearing (Supplementary Table 3.2).

Six of the seven patients had facial dysmorphisms including coarse facies and macroglossia. Four (St2, St4, St5 and St6) had cranial shape anomalies and three (St1, St2 and St3b) had pectus excavatum. Other findings included inverted nipples (St1), scoliosis (St2), delayed dentition (St2, St3b and St5), bilateral pulmonary interstitial emphysema (St3a), an accessory spleen (St3a), increased nuchal redundancy, short stature, hyperextensive interphalangeal joints and deep palmar and plantar creases (St4), and an enlarged pinna (St5) (Supplementary Table 3.2).

Cardiac anomalies were observed in six patients, including prolapsed mitral valve (St2), pulmonary stenosis (St5), pulmonary hypertension (St6), heart block and arrythmia (St2,

St3b, St4), and right ventricular hypertrophy with poor heart function (St3a, though hypertrophy was not found on autopsy) (Supplementary Table 3.2). Genitourinary issues included incontinence (St1, St2, St5, St6), bilateral hydronephrosis (St4, St5), renal stones with slightly enlarged kidneys (St4) and vesicoureteral reflux (St5). Autopsy of St3a revealed dilated/tortuous ureters with hypoplastic renal pelvis and calyces. Most patients had significant gastrointestinal issues including G-tube dependency (St2, St3b, St4, St5, St6), constipation (St1, St2, St6), volvulus (St4 and St5 had Ladd's procedure) and duodenal web (St5) (Supplementary Table 3.2).

EEG findings were in keeping with clinical presentations and ranged from normal findings early in the disease course, to burst-suppression patterns, background slowing with interictal multifocal sharp waves, hypsarrhythmia and ictal focal spike and slow wave complexes (Supplementary Table 3.3).

MRI findings showed no initial abnormalities in the cerebral cortex, but subsequent imaging showed progressive cortical volume loss (St4, Figure 3.1B/C; St5). There was poor or incomplete myelination or demyelination in four of the six subjects with available imaging study results (St1, St3b, St4, St5) (Supplementary Table 3.4). While St3a did not have brain imaging studies, an autopsy showed pyknotic nuclei of the cerebral cortex, as well as devitalization of the white matter with necrosis and karyorrhexis. There was a strongly positive glial fibrillary acidic protein signal and no striking anoxic changes, giving an overall impression of periventricular leukomalacia. Additional MRI findings included broad periventricular spaces (St1, St3b), prominent frontal horns of the lateral ventricles (St2), volume loss of the vermis (St3b, St5), dangling choroids (St5) and pituitary hypoplasia with preservation of the stalk (St5) (Supplementary Table 3.4). MRS showed borderline lactate

peaks (St2) and diffusion-weighted imaging (DWI) showed increased intensity in the bilateral medial lemniscus tracts (St4, Figure 3.1D) (Supplementary Table 3.4). Serum alkaline phosphatase levels were elevated in St3b, and intermittently elevated in St2 and St4.

3.4.3 Flow cytometry

In blood, both St4 and St5 had very low levels of FLAER and CD16 cell surface localization. In brief, granulocytes from St4 had only 6% the level of FLAER compared to normal while this marker in St5 was 35% (mean fluorescence intensity). For CD16, expression was 28% compared to normal for St4, and 20% in St5. CD55 and CD59 in St5 were normal whereas CD55 was decreased to 68% in St4. However, this patient has an increase in CD59 (Figure 3.2). Analysis of granulocytes by a clinical lab for St1 showed that the level of FLAER was 64.7% relative to the control.

For fibroblasts, levels of all markers were decreased in St3b and St5. St3b showed decreases in FLAER, CD73 and CD109 to 45%, 56% and 20%, respectively relative to control, and these markers in St5 were reduced to 45%, 28% and 20%, respectively (Figure 3.3). Analysis of CD59 expression in an independent lab showed a mean fluorescence intensity of 65.2% in St2-derived fibroblasts relative to the control (Supplementary Figure 3.2). While transduction with an empty lentivirus did not affect GPI-AP levels, a lentivirus expressing wildtype *PIGQ* completely restored GPI-AP expression in St3b, and there was partial rescue in St5 (FLAER, CD73 and CD109 were increased to 56%, 70% and 46% versus control) (Figure 3.3).

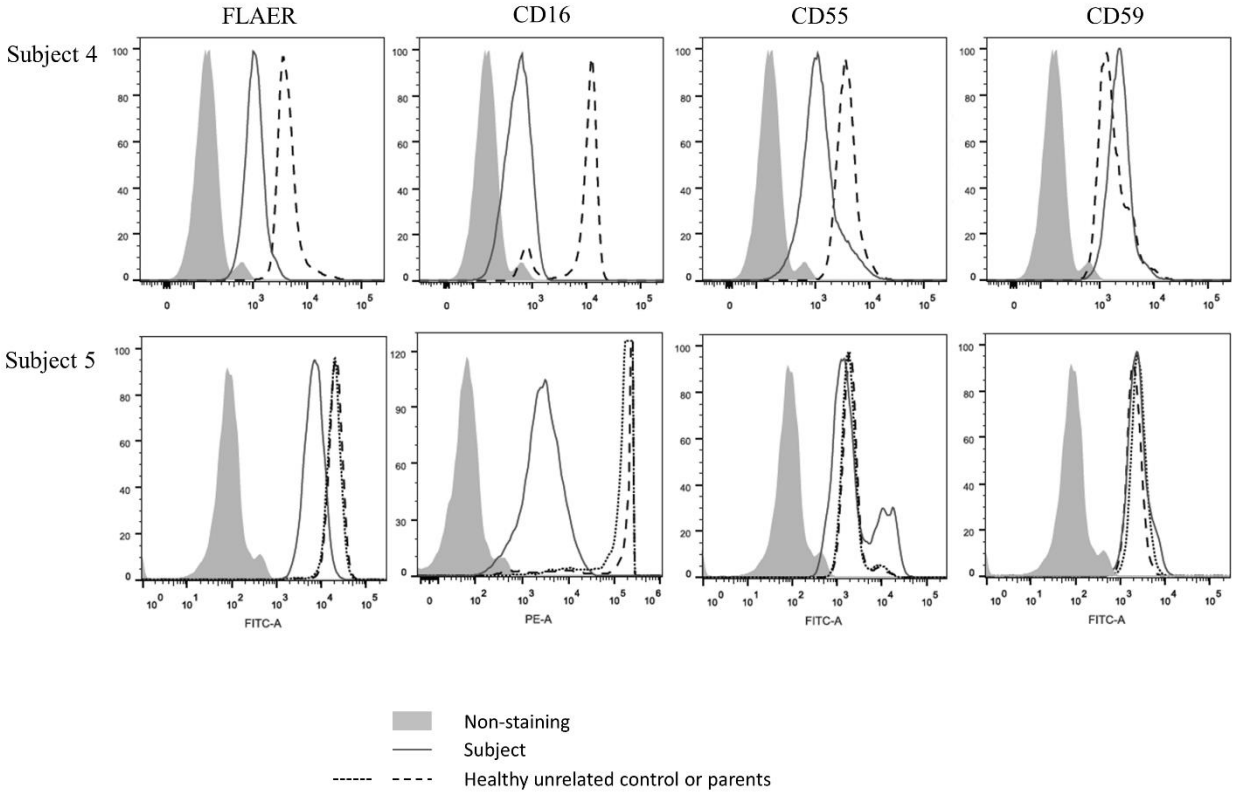
FLAER
CD16
CD55
CD59
Subject 4
Subject 5
FITC-A
PE-A
FITC-A
FITC-A
Non-staining
Subject
Healthy unrelated control or parents

Figure 3.2 Impact of the *PIGQ* variants on the expression of GPI-APs in granulocytes.

Flow cytometry analysis of granulocytes from fresh blood from subject 4 (top row) and subject 5 (bottom row) and compared to healthy controls and parents, respectively. Fluorescently labeled proaerolysin 'FLAER' directly binds the GPI-anchor, whereas CD16, CD55 and CD59 all stain for GPI-APs.

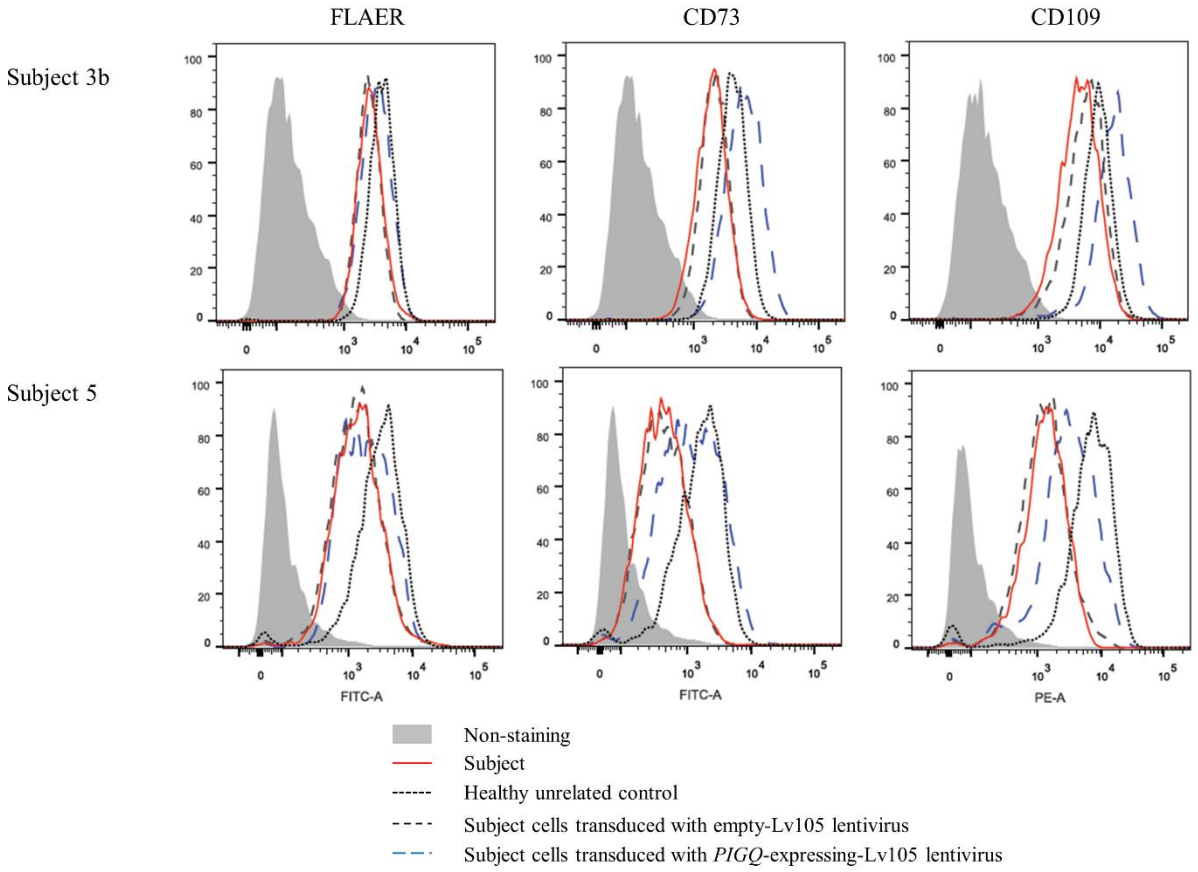
FLAER
CD73
CD109
Subject 3b
Subject 5
FITC-A
FITC-A
PE-A
Non-staining
Subject
Healthy unrelated control
Subject cells transduced with empty-Lv105 lentivirus
Subject cells transduced with PIGQ-expressing-Lv105 lentivirus

Figure 3.3 Impact of the *PIGQ* variants on the expression of GPI-APs in fibroblasts.

Flow cytometry analysis of fibroblasts derived from subject 3b (top row) and subject 5 (bottom row) and compared to healthy controls and parental derived cell-lines, respectively. Subject cell lines were further transfected with empty lentivirus or lentivirus expressing WT *PIGQ* cDNA. Fluorescently labeled proaerolysin 'FLAER' directly binds the GPI-anchor, whereas CD73 and CD109 stain for GPI-APs.

3.5 Discussion

This cohort of seven new individuals affected by biallelic pathogenic variants in *PIGQ* enables us to broaden the phenotypic spectrum of this rare condition (Table 3.1, Supplementary Table 3.2) and also to demonstrate the impact of *PIGQ* on GPI-anchored proteins.

Patients with biallelic *PIGQ* variants show a broad phenotypic spectrum including epileptic seizures, GDD, hypotonia, feeding difficulties, and multiple congenital anomalies (Table 3.1, Supplementary Table 3.2), clinical features also observed in other inherited GPI-deficiencies (IGDs) (104). Most affected individuals with biallelic *PIGQ* variants have delayed myelination, but generally lack gross structural lesions on MRI. Of note, while the affected individual reported by Starr *et al* (206) had significant left-sided ventriculomegaly, we did not observe this in our cohort. A limiting factor could be that our subjects generally underwent MRI before the age of 10 months and that a long-term follow-up of MRI findings was not available. Individuals with pathogenic variants affecting other genes in the pathway have shown development of both cerebral and cerebellar loss of tissue over time (176, 201).

While we also did not observe long bone radiolucent lesions as previously described (206), skeletal anomalies and delayed dentition were common. Of note, St4 and St5 had midgut volvulus requiring surgery, and St5 had a duodenal web requiring resection. Furthermore, our cohort showed a variety of cardiac issues, including arrhythmia and fatal heart block.

Seizure type and control were highly variable (Supplementary Tables 3.2 and 3.3). Martin *et al* reported a burst-suppression pattern on EEG and Ohtahara syndrome (154), which was not observed in subsequent patients, but has been reported in other IGDs (207), Two

patients developed epileptic spasms and St3b showed a recurrent pattern of seizure activity. Interestingly, St6 was diagnosed with epilepsy of infancy with migrating focal seizures (EIMFS), which is a very severe epileptic syndrome with poor outcome, previously known as malignant migrating partial seizures of infancy or Coppola-Dulac syndrome (208). The most common genetic cause of this syndrome is gain-of-function mutations in a gene encoding a potassium channel (*KCNT1*), but recently, in a cohort of 135 patients with EIMFS, two were found with *de novo* heterozygous pathogenic variants in *PIGA*, an X-linked gene involved in GPI-anchor biosynthesis, implicating this pathway in this particular epileptic syndrome (209). Presently, the downstream GPI-AP target(s) involved in the pathogenesis of IGDs remain unidentified.

St1, who was homozygous for the p.(R538Afs*24) variant, seems to have the mildest phenotype in our cohort. She is currently 11 years old and although she has chewing difficulties, she remains the only living patient who is not G-tube dependent. While she has limited fixing/tracking abilities, she is also the only patient without a cortical visual impairment. While she is homozygous for a frameshift in the last exon, it is unclear if this can explain her milder phenotype, as St6, with a more severe phenotype and who eventually died, had an even later frameshift p.(G557Dfs*4). This may be in part because St6 was born from consanguineous parents thus other recessive genes may be contributing, or there may not be a clear genotype-phenotype correlation. Indeed, even the two siblings in our cohort (St3a, St3b) had different clinical presentations and survived to two days and five years, respectively. Analysis of further affected individuals may reveal a genotype-phenotype correlation, and given that PIGQ is part of the N-acetylglucosamine complex, the protein location of the disease-causing variants may result in differential impact for the binding of other enzymes in

the complex. Compared to other IGDs, there are more often bi-allelic nonsense and/or frameshift variants in *PIGQ*, but there is also increased mortality (210). This might be because bi-allelic loss-of-function mutations in other GPI-biosynthesis genes lead to embryonic lethality, while it does not for *PIGQ*.

Previous studies have correlated variants in *PIGT*, another key component to GPI-biosynthesis, to preferential atrophy of the cerebellar vermis (175, 211-213), a finding found inconsistently in a subsequent cohort (201). Similarly, only two of our patients (St3b and St5) had MRI results showing atrophy affecting the cerebellar vermis, however, interestingly, an MRI of St5 at age 2 years found diffuse cerebral atrophy, but cerebellar atrophy was not appreciated. Given that variants in other genes in this pathway have been linked to cerebral and cerebellar loss of tissue over time, it is worth considering further imaging later in childhood.

Although serum alkaline phosphatase (ALP) has been linked with IGDs, evidence suggests that elevated ALP levels are most often associated with variants in later steps of GPI biosynthesis, whereas earlier steps are associated with ER-associated degradation of the anchor (177, 214). Thus, it is not surprising that elevated serum ALP is not common among subjects with *PIGQ* pathogenic variants.

Treatments remain limited, though butyrate helped treat intractable epilepsy due to variants in the *PIGM* promoter (215), and IGDs due to variants in *PIGV*, *PIGO* and *PIGS* have been partially treated with vitamin B6 supplementation (172, 216, 217). In St6, there was phenotypic overlap with cerebral folate deficiency due to *FOLR1*-mutations (197), in which the GPI-anchored folate receptor alpha fails to provide folate to the brain. This can be by-

passed by providing folinic acid supplementation, however, unfortunately, St6 did not respond to this therapy, though it should be noted it was initiated late in his disease course.

Given the function of the proteins involved in GPI-anchor biosynthesis, the gold standard for evaluation of functional defects in this pathway is using flow cytometry to assess the effect of the variants on GPI-anchored proteins (172). In granulocytes from fresh blood and fibroblasts, we show reduced expression of GPI-anchored proteins in five unrelated affected individuals, a phenotype that was partially or fully reversible in fibroblasts by transfecting WT cDNA. Taken together with previous work on CHO cells, we show that biallelic *PIGQ* variants impact GPI-AP expression.

In summary, we expand the phenotypic spectrum of IGDs related to biallelic *PIGQ* pathogenic variants and show that the impaired expression of GPI-APs in human cells can be improved *in vitro* by the transduction of WT *PIGQ* cDNA. These variants lead to impaired GPI-biosynthesis and subsequently reduced localization of GPI-APs, resulting in a broad phenotypic spectrum. While the phenotypic spectrum is broad, the clinical overlap of IGDs is significant, and collectively they may represent as much as 0.15% of all developmental disorders (218). Thus, there is a need for future work to develop therapies that reduce the impact of these devastating diseases (195).

3.6 Supplementary materials

Supplementary methods

Patient recruitment

Subject 1 (St1) was recruited by the EuroEPINOMICS Rare Epilepsy Syndromes (RES) consortium. Subject 2 (St2) was recruited by the DuPont Hospital for Children/Nemours and the Children's Hospital of Philadelphia. Ethics approvals were obtained from the local institution review boards and informed consent was obtained from patients´ parents.

Subject 3a, 3b and 4 (St3a, St3b, St4) were recruited as part of a Care4Rare Canada research study, which was approved by the Children's Hospital of Eastern Ontario Research Ethics Board (REB #11/04E).

For subject 5 (St5), oversight for the human subjects research protections was provided by the institutional review board (IRB) of the National Human Genome Research Institute (protocol 15-HG-0130, Clinical and Genetic Evaluation of Patients with Undiagnosed Disorders through the Undiagnosed Diseases Network) and the Duke University School of Medicine IRB (Pro00056651).

Subject 6 (St6) was recruited as part of the Swedish MIDIC (Mitochondrial Disease in Children) study, reviewed by the local Ethical Review Board in Lund (protocol #2009/97; amended #2017/266).

Sequencing methods

Primers used for Sanger sequencing validations are listed in Supplementary Table 3.1. Exome sequencing details for each patient/family are as follows:

St1

Exome sequencing was performed on an Illumina HiSeq2000 by BGI-Europa, after exome enrichment with the Agilent SureSelectXT Human All Exon 50Mb Kit using blood-derived DNA from the patient and both parents. Read alignment was performed with Burrows-Wheeler Aligner (219), and variant calling using GATK (220), with annotation performed by the Department of Genetics of the Radboud University Medical Center with an in-house developed program. The variants in genes were selected based on possible pathogenicity (deletions, insertions, nonsense and canonical splice site mutations and missense mutations (PhyloP score base change >3.5)). Variants were confirmed by Sanger sequencing (Supplementary Table 3.1).

St2

Exome sequencing was performed on an Illumina HiSeq2000 by GeneDx, after exome enrichment with the Agilent SureSelect XT2 All Exon V4 kit using blood-derived DNA from the patient and both parents. The DNA sequence compared to human genome build GRCh37 (hg19) reference sequence. The targeted coding exons and splice junctions of known protein coding RefSeq genes were assessed. The Xome Analyzer was used to evaluate sequence changes of the proband relative to the parents. Variants were confirmed by Sanger sequencing (Supplementary Table 3.1).

St3a and St3b

Exome sequencing was performed on an Illumina HiSeq2000, after exome enrichment with the Agilent SureSelect Clinical Research Exome kit using blood-derived DNA from the proband (St3b) and both parents. A pipeline based on Burrows-Wheeler Aligner (219), Picard (http://broadinstitute.github.io/picard/), ANNOVAR (221) and custom annotation scripts was used. The GRCh37 (hg19) human reference genome assembly was used for alignment. Variants were compared to the 1000 genomes phase 1 data set (April 2012 release)(186), the Exome Variant Server (http://evs.gs.washington.edu/EVS/), ExAC (222), and an in-house database of ~2000 exomes previously sequenced at the McGill University and Génome Québec Innovation Centre. Variants with greater than 1% frequency in any database were excluded from further analysis. Variants were confirmed by Sanger sequencing (Supplementary Table 3.1), and DNA from the sibling, St3a, was subsequently Sanger sequenced to confirm the presence of the variants.

St4

Exome sequencing was performed at Prevention Genetics as per their protocol (https://www.preventiongenetics.com/ClinicalTesting/TestCategory/PGxome.php) using blood-derived DNA from patient and both parents. The GRCh37 (hg19) human reference genome assembly was used for alignment. Bam files were analyzed using SAMtools mpileup (223), Freebayes *(*arXiv preprint arXiv:1207.3907), Platypus (224) and GATK-haplotype (225) to identify single nucleotide variants and short insertions or deletions (indels). Variants were further analyzed if identified in $\geq$2 programs. Variants were annotated using Ensembl variant effect predictor (226) and the ENSEMBL/Gencode gene set, and annotated with VEP using the Refseq gene set (227) and GEMINI framework (228). Variants that were previously

detected in more than 20 of local control samples and/or have had a minor allele frequency greater than 1% in the 1000 genomes/ ESP/ NHLBI exome database and/or those identified in one or more NHLBI exomes and had been called with a homozygous genotype were excluded. Clinical significance of the remaining variants was assessed using Alamut Visual in accordance with ACMG recommendations (229). All rare variants were checked for prior reports in the literature, the ClinVar, ExAC, Exome Variant Server databases and other relevant sources of information. Variants were confirmed by Sanger sequencing (Supplementary Table 3.1).

St5

Exome sequencing and data analysis was performed at Baylor Genetics following their standard protocol (https://www.bcm.edu/research/medical-genetics-labs/test_detail.cfm?testcode=1600) using blood-derived DNA from the patient and both parents. Variants were confirmed by Sanger sequencing (Supplementary Table 3.1).

St6

Exome sequencing was performed on an Illumina HiSeq2500, after exome enrichment with the Agilent SureSelect Clinical Research Exome kit using blood-derived DNA from the patient and mother. Bioinformatic analysis was performed using an in-house Mutation Identification Pipeline (MIP) (230). Variants were filtered using an epilepsy panel using version six of our database (https://www.karolinska.se/for-vardgivare/karolinska-universitetslaboratoriet/centrum-for-medfodda-metabola-sjukdomar/genetisk-diagnostik/). Variants were confirmed by Sanger sequencing (Supplementary Table 3.1).

Clinical descriptions

St1

Subject 1 was the third child to non-consanguineous healthy Turkish parents with an unremarkable family history. She was born at 38 weeks and 2 days gestation following an uncomplicated pregnancy and delivery and weighed 3420g (65.5%). She met early developmental milestones however her development plateaued at 6 months of age, coinciding with the onset of seizures. Currently, at 11 years of age, she continues to have intermittent seizures of multiple semiology including focal, tonic, bilateral tonic-clonic, with impaired awareness, but no classical absences. These tend to be clustered and often precipitated by fever. She sometimes has long seizure-free intervals (months) between episodes. She is currently treated with carbamazepine, phenobarbital and clobazam. She has severe developmental and intellectual disability; she makes few sounds and is unable to ambulate independently. She has some purposeful hand movements and can sit independently for brief periods when placed in position. She can fix and follow intermittently. She is incontinent of urine and stool and has difficulties with constipation, swallowing and sleep. She has stereotypies including, shaking of her head, closure of her eyes, rolling of her eyes, intermittent groaning and hyperventilation. She has abnormal movements including, dystonic posturing of her left foot, choreatic movements of her hand and on examination has axial hypotonia, limb hypertonia, ankle contractures and brisk deep tendon reflexes. She is non-dysmorphic and has strabismus, pectus excavatum, inverted nipples and hip dysplasia.

Exome sequencing demonstrated a homozygous *PIGQ* variant: Chr16(GRCh37):9.632962del; NM_148920.2:c.1611del, p.R538Afs*24. Clinical flow cytometric analysis confirmed that the GPI anchor is involved, with a mean fluorescence

intensity (FLAER) of granulocytes of 22249 versus 34385 in the control (64.7%) (histogram not available).

St2

Subject 2 was the second child to a healthy non-consanguineous couple of European and Puerto Rican descent. The patient's parents had a prior early trimester miscarriage and a healthy daughter; there was also a paternal half-sibling. The pregnancy was complicated by polyhydramnios and elevated alpha-fetoprotein (AFP) on maternal serum screening. Routine anatomy ultrasound was normal. Given the prenatal findings, an amniocentesis was performed showing normal female karyotype. She was born at 38 weeks gestation, weighing 4850g (99.9%). Issues during the neonatal period included the need for CPAP respiratory support, intermittent hypoglycemia and she failed the newborn hearing screen (left ear). Following discharge, her parent's initial concerns were global developmental delay.

At age 7 months of age she developed focal seizures with secondary generalization. Seizures were well controlled on topiramate and levetiracetam with occasional breakthrough seizures with illness. She had a brain magnetic resonance imaging (MRI) which showed slightly diminutive frontal lobes and slightly prominent frontal horns of the lateral ventricles but was an otherwise unremarkable contrast-enhanced MRI of the brain. Magnetic resonance spectroscopy (MRS) of the brain showed a borderline lactate peak identified in nearly all the voxels placed over the basal ganglia (Supplementary Table 3.4).

At last assessment (6 years, 6 months of age), she had chronic static encephalopathy with global developmental delay and severe intellectual disability. She was G-tube dependent with chronic constipation. She had respiratory insufficiency with bilevel positive airway pressure (BPAP) dependence, neuromuscular scoliosis and pectus excavatum. She had

frequent hospitalizations for respiratory illnesses leading to acute respiratory failure. During one hospitalization for respiratory infection she developed hyperkinetic involuntary movements without correlate on electroencephalogram (EEG) which resolved with clinical improvement (Supplementary Table 3.3). She was also found to have subglottic stenosis requiring laryngeal dilation. Echocardiogram showed prolapsed mitral valve with mild left ventricular dysfunction and an electrocardiogram (ECG) showed 1st degree AV block. She is legally blind and electroretinograms (ERG) performed at 1 and 4 years of age suggested a transmission problem at the level of the photoreceptor-bipolar cell synapse in the retina. At age 3 ½ years of age she developed an episode of rhabdomyolysis.

She was evaluated by Clinical Genetics and Metabolism over several years. She was noted to have dysmorphic facial features with somewhat coarse appearance, gingival hyperplasia, midface hypoplasia, wide mouth, thickened lips, thick eyebrows and prognathism (Supplementary Figure 3.1). Investigations were non-diagnostic including chromosomal microarray, Noonan syndrome panel, acylcarnitine profile, plasma amino acids, lactate/pyruvate ratio, carbohydrate deficient transferrin via mass spec matrix-assisted laser desorption/ionization time-of-flight (MALDI-TOF) and clinical exome sequencing. Reanalysis of clinical exome revealed two variants in *PIGQ*: NM_148920.2:c.1199_1201delACT, p.Y400del (maternal) and NM_148920.2:c.942+1G>A, IVS4+1G>A (paternal)). The average depth of coverage for the analysis was 167x, with a quality threshold of 98.8%. 100% of the coding region of the *PIGQ* gene was covered at a minimum of 10X in the XomeDx test.

Additional variants of uncertain significance reported as possibly related to the phenotype of failure to thrive, hypotonia, seizures and developmental delay, but which were clinically not thought to explain the phenotype included maternally inherited VUS in *ATP5A1*

c.171G>T, p.E57D and paternally inherited VUS in *EFHC1* c.694C>T, p.L232F. In silico analysis was inconsistent in its predictions as to whether these variants are damaging to the protein structure/function.


IN THE SAME
LANGUAGE

Supplementary Figure 3.1: Photographs of patient St2.

Patient St2 shows dysmorphic facial features with somewhat coarse appearance, midface hypoplasia, wide mouth, thickened lips, thick eyebrows and prognathism.

St3a and 3b

Subjects 3a and 3b were sisters. Their parents were healthy, non-consanguineous and of British and French-Canadian ancestry. They had an older healthy brother and the remainder of the family history was non-contributory.

Anatomy ultrasound for Subject 3a showed prominent fetal kidneys at 26 weeks gestation. She was the product of a healthy early pregnancy later complicated by premature rupture of membranes at 28 weeks gestation, with a birth weight of 1344g. APGAR scores were 6 and 7. During the immediate neonatal period she developed respiratory distress requiring intubation and renal failure. She passed away on day 2 of life. Physical examination revealed minor dysmorphic facial features including down-slanting palpebral fissures, hypertelorism and flattened nasal bridge. Post-mortem autopsy showed tortuosity of the ureters with hypoplasia of the renal pelvis and calyces and an accessory spleen. The brain showed evidence of periventricular leukomalacia. Karyotype was normal female.

Subject 3b was born at born at term after an uncomplicated pregnancy. She weighed 3.5 kg (75%) with no resuscitation required. She developed jaundice on day two of life which responded to phototherapy. She was discharged home on day of life 3. Parents first became concerned about her development just before three months of age. She had central hypotonia, increased peripheral tone and dysconjugate gaze. She was evaluated at 4 months of age for the question of seizures however EEG was normal (Supplementary Table 3.3) and MRI showed increased CSF spaces (Supplementary Table 3.4). Eye examination at 5 months of age showed cortical visual impairment. During infancy, hypotonia evolved into spasticity and dystonia. She required G-tube feeds. At the age of two years she presented again with episodes concerning for seizures and EEG confirmed seizure activity in the right temporal lobe (Supplementary Table 3.3). The seizures proved to be refractory to multiple anticonvulsants.

She developed progressive microcephaly; OFC as a neonate was at the 70th centile and 3rd centile at the age of 4 years. She had delayed dental eruption and gingival hyperplasia but was otherwise non-dysmorphic. She developed first-degree AV block and continued to be followed for this for several years with no intervention required.

She was followed by the Genetics and Metabolics services and investigations were non-diagnostic including chromosomal microarray, enzymology for Krabbe disease, Metachromatic Leukodystrophy and Niemann-Pick A, and muscle biopsy and fibroblast studies for Pallister-Killian syndrome.

At 5 years of age she developed increasing discomfort with feeds of unknown etiology. She subsequently developed increased work of breathing and had two episodes of asystole and was unable to be revived from the second episode. Exome sequencing had been initiated prior to her passing. It revealed two variants in *PIGQ*: NM_148920.2:c.1578_1579delCC, p.Q527Afs*75, (maternal) and NM_148920.2:c.1199_1201delACT, p.Y400del (paternal). The *PIGQ* variants were confirmed by Sanger sequencing in the DNA sample from Patient 3a.

A heterozygous VUS in *PKDH1* (c.12133G>T, p.G4045W) was also identified but was not considered likely to explain the clinical presentation.

St4

Subject 4 was the first child to non-consanguineous Lebanese and Iraqi ancestry parents. Prenatal history included maternal Remicade exposure until 17 weeks gestational age when mother became aware of the pregnancy. Pregnancy was complicated by severe polyhydramnios, first noted at 28 weeks gestation, requiring multiple amnio reductions and severe fetal hepatomegaly (liver extending into iliac crest). Antenatal testing included a normal chromosomal microarray and no serological evidence for an intrauterine infection. Mild

bilateral hydronephrosis was noted at 35 weeks gestation. She was born via uncomplicated C-section at 36+3 weeks gestation with APGARS of 8 and 9. Her birthweight was 3389 g (96%ile), birth length was 47.5cm (68.2%ile) and head circumference was 33.5 cm (84%ile). Neonatal abdominal ultrasound revealed intestinal malrotation (surgically corrected by a Ladd procedure on the first day of life). She was grossly hypotonic and significantly dysmorphic at birth with coarse facial features, increased nuchal fold, macroglossia, wide nasal bridge with a short-upturned nose, clenched hands with deep palmar and plantar creases and an impression of rhizomelic shortening. She was also noted to have hepatomegaly, a soft palate cleft and inverted nipples. She did not blink to visual threat however ophthalmological examination was structurally normal. Deep tendon reflexes were diffusely brisk (3+) and her appendicular tone was increased with episodes of extensor posturing of her upper extremities noted. An awake EEG revealed episodic slowing of background cerebral activity with intermittent asynchrony (Supplementary Table 3.3). Several of the posturing episodes were captured which were not associated with any electrographic changes noted; felt to be clinically consistent with dystonia. MRI of the brain revealed no intracranial abnormalities (Supplementary Table 3.4). Echocardiogram was reassuring although she had significant arrhythmic episodes in the first week of life.

Baseline investigations including serum creatine kinase, lactate alanine aminotransferase (ALT), acylcarnitine profiles were normal. Very long chain fatty acids (VLCFA) were normal. Enzyme (WBC) testing for beta-glucosidase, beta-galactosidase were negative. Plasma amino acids and urine organic acids were normal.

Due to feeding issues and failure-to-thrive, a gastrostomy tube was placed at 6 weeks old. She was re-admitted to hospital at 3 months old with *Klebsiella* pneumonia. Supplemental oxygen was required from which she could never be fully weaned. Central apneas were noted

during sleep and repeat echocardiogram at 3 months' old noted mild right ventricular hypertrophy and pulmonary hypertension. Repeat awake EEG at 4 months old showed generalized slowing of background activity (Supplementary Table 3.3).

Over subsequent months, she demonstrated no neurodevelopmental gains. At 6 months old she demonstrated no head control and no social smile. Her eye movements were dysconjugate and she was unable to visually fixate or track consistent with cortical blindness. Her hands were closed at rest. Her head circumference was 41.0 cm (10%). Appendicular tone was increased with brisk reflexes and sustained ankle clonus.

Repeat MRI brain at 7 months old revealed progressive cortical and subcortical volume loss (Figure 3.2, Supplementary Table 3.4) with a mild delay in myelination reported. Restricted diffusion was seen in the brainstem (Figure 3.2) corresponding to the location of the medial lemniscus tracts, bilaterally. No restricted diffusion was apparent elsewhere and MR spectroscopy was normal. Evoked potentials were performed at 7 months old. Visual evoked potentials revealed no cortical responses. Brainstem auditory evoked potentials revealed no response on the right and low amplitude and prolonged absolute and interpeak latencies on the left. EEG at 7 months old revealed hypsarrhythmia and bursts of generalized polyspike and wave discharges (Supplementary Table 3.3). Several decremental events were captured which were clinically associated with subtle shoulder elevation, clinically consistent with epileptic spasms. Vigabatrin therapy was initiated. Within 2 weeks she was admitted to the pediatric intensive care unit (PICU) with episodes of autonomic dysfunction characterized by intermittent bradycardia, apneic episodes, hypoxia and hypothermia requiring intubation. No viral or bacterial infection could be identified. Muscle biopsy was performed during this admission which was unrevealing. mtDNA sequencing revealed no pathogenic variants. During her first week of ICU admission she developed an episode of sustained ventricular

tachycardia treated with amiodarone. Repeat echocardiogram confirmed good biventricular function. Once a genetic diagnosis was made, her parents requested palliation and she died at 9 months of age.

Following unrevealing clinical exome sequencing, a re-analysis was performed under the Care4Rare Canada research protocol and revealed compound heterozygous mutations in *PIGQ*: NM_148920.2:c.1130_1168del, p.A377_S389del (maternal) and NM_148920.2:c.1345G>C, p.G449R (paternal).

St5

Subject 5 was the fifth pregnancy to healthy, non-consanguineous parents of Mexican ancestry. The couple had a history of a son who died shortly after birth, at 9 hours of life. He was born via C-section due to being large for gestational age and had abdominal distention and brain abnormalities noted birth; however, details are limited. The couple also had two healthy daughters. The patient was born following a pregnancy that was complicated by abnormal ultrasound findings during the second trimester that included right ventricular hypertrophy, lateral ventricles at 8mm with dangling choroids, hypoplastic inferior cerebellar vermis, leading to impression of a Dandy Walker variant, bilateral urinary tract dilation and ambiguous genitalia. He was born via a C-section at 37 weeks due to being large for gestational age and weighed 4519g (98.5%) at birth with normal APGAR scores. He spent 13 days in the NICU due to respiratory distress, jaundice and hypoglycemia. During his stay in the NICU, he was diagnosed with a patent ductus arteriosus (PDA), patent foramen ovale (PFO), mild right ventricular hypertrophy, and bilateral hydronephrosis with reflux and a connection of the distal ureters to the posterior urethra.

Concerns about his development began shortly after birth and currently at the age of 26 months he has not made neurodevelopmental gains. He has no gross or fine motor skills and is unable to smile, laugh or track objects. He was found to have cortical visual impairment at 10 months of age. Initial EEG and brain MRI were normal. However repeat EEG in infancy showed multifocal spikes and sharp waves with background slowing consistent with epileptic potential (Supplementary Table 3.3). He has multiple seizures daily. A repeat brain MRI at 24 month showed abnormal myelination characterized by increased T2 signal in the peripheral and periatrial white matter, pituitary hypoplasia, diffuse cerebral volume loss, and abnormal skull shape with right plagiocephaly (Supplementary Table 3.4). He experiences abdominal distension and feeding intolerance that required G-tube placement.

Previous nondiagnostic testing included plasma amino acids, urine organic acids, total and free carnitine, acylcarnitine profile, urine MPS screen, 7-dehydrocholesterol, BWS methylation testing, VLCFA, karyotype, Fragile X, and chromosomal microarray.

He was enrolled in the Undiagnosed Diseases Network (UDN) at 23 months of age. On exam he was found to have dysmorphic features including course facies, large ears, and open mouth with protruding, large tongue. He has no meaningful social interactions, his hands were primarily fisted, did not fix/track, and had profound axial and limb hypotonia with significant head lag. Trio whole exome sequencing through the UDN identified two variants in trans in the *PIGQ* gene: NM_148920.2:c.49G>A, p.G17R (maternal) and NM_148920.2:c.942+1G>A, IVS4+1G>A (paternal).

VUSs included a maternally inherited heterozygous variant in *KMT2D* (c.15736A>G, p.I5246V), a paternally inherited heterozygous variant in *LZTR1* (c.370G>A, p.V1241), and he was compound heterozygous for the variants c.868A>G, p.S290G (maternal) and

c.2891C>A, p.T964N (paternal) in *ASTN1*. These variants were ruled out due to phenotype incompatibility, benign predicted pathogenicity or inheritance.

St6

Subject 6 was the only child to a consanguineous Afghani couple (first-cousin union). The pregnancy was unremarkable with routine prenatal care. The delivery was complicated by failure to progress requiring vacuum-assist at term. He was born at 40+1 weeks, with a birthweight of 2.94 kg (19.3%). APGAR scores were 8 and 9. There were no immediate neonatal concerns and he was discharged home. During the first week of life, he developed feeding difficulties and irritability and at 3 weeks of age he developed opisthotonos when crying, central hypotonia, appendicular hypertonia and spasticity with clenched hands. He had coarse facial features but was otherwise non-dysmorphic. An MRI scan completed at the time was normal (Supplementary Table 3.4). Metabolic investigations including ammonia, lactate, plasma and urine amino, urine organic acids, acylcarnitine profile, water soluble vitamins, glycoconjugates in urine and cerebrospinal fluid analysis (cells, lactate, pyruvate, amino acids, protein, albumin) were all normal.

At 2.5 months he was hospitalized after a suspected seizure with eye deviation towards the upper left corner and an increased tone in all extremities. EEG at this time was normal and as was a repeat MRI of the brain (Supplementary Tables 3.3 and 3.4). He thereafter showed a profound stagnation of development making no meaningful gains. His clinical seizures continued and at 6 months of age an EEG showed asymmetry with sharp-waves on the left hemisphere and rhythmic sequences up to 30 seconds in keeping with electrographic seizures (Supplementary Table 3.3). He was started on phenobarbital, topiramate and levetiracetam with initial improvement. Seizures re-occurred again at one year of age with focal seizures

from both hemispheres and the EEG, consistent with the diagnosis of epilepsy of infancy with migrating focal seizures (Coppola-Dulac syndrome) (Supplementary Table 3.3). At this time he also had a G-tube inserted for feeding. Benzodiazepines and valproate were added in conjunction to his other anti-epileptics; however, from the age of 1-2.5 years seizures were refractory. He has repeated respiratory infections leading to chronic respiratory insufficiency and at the age of 3 years and 9 months, he died from complications secondary to pneumonia. Autopsy was declined.

Exome sequencing of the patient and his mother revealed a homozygous *PIGQ* variant: NM_148920.2:c.1670del, p.G557Dfs*4. The average depth of sequencing was 330X for the patient and 263X for the mother.

Only one other mutation of potential significance was noted after the filtering process. This was a heterozygous mutation in *SPTAN-1* (c.6503C>T, p.A2168V), which was benign by PolyPhen2 and exists in low frequency in population databases. As only the mother's DNA was available, it is not known whether this variant is *de novo* or inherited from the father.

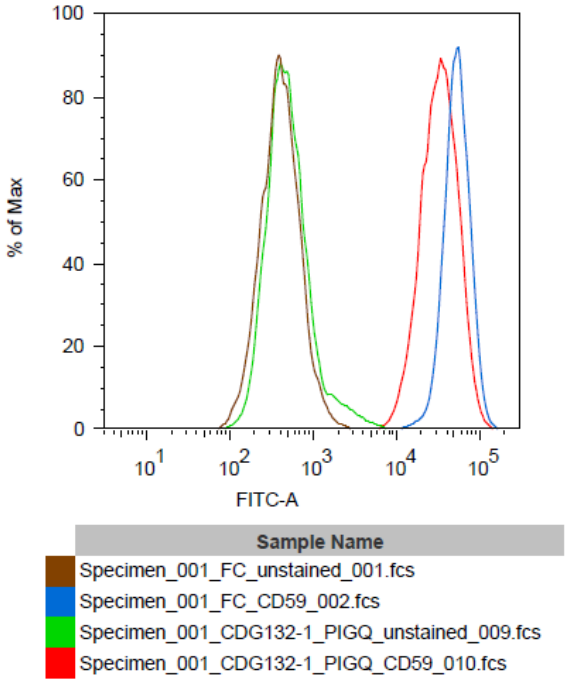
100
80
60
40
20
0
% of Max
10^1
10^2
10^3
10^4
10^5
FITC-A
Sample Name
Specimen_001_FC_unstained_001.fcs
Specimen_001_FC_CD59_002.fcs
Specimen_001_CDG132-1_PIGQ_unstained_009.fcs
Specimen_001_CDG132-1_PIGQ_CD59_010.fcs

Supplementary Figure 3.2 Flow cytometry histogram of fibroblasts from St2 relative to control.

FITC-CD59 stained fibroblasts from St2 (red) relative to control (blue).

Supplementary Table 3.1 Primers used for Sanger sequencing confirmation of exome sequencing results.

Variant	Forward Primer (5'-3')	Reverse Primer (5'-3')
c.1611del; p.R538Afs*24	ATGTCTGAGACAGCACTGGC	CCAGCAGTTCCCTCAGTCCT
c.1578_1579del; p.Q527Afs*75	GAGCTCAGACCACCCCACT	TTCCCTCAGTCCTGCTTGTC
c.1199_1201del; p.Y400del	CTTCGTGGAGCACATCCTTT	CGCAGAACGTTCCACTTCTT
c.1130_1168del; p.A377_S389del	CTGTGTGTGTGAGGGTTGTG	CCCACCTGGCTCCATAGAC
c.1345G>C; p.G449R	CTGCTACTGGGACTGCTTCT	GTGCTCAGCTCACCAGGG
c.942+1G>A; IVS4+1G>A	CCTTCTCCATCCCCCTCTG	CCTGGAGTTCCTGCTTCTGG
c.49G>A; p.G17R	AGCCGAGCCTCTCCTCTTCT	CTGCGGAAGAGCACCTCACT
c.1670del; p.G557Dfs*4	Not available	Not available

Supplementary Table 3.2 Detailed clinical features of seven novel patients from six families with biallelic variants in PIGQ and review of the literature.

Abbreviations**:** DD (developmental delay), GFAP (glial fibrillary acidic protein), ID (intellectual delay), N/A (not applicable or not available), PDA (patent ductus arteriosus), PFO (patent foramen ovale). Centiles expressed according to WHO scale and corrected for prematurity where applicable.

Subject ID/Source	**St1 (this report)**	**St2 (this report)**	**St3a (this report)**	**St3b (this report)**	**St4 (this report)**	**St5 (this report)**	**St6 (this report)**
Variants & Inheritance (NM_148920.2)	Homozygous: c.1611del p.R538Afs*24	Maternal c.1199_1201del p.Y400del Paternal: c.942+1G>A IVS4+1G>A	Maternal: c.1578_1579del p.Q527AfsX75 Paternal: c.1199_1201del p.Y400del	Maternal: c.1578_1579del p.Q527AfsX75 Paternal: c.1199_1201del p.Y400del	Maternal: c.1130_1168del p.A377_S389del Paternal c.1345G>C p.G449R	Maternal: c.49G>A p.G17R Paternal: c.942+1G>A IVS4+1 G>A	Homozygous: c.1670del p.G557Dfs*4
Gender	Female	Female	Female	Female	Female	Male	Male
Ancestry	Turkish	European/Puerto Rican	British Isles/French Canadian	British Isles/French Canadian	Lebanese/Iraqi	Mexican	Afghani
Consanguinity?	No	No	No	No	No	No	Yes, cousins
History of miscarriages	Yes 1	1 early trimester loss	No	No	No	Yes 1	No
Affected siblings	None	None	St3b	St3a	None	Yes, older brother who passed away at 9 hours old	None
Unaffected siblings	2 older, healthy brothers	Full sister and paternal half- sister	11 year old sibling healthy	11 year old sibling healthy	None	2 healthy older sisters	None
Prenatal issues or findings	None	Elevated AFP on maternal serum screening, polyhydramnios, amniocentesis performed with normal 46,XX karyotype.	U/S 26 weeks showed prominent kidneys. Premature rupture of membranes and delivery at 28 weeks.	None	Severe fetal hepatomegaly (to iliac crest) and hydronephrosis at 29+6 weeks gestation; maternal Infliximab use until 17 weeks gestation. Severe polyhydramnios.	Prenatal ultrasound during second trimester noted RVH, and lateral ventricles at 8mm with dangling choroids, hypoplastic cerebellar vermis, inferiorly leading to impression of Dandy Walker Variant, bilateral urinary tract dilation, and ambiguous	None

Subject ID/Source	St1 (this report)	St2 (this report)	St3a (this report)	St3b (this report)	St4 (this report)	St5 (this report)	St6 (this report)
						genitalia. Also noted to be LGA.	
Polyhydramnios	-	+	-	-	Severe	-	-
Gestational period	38 weeks 2/7 days	38 weeks 0/7 days	28 weeks 1/7 days	41 weeks 4/7 days	36 weeks 3/7 days	37 weeks 3/7 days	40 weeks 1/7 day
APGAR scores	Normal	Unavailable	6 and 7	9 and 9	7 and 9	8 and 8	8 and 9
Neonatal complications	None	Required CPAP respiratory support, hypoglycemia, failed newborn hearing screen in left ear.	Significant respiratory distress requiring intubation and ventilation. Cardiac failure with subsequent renal failure and death at 2 days of life.	Admitted to hospital for 3 days for hyperbilirubinemia. Secundum atrial ventricular defect detected after birth.	Received antenatal steroids 2-24 hours prior to delivery. Was holding breath, given CPAP at 1 minute	Feeding difficulties, respiratory distress, jaundice, PDA/PFO.	Feeding difficulties, irritability, extremity hypertonia.
Birth weight	3420 g (65.5%)	4.85 kg (99.9%)	1344 g (91.5% corrected)	3560 g (75.6%)	3389 g (96%)	4519 g (98.5%)	2.94 kg (19.3%)
Birth height	N/A	52 cm	38.5 cm (71.2% corrected)	51 cm (84%)	47.5 cm (68.2%)	50.8 cm (68.6%)	46 cm (2%)
Birth head circumference	N/A	unknown	26.5 cm (68.1% corrected)	34.5 cm (70%)	33.5 cm (84.1%)	36 cm (88.7%)	33.3 cm (18%)
Age at last follow-up	8 years	6 years, 6 months	2 days	4 years 4 months	8 months (passed away)	2 years 2 months	3 year 7 months (deceased)
Weight	24 kg (39.7%)	18.4 kg (16.4%)	1460 g	14.4 kg (13.3%)	5.39 kg (<0.1%)	11.4kg (20.2%)	18.4 kg (91.2%)
Height	125 cm (39.4%)	109 cm (4.5%)	38.5 cm	88 cm (<0.1%)	N/A	81 cm (0.7%)	105.5 cm (89.5%)
Head circumference	51.5 cm	50 cm	26.5 cm	47 cm (3.6%)	N/A	46 cm (3.4%)	46 cm (0.3%)
Current age	11 years	6 years 6 months	Deceased 2d	Deceased 5y	Deceased 9m	2y2m	Deceased 3y9m
DD/ID	Severe DD/ID (makes sounds, does not understand simple tasks, grabs objects and brings them to her other hand, is able to sit for a short time, able to roll to her flank, not able to walk).	Severe DD/ID – chronic static encephalopathy	N/A (death at 2 days)	Global developmental delay, no walking, sitting or rolling over, very little head control.	Severe DD/ID, failure to thrive.	Profound global developmental delays (does not have head control, sit up, hands clenched, does not track or fix).	Profound global ID (no track or fix, no language, no head control, cannot sit or roll).
Seizures?	Yes	Yes	N/A	Yes	Yes	Yes	Yes
Seizure onset	6 months	7 months	N/A	Almost 4 months	7 months	6 months	2.5 months
Seizure types	Tonic seizures and seizures during which she turns her eyes upwards and does not react to her surrounding	Focal status epilepticus, generalized tonic-clonic	N/A	Myoclonus. hand extends, full body shifting, nystagmus and 4 limb shakes.	Epileptic spasms, status epilepticus	Myoclonic jerks and generalized tonic clonic seizures.	Initially tonic seizures with eye deviation. Then status epilepticus. Thereafter epilepsy of infancy with migrating focal seizures.

Subject ID/Source	St1 (this report)	St2 (this report)	St3a (this report)	St3b (this report)	St4 (this report)	St5 (this report)	St6 (this report)
Seizure control	Seizures are clustered, mostly during episodes of fever. In between a period of several months without seizures (from the outside).	Controlled on medication, breakthroughs with illness	N/A	No seizures 4 months>2 years. Thereafter, seizures occurred in cycles: 1-3 daily over 10 to 14 days, then increased to at least 8 per day then tapered off. She would then be seizure free for 7 to 12 days and the cycle would restart. Seizures would occur mainly around transition to sleep/wake.	Poor	10 clusters of myoclonic jerks per day more with illness. Other seizure types vary (from days to months).	Started AED at 6 months. Initially well controlled with topiramate, levetiracetam and phenobarbital. Then daily migrating focal seizures with varying frequency.
Seizure current medication	Carbamazepine, phenobarbital, clobazam	Topamax and Keppra	Deceased	Deceased	Deceased	Keppra, Onfi, Vimpat	Deceased
Seizure drugs tried (AEDs)	Carbamazepine, valproic acid, phenobarbital, clobazam	Topamax and Keppra	N/A	Carbamazepine, valproate (initial response), topiramate (no response), lamotrigine (little response), nitrazepam (some response), oxcarbazepine (some response), clobazam	Vigabatrin, Lorazepam, midazolam, phenobarbital	N/A	Levetiracetam Topiramate Phenobarbital Clonazepam Valproate Lorazepam
Other medications	Midazolam nasal spray when seizures last > 5 minutes, no other medications	Albuterol, cetirizine, enalapril, fluticasone, polyethylene glycol, simethicone, vitamin D3	Nitrous oxide for cardiac failure	Vitamin D, ranitidine, PEG3350	Trimethoprim, Lansoprazole, Vitamin D 400U daily, Lactulose 5ml BID	Diastat as needed	Sildenafil (pulmonary hypertension) Furosemide Ventolin Budesonide Diazepam (rectal)
Hypotonia	Axial hypotonia, hypertonia of arms and legs.	Muscle tone axial and appendicular hypotonia with severe head lag.	N/A	Axial hypotonia, with appendicular hypertonia and mild spasticity.	Axial hypotonia, appendicular spasticity, tonic posturing of upper limbs.	Axial and appendicular hypotonia with significant head lag.	Pronounced axial hypotonia and appendicular hypertonia with clenched fists. Significant head lag
Other neurological findings	Stereotypic movements (turning of her head, closure of her eyes, rolling	hyperkinetic involuntary movements.	Autopsy: normal meninges,	Random myoclonic jerks throughout the day.	Opisthotonos	Involuntary movements of all 4 extremities,	Opisthotonos in the infancy

Subject ID/Source	St1 (this report)	St2 (this report)	St3a (this report)	St3b (this report)	St4 (this report)	St5 (this report)	St6 (this report)
	of her eyes, intermittent groaning/hyperventilation). strabismus convergence, dystonic positioning of her left foot, choreatic movements of her hands Hyperlaxicity Sleep disturbances – difficulties to falling asleep.		cranial nerves and vessels. Cerebral hemispheres were normal and no evidence of malformation. Sections of the cerebral cortex show pyknotic nuclei, demonstrating karyorrhexis. There were numerous changes within the white matter. There were areas of devitalization of white matter with necrosis and karyorrhexis of cells. There are astrocytes with enlarged nuclei in these areas. The GFAP was strongly positive. This is indicative of periventricular leukomalacia. No striking anoxic changes.			sleep disturbances, nystagmus.	Suspected blindness, uncoordinated eye movements.
Facial dysmorphism	No	Dysmorphic facial features with somewhat coarse appearance, midface hypoplasia, wide mouth, thickened lips, thick eyebrows, prognathism.	Small chin, macroglossia, flat nasal bridge, down slanting palpebral fissures.	High arched palate	Coarse facial features, thick lips, macroglossia, short neck, prominent forehead, wide nasal bridge and short upturned	Coarse facial features	Coarse facial features

Subject ID/Source	St1 (this report)	St2 (this report)	St3a (this report)	St3b (this report)	St4 (this report)	St5 (this report)	St6 (this report)
					nose, large ears, micrognathia.		
Cranial shape anomalies	-	Mild brachycephaly	-	-	Cleft soft palate and high arched hard palate, progressive microcephaly (90th% at birth which had dropped to the 10th centile by age 7 months).	Plagiocephaly, small maxilla, mild brachycephaly.	Positional plagiocephaly
Craniosynostosis	-	-	-	-	-	Possible premature closure of the right coronal suture, the left is probably open.	-
Pectus excavatum	+	+	-	+	-	-	-
Other skeletal anomalies	-	Neuromuscular S-shaped scoliosis	-	-	Short stature, abnormal bone mineralization, hyperextensive interphalangeal joints.	-	-
Other dysmorphic features	Inverted nipples	-	Bilateral pulmonary interstitial emphysema, accessory spleen	-	Increased nuchal redundancy, deep palmar and plantar creases.	Subjectively large pinna	-
Deafness	-	-	N/A	-	Mild left conductive hearing deficit.	-	-
Ophthalmological anomalies	Short fix/track	Dysconjugate gaze, cortical visual impairment Synaptic, midretinal disease with fundoscopically normal looking fundi, no optic nerve atrophy ERG (performed at 1 year and 4 years of age) suggests	N/A	Cortical visual impairment	Cortical blindness, strabismus exotropia, Lagophthalmos of approximately 3-4mm of each eye, reaction to light with faint blinking,	Cortical visual impairment, unable to fix/track, nystagmus.	Cortical visual impairment, unable to fix/track.

Subject ID/Source	St1 (this report)	St2 (this report)	St3a (this report)	St3b (this report)	St4 (this report)	St5 (this report)	St6 (this report)
		that there is a transmission problem at the level of the photoreceptor-bipolar cell synapse in the retina			corneal ulcer of right eye.		
Cardiac anomalies	-	Prolapsed mitral valve with mild left ventricular dysfunction, 1st degree AV block.	Right ventricular hypertrophy and poor heart function. Hypertrophy not supported on autopsy exam.	Holter monitor revealed first and second degree heart block with some complete heart block and vestibular escape beat.	Arrhythmia	PDA, PFO (both resolved) mild pulmonary stenosis.	Tricuspid insufficiency Pulmonary hypertension
Genito-urinary malformation	Incontinence	Incontinence	Dilated and tortuous ureters, hypoplastic renal pelvis, hypoplastic renal calyces.	None noted- no ultrasound done	AUS at 8 months: bilateral grade 4 hydronephrosis, new renal stones. Kidneys slightly increase in size.	Incontinence, vesico-ureteral reflux, and bilateral hydronephrosis.	Incontinence
Gastrointestinal issues	Constipation, chewing difficulties, incontinence.	Constipation, reflux, G-tube dependent.	-	Recurrent aspirations, G-tube.	G-tube at 6 weeks, Volvulus (Ladd's procedure performed), SMA/SMV reversal, constipation, GERD.	G-tube dependent, duodenal web s/p resection, malrotation s/p Ladd procedure, intestinal dysmotility, volvulus, dysphagia.	G-tube dependent, constipation.
Nephrocalcinosis	-	-	-	-	-	-	-
Teeth anomalies	Gingival hyperplasia	Small appearing teeth with delayed dentition.	Not applicable	Delayed eruption with gingival hyperplasia.	Too young	No teeth (delated dentition)	N/A
Nail anomalies	-	-	-	-	-	-	-
Short fingers or hands	-	-	-	-	-	-	-
Joint contractures	Yes, of ankles. Her hips are out of the hip-bowls	-	-	Mild spasticity of the lower extremities requiring AFOs	+		-
Serum alkaline phosphatase	194 U/l (age 1.5 year), normal range 100-310 U/L	Intermittently elevated (range 212	Not done	762 (2yrs), 486 (5yrs), normal range 176-530 U/L	255-533, normal range 110-320 U/L	Not measured	Normal

Subject ID/Source	St1 (this report)	St2 (this report)	St3a (this report)	St3b (this report)	St4 (this report)	St5 (this report)	St6 (this report)
		– 1,360), normal range 150-380 U/L					At 2 yrs 5 months 330 (42-408); at 3 yrs 2 months 258.
Other		Repeated pneumonia, chronic respiratory insufficiency, Subglottic stenosis requiring multiple episodes of Microlaryngoscopy & Bronchoscopy (MLB) with laryngeal dilation, thoracic insufficiency, asthma, Nocturnal BIPAP dependence, one episode of rhabdomyolysis.			Coarse cry, Sandifer syndrome. Failure to thrive. Abnormal control of respiratory rate. Lack of interaction. Pneumonia.		Repeated pneumonias. Respiratory insufficiency. Died from pneumonia + worsening in pulmonary hypertension.

Supplementary Table 3.2 continued

Subject ID/Source	Martin *et al* 2014(154)	Alazami *et al* 2015(205)	Starr *et al* 2018(206)
Variants & Inheritance (NM_148920.2)	Homozygous: c.690-2A>G	NM_004204.3: c.619C>T p.R207*	Maternal: c.968_969del p.L323Pfs*119 Paternal: c.1199_1201del p.Y400del
Gender	Male	N/A	Male
Ancestry	West African	N/A	N/A

Subject ID/Source	Martin *et al* 2014(154)	Alazami *et al* 2015(205)	Starr *et al* 2018(206)
Consanguinity?	Reported no, but extensive regions of homozygosity	N/A	No
History of miscarriages	N/A	N/A	N/A
Affected siblings	None	N/A	None
Unaffected siblings	2	N/A	2
Prenatal issues or findings	None reported	N/A	Severe polyhydramnios requiring multiple amniocentesis fluid reduction procedures.
Polyhydramnios	-	N/A	Severe
Gestational period	41 weeks	N/A	39 weeks (C-section)
APGAR scores	N/A	N/A	N/A
Neonatal complications	At 4 weeks: cyanotic episodes with eye twitching, brief stiffening of upper body.	N/A	Feeding difficulties, trembling episodes.
Birth weight	3.83 kg (82.8%)	N/A	3.6 kg (69.5%)
Birth height	N/A	N/A	N/A
Birth head circumference	32.5 cm (6.1%)	N/A	N/A
Age at last follow-up	2 years	N/A	10 months
Weight	N/A	N/A	7.8 kg (5%)
Height	N/A	N/A	69 cm (3%)
Head circumference	N/A (0.4^{th} centile at 14 months)	N/A	45cm (37.2%)
Current age	Deceased 2y4m	N/A	Deceased 10m
DD/ID	Profound developmental delay, lack of head control, does not smile.	Developmental delay	Lack of head control, episodes of gasping with lip quivering.
Seizures?	Yes	Yes	Yes
Seizure onset	4 weeks	N/A	7 months
Seizure types	Focal, tonic, tonic-clonic, cyanotics spells	N/A	Clustered myoclonic jerks with extremity stiffening, lip quivering, back arching with upper extremities appearing floppy, status epilepticus
Seizure control	Poor	Intractable	Refractory to Levetiracetam, controlled on Fosphenytoin
Seizure current medication	Deceased	N/A	Deceased
Seizure drugs tried (AEDs)	Diazepam Phenytoin Phenbarbital Paraldehyde Vigabatrin Valproic acid Topiramate Clonazepam	N/A	Levetiracetam Lorazepam Fosphenytoin Phenobarbitol Gabapentin
Other medications	Biotin Pyridoxine	N/A	Clonidine
Hypotonia	Yes	N/A	Progressive truncal hypotonia

Subject ID/Source	Martin *et al* 2014(154)	Alazami *et al* 2015(205)	Starr *et al* 2018(206)
Other neurological findings	Dystonic movements	N/A	Central apnea, decreased deep tendon reflexes (1+)
Facial dysmorphism	Thick lips, thick alveolar margins, narrow palate.	N/A	Coarse and dysmorphic facial features, hooded upper eyelids with mild ptosis, telecanthus, fleshy and uplifted earlobes, thick alae nasi with broad nasal tip, anteverted nares. Full almost pendulous cheeks, long and smooth philtrum, thin vermillion of upper lip, downturned corners of mouth, mild micrognathia.
Cranial shape anomalies	-	N/A	Large anterior fontanelle, sphenoid wing dysplasia.
Craniosynostosis	-	N/A	Intrasutural bone of the coronal suture
Pectus excavatum	-	N/A	+
Other skeletal anomalies	-	N/A	Progressive scoliosis, metaphyseal radiolucent lesions in femora and tibiae
Other dysmorphic features	Inverted nipples	N/A	Deep plantar creases, marked abdominal laxity, prune-belly-like abdomen
Deafness	-	N/A	-
Ophthalmological anomalies	Poor vision	Optic atrophy	Vertical nystagmus, bilateral hyperopia with astigmatism, cortical visual impairment, delayed visual maturation, punctate keratitis of both eyes, alacrima with decrease of corneal sensation.
Cardiac anomalies	-	N/A	Patent foramen ovale discovered at 17 weeks old.
Genito-urinary malformation	-	N/A	Bilateral cystic renal dysplasia, bilateral inguinal hernias, small right kidney with increased cortical echogenicity and diminished cortical medullary differentiation, grade 3 vesicoureteral reflux on the right, 1 on the left.
Gastrointestinal issues	Recurrent vomiting, G-tube dependent (feeding difficulties).	N/A	Cyclic vomiting, hepatic nodule, poor feeding, diastasis recti.
Nephrocalcinosis	-	N/A	+
Teeth anomalies	-	N/A	Too young
Nail anomalies	-	N/A	-
Short fingers or hands	-	N/A	-
Joint contractures	-	N/A	-
Serum alkaline phosphatase	N/A	N/A	480-836U/L (150-440 U/L)
Other	Aspiration pneumonia		

Supplementary Table 3.3 EEG findings for each *PIGQ* patient reported here and from the literature.

Subject	EEG findings
St1	(8 years): Slow, encephalopathic, no occipital rhythm, no reaction on eye closure and opening of her eyes. During wake in 1-10% of time multifocal epileptiform discharges, mainly left temporal/fronto-temporal. During sleep still a slight increase in epileptiform discharges to 10-50% of time. After awakening a slight decrease to 1-10% No seizures. During the moments of decreased consciousness during wakefulness there are no epileptiform discharges. Conclusion: localization related epilepsy.
St2	(5 years): Overall Final Impression: Abnormal. This is an abnormal EEG during wakefulness and sleep due to: - A poorly organized and diffusely slow background without the expected features of wakefulness - Intermittent high amplitude left posterior slowing - Intermittent right posterior slowing with admixed right parietal sharp waves - Frequent right frontal or right parietal sharp waves that are sleep potentiated - Occasional left frontal and left parietal sharp waves that are sleep activated. - This EEG suggests diffuse cerebral dysfunction. There is frequent intermittent polymorphic high-amplitude 2-3 Hz delta slowing in the left temporal parietal region. There is intermittent polymorphic, semi rhythmic, moderate amplitude 3 Hz slowing in the right posterior quadrant with embedded P4 sharp waves. Sporadic Epileptiform Discharges: Type # 1: Focal. Morphology: Sharp. Qualification: Frequent. Location: Independent sharp waves at F4, and P4 which are present during wakefulness and potentiated by sleep. In sleep, F4 sharps occur in runs of 3-10 seconds.. Type # 2: Focal. Morphology: Sharp. Qualification: Occasional. Location: Independent sharp waves at F3, P3 which are seen only in sleep; there are rare F3 runs up to 3-5 seconds.
St3a	-
St3b	(5 months): Normal, repeat showed mild slow waves over left temporal lobe. (2 years): 3 events localized to L posterior head region. Interictally some left posterior head spike and slow wave complexes, some sharp waves in both central head regions. (3 years): Generalized slow wave excess out of keeping with subject age. Single right posterior temporal lobe spike.
St4	(Neonatal): Negative for seizures but shows episodic slowing of background activity and asynchrony. (8 months; admitted with epileptic spasms): Confirmed hypsarrhythmia.
St5	(6 months): 4-5 hz, multifocal spikes intermittently at T5, F8 and T4. (8 months): Generalized slowing with multifocal sharp waves and excessive beta activity no seizures. (14 months): EEG with LTM noted abundant sleep activated multifocal spikes and sharp waves with background slowing.
St6	(7 weeks): Within normal boundaries. (4 months): Normal. (6 months): Asymmetric EEG with slowing left side. Sharp-waves left side with short rhythmic sequences up to 30 seconds. (14 months): Full EEG + video monitoring 24 hours. Continuous background. Repeating 2-3 min long focal seizures left and right side independently (EIMFS).
Martin *et al* 2014(154)	(3 months): Burst-suppression pattern with bursts of high amplitude multifocal, irregular sharp and slow wave discharge, interrupted by 1-1.5 seconds of flattening in wake/drowsiness when posterior discharges were prominent, subtle focal seizure. (2 years): Very abnormal but more continuous in wake and sleep over right hemisphere, with very active multifocal sharp waves on left side, left discharge interrupted in sleep by brief periods of EEG attenuation over the left hemisphere. Left temporal focal seizure.
Alazami *et al* 2015(205)	N/A
Starr *et al* 2018(206)	(2 months): Unremarkable, but clinical episodes not captured during recording. (7 months): EEG1 frequent epileptiform discharges arising from right temporal, central, and bilateral occipital areas; EEG 2 high amplitude diffuse background slowing. (9 months): Multifocal epileptiform activity in the form of high amplitude spike and slow wave complexes in the right occipital region, spikes and polyspikes associated with slow potentials in bilateral temporal and posterior temporal regions.

Supplementary Table 3.4 MRI findings for each subject for each PIGQ patient reported here and from the literature.

Subject	MRI findings
St1	(8 months): Broad periventricular cerebral fluid spaces, almost no myelination to the central areas and no myelination to the occipital area. No abnormalities of the cerebral cortex.
St2	(5 months): Slightly diminutive frontal lobes and slightly prominent frontal horns of the lateral ventricles. Otherwise, unremarkable contrast-enhanced MRI of the brain. MRS: There is borderline lactate peak identified in nearly all the voxels placed over the basal ganglia. The minimal lactate peak is also seen in voxels overly CSF and the ventricles. This is nonspecific marker of parenchymal injury. The major metabolites are otherwise normal for age. No repeat MRI obtained.
St3a	No imaging.
St3b	(19 months): Mild volume loss involving the cerebellum, particularly the vermis. There remain areas of incomplete myelination in the subcortical white matter of the bilateral frontal lobes, anterior temporal lobes, subinsular white matter and periventricular white matter around the frontal horns, atria and occipital horns of the lateral ventricles. Mild prominence of the extra-axial subarachnoid space overlying the bilateral frontal convexities, right greater than left and in the intrahemispheric fissure.
St4	(9 days): Normal but spine images show low lying conus medullaris. (7 months): Nonspecific increased T2/FLAIR intensity in bilateral medial lemniscus tracts. Prominent extra axial spaces and ventricles, showing progressive cortical volume loss and loss of subcortical white matter volume compared to prior study. Slightly delayed myelination.
St5	Prenatally, lateral ventricles at 8mm with dangling choroids, hypoplastic cerebellar vermis, inferiorly leading to impression of Dandy Walker Variant. (2 years): 1. Abnormal myelination characterized by increased T2 signal in the peripheral and periatrial white matter, but with more age-appropriate T2 signal in the deep white matter. This is favored to represent delayed myelination. The basal ganglia and cerebellum are normal. 2. Pituitary hypoplasia with the preservation of the pituitary stalk. 3. Diffuse cerebral volume loss. 4. Abnormal skull shape with right plagiocephaly, possibly positional plagiocephaly.
St6	MRI at 6 weeks and 3 months normal.
Martin *et al* 2014(154)	(3 months): Normal. (9 months): Delayed/limited myelination but no gross structural lesion.
Alazami *et al* 2015(205)	N/A
Starr *et al* 2018(206)	(5 months+10 months CT): Plagiocephaly with ventriculomegaly (left>right).

Chapter 4: PLPHP deficiency: Clinical, genetic, biochemical, and mechanistic insights

Published in:

Johnstone DL, Al-Shekaili HH, Tarailo-Graovac M, Wolf NI, Ivy AS, Demarest S, Roussel Y, Ciapaite J, van Roermund CWT, Kernohan KD, Kosuta C, Ban K, Ito Y, McBride S, Al-Thihli K, Abdelrahim RA, Koul R, Al Futaisi A, Haaxma CA, Olson H, Sigurdardottir LY, Arnold GL, Gerkes EH, Boon M, Heiner-Fokkema MR, Noble S, Bosma M, Jans J, Koolen DA, Kamsteeg EJ, Drogemoller B, Ross CJ, Majewski J, Cho MT, Begtrup A, Wasserman WW, Bui T, Brimble E, Violante S, Houten SM, Wevers RA, van Faassen M, Kema IP, Lepage N, Care4Rare Canada C, Lines MA, Dyment DA, Wanders RJA, Verhoeven-Duif N, Ekker M, et al. 2019. **PLPHP deficiency: clinical, genetic, biochemical, and mechanistic insights**. *Brain* 142:542-559.

Permission for use from Oxford University Press:

4.1 Abstract

Biallelic pathogenic variants in *PLPBP* (formerly called "*PROSC"*) have recently been shown to cause a novel form of vitamin B6-dependent epilepsy, the pathophysiological basis of which is poorly understood. When left untreated, the disease can progress to status epilepticus and death in infancy. Here we present 12 previously undescribed patients and six novel pathogenic variants in *PLPBP*. Suspected clinical diagnoses prior to identification of *PLPBP* variants included mitochondrial encephalopathy (two patients), folinic acid-responsive epilepsy (one patient) and a movement disorder compatible with AADC deficiency (one patient). The encoded protein, PLPHP is believed to be crucial for B6 homeostasis. We modelled the pathogenicity of the variants and developed a clinical severity scoring system. The most severe phenotypes were associated with variants leading to loss of function of *PLPBP* or significantly affecting protein stability/PLP-binding. To further explore the pathophysiology of this disease, we developed the first zebrafish model of PLPHP deficiency using CRISPR/Cas9. Our model recapitulates the disease, with *plpbp*$^{-/-}$ larvae showing behavioral, biochemical, and electrophysiological signs of seizure activity by 10 days post-fertilization and early death by 16 days post-fertilization. Treatment with pyridoxine significantly improved the epileptic phenotype and extended lifespan in *plpbp*$^{-/-}$ animals. Larvae had disruptions in amino acid metabolism as well as GABA and catecholamine biosynthesis, indicating impairment of PLP-dependent enzymatic activities. Using mass spectrometry, we observed significant B6 vitamer level changes in *plpbp*$^{-/-}$ zebrafish, patient fibroblasts and PLPHP-deficient HEK293 cells. Additional studies in human cells and yeast provide the first empirical evidence that PLPHP is localized in mitochondria and may play a

role in mitochondrial metabolism. These models provide new insights into disease mechanisms and can serve as a platform for drug discovery.

4.2 Introduction

The vitamin B6-responsive disorders (B6RDs) are a clinically and genetically heterogeneous group of rare, autosomal recessive conditions (231) with the hallmark feature of seizures uniquely responsive to treatment by the B6 vitamers pyridoxine (PN) and/or pyridoxal-5'-phosphate (PLP) (232, 233). PLP is a cofactor for over 160 distinct catalytic functions (113), including enzymes involved in glucose, lipid and amino acid metabolism (116-118), and for the synthesis of neurotransmitters, making it an essential vitamer for normal brain function (234).

The B6RDs are characterized by recurrent seizures in the prenatal, neonatal, or postnatal period and are resistant to anti-epileptic medication (123, 125, 232, 235). Intellectual disability, behavioral abnormalities, and psychiatric disturbances, as well as abnormalities in brain structure and myelination are frequently observed (236). If untreated, B6RDs may lead to status epilepticus and death (237). B6RDs have been attributed to a number of genetic variants disrupting B6 metabolism, including those leading to the accumulation of toxic metabolites that inactivate PLP (*ALDH7A1* (MIM#266100), *ALDH4A1*, (MIM#239510)), those interfering with the interconversion of B6 vitamers (*PNPO* (MIM#610090), *TNSALP* (MIM#171760) (123, 125, 204, 231, 236), and those impairing PLP homeostasis ((*PLPBP* (encoding PLP homeostasis protein, PLPHP), MIM#604436, previously named "*PROSC"*) (131, 132).

In bacteria (YggS) and yeast (YBL036C), the structures of PLPHP orthologous proteins show PLP covalently bound to a lysine residue, phosphate-binding motifs, and a typical triosephosphate isomerase (TIM)-barrel domain (128, 238). Purified human PLPHP is also bound to PLP in the native state, but little is known about the molecular function of this protein (239). Studies in YggS-deficient *Escherichia coli* revealed growth impairment and disrupted amino and keto acid homeostasis (128, 129). In cyanobacteria, it has been suggested that the C-terminal helix may play a role in PLP exchange with apoenzymes (240). B6 vitamer levels were significantly altered in human PLPHP loss-of-function (LOF) patient samples, and it has been hypothesized this protein has a key role in B6 homeostasis (129, 131), possibly acting as a PLP-carrier that prevents PLP from reacting with other molecules, supplying it to dependent enzymes and/or protecting PLP from phosphatases.

PLPHP deficiency in humans is manifested by early-onset intractable seizures responsive to PN and/or PLP, developmental delay, and structural brain abnormalities, most notably simplified gyral pattern and cyst-like structures adjacent to the anterior horns (131). We undertook a comprehensive genetic and biochemical study of PLPHP deficiency in a cohort of 12 previously undescribed patients, highlighting a unique movement disorder phenotype (without epilepsy) as well as fatal mitochondrial encephalopathy phenotype, which both to our knowledge, have not previously been described. To better characterize the pathophysiology of this neurometabolic disease, we generated knockout models in zebrafish (*Danio rerio*), yeast (*Saccharomyces cerevisiae*) and HEK293 cells, providing insights into the biochemical consequences of PLPHP deficiency.

4.3 Materials and methods

4.3.1 Patients

This study was approved by the clinical research ethics board of BC Children's and Women's Hospital, University of British Columbia (H12-00067), the Children's Hospital of Eastern Ontario Research Ethics Board, and local institutional review boards at the University of Colorado. Many of the patients were recruited through international collaboration as part of an ongoing TIDEX neurometabolic gene discovery project (241). After obtaining signed informed parental consent, referring clinicians provided detailed reports of clinical, MRI and EEG features of study patients.

4.3.2 Whole-exome sequencing, Sanger sequencing and *in silico* analysis

Detailed descriptions of whole-exome sequencing, bio-informatic analyses, Sanger sequencing and *in silico* analysis strategies are provided in the Supplementary Material. All exomes were aligned to the human reference genome, February 2009 assembly (GRCh37/hg19).

4.3.3 Structural model of human PLPHP

The 3D model of PLPHP protein (NP_009129.1) was obtained by homology modelling using MODELLER (242) and the yeast ortholog (YBL036C, PDB 1CT5, (238), 41% identical, 57% similar) as template. DOPE (discrete optimized protein energy) score was used to select the best model for subsequent refinement using Coot (v0.8.6.1, (243)). Prosa-Web (244) and

Coot's Ramachandran plot analysis module were used to validate model quality. PyMOL (245) was used for structural superimposition of the human PLPHP model with yeast 1CT5, and the coordinates of the PLP co-crystalized with the yeast ortholog were transferred to the PLPHP model, with PLP covalently bound to p.Lys47. Images were prepared using PyMOL. Arpeggio was used to calculate contacts (246). DUET (247) was used to calculate stability changes.

4.3.4 Clinical severity score

We assessed the clinical severity of patients within this study and previous studies (131, 132) based on published data. We adapted a scoring system of patients with B6RD due to pathogenic variants in *ALDH7A1* (248). The following criteria were used: A) global and/or intellectual delay: 0=normal; 1=mild; 2=moderate; 3=severe; B) age of onset of seizures and/or movement disorder: 0=absent; 1=>1month; 2=≥7 days; 3=<7 days; C) therapeutic response: 0=full cessation of seizures and normalization of EEG (if available) on <200mg B6 (PN and/or PLP) total daily; 1=no clinical seizures or abnormal movements on ≥200mg B6 total daily, with or without electrographic normalization OR clinical response to <200mg B6 total daily dose with persistently abnormal EEG; 2=no seizures with B6 (any dose) AND other antiepileptic drug (AED) medication, with or without EEG normalization; 3=breakthrough seizures and/or persistent movement disorder, no responsiveness. We calculated the sum for each clinical feature (A, B and C, above), and classified each patient as mild (1-3), moderate (4-6) or severe (7-9)(248).

4.3.5 Isolation of pure mitochondrial fractions and western blotting

Pure mitochondrial fractions were isolated from HeLa cells having HA-tagged mitochondria using an immunoprecipitation protocol as outlined previously (249). Whole cell and pure mitochondrial fractions were run on SDS-PAGE, and western blots were blocked in TBS-T 5% milk and probed with the following primary antibodies: rabbit anti-PROSC (Proteintech 25154-1-AP; 1:1000), rabbit anti-SHMT2 (SIGMA HPA020549; 1:1000), rabbit anti-VDAC (Cell Signaling 4661S; 1:1000), mouse anti-LAMP2 (Abcam ab25631; 1:1000), mouse anti-GAPDH (Santa Cruz sc-47724; 1:2000), and rabbit anti-GOLGIN-97 (Cell Signaling 13132; 1:1000). All antibodies were prepared fresh in TBS-T 5% BSA. HRP-conjugated goat anti-mouse (cat. no. sc-2055) and anti-rabbit (cat. no. sc-2054) secondary antibodies obtained from Santa Cruz Biotechnology were used at 1:3000.

4.3.6 Yeast strains and culture conditions

Saccharomyces cerevisiae BY4742 (MATα *his3Δ1 leu2Δ0 lys2Δ0 ura3Δ0*) was used as the Wild Type (WT) strain along with derivative strains: *fox1*::KAN, carrying a deletion of peroxisomal acyl-CoA oxidase and *ybl036C*::KAN mutant (Euroscaft). Yeast strains and transformants containing the expression plasmids p*PROSC1a* and p*PROSC2a* (human *PLPBP*) were selected and grown in minimal medium containing 6.7 g/L yeast nitrogen base without amino acids (YNB-WO), supplemented with 5 g/L glucose and amino acids (20 mg/L), and growth was measured. For the induction of peroxisome and mitochondrial proliferation, cells were shifted to ethanol (YPE) 20g/L, glycerol (YPG) 20g/L, or oleate (YPO) medium containing 5g/L potassium phosphate buffer, pH 6.0, 3g/liter yeast extract,

5g/L peptone. YPO media were supplemented with 1.2 g/L oleate, and 2g/L Tween-80. Prior to shifting to these media, the cells were grown in minimal medium with 5 g/L glucose for at least 24h.

4.3.7 Generation of mutant zebrafish lines

Zebrafish were maintained following standard protocols (250), and experiments were in accordance with the animal care guidelines of the Canadian Council on Animal Care, the University of Ottawa animal care committee (protocol BL-2678), and the ARRIVE guidelines (251). Handling, treatments, husbandry and nursery were performed as outlined previously (149). CRISPR/Cas9 was used to induce targeted indel mutations in the *plpbp* gene of zebrafish embryos as previously described (252), using ZiFit targeter (253) to select CRISPR targets and design oligonucleotides (5' TAGGTGGAGCGGGTGAATCAAG 3' and 5' AAACCTTGATTCACCCGCTCCA 3') in the first exon. The target was chosen as having the fewest predicted off-targets (minimum three mismatches with any predicted off-target sequence). Generation of the sgRNA and CRISPR/Cas9 injection, as well as screening for mutants by PCR/HMA-PAGE, were performed as previously described (149, 254). Genotyping PCR was performed as described in (148) and in Supplementary Material. F0 larvae were raised to adulthood and backcrossed with WT to generate heterozygous F1 fish. These were again backcrossed with WT to minimize off-targets. Experimental compound heterozygous animals were obtained by crossing F2 heterozygotes.

4.3.8 Behavioral phenotyping

Sixteen 11 days post-fertilization (dpf) larvae per group were dispensed (one per well) in 48-well flat-bottomed culture dishes (Corning) containing 500µL of system water. Behavior was monitored as previously described (149) using a ZebraBox system (ViewPoint Behavior Technology). Videos were also analyzed blindly by two observers to classify seizure scores using the S0-S3 system (255).

4.3.9 Electrophysiology and *c-fos* expression

Electrophysiological local field potential recordings of activity in the optic tectum of five 11 dpf larvae per group selected randomly were obtained as previously described (149). Since *c-fos* expression can be used as a biomarker for increased neuronal activity and is known to increase with seizure activity (255), we measured *c-fos* mRNA expression in pools of five 11 dpf larvae (mutants and WT) as well as in WT larvae treated with 15mM pentylenetetrazol (PTZ) as a positive control. RNA was extracted, reverse transcribed and quantified by qPCR as previously described (149). Primers used were: *cfos*-F 5' AACTGTCACGGCGATCTCTT 3' and *cfos*-R 5' TCTTCTGGAGAAAGCTGTTC 3' with β-*actin* as internal control: *actin*-F 5' CATCCATCGTTCACAGGAAGTG 3' and *actin*-R 5' TGGTCGTTCGTTTGAATCTCAT 3'.

4.3.10 Metabolite extraction and mass spectrometry

For analysis of B6 vitamers, three pools of six 10 dpf larvae (*plpbp*$^{-/-}$, WT) were analyzed as previously described (149). Measurement of amino acid panels was performed using three pools of five larvae per group (*plpbp*$^{-/-}$, WT, heterozygotes) following established protocols (149, 256), with the modification that 10 dpf larvae were fasted for 24 hours prior to collection with metabolite extraction at 11 dpf. Neurotransmitter analytes (5 pools of *plpbp*$^{-/-}$ and 4 pools of WT; 6 larvae per pool) were measured following established methods (257).

4.3.11 Statistical analysis

All statistical analyses and graphing were performed using GraphPad Prism. Where appropriate, one-way ANOVA with Tukey's test, or Krustal-Wallis with Dunn's *post hoc* test was performed. Student's t-test was used for pairwise comparisons.

4.4 Results

4.4.1 Phenotypic spectrum of patient cohort with biallelic pathogenic *PLPBP* variants

The 12 previously unreported patients described here presented with encephalopathic phenotypes comprising neonatal-onset of refractory epilepsy (or a movement disorder in one case), with or without additional clinical features (Table 4.1 and Supplementary Material). This cohort comprised six male and six female patients from seven different ethnic backgrounds. For patients 1 and 6, the pregnancy history was notable for excessive fetal movements, possibly indicating seizures *in utero*. Three patients experienced respiratory insufficiency after birth, including patient 3 who had progressive respiratory failure.

Epileptic seizures started within the first week of life in all affected infants except patient 7, who instead presented with a movement disorder (opisthotonos, oculogyric crises) at two months of age. Patients manifested multiple seizure types, and initial EEG showed various patterns of abnormal electrographic activity with burst suppression being common (6/11 reported). Seizures were refractory to AED treatment in all patients (Table 4.1, Supplementary Material). All patients who received vitamin B6 (10/12) showed responsiveness and improvement of seizures or abnormal movements upon its institution. Vitamin B6 therapy was first trialed as PN in eight patients, PLP in one patient and a combination of both vitamers in another patient (Table 4.1). The incomplete response to PN or PLP in patient 1 prompted the clinicians to add folinic acid to his treatment, which produced a marked reduction in seizure frequency (only two brief episodes in a three-month period). In patient 3, PLP was initially started but failed to exert sufficient seizure control, and adjuvant AED treatment was necessary.

Table 4.1: Clinical features of PLPHP-deficient patients.
Abbreviations: GA: Gestational Age, NA: Not Available, HC: Head Circumference, AEDs: Anti-Epileptic Drugs, GTCs: Generalized Tonic-Clonic seizures, PN: Pyridoxine, PLP: Pyridoxal 5'-Phosphate, EEG: Electroencephalography, MRI: Magnetic Resonance Imaging, MRS: Magnetic Resonance Spectroscopy, wk(s): week(s), mo: month(s), yr: year(s), nb: nota bene.

Patient's ID (sex, current age)	Patient 1 (Male, 3 11/12 yr)	Patient 2 (Male, 14 yr)	Patient 3 (Female, 5 2/12 yr)	Patient 4 (Female, died at 2 wks)	Patient 5 (Female, died at 8 wks)	Patient 6 (Male, 4 3/12 yr)
Ancestry (domicile)	Arab (Oman)	Arab (Oman)	African/Creole (Curacao)	Dutch (Netherlands)	Cree First Nation (Canada)	Arab (United Arab Emirates)
Consanguinity (degree)	+ (first cousin)	+ (first cousin)	+ (degree NA)	-	+ (second cousin)	+ (second cousin)
***PLPBP* cDNA change (NM_007198)**	347C>T (homozygous) 823C>G (homozygous VUS)	122G>A (homozygous)	199G>A (homozygous)	320-2A>G; 671G>C	370_373del (homozygous)	347C>T (homozygous)
Amino acid change	p.Thr116Ile; p.His275Asp (VUS)	p.Arg41Gln	p.Glu67Lys	Splicing; p.Gly224Ala	p.Asp124Lysfs*2	p.Thr116Ile
Pregnancy / delivery complications	Abnormal fetal movements	-	C-section due to fetal distress	DCDA-gemelli pregnancy	C-section due to fetal distress	Abnormal fetal movements
Birth HC percentile	66th centile	10th centile	<2nd centile	1st centile	82nd centile	NA
Lactic acidosis	-	-	+	+	+	NA
Seizure onset	Day 5	Day 7	Day 2	Day 1	Day 1	Day 4
Seizure type [5]: myoclonic	-	-	-	-	+	-
Seizure type: tonic	_	_	+	+	+	_
Seizure type: clonic	_	_	_	_	_	+
Seizure type: tonic-clonic	+	+	+	_	_	_
Seizure type: infantile spasms	_	_	_	+	_	+
Initial EEG pattern (at age)	Burst suppression (1 wk)	NA	Discontinuous with tendency to burst suppression (5 days)	Discontinuous (day 1)	Burst suppression (age NA)	Multifocal epileptiform activity (4 mo)
Response to initial AED treatment [3]	Partial response	No response	NA	Partial response	Partial response	Partial response
Initial B6 treatment (age/response [3])	PN (5 wks) PLP (2 yr, 6 mo / partial response)	PN (< 1 mo/ (seizure free)	PLP (5 days) PN (3 yr, 10 mo / good response)	Not tried	Not tried	PN (6 mo/ seizure free [4])
B6 withdrawal (vitamer/ response)	-	-	+ (PLP/ seizure relapsed)	Not applicable	Not applicable	+ (PN/ seizure relapsed)
B6 vitamer switch (type/ response)	+ (PN→PLP/ no improvement)	-	+ (PLP→PN/ no improvement)	Not applicable	Not applicable	-
Current treatment (dose)	PLP (58 mg/kg/day) Folinic acid (2mg/kg/day)	PN (5 mg/kg/day)	PN (9 mg/kg/day) Midazolam (used during seizures only)	Not applicable	Not applicable	PN (12.8 mg/kg/day) oxcarbazepine (53.8 mg/kg/day)

Patient's ID (sex, current age)	Patient 1 (Male, 3 11/12 yr)	Patient 2 (Male, 14 yr)	Patient 3 (Female, 5 2/12 yr)	Patient 4 (Female, died at 2 wks)	Patient 5 (Female, died at 8 wks)	Patient 6 (Male, 4 3/12 yr)
Breakthrough seizures with fever	+	+	+ (seizure relapse on viral infections or sleep deprivation)	Not applicable	Not applicable	+
Motor neurological exam	Unremarkable	Unremarkable	Hypertonia, stereotypies	NA	NA	Mild axial hypotonia, stereotypies
Developmental delay	+, with ASD	-	+	Not applicable	Not applicable	+, with ASD
Speech delay	+	-	+	Not applicable	Not applicable	+
School performance or IQ	NA	Average school performance	NA	Not applicable	Not applicable	DQ=70, 2nd percentile (Bayley-III Cognitive Composite score)
Minor dysmorphic features	-	-	+ [7]	-	-	-
Neuro-imaging (age) [10]	MRI (6 wks): mild WM changes MRI (9 mo): mild hydrocephalus. MRI (3.5 yrs): normal.	Not performed	MRI (day 10): WM changes, large paraventricular (pseudo)-cysts, thin posterior CC, PLIC is not myelinated.	MRI (day 1): WM changes, large paraventricular (pseudo)-cysts, thin posterior CC, PLIC is not myelinated.	MRI (day 6): cystic leukencephalopathy	MRI (8 mo): normal.

Table 4.1 continued:

Patient's ID (sex, current age)	Patient 7 (Male, 23 mo)	Patient 8 (Male, 8 1/12 yr)	Patient 9 (Male, 14 mo)	Patient 10 (Female, 10 6/12 yr) (sister of Patient 11)	Patient 11 (Female, 6 10/12 y) (sister of Patient 10)	Patient 12 (Female, 5 mo)
Ancestry (domicile)	Hispanic (Guatemala)	Arab (Oman)	Arab (Oman)	Kurdish (USA)	Kurdish (USA)	African American (USA)
Consanguinity (degree)	-	+ (first cousin)	+ (first cousin)	+ (first cousins)	+ (first cousin)	1st degree relatives
***PLPBP* cDNA change (NM_007198)**	280A>T (homozygous)	122G>A (homozygous)	122G>A (homozygous)	199G>A (homozygous)	199G>A (homozygous)	370_373del (homozygous)
Amino acid change	p.Ile94Phe	p.Arg41Gln	p.Arg41Gln	p.Glu67Lys	p.Glu67Lys	p.Asp124Lysfs*2
Pregnancy / delivery complications	-	-	-	C-section due to fetal decelerations and meconium stained amniotic fluid	-	-
Birth HC percentile	12.5th centile	50th centile	50th centile	NA	2nd centile	22nd centile
Lactic acidosis	+	- [1]	NA	- [2]	NA	+
Seizure onset	2 mo	1st wk	Day 5	Day 1	Day 1	Day 1
Seizure type [5]: myoclonic	- [6]	+	-	+		+
Seizure type: tonic	–	–	+	–	–	+
Seizure type: clonic	–	–	–	–	+	–
Seizure type: tonic-clonic	–	–	–	–	–	–
Seizure type: infantile spasms	–	–	–	+	+	–
Initial EEG pattern (at age)	Continuously disorganized background with bursts of higher-amplitude activity (2 mo)	Burst suppression (3 wks)	Burst suppression (10 days)	Discontinuous (2 days)	Discontinuous with multifocal sharps (age NA)	Burst suppression (2 days)
Response to initial AED treatment [3]	Partial response	No response	Not tried	Partial response	No response	Partial response
Initial B6 treatment (age/response [3])	PN and PLP (2.5 mo/ seizure free)	PN (25 days/ seizure free)	PN (2nd week/ seizure free)	PN (2nd week/ seizure free[4])	PN (age NA/ good response)	PN (age NA/ no response) PLP (1 mo/seizure free)
B6 withdrawal (vitamer/ response)	-	-	-	+ (PN/ seizure relapsed)	+ (PN/ increased seizures)	-

Patient's ID (sex, current age)	Patient 7 (Male, 23 mo)	Patient 8 (Male, 8 1/12 yr)	Patient 9 (Male, 14 mo)	Patient 10 (Female, 10 6/12 yr) (sister of Patient 11)	Patient 11 (Female, 6 10/12 y) (sister of Patient 10)	Patient 12 (Female, 5 mo)
B6 vitamer switch (type/ response)	-	-	-	-	-	+ (PN→PLP/ complete response)
Current treatment (dose)	PN (23 mg/kg/day) PLP (30 mg/kg/day)	PN (6 mg/kg/day)	PN (8.5 mg/kg/day)	PN (4.7 mg/kg/day) Lamotrigine (3.5 mg/kg/day) Clobazam (0.75 mg/kg/day)	PN (7.8 mg/kg/day) Lamotrigine (4.5 mg/kg/day) (1.25mg/kg/day)	PLP (40 mg/kg/day) Phenobarbital (9 mg/kg/day)
Breakthrough seizures with fever	-	+	-	+	+	-
Motor neurological exam	Unremarkable	Unremarkable	Hyperreflexia of all limbs	Hypotonia, mild dysmetria, wide based gait	Hypotonia, mild dysmetria, wide based and ataxic gait.	Mild hypotonia
Developmental delay	-	-	-	+	+	-
Speech delay	-	-	NA	+	+	Not applicable
School performance or IQ	NA	Excellent school performance	NA	NA	NA	Not applicable
Minor dysmorphic features	+ [8]	-	-	+ [9]	-	-
Neuro-imaging (age) [10]	MRI (2 mo): normal	MRI (4 wks): normal	MRI (10 mo): normal	MRI (2 days): underdeveloped frontal gyri. Subsequent MRI (age NA): thin posterior CC.	Initial MRI (age NA): normal. Subsequent MRI (age NA): Slight asymmetry in height of the hippocampi, WM changes.	2 MRI's (2 days and 3 weeks): WM changes, mild dilatation of the lateral and third ventricles, PLIC is not myelinated.

necessary. A similar picture was seen for patients 6, 11 and 12, who required treatment with PN and adjuvant AED.

Patients 1 (Fig. 4.1), 6, 7, 8 and 9 had normal brain MR imaging studies (with the exception of mild T2-hyperintense white matter signal in the neonatal period for patient 1) (Supplementary Table 4.1). The remainder (6/11 patients for whom brain imaging was done) had structural brain abnormalities (Fig. 4.1, Supplementary Table 4.1). Four patients (3, 4, 5 and 12) had simplified gyral pattern, suggesting prenatal onset of the disease and possible effect of PLPHP-deficiency on neuronal migration. In addition, these patients displayed large cysts adjacent to the anterior horns. In two patients, a lactate doublet was present in single voxel MR spectroscopy of the basal ganglia.

Clinical presentations deviating from previous descriptions of this disease were also reported. Patient 7 showed a prominent movement disorder and biochemical picture resembling aromatic l-amino acid decarboxylase (AADC) deficiency (MIM#608643) (Supplementary Material). This patient had no pathogenic variant in *DDC* on exome sequencing. Patients 4 and 5 presented with signs and symptoms suggestive of severe mitochondrial disease with fatal epileptic encephalopathy, lactic acidosis and brain white matter lesions. Both patients deteriorated rapidly

and died at two and eight weeks of age, respectively, due to uncontrolled seizures and respiratory failure. In neither case was the presentation deemed typical of pyridoxine-dependent epilepsy, nor was a trial of B6 vitamers administered (Supplementary Material).

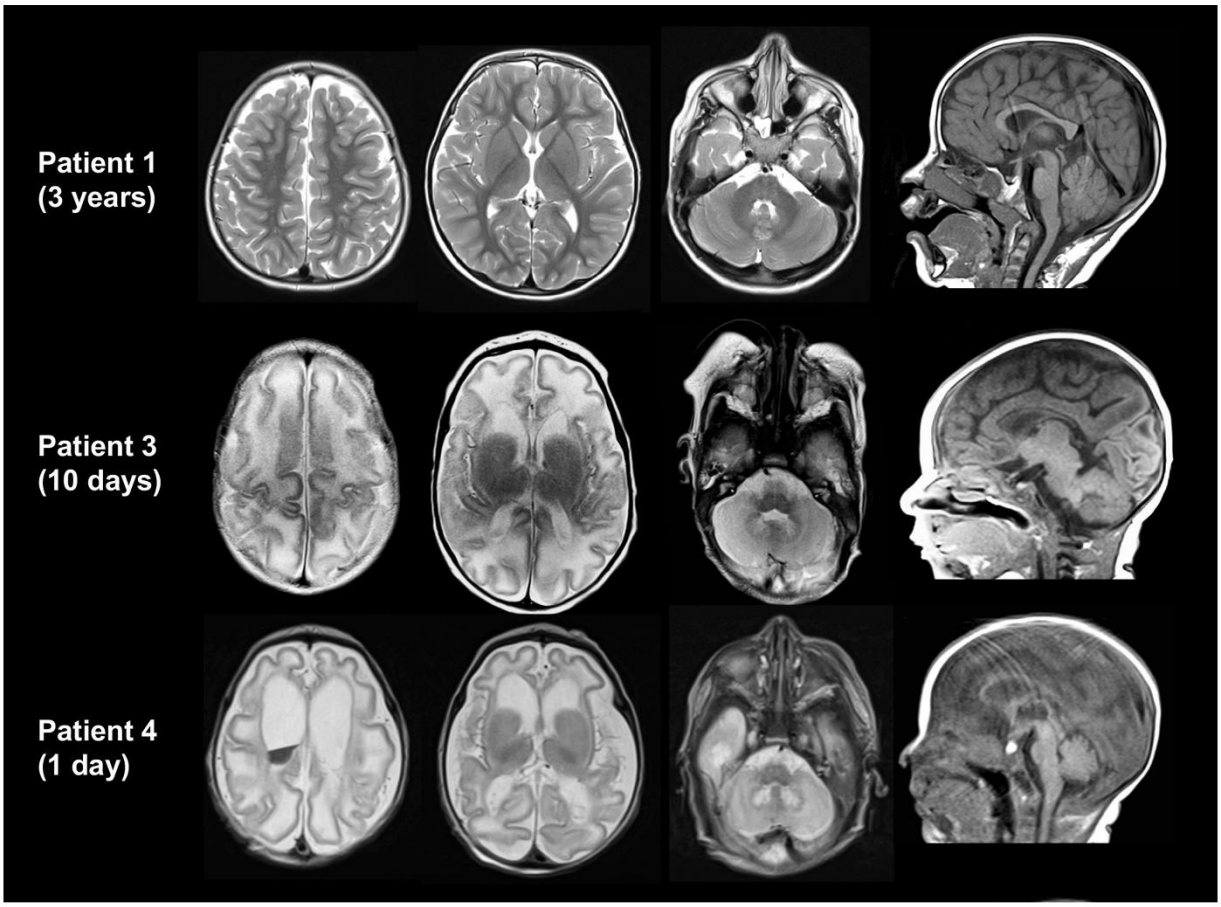
Patient 1
(3 years)
Patient 3
(10 days)
Patient 4
(1 day)

Figure 4.1: Patient MRI findings.

Axial T2 (first 3 columns) and sagittal (last column) T1-weighted images of patients 1, 3 and 4. At age 3 years, the MRI of patient 1 is normal. Patient 3 and 4 show a simplified gyral pattern, cyst-like structures connected to the anterior horns and a T2-hyperintense signal of the hilus of the dentate nuclei. White matter signal is T2 hyperintense and appears swollen. These abnormalities are more severe in patient 4 (who additionally has intraventricular blood) than in patient 3. The corpus callosum lacks the most posterior part.

4.4.2 Genotypic spectrum, variant effect prediction and clinical severity

Eight variants in *PLPBP* were identified in our patient cohort, mostly novel missense variants (Fig. 4.2, Supplementary Table 4.2). The exceptions are a novel homozygous frameshift deletion (c.370_373del) leading to a premature stop codon in two patients (5, 12) and the splice site variant (c.320-2A>G) previously reported by Darin *et al* 2016 (Supplementary Table 4.2) in another patient. To investigate potential genotype-phenotype correlations, we developed a clinical severity score to classify patients into three categories: mild, moderate and severe (Table 4.2). This score reflects the broad spectrum of clinical severity observed, ranging from B6-responsive epilepsy with normal developmental outcome, to perinatal lethality with lactic acidosis and structural brain malformations (e.g., patients 4 and 5). All truncating variants leading to complete LOF of PLPHP (c.207+1G>A, c.320-2A>G; p.Ser78Ter, p.Gln71Ter and p.Asp124Lysfs*2) are associated with the most severe forms of the disease (Table 4.2). In our cohort, this is evidenced in patients 5 (deceased) and 12, both affected by biallelic exon 5 frameshift variants (p.Asp124Lysfs*2) leading to absence of protein expression in patient fibroblasts (Supplementary Fig. 4.1).

To study the pathogenic effect of the missense variants in our cohort on PLPHP function (here based on PLP-binding, folding or stability), we modeled the tridimensional structure of the human PLPHP protein (Fig. 4.2B-D). The model indicates that PLPHP folds in a typical (β/α)8-TIM barrel structure, with PLP covalently bound to Lys47 (Schiff base). As with several TIM barrel fold members, a structurally conserved “phosphate binding motif” exists; this is formed by the end of β-strands and loops, especially at the C-terminal (258). Bound PLP interacts with R241, M225, S226, I242, G243, S244, V45, N68, I94 and M181 (Fig. 4.2C-D). Combining the novel and previously described variants (131, 132), 12 missense

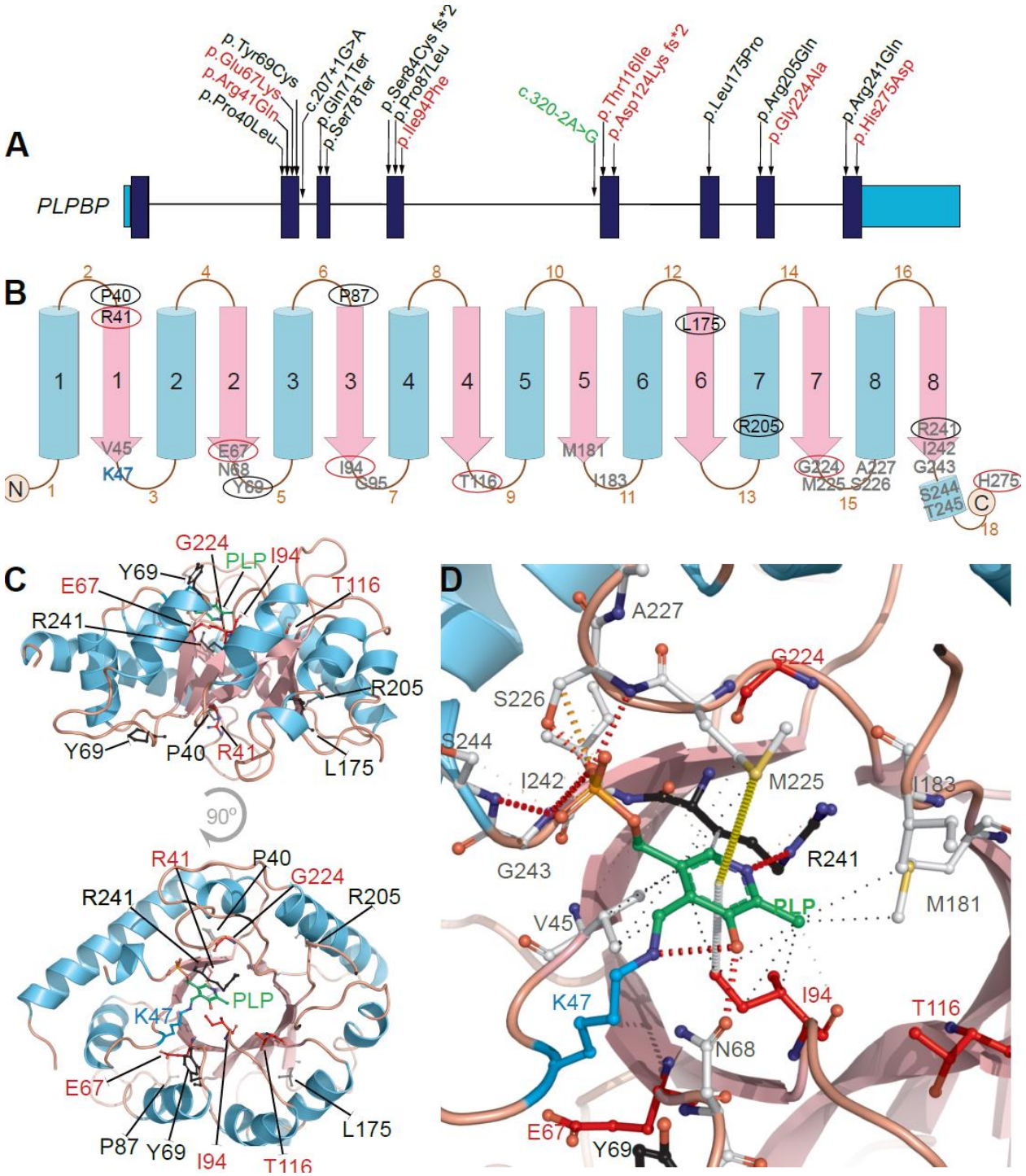
A
PLPBP
p.Tyr69Cys
p.Glu67Lys
p.Arg41Gln
p.Pro40Leu
c.207+1G>A
p.Gln71Ter
p.Ser78Ter
p.Ser84Cys fs*2
p.Pro87Leu
p.Ile94Phe
c.320-2A>G
p.Thr116Ile
p.Asp124Lys fs*2
p.Leu175Pro
p.Arg205Gln
p.Gly224Ala
p.Arg241Gln
p.His275Asp
B
N
C
P40
R41
P87
L175
R205
R241
V45
K47
E67
N68
Y69
I94
G95
T116
M181
I183
G224
M225
S226
A227
I242
G243
S244
T245
H275
C
PLP
I94
T116
90°
D
A227
G224
S226
S244
I242
M225
I183
R241
G243
M181
V45
K47
N68
E67
P87
L175

Figure 4.2: PLPBP variants and protein structure.

Pathogenic variants reported so far and their genetic location, predicted secondary structure and tridimensional structure in the PLPHP protein in the context of PLP-binding. (A) Human *PLPBP* gene structure, protein coding exons shown in dark blue and 5' and 3' UTR shown in light blue. Position of the variants reported previously by Darin *et al* (2016) and Plecko *et al* (2017) are shown in black, seven novel variants identified by this study are shown in red and a splicing variant reported previously but also observed in our cohort is shown in green. (B) 2D graphical representation of the PLPHP protein based on secondary structure prediction and the tridimensional model (shown in D). Blue cylinders represent the outer α-helices and pink arrows represent the inner β-strands that comprise the (β/α)8-TIM barrel structure. Residues observed mutated in PLPHP-deficiency are shown in circles, black for variants reported previously or red for novel variants reported here. Residues located within 6Å of the modeled PLP position are shown in blue, from which the residues that establish contacts with PLP shown in cyan. (C) Predicted PLP-binding pocket showing the key Lysine 47 predicted to form the PLP-Lys adduct, black dashed lines indicate hydrogen bonds and salt bridges, green solid line show hydrophobic interactions. (D) tridimensional structure of the human PLPHP model showing the PLP molecule in green and the positions of the residues found mutated in PLPHP-deficiency in black or red according to A. Note that the variant p.His275Asp was co-inherited homozygously with p.Thr116Ile in patient 1, we report this as a variant of unknown significance, however we also modelled it in panels B-D.

Table 4.2: Clinical severity scores.
Based on system adapted from (248). Variants are organized by whether seen homozygously vs. compound heterozygous, then based on variant type (missense, truncating, splicing). Note that truncating variants are associated with the most severe phenotypes. NA[a], NA[b], NA[c], full clinical scores could not be calculated due to early death of these patients but assumed severe based on lethality. NA* full clinical score could not yet be calculated due to early age of patient, so GDD/ID cannot yet be assessed. [1]Variant reported by (131). [2] Variant reported by (132). [3]Variant experimentally studied by (239).

Patient ID	Variant type	Amino acid change	First seizure/ movement episode score	GDD/ ID score	B6 response score	Severity score sum	Protein effect
Patients reported in this study							
1	Homozygous missense	p.Thr116Ile;	3	2	2	Severe (7)	Predicted LOF - variant likely impacts PLP binding
	Homozygous missense	p.His275Asp					Variant of unknown significance: variant likely impacts PLP binding
2	Homozygous missense	p.Arg41Gln	2	0	0	Mild (2)	Predicted to still bind PLP, but stability is reduced
3	Homozygous missense	p.Glu67Lys	3	3	2	Severe (8)	Predicted LOF - variant likely impacts PLP binding
4	Compound heterozygous nonsense & missense	c.320-2A>G;	3	NA[a]	NA[a]	Deceased: Severe (9)	LOF - Truncated protein[1]
		p.Gly224Ala					Predicted LOF - Variant likely disrupts loop 15 structure and orientation of several PLP binding residues
5	Homozygous nonsense	p.Asp124Lys fs*2	3	NA[b]	NA[b]	Deceased: Severe (9)	LOF - Truncated protein (band absent as in Supp. Fig 1)
6	Homozygous missense	p.Thr116Ile	3	2	3	Severe (8)	Predicted LOF - variant likely impacts PLP binding

Patient ID	Variant type	Amino acid change	First seizure/ movement episode score	GDD/ ID score	B6 response score	Severity score sum	Protein effect
7	Homozygous missense	p.Ile94Phe	1	1	1	Mild (3)	Predicted LOF? Variant likely impacts PLP binding, but it is possible Phe could still establish aromatic/hydrophobic contacts with PLP;
8	Homozygous missense	p.Arg41Gln	3	0	0	Mild (3)	Predicted to still bind PLP, but stability is reduced
9	Homozygous missense	p.Arg41Gln	3	0	0	Mild (3)	Predicted to still bind PLP, but stability is reduced
10	Homozygous missense	p.Glu67Lys	3	2	2	Severe (7)	Predicted LOF - variant likely impacts PLP binding
11	Homozygous missense	p.Glu67Lys	3	2	2	Severe (7)	Predicted LOF - variant likely impacts PLP binding
12	Homozygous deletion	p.Asp124Lys fs*2	3	NA*	2	NA*	LOF - Truncated protein (band absent as in Supp. Fig 1)
			Patients reported by (131)				
1	Homozygous nonsense	p.Ser78Ter	3	NA[c]	NA[c]	Deceased Severe (9)	LOF - Truncated protein[1]
2	Homozygous nonsense	p.Ser78Ter	3	2	3	Severe (8)	LOF - Truncated protein[1]
3	Homozygous nonsense	p.Ser78Ter	3	3	3	Severe (9)	LOF - Truncated protein[1]
4	Homozygous missense	p.Leu175Pro	3	3	2	Severe (8)	LOF - Misfolded protein[1,3]
5	Compound heterozygous missense & missense	c.207+1G>A; .320-2A>G	3	3	2	Severe (8)	LOF - Truncated protein[1]; absent band in Western blot1
6	Homozygous nonsense	p.Gln71Ter	3	2	3	Severe (8)	LOF - Truncated protein[1]
7	Compound heterozygous missense	p.Pro87Leu; p.Arg241Gln	1	1	1	Mild (3)	Lower solubility and some precipitated; Folded forms still binds to PLP [3] LOF - variant abolishes PLP binding3, drastic reduction in stability (Tm shift - 14ºC)[3]

Patient ID	Variant type	Amino acid change	First seizure/ movement episode score	GDD/ ID score	B6 response score	Severity score sum	Protein effect
			Patients reported by (132)				
1	Compound heterozygous missense & missense	p.Pro40Leu;	2	0	1	Mild (3)	Reduced stability (Tm shift - 6ºC); Still binds to PLP [3]
		p.Arg241Gln					LOF - variant abolishes PLP binding, drastic reduction in stability (Tm shift - 14ºC)[3]
2	Compound heterozygous truncating & missense	p.Ser84Cysfs*21;	2	1	1	Moderate (4)	LOF - Truncated protein [2]
		p.Arg205Gln					Reduced stability (Tm shift - 7ºC); Still binds to PLP 3
3	Homozygous missense	p.Pro87Leu	3	3	1	Severe (7)	Lower solubility and some precipitated; Folded forms still binds to PLP [3];
4	Homozygous missense	p.Tyr69Cys	2	0	2	Moderate (4)	Cys forms disulfide bridges that creates an artificial dimer that hides PLP. Decreased PLP binding in 30%[3]

PLPHP variants have been reported so far in B6RD patients (Fig. 4.2A), seven in homozygosity (Table 4.2). Patients 1, 3, 6, 10 and 11 from our cohort were classified as severe, with either p.Glu67Lys or p.Thr116Ile homozygous variants identified. Both substitutions were computationally predicted as damaging (Table 4.2, Supplementary Table 4.2). Residues 67 and 116 are conserved (Supplementary Fig. 4.4) and adjacently located to the predicted PLP-binding site (Fig. 4.2B-D); variants to Lys and Ile, respectively, likely lead to disruption of PLP-binding properties (Supplementary Table 4.2). Patients 4 and 2 were also classified as severe; patient 4 is compound heterozygous for the splice variant leading to LOF (c.320-2A>G) and the substitution of the highly conserved Gly224 (Supplementary Fig. 4.4) to Ala (Supplementary Table 4.2). The p.Gly224Ala variant likely impacts loop 15 structure and orientation of key PLP-binding residues, especially due to alanine's reduced degree of freedom (φ and ψ angles). Patient 1 is uniquely homozygous for two missense variants; p.Thr116Ile (discussed above) and p.His275Asp (an American College of Medical Genetics and Genomics variant of uncertain significance). The importance of the C-terminal residues for ligand binding, stability and activity of proteins that fold as a TIM barrel is well known (259, 260); therefore, a drastic chemical change like replacing a positively-charged amino acid by a negatively-charged amino acid at the C-terminus in the p.His275Asp variant may negatively impact these functions.

Of the four mild cases reported here, three patients (2, 8 and 9) are homozygous for p.Arg41Gln. Normal intellectual development, average-excellent school performance, seizures that are well controlled with relatively low doses of pyridoxine, and normal brain structure on MRI were reported in each of these patients. Arg41 is not an invariant residue (Supplementary Fig. 4.4) and is located in the distal face of the TIM-Barrel structure, not directly involved in PLP-binding. The p.Pro40Leu variant (adjacent residue) seen in a

previously reported mild case (132) still binds PLP but has reduced stability (239); it is possible that p.Arg41Gln has similar impact.

Patient 7 was also classified as mild and is homozygous for a p.Ile94Phe variant. This substitution is predicted to be damaging, destabilizing and likely inducing misplacement of PLP due to the large size of Phe compared to Ile (Supplementary 4.Table 2, Table 4.2). Although Phe has not been observed at this position among known orthologues (Supplementary Fig. 4.4), the milder phenotype in our patient with a p.Ile94Phe variant suggests that a hydrophobic/aromatic residue can be accommodated within the PLP-binding site.

4.4.3 Biochemical and vitamer profiles of PLPHP deficiency patients

Biochemical investigations performed in patients prior to B6 treatment uncovered several abnormal profiles. The most consistently observed alterations were hyperlactatemia (6 patients) and hyperglycinemia (3 patients). Urine organic acids investigation in patient 7 revealed the presence of vanillactic acid, vanillpyruvic acid, and n-acetyl-vanilalanine, similar to what is seen in AADC deficiency. Minor elevations of urine lactic, malic, 2-ketoglutaric, and n-acetylaspartic acids were also observed. Pre-treatment CSF metabolomics analysis showed elevated 3-methoxytyrosine (Z score = 4.2) with normal 3-methoxytyramine levels, and mild elevations of: palmitoyl-GPA 16:0 (Z-score= 3.7), α-ketoglutarate (Z-score= 3.2), adenosine (Z-score= 2.6), 2-aminooctanoate (Z-score= 2.6) and tryptophan (Z-score= 2.5).

B6 vitamer analysis in plasma from patient 4 (on no B6 treatment) revealed low levels of PLP (1.1nM, reference >20.5nM) and elevation of 4-pyridoxic acid (PA) (130 nM, reference

<84 nM). In a plasma sample from patient 3 collected during treatment with vitamin B6, accumulations of PLP (685 nM), PA (365 nM), and pyridoxal (PL) (276 nM) were observed (Supplementary Table 4.3). Analysis of B6 vitamers from patient 5 primary skin fibroblast lysates revealed significant decreases in PLP ($p<0.0001$), pyridoxamine 5'-phosphate (PMP) ($p=0.007$) and PN ($p=0.0018$), along with accumulation of pyridoxine 5'-phosphate (PNP) ($p<0.0001$, ANOVA) in the patient cells compared to the controls, whereas PL, pyridoxamine (PM) and PA showed no difference (Supplementary Fig. 4.2). Similarly, in PLPHP-deficient HEK293 cells, PLP was markedly decreased ($p<0.0001$) and PNP was greatly increased ($p<0.0001$) (Supplementary Fig. 4.3).

4.4.4 PLPHP mitochondrial localization and effects on energy metabolism

To provide further insights on PLPHP function, we investigated its subcellular localization in human cells. Some evidence suggests that PLPHP resides primarily in the cytoplasm (127, 261) (Human Protein Atlas available from www.proteinatlas.org). The MitoCarta 2.0 database, however, suggests a mitochondrial localization for human and mouse PLPHP (262, 263). Furthermore, MitoMiner 4.0 rates the protein as "known mitochondrial" (Integrated Mitochondrial Protein Index score 0.991), based on mass-spectrometry evidence (264).

To test if PLPHP does indeed localize to the mitochondria, we purified mitochondrial fractions using a recently developed method for immunoprecipitation of HA-tagged mitochondria in HeLa cells (249). The pure mitochondrial fractions were enriched for PLPHP, further evidencing the mitochondrial localization of this protein (Fig. 4.3A). Cytosolic and mitochondrial localization were also evidenced by immunofluorescence assays (Supplemental

Fig. 4.3B-C). Furthermore, we observed that the skin fibroblast cell line obtained from Patient 5 displays reduced growth in the presence of galactose as carbon source in the culture medium while normal growth was observed in the presence of glucose (Suppl. Fig 4.3C-D). Patient 5 fibroblasts also showed an elevated lactate-to-pyruvate ratio (41.65±7.13 SD; reference 9.57-26.49), which is consistent with NADH accumulation. Activities of mitochondrial pyruvate dehydrogenase and respiratory complexes II-IV were normal, as were mitochondrial morphology and inner membrane potential (data not shown). Extracellular flux testing showed an apparent reduction of carbonyl cyanide-*4*-(trifluoromethoxy)phenylhydrazone (FCCP)-stimulated spare respiratory capacity. These data may indicate that a direct role in electron transport is unlikely. However, considering that primary skin fibroblasts do not always replicate the disease phenotype in mitochondrial disorders (265), we decided to test other cell models.

Yeast is a well-established model to study mitochondrial function and disease (266). In yeast cells, ATP is produced through two mechanisms. In the presence of glucose, ATP is primarily generated via glycolysis, while gluconeogenesis and mitochondrial respiration are repressed. In the absence of fermentable carbon sources, the cell resorts to oxidative phosphorylation (OXPHOS) for the production of ATP. As a result, mutations affecting OXPHOS components are not lethal and the levels of expression of these components can be manipulated simply by changes in culture conditions (267).

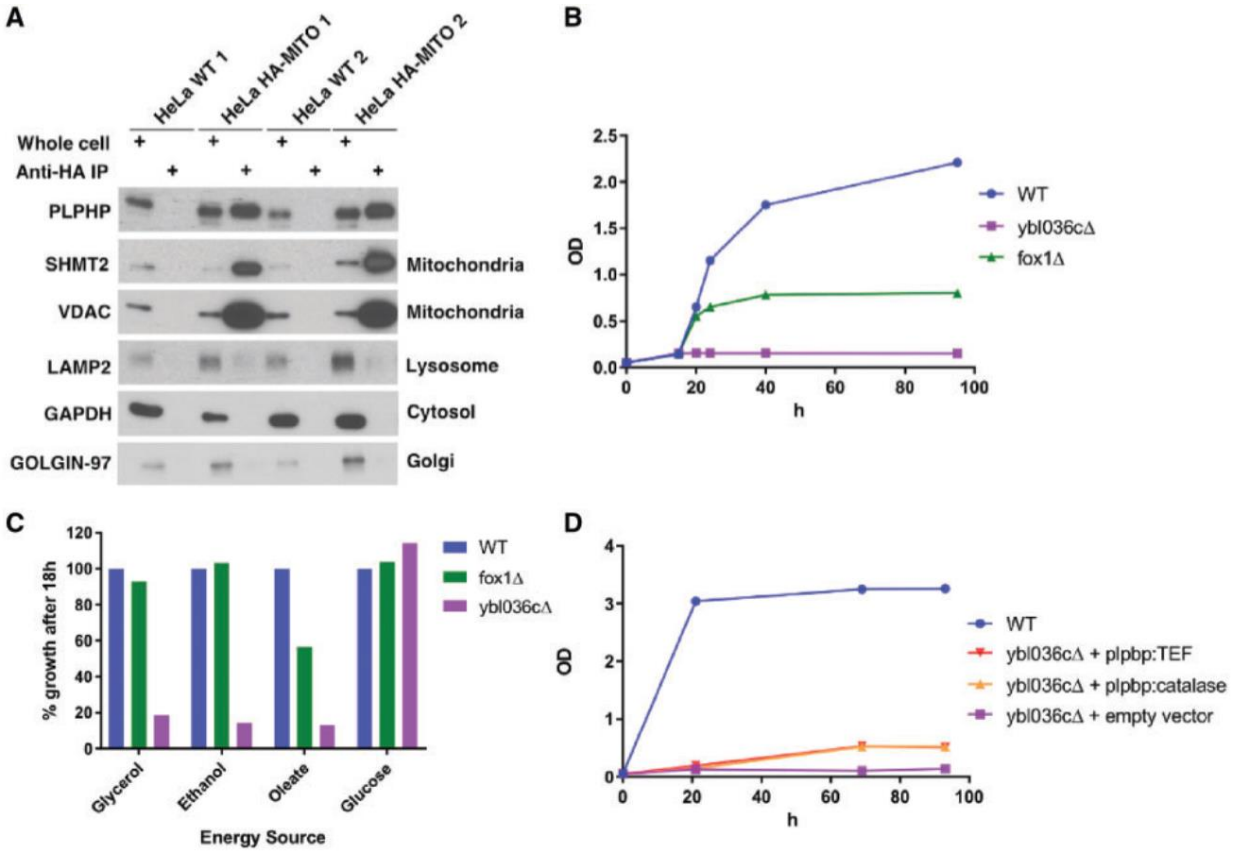
A
HeLa WT 1
HeLa HA-MITO 1
HeLa WT 2
HeLa HA-MITO 2
Whole cell
Anti-HA IP
PLPHP
SHMT2
VDAC
LAMP2
GAPDH
GOLGIN-97
Mitochondria
Mitochondria
Lysosome
Cytosol
Golgi
B
OD
h
WT
ybl036cΔ
fox1Δ
C
% growth after 18h
Glycerol
Ethanol
Oleate
Glucose
Energy Source
WT
fox1Δ
ybl036cΔ
D
OD
h
WT
ybl036cΔ + plpbp:TEF
ybl036cΔ + plpbp:catalase
ybl036cΔ + empty vector

Figure 4.3: Evidence of mitochondrial enrichment of PLPHP in HeLA cells and yeast.

(A) Western blot of WT HeLa cells and HeLa cells with HA-tagged mitochondria (HeLa HA-MITO) that were immunoprecipitated for mitochondrial purification, showing PLPHP enrichment in the mitochondrial fraction, other antibodies show minimal contamination from the cytosol or other organelles; (B) Growth curves of wild-type yeast cells and mutant strains on rich oleate medium. The strains shown are: WT (BY4742) (blue), *fox1Δ* (green) and *ybl036cΔ* (purple). (C) Growth of wild-type and mutant cells after 18 hours on 20g/L glucose and non-fermentable carbon sources: rich oleate, 2% ethanol and 2% glycerol medium. Values are expressed as % growth relative to WT. The strains shown are: WT (BY4742) (blue), *fox1Δ* (green) and *ybl036cΔ* (purple). (D) Growth of wild-type cells and mutant cells on 2% ethanol medium. The strains shown are: WT (BY4742) (blue), *ybl036cΔ* + pPROSC1a (human PLPHP under catalase promoter (orange) or pPROSC2a (human PLPHP under Tef promoter) (red) and *ybl036cΔ* + empty vector (purple).

To determine if PLPHP could play a role in energy metabolism, we studied the function of the PLPHP ortholog of *S. cerevisiae*: YBL036C. Growth of *ybl036Δ* yeast cells was completely normal on glucose medium but markedly reduced under conditions in which either glycerol, oleate, or ethanol was used as a carbon source (Fig. 4.3B-D). Since oxidation of the latter three substrates (but not glucose) is fully dependent on the proper functioning of the mitochondrial citric acid cycle and oxidative phosphorylation system, these findings suggest that YBL036C affects mitochondrial metabolism. Introduction of human PLPHP in *ybl036cΔ* yeast partially rescued the growth phenotype, which is consistent with a conserved function (Fig. 4.3D). Because PLP is a cofactor for key mitochondrial metabolism enzymes (118) including aspartate aminotransferase (AST) in the malate-aspartate shuttle and serine hydroxymethyltransferase (SHMT2) involved in one-carbon metabolism, the metabolic pleiotropy of PLPHP deficiency is expected, although the mechanisms through which *PLPBP* variants produce mitochondrial dysfunction remain to be elucidated in detail.

4.4.5 Loss of Plphp in zebrafish leads to spontaneous seizures and early death

We developed zebrafish lines carrying two different *plpbp* mutant alleles: a 4bp deletion (chr23:34037190-chr23:34037193) (NM_001126409; p.Asp23Lysfs*138) (*plpbp*^{ot101}) and the mutation CGG**GTGAATCA**A>CGG**TGG--TGG**A (chr23:34037185-34037192) (*plpbp*^{ot102}), the latter resulting in a 2bp frameshift, in the transcript (NM_001126409; p.Asp23Trpfs*56) (Fig. 4.4A). We crossed the F2s from each heterozygous line (*plpbp*$^{+/ot101}$ x *plpbp*$^{+/ot102}$) to generate compound heterozygous *plpbp*$^{ot101/ot102}$ (henceforth referred to as *plpbp*$^{-/-}$). F3 homozygous mutants and/or compound-heterozygous *plpbp*$^{-/-}$

displayed LOF of Plphp as evidenced by Western blot analysis (Fig. 4.4B). There were no phenotypic differences between homozygous and compound heterozygous mutants (Supplementary Fig. 4.7), and the latter was used for experiments due to the relative ease of genotyping (Supplementary Material). In the F3 generation, there were no obvious morphological or behavioral differences between genotypes up until ~9 dpf. As early as 10 dpf, *plpbp*$^{-/-}$ larvae showed spontaneous seizure-like behavior, and all mutants died by 16 dpf (Fig. 4.4C).

Epilepsy in zebrafish can be characterized by episodes of excessive locomotion, sustained rhythmic jerking (clonus), stiffening (tonus) and/or tonic-clonic seizures (140, 145, 255, 268). We measured the amount of high-speed movements as a correlate of hyperactivity and found that untreated *plpbp*$^{-/-}$ larvae spent significantly more time ($p<0.01$) and moved a greater distance in high-speed movements ($p<0.01$) than WT or heterozygous siblings (Fig. 4.4D-E). 11 dpf *plpbp*$^{-/-}$ larvae displayed increased *c-fos* mRNA expression (a biomarker of neuronal activity (255)) compared to WT larvae, but less than WT treated with 15mM PTZ (Fig. 4.4F). Finally, tectal field recordings of agar-immobilized 11 dpf larvae showed that mutant larvae (n=5) displayed spontaneous electrical discharges with high amplitude and duration, similar to ictal-like events previously reported in other zebrafish models, whereas WT siblings (n=5) showed only normal activity (Fig. 4.4G/4.5G). We conclude that *plpbp*$^{-/-}$ larvae recapitulate a seizure phenotype.

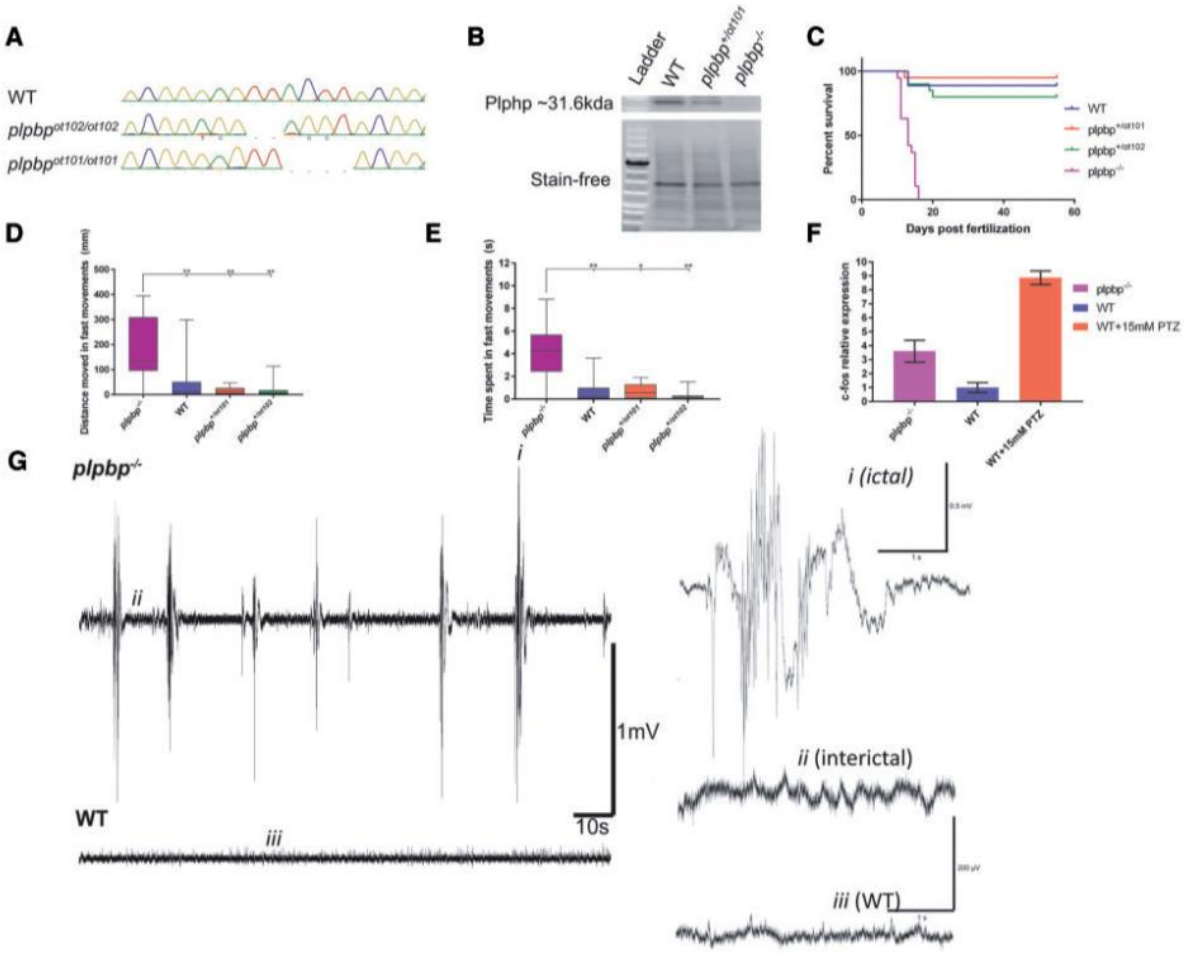
A
WT
plpbp ot102/ot102
plpbp ot101/ot101
B
Ladder
WT
plpbp +/ot101
plpbp -/-
Plphp ~31.6kda
Stain-free
C
Percent survival
Days post fertilization
WT
plpbp +/ot101
plpbp +/ot102
plpbp -/-
D
Distance moved in fast movements (mm)
E
Time spent in fast movements (s)
F
c-fos relative expression
plpbp -/-
WT
WT+15mM PTZ
G
plpbp-/-
i
ii
iii
1mV
10s
WT
i (ictal)
ii (interictal)
iii (WT)

Figure 4.4: Development of *plpbp*$^{-/-}$ zebrafish model by CRISPR/Cas9 and epileptic phenotypic analysis.

A) Chromatograms of zebrafish larvae showing WT and the genotypes for homozygous mutants *plpbp*$^{ot101/ot101}$ *and* *plpbp*$^{ot102/ot102}$. Compound heterozygous mutant larvae (*plpbp*$^{ot101/ot102}$) (not shown) were used for most experiments with the same phenotype as the homozygotes. (B) Cropped WB (for clarity) showing that no Plphp protein was detected in mutant larvae. Total protein (Stain free blot) is shown underneath for standardization. Full blot available in Supplementary Material. (C) Survival curves showing reduced survival of mutant larvae compared to WT and the two heterozygous parental types (n=20 larvae per group). (D and E) Mutant larvae moved a greater total distance during fast speed (>20mm/s) movements and spent more time in fast movements, respectively (n=16 larvae per group). (F) Relative mRNA expression showing increased expression of *c-fos* in mutant larvae compared to WT larvae, PTZ treatment was used as a positive control. (G) Example electrophysiology recordings of mutant (top) and WT (bottom) larvae showing increased number of ictal-like events. Inset are zoomed-in examples (4 seconds) of ictal-like, interictal and WT recordings. Significance: ** ($p<0.01$), * ($p<0.05$).

4.4.6 Vitamin B6 responsiveness and dependency in *plpbp*$^{-/-}$ larvae

We tested if seizures in *plpbp*-null zebrafish larvae show beneficial response to PLP and PN. Although we observed a PLP dose-dependent increase in the lifespan, all larvae died by 26 dpf, even at the highest dose (500 µM PLP) (Fig. 4.5A). Treatment with PN showed a more remarkable effect, with dose-dependent rescue of survival to nearly 100% until juvenile stages using 5 or 10 mM PN (Fig. 4.5B). Removal of PN daily treatments induced seizures and death within days, indicating B6-dependence, as previously reported for *aldh7a1*$^{-/-}$ larvae (149).

In agreement with the B6-dependency and rescue, PN treatment significantly reduced the number of hyperactive movements as measured by the time spent ($p=0.0028$) and distance travelled in high-speed movements ($p<0.0001$) (Fig. 4.5D-E). Additionally, by classifying larval movements as little movement (S0), increased spontaneous swim bursts (S1), whirlpool-like swimming (S2) or whole-body convulsions with loss of posture (S3) (255) through blinded analysis, we observed that only untreated *plpbp*$^{-/-}$ larvae displayed S2 or S3 swimming behavior (Fig. 4.5F). Similarly, treatment with 5mM PN resulted in a 5-fold reduction of the number of high-amplitude spikes of electrographic activity in tectal field recordings ($p=0.0458$) (Fig. 4.5G). We conclude that *plpbp*$^{-/-}$ larvae have B6-responsive and dependent epilepsy.

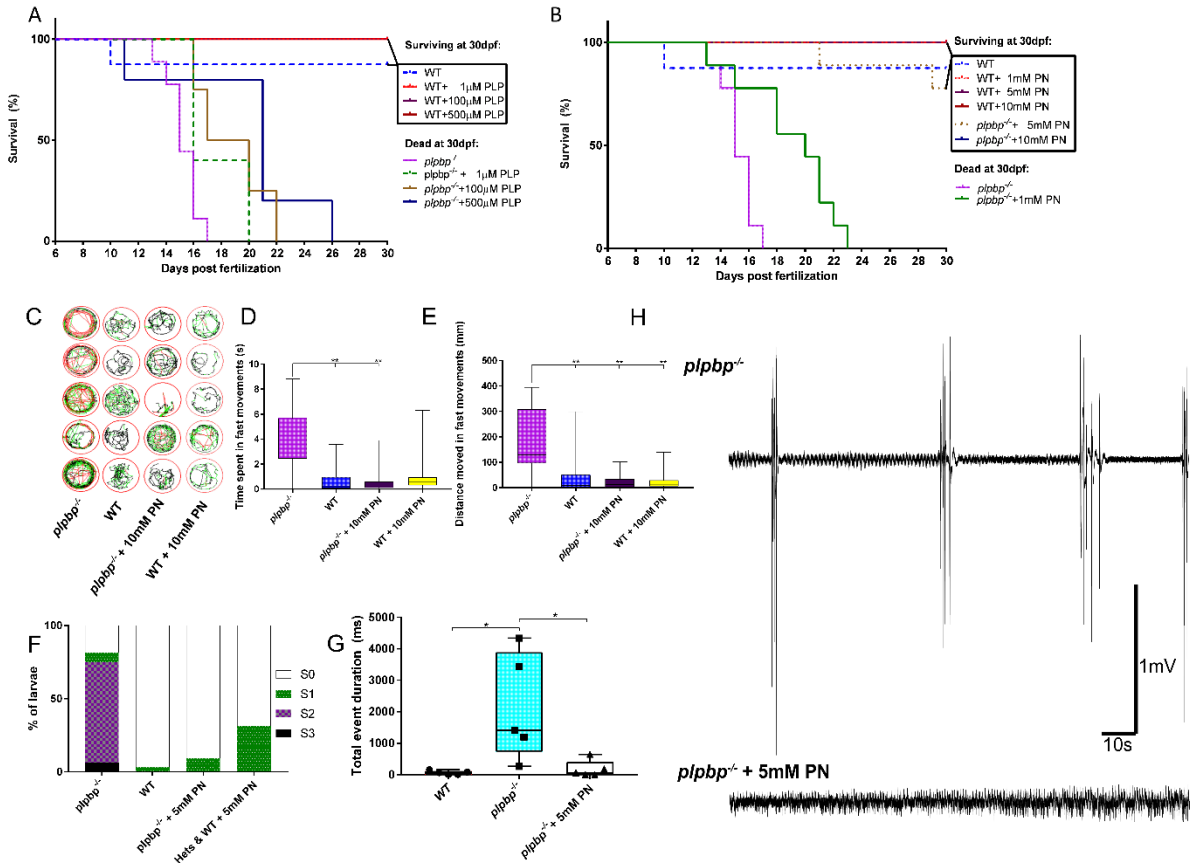
A
Survival (%)
Days post fertilization
Surviving at 30dpf:
WT
WT+ 1μM PLP
WT+100μM PLP
WT+500μM PLP
Dead at 30dpf:
plpbp-/-
plpbp-/- + 1μM PLP
plpbp-/-+100μM PLP
plpbp-/-+500μM PLP
B
Survival (%)
Days post fertilization
Surviving at 30dpf:
WT
WT+ 1mM PN
WT+ 5mM PN
WT+10mM PN
plpbp-/-+ 5mM PN
plpbp-/-+10mM PN
Dead at 30dpf:
plpbp-/-
plpbp-/-+1mM PN
C
plpbp-/-
WT
plpbp-/- + 10mM PN
WT + 10mM PN
D
Time spent in fast movements (s)
E
Distance moved in fast movements (mm)
H
plpbp-/-
1mV
10s
plpbp-/- + 5mM PN
F
% of larvae
S0
S1
S2
S3
plpbp-/-
WT
plpbp-/- + 5mM PN
Hets & WT + 5mM PN
G
Total event duration (ms)
WT
plpbp-/-
plpbp-/- + 5mM PN

Figure 4.5: Vitamin B6-responsive epilepsy in *plpbp*$^{-/-}$ zebrafish larvae.

Survival in mutants was moderately improved using PLP (A) but showed a better response that was clearly dose-dependent with pyridoxine (B). (C) 5-minute trace recordings of 11 dpf zebrafish larvae showing increased hyperactivity in the mutants which was alleviated with 10mM pyridoxine treatment, as measured by (D) time spent in fast movements and (E) distance moved in fast movements. (F) Highest seizure-like behavior category identified by blinded observers. Only untreated mutant larvae showed evidence of S2 or S3 seizure-like activity. (G) Electrographic activity in mutant larvae was normalized by treatment with 5mM pyridoxine. (H) Example electrophysiology recordings of untreated and treated mutant larvae. Significance: ** ($p<0.01$), * ($p<0.05$).

4.4.7 Biochemical abnormalities in *plpbp*$^{-/-}$ zebrafish

B6 vitamer levels were quantified in untreated 10 dpf larval lysates. The *plpbp*$^{-/-}$ larvae displayed significant reductions in systemic concentrations of PLP and PL (1.4 and 5.5-fold reductions, p=0.0026 and p=0.0003, respectively) compared to WT siblings, together with non-significant reductions in PMP and PN levels (Fig. 4.6A). PNP was not detectable in either group. As PLP was markedly low in *plpbp*$^{-/-}$ larvae, we hypothesized that neurotransmitter and amino acid metabolism would be greatly affected since most transamination/decarboxylation reactions require PLP. Neurotransmitters were also analyzed in fasted 11 dpf larval lysates (Fig. 4.6B). We noted a significant decrease in levels of adrenaline ($p<0.001$) as well as significant accumulations of 3-methoxytyramine (3-MT), normetanephrine and 5-hydroxyindoleacetic acid (5-HIAA) ($p<0.001$).

Analysis of amino acid levels by liquid chromatography-mass spectrometry in fasted larvae revealed 17 analytes significantly different between homozygous mutants and the heterozygous/WT siblings (Fig. 4.6C). Nine analytes were found reduced in *plpbp*$^{-/-}$ larval extracts: threonine, asparagine, glutamate, glutamine, proline, alanine, α-aminobutyric acid, γ-aminobutyric acid (GABA), and lysine (Tukey's post-hoc comparison: p= 0.0315, <0.0001, 0.0015, <0.0001, 0.0020, <0.0001, 0.0006, <0.0001, and 0.0068, respectively). Eight compounds were significantly elevated in *plpbp*$^{-/-}$ larvae compared to WT: methionine, cystathionine, isoleucine, tyrosine, ß-alanine, phenylalanine, aminoisobutyric acid and tryptophan (p=0.0147, <0.0001, <0.0001, 0.0005, <0.0001, <0.0001, <0.0001, and 0.0013,

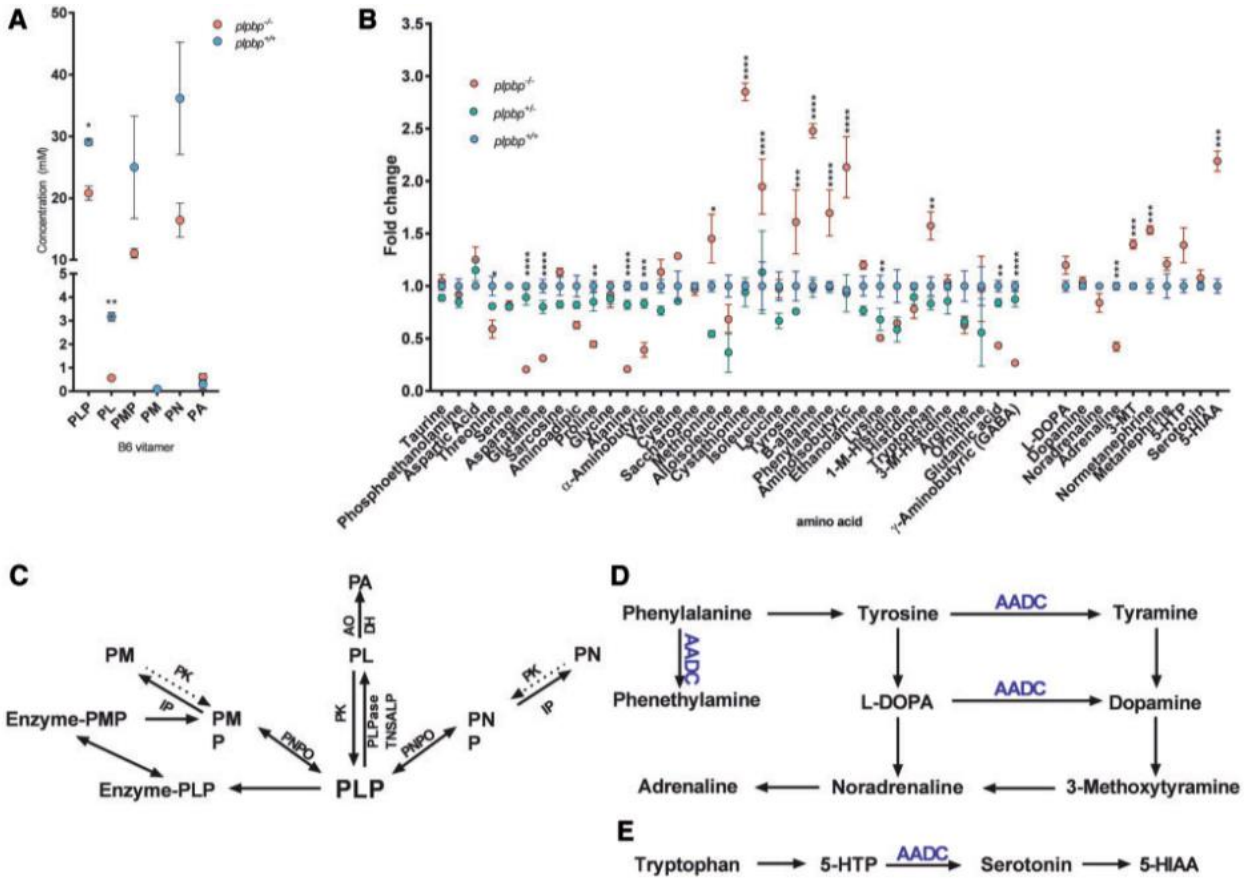
A
B
C
D
E
Concentration (mM)
B6 vitamer
PLP
PL
PMP
PM
PN
PA
Fold change
amino acid
PM
PK
PP
Enzyme-PMP
PNPO
Enzyme-PLP
PA
AO
DH
PL
PLPase
TNSALP
PLP
PN
Phenylalanine
Tyrosine
AADC
Tyramine
Phenethylamine
L-DOPA
Dopamine
Adrenaline
Noradrenaline
3-Methoxytyramine
Tryptophan
5-HTP
Serotonin
5-HIAA

Figure 4.6: Targeted mass spectrometry studies of *plpbp*$^{-/-}$ zebrafish larvae indicates changes in B6 vitamer, amino acid, and neurotransmitter profiles.

(A) B6 vitamer profile of Mutant and WT 10 dpf larvae. (B) Amino acid and neurotransmitter profile of whole larval mutant, heterozygous and WT 11 dpf larvae after 24 hours fasting. (C) Metabolic pathways for the synthesis and degradation of PLP. (D). Biosynthetic pathways of catecholamines and trace amines, highlighting (in blue) the role of AADC. (E) The serotonin biosynthesis pathway, highlighting the role of AADC.
Abbreviations: 3-MT: 3-methoxytyramine, 5-HIAA: 5-hydroxyindoleacetic acid, 5-HTTP: 5-hydroxytrytpophan, AADC: aromatic-L-amino acid decarboxylase, AO: *aldehyde oxidase I*, DH: β-NAD dehydrogenase, PA: 4-pyridoxic acid, PK: pyridoxal kinase, PL: pyridoxal, PLP: Pyridoxal 5'-Phosphate, PM: pyridoxamine, PMP: pyridoxamine 5'-phosphate, PN: pyridoxine, PNP: pyridoxine 5'-phosphate, PNPO: PNP oxidase Significance: ****($p<0.0001$), ***($p<0.001$), ** ($p<0.01$), * ($p<0.05$).

respectively). Low GABA levels were also observed in *aldh7a1*$^{-/-}$ zebrafish and could constitute part of the pathophysiologic mechanism for seizure occurrence. We conclude that Plphp deficiency leads to significant disruptions in amino acid and neurotransmitter metabolism and likely other metabolic pathways that are dependent on PLP in zebrafish.

4.5 Discussion

Here we report a cohort of 12 patients, six novel disease-causing variants in *PLPBP*, and experimental models to further elucidate the pathophysiology of this B6RD. Many of the clinical features of PLPHP deficiency in this new cohort of patients concur with those described by Darin *et al* 2016 and Plecko *et al* 2017, thus confirming the previously described phenotypic spectrum (131, 132). Additionally, our patients presented with novel features; one patient required folinic acid in addition to B6 for adequate seizure control, two patients suffered a lethal mitochondrial encephalopathy phenotype, while another patient presented with an AADC deficiency-phenocopy without clear epilepsy. Darin *et al* (131) described increased levels of AADC substrates in another PLPHP-deficient patient, and our zebrafish *plpbp*$^{-/-}$ model accumulated phenylalanine, tryptophan and tyrosine, in keeping with reduced AADC function. It is possible that reduction of AADC function may contribute to the clinical picture in PLPHP-deficient patients, given it is a PLP-dependent enzyme important in the biosynthesis of serotonin, dopamine, epinephrine and norepinephrine (269).

The severe clinical presentation of patients 4 and 5 with respiratory failure, chronic lactic acidosis, NADH accumulation, and periventricular cerebral cysts prompted us to investigate whether PLPHP could have a role in mitochondrial energy metabolism. We observed enrichment of PLPHP in pure mitochondrial fractions extracted from HA-tagged

mitochondria in HeLa cells (Fig. 4.3). The mitochondrial enrichment was also evidenced by immunofluorescence studies (Supplemental Fig 4.3). *In silico* prediction tools and previous high-throughput mass spectrometry experiments suggested intracellular localization of PLPHP for both the cytoplasm and mitochondria (263, 264). Although we could not identify clear electron transport chain defects in in the primary skin fibroblast cell line obtained from patient 5 by Seahorse assay, its reduced growth in galactose and our identified mitochondrial enrichment of PLPHP encouraged us to investigate other models.

S. cerevisiae is a well-established model to study mitochondrial defects (266), and we observed that energy metabolism is affected in yeast cells deficient for the PLPHP ortholog, YBL036C (*ybl036cΔ* cells) (Fig. 4.3B-D). It is not yet clear if this is due to a direct effect or to indirect changes in key energy metabolism substrates. Several PLP-dependent enzymes, such as SHMT2 (270), AST and the glycine cleavage system (271) have mitochondrial localization. It has also recently been shown that LOF variants in *KYNU*, encoding a PLP-dependent enzyme, lead to deficiencies in the synthesis of NAD (272). The kynurenine pathway uses tryptophan as a precursor for NAD biosynthesis, and several PLP-dependent enzymes are involved (273). The multitude of enzymatic functions of PLP may explain the complex array of biochemical phenotypes associated with B6RDs, suggestive of a key role of PLPHP in PLP homeostasis.

By adapting a clinical severity score used for another B6RD (248), we observed that the patients with severe phenotypes (scores 7-9) and/or early mortality were usually associated with proven or predicted LOF variants (Table 4.2). These included splicing defects, truncating variants, and missense variants predicted or experimentally proven (239) to affect PLP binding negatively. A missense variant associated with a severe disease presentation (131),

p.Leu175Pro, was experimentally proven to induce PLPHP LOF due to protein misfolding (239). In contrast, it seems that missense variants in residues not associated with the PLP-binding site are seen in patients with milder disease presentations (Table 4.2). When stability and folding are not drastically affected, it is possible that PLPHP is still able to bind PLP, as evidenced experimentally for p.Pro40Leu and p.Arg205Gln (239). Residual PLP binding and PLPHP function may be associated with milder presentations of the disease. *In silico* molecular dynamics simulations or *in vitro* assessment of PLP binding, PLPHP folding and stability should be performed to further access these scenarios in the missense variants reported here. We acknowledge that the clinical data presented and used to assess clinical severity was collected retrospectively after patients were identified, which limited the level of detail available. Future prospective natural history studies would be valuable in further clarifying the phenotype.

In both lysates derived from patient fibroblasts and PLPHP-deficient HEK293 cells, decreases in intracellular PLP were observed. Intracellular PLP was found to accumulate as reported by Darin *et al* 2016; further work may be necessary to resolve this discrepancy. A significant accumulation of PNP levels was found in PLPHP-deficient cells, but our methods were not sensitive enough for the detection of PNP in plasma, CSF or whole zebrafish larvae. PNP accumulation, therefore, may be of limited use as a biomarker of the disease, but it may help to unravel the functional role of PLPHP.

To enable analysis of the untreated biochemical status, improve our understanding of the pathophysiology of this disease, and establish a platform for potential drug discovery, we successfully developed a *plpbp*-null zebrafish model. The *plpbp*$^{-/-}$ larvae recapitulated the disease, and seizure activity was detected as early as 10 dpf, with 100% mortality by 16 dpf. Treatment with PN fully reversed these phenotypes, and treated *plpbp*$^{-/-}$ larvae often survived

to adulthood, but PLP was not very effective, similar to *aldh7a1*$^{-/-}$ larvae (149). It is possible that low water solubility, instability, or light sensitivity of PLP play an important role in the ineffectiveness of PLP. Larvae showed significant changes in the levels of B6 vitamers, particularly PLP and PL, which lend further support to the hypothesis that PLPHP is important for PLP homeostasis (129, 131). By quantifying systemic amino acid levels, our results indicate disruption of many key PLP-dependent enzymes. Furthermore, the reduction of GABA may provide a possible explanation for the increased neuronal activity of mutants, as has been previously reported in *aldh7a1*$^{-/-}$ zebrafish (149). Another mechanism to consider as part of disease pathophysiology is altered biosynthesis of catecholamines (especially adrenaline), likely due to reduced availability of PLP for AADC activity (Fig. 4.6D). This is further evidenced in the mutant animals by the accumulation of phenylalanine, tryptophan and tyrosine (precursors to monoamine neurotransmitter synthesis). PLPHP-deficiency patients with AADC deficiency-like symptoms may provide support to this observation. Given that systemic dopamine levels were unchanged, a reduction of metabolic flux towards AADC is likely taking place, rather than a complete inactivation of this enzyme; alternatively, small amounts of dopamine may be formed via tyramine hydroxylation by renal CYP2D6, as suggested by (274). Our results illustrate the dynamic and complex nature of PLP binding to dependent enzymes and its turnover in the context of PLPHP deficiency.

In conclusion, we presented detailed profiles of the clinical, genetic and biochemical alterations of PLPHP deficiency in a series of 12 new patients. Given the broad phenotypic spectrum of B6RDs, PLPHP deficiency should be considered in neonatal/infantile epilepsy and possibly also in patients who present with a movement disorder ‘only’ and/or a phenotype suggestive of mitochondrial epileptic encephalopathy. In the latter case, we note that patients with severe forms of this disease may show increased levels of glycine in combination with

marked lactic acidosis, a finding not typical of similar presentations such as pyruvate dehydrogenase deficiency (275). When PLPHP deficiency is suspected, B6 therapy should be initiated. A lack of response to PN may not rule out this condition, and PLP should be trialed as well. We recommend obtaining diagnostic samples prior to B6 treatment and screening for vitamer levels, with low PLP suggestive of this condition.

We report the first animal model organism for PLPHP deficiency, which replicated the human epileptic disorder. Research using the zebrafish *plpbp*$^{-/-}$ has added insight into which PLP-dependent pathways are mostly affected and increased our understanding of systemic B6 vitamer dysfunction. The pathophysiology of the seizure phenotype in zebrafish seems to be connected with impaired PLP-dependent neurotransmitter biosynthesis and homeostasis. This model may be used to investigate other disease mechanisms and to search for biomarkers that may facilitate diagnosis. Finally, our zebrafish model provides a steppingstone for preclinical treatment trials, which are necessary, given the poor developmental outcomes and incomplete seizure control seen in many patients with this form of B6-dependent epilepsy.

4.6 Supplemental Materials

Clinical Patient Descriptions

note: MRI findings detailed in Fig. 4.1 and Supplementary Table 4.1

Case vignettes with phenotypic features not previously described

Fatal mitochondrial encephalopathy

Patient 4

This girl of Dutch non-consanguineous origin, who died at 2 weeks of age, was the first of DCDA twins, born via spontaneous vaginal delivery at 36+6 weeks gestation (birth weight: 2215 g (10^{th} percentile), head circumference 30.7 cm (-2.5 SD corrected for gestational age) and APGAR 6/7/8). The family history was negative for epilepsy or developmental problems. Her twin sib is healthy with normal development. Directly postpartum, spontaneous breathing was insufficient, requiring assisted ventilation for 5 minutes followed by CPAP with oxygen. Spontaneous ventilation was restored. Glucose was 4.5 mmol/L but rapidly decreased to <0.6 mmol/L one hour postpartum and remained between 0.8 and 1.8 for four hours despite extreme supplementation dosages; at 6 hours postpartum normoglycemia was first reached (6.6 mmol/L). Initial lactate was 19 mmol/L, CK 3137 U/L (normalized to 232 U/L at day 9). A brain ultrasound on postnatal day 1 showed a dilation of the ventricular system, intraventricular bulkheads, an abnormal gyral pattern and abnormal white matter.

Neurologically the girl showed strong motor unrest and progressive axial hyperextension upon light touch. Seizures probably started at day 1 postnatally (but could not be proven by EEG at that time) and escalated at day 3 (irritability, nystagmus, tonic spasms of

the face, thorax and arms, later on also tachycardia, hypertension, apneas, and desaturations, followed by crying and grimacing). The first EEG (postnatal day 1) showed a diffusely abnormal and excessively discontinuous pattern. Upon external stimulation, there was sharp polymorphic and asynchronous activity in the central areas and sometimes more generalized. EEGs on day 4 and 7 displayed a similar background, progressively frequent BIRDS (brief ictal rhythmic discharges) and progressive episodes of rhythmic sharp activity compatible with electrographic neonatal seizures, sometimes without clinical correlate. Over the course of two weeks several AEDs were trialed, all leading to unsustained (minutes to one hour) and only partial seizure control. Because of the severe structural brain abnormalities on ultrasound and MRI, pyridoxine treatment was not considered. Phenobarbital loading doses up to 40 mg/kg were followed by 5 mg/kg/day. Levetiracetam was given twice daily (60 mg/kg) after 2 loading dosages of 20 mg/kg. Continuous intravenous midazolam (0.8 mg/kg/hour) with several additional loading doses had a similar effect. Finally, repeated doses of oral chloral hydrate (50 mg/kg) accomplished a good clinical response for several hours. However, seizures became intractable and on day 16, after elevating midazolam and adding morphine for comfort control the girl died of respiratory depression and bradycardia. Permission for restricted brain autopsy was granted by the parents (only one slice). Histopathological examination showed focal abnormalities, mainly of the white matter consistent with hypoxic-ischemic injury. WES open exome trio-analysis came back negative at first. However, re-analysis of open exome data revealed a compound heterozygous mutation in *PLPBP*.

Patient 5

This female neonate was the first child to consanguineous parents (second cousins) of Cree First Nation ancestry. The pregnancy was unremarkable, but a Caesarean delivery was performed at term due to a non-reassuring fetal heart rate. Her birthweight was 3470 g (76th percentile), head circumference was 35 cm (82nd percentile) and height was 47cm (14th percentile). The child briefly (10-15 seconds) received positive pressure ventilation for poor respiratory effort, being initially stable. Over the first hours of life, she developed progressive respiratory failure requiring intubation and transfer to a tertiary care NICU.

The admitting diagnosis was suspected birth asphyxia. Her neurological examination was notable for hypertonia, hyperreflexia, and abnormal movements (persistent flexion and clenching of her upper extremities). Clinical seizures were noted on the first day of life; EEG was markedly abnormal with a burst-suppression pattern, and she was given a neurological diagnosis of early infantile epileptic encephalopathy (Ohtahara syndrome). Routine lab studies were notable for a persistently increased lactate level in blood (range 1.5 - 11.2 mmol/L) and cerebrospinal fluid (5.6 mmol/L).

The patient was successfully extubated post-transport, however her seizures proved to be refractory. Seizures were managed, to the extent possible, with an intravenous midazolam infusion (150 µg/kg/hour), followed by an escalating series of up to six simultaneous anticonvulsant agents, and high-dose prednisone. Empiric therapy with biotin and thiamine produced no obvious benefit (pyridoxine was not tried). Seizures and apneic episodes persisted, becoming increasingly frequent despite these treatments. At eight weeks of age, she acutely deteriorated with recurrent apneas, acute renal failure, and hemodynamic compromise, and care was recognized to be futile, and withdrawn.

The patient's clinical presentation and imaging were considered most consistent with a mitochondrial disorder. Plasma amino acids were notable for hyperglycinemia (943-1010 µmol/L; reference interval 81-436) with corresponding high glycine in CSF (28 µmol/L; reference interval 3-23); of note, alanine and proline concentrations in blood and CSF were normal. Acylcarnitine profile was normal. Urine organic acids showed increased excretion of lactic, pyruvic, and 2-hydroxybutyric acids, consistent with lactic acidosis. Muscle biopsy was refused; cultured skin fibroblasts showed an elevated lactate-to-pyruvate ratio (41.7 +/- 7.13; reference interval 9.6-26.5), normal activities of several enzymes (pyruvate dehydrogenase (PDH) native: 0.94±0.06nmoles/min/mg protein, ref 0.46-1.60; PDH: 1.32±0.06nmoles/min/mg protein, ref 0.87-2.33; pyruvate carboxylase: 0.51, ref 0.35-5.18; and respiratory complexes II-IV), and normal mitochondrial morphology and inner membrane potential. Extracellular flux testing showed an apparent reduction of carbonyl cyanide-*4*-(trifluoromethoxy)phenylhydrazone (FCCP)-stimulated spare respiratory capacity.

Genetic investigations which were normal or inconclusive in the patient included oligonucleotide microarray, mtDNA point mutation panel, and an NGS-based nuclear mitochondrial gene panel (Mitome200, Baylor College). She was enrolled into a local research program and an NGS-based panel of 4,813 genes associated with any clinical phenotype (Illumina TruSight One) was performed and negative. Whole-exome sequencing of the proband and both parents was performed as described (185, 276), identifying a homozygous frameshift mutation in NM_007198(*PLPBP*):c.370_373del (p.Asp124Lysfs*2). Absence of PLPHP protein expression was confirmed by immunoblot of fibroblast lysates from the patient and controls (Supplementary Fig. 4.1).

Movement disorder without epilepsy

Patient 7

This boy, currently 23 months old, was born at term to non-consanguineous parents who originate from a small town in Guatemala. He was born with bilateral syndactyly of the third and fourth fingers. His birth weight was 3.317 kg (47.6th percentile, Z = -0.06), head circumference was 33 cm (12.5th percentile, Z = -1.15) and APGAR 9, 9. He initially presented at 2 months of age for abnormal movements: flexor posturing with arm abduction, tonic posturing of his UE and LE with internal rotation of his arms, jerking of the left arm and upward eye deviation with each event. There were no recognized triggers of these events, and they clustered for minutes to over an hour. He did not present with clear epilepsy. His initial routine EEG was read as disorganized background and bursts of higher-amplitude activity, with several spike and slow wave complexes followed by electro-decrement with clinical correlate of subtle twitch. Although this EEG did not meet criteria for hypsarrhythmia, there was high clinical suspicion for infantile spasms with emerging hypsarrhythmia on EEG; he was thus treated for infantile spasms with high dose prednisolone. CSF analysis of cell count, chemistry and culture were unremarkable.

His parents discontinued prednisolone on the 8th day of treatment due to side effects of irritability, diarrhea, persistence and worsening of his abnormal movements. An inpatient video EEG captured non-epileptic opisthotonic-like events (back arching, sometimes twisting at the trunk, occasional arm stiffening) and oculogyric crises. These movements did not correlate with electrographic changes on the EEG suggestive of seizures or spasms and were determined non-epileptic. He would become extremely tachycardic with the events. Cardiac and GI workups were negative. His movements did not respond to lorazepam (0.1 mg/kg),

though reduced in frequency during levetiracetam treatment (30 mg/kg twice daily), and parenteral hydration. Biochemical labs revealed a profile suggestive of aromatic L-amino acid decarboxylase (AADC) deficiency (see details below) and he was started on recommended treatment for this disorder: PN 50 mg BID, PLP 60 mg TID and Sinemet 0.4 mL TID (approximately 1 mg/kg/day based on levodopa component) at 2.5 months of age with complete resolution of symptoms on this regimen. Once *PLPBP* mutation was identified, Sinemet was later discontinued (at age of 8 months) and he is currently on a mixed regimen of PN (23 mg/kg/day div BID) and PLP (30 mg/kg/day div TID). Following initiation of treatment, all subsequent EEGs have been normal.

Early developmental milestones were achieved within the normal age range; more recently, asymmetric delays were identified. At the age of 20 months, his vision and hearing grossly intact and motor neurological exam was normal: normal bulk, full strength at all extremities at distal and proximal muscles in BUE and BLE, no hypotonia, sits, crawls, walks independently, stands flat footed; sensation: intact grossly at all extremities; coordination: no tremor, reaches for objects with both hands, transfers objects between hands, pincer grasp, using hands equally; reflexes: 2+ bilateral bicep and BR, symmetric brisk 2+ at patella, symmetric 2 at ankles, no clonus. At 23 months of age, significant delays were noted in expressive and receptive language skills with preservation of gross and fine motor development.

Biochemical investigations: Lactate remained normal when checked on hospital readmission (1.7 mM, reference range: <2.0 mM). However, during a third admission, he was confirmed to have elevated lactate (8.46) and metabolic acidosis on VBG with elevated anion gap (23) as well as hyperglycemia (325) in the setting of repeated opisthotonic events. His UA

showed 4+ glucose and 1+ ketones. His hyperglycemia and elevated lactate corrected quickly following a NS bolus. CRP and ammonia were normal.

Urine organic acids resulted positive for presence of vanillactic acid, vanilpyruvic acid, and n-acetyl-vanilalanine; also, minor elevations of lactic, malic, 2-ketoglutaric, and n-acetylaspartic acids. This profile is typical of aromatic AADC deficiency, an enzyme necessary for synthesis of neurotransmitters (DA, Epi, NE, 5HT). The rest of the metabolic workup (including plasma amino acids, acylcarnitine profiling) was negative. Confirmatory testing with AADC enzyme assay revealed partial enzymatic activity (18.84 pmol/min/mL), suspicious for carrier status of the condition but not complete AADC enzyme deficiency. Biochemical analysis of CSF at age of 2 months (before B6 treatment) showed normal levels of glucose (71 mg/dL, reference range: >40 mg/dL) but elevated protein concentration (75 mg/dL, reference range: <45 mg/dL) which normalized after B6 treatment (25 mg/dL at age of 2.5 months). Pre-B6 treatment CSF metabolomics (at age of 2 months) revealed several minor elevations of (Z score): 3-methoxytyrosine (4.2), palmitoyl-GPA 16:0 (3.7), alpha-ketoglutarate (3.2), adenosine (2.6), 2-aminooctanoate (2.6) and tryptophan (2.5).

Clinical whole-exome sequencing (WES) on the proband identified a homozygous variant in the *PLPBP* (c.280 A>T, p.Ile94Phe in exon 4). A homoplasmic variant in MT-ND1 was also described. A dopamine-related disorders gene panel identified a heterozygous pathogenic splice variant in *DBH* (c.339+2T>C). No variants were detected in *DDC*, the gene that encodes AADC. Sinemet (Levodopa/carbidopa) treatment was successfully discontinued after WES resulted, further supporting PLPHP dysfunction, rather than AADC deficiency, as disease-causing.

Folinic acid responsive seizures

Patient 1

This Omani boy, now 3 years and 10 months old, was born to a G3P3 mother. His parents are first cousins, who are healthy with normal learning abilities and there is a family history of similar disease in a younger newly born sibling. Antenatally, the mother experienced increased fetal movements. He was born at term, cried immediately and APGAR scores were 9 / 10. His birth weight was 2.95 kg (10^{th} percentile), length: 49 cm (50^{th} percentile) and HC: 35 cm (50^{th} percentile).

Seizures were first observed on the 5^{th} day of life, presenting with decreased consciousness, uprolling of the eyes and tonic-clonic movements of the body; each episode lasted 10-15 minutes and recurred every few minutes. He then developed myoclonic seizures. He was treated with phenytoin, phenobarbitone and midazolam infusion without clinical response; subsequently he was started on clonazepam and topiramate with initial reduction of seizures but subsequent relapse. His EEG showed burst suppression.

At 5 weeks of age, he was started on oral pyridoxine (25 mg BD) with immediate effect; he was sedated yet hemodynamically stable. All anti-epileptics were discontinued after the first dose of pyridoxine because of excessive sleepiness. He continued to be sleepy (remained sleepy for almost 72 hours) and therefore pyridoxine was withheld for 48 hours then restarted at 5 mg BD with gradual increment to 25 mg BD. EEG was repeated, and it showed marked improvement with no burst suppression on the lower pyridoxine dose. At the age of one year, seizures relapsed in the form of generalized tonic-clonic seizures but were brief (lasting one to two minutes) and infrequent (once or twice per month) and mostly occurred

during febrile illness. He was started on levetiracetam but there was no response, so it was tapered and discontinued.

At the age of 2 years and 4 months, the dose of pyridoxine was increased to 120 mg BD p.o. (= 24 mg/kg/d) that is increased to TID during febrile illness and his seizures were controlled for around 2 months but then he was admitted again with *status epilepticus*. Pyridoxine was thus substituted by PLP starting at a dose of 200 mg TID (= 42 mg/kg/d) which was then increased to PLP 300 mg TID (=58mg/kg/day) with no notable improvement of his seizure control. Subsequently, folinic acid 15 mg BID (= 2mg/kg/day) was added to his PLP regimen, this combination resulted in the best seizure control during his entire course of treatment. He was last seen at the age of 3 years and 11 months in February 2018, where his parents reported marked reduction in the frequency of his seizures. They reported only 2 brief episodes in 3 months period, mainly fever provoked.

He suffered global developmental delay, of a moderate to severe degree: When he was assessed at 2.5 years of age, his developmental age was around 12-18 months. Speech and language developmental age is around 7-8 months of age (he had 4 syllable babbles, had 1 word (unspecific) – Mama-, could not do head shaking for "No," was not able to babble monologs, could know his own name). He is hyperactive and was diagnosed with autism spectrum disorder (ASD). After improving his seizure control following folinic acid supplementation, his development improved, and he started to gain some milestones. He is currently walking without support and steadily and is able to run and climb the stairs. He can say around 10 words with meaning, he obeys commands and can scribble. He has also become less hyperactive. Physical exam revealed no dysmorphic features with biometry on the 50th

centile; systemic exam was also unremarkable without organomegaly. Motor neurological examination showed no focal deficits.

Biochemical investigation at the age of 15 months showed high-normal urinary α-aminoadipic semialdehyde (α-AASA, 0.19 µmol/l, reference range: 0-0.2 µmol/l) but plasma pipecolic acid was within the reference range. Antiquitin deficiency was subsequently ruled out by Sanger sequencing of *ALDH7A1*. Plasma amino acids were measured twice and were normal while blood lactate was high-normal (1.7 mmol/l, reference range: 0.5-2.2 mmol/l) (tests were done at the age of 6 weeks).

Whole-exome sequencing performed in this proband identified a pathogenic homozygous missense variant in *PLPBP*: chr8(GRCh37): g.37630300C>T; NM_007198: c.347C>T; p.Thr116Ile. In addition to this variant, this patient was found have another rare variant of unknown significance: chr8(GRCh37): g.37635617C>G; NM_007198: c.823C>G; p.His275Asp (homozygous missense). The variant affects last amino acid in the protein and two of the *in silico* prediction tools described in Supplementary Table 4.2 proposed a benign/non-functional effect for this variant.

Other cases according to phenotypic severity:

Severe phenotypes

Patient 3

This girl from Curacao Island in the Dutch Antilles (African/Creole descent), now 5 years and 2 months old, was born at 37+5 weeks of gestation after an emergency caesarian section because of fetal distress. She is the first and only living child of possibly consanguineous parents. The pregnancy was complicated by a vanishing twin at 9 weeks of

gestation. APGAR scores were 8/9. There was meconium in the amniotic fluid. Umbilical cord blood gas had pH 7.00. Birth weight was 2422 grams (5-10th centile / -1,91 SD), birth length was 47 cm (25th centile/ -1.23SD) and head circumference was 30 cm (<2nd centile / -4,01 SD). Her fontanel was small. After birth, she needed CPAP for breathing difficulties and she had trouble keeping her temperature. She received antibiotics because of suspicion of a perinatal infection. Blood lactate was 13.2 mmol/L (reference range: <2.2 mmol/L); blood gas at day 0: pH 7.15 (normal range: 7.35-7.45); pCO_2 4.2 kPa (normal range: 4.7-6.4 kPa); pO2 7.5 kPa (normal range: 10.0-13.3 kPa); HCO_3 11 mmol/L (normal range: 22-29 mmol/L); and base excess -17.3 mmol/l (normal range: -3 - +3 mmol/L). Lactate was between 4.2 and 8.8 mmol/L on days 1-5 (normal range =<2.2 mmol/L). Blood glucose was normal, creatine kinase was 6593 U/L (normal range: <600 U/L) at day 1 and went down to 460 U/L at day 5.

On day 1, she had clinically evident tonic seizures and an abnormal cerebral function monitoring (CFM)[1]. On the third day she manifested tonic-clonic seizures despite phenobarbitone (20+10 mg/kg), clonazepam (for a seizure, dose not known) and midazolam until 0.2 mg/kg/hour. During the first days she was sometimes quiet but could be hyperkinetic with somewhat shaking movements. She had dysregulation of muscle tone. Head circumference was at -4SD.

She was variable hypo- and hypertonic. EEG at day 5 was in keeping with encephalopathy showing a discontinuous pattern, and a tendency to burst suppression. Epileptiform discharges in the form of sharp waves were frequently observed during the burst

[1] CFM is a device used for continuous recording and monitoring of fluctuations in the amplitude of EEG, usually using one or two pairs of electrodes. In newborns, it is exploited for detection of seizure activity, tracking the response to AEDs and determining prognosis (277. Azzopardi D. 2015. **Clinical applications of cerebral function monitoring in neonates**. Semin Fetal Neonatal Med 20:154-163.

but without clear clinical correlate. The liver projected two centimeters below the costal margins.

At day 5, PLP was started orally (40 mg 3 dd = 48mg/kg/d) after which the convulsions vanished, and blood lactate started to normalize after day 6 (between 1.6 and 2.9 mmol/L). At 2.5 months of age there were no clinical signs of epileptic activity, the EEG was normal, and the head circumference had shown catch-up growth to -2.5 SD. The PLP dose was lowered to 20 mg 3dd (15mg/kg/d) because of vomiting. At six months of age the development was still normal. There was a short possibly epileptic episode after which the dose of PLP was adjusted to 40 mg 3dd (16mg/kg/d).

At 10 months of age, she had 15-20 minute long tonic-clonic seizures shortly after stopping the PLP because *PNPO* Sanger analysis was normal as was urine concentration of α-AASA. The next days she had several epileptic insults and the EEG results were slower and less differentiated showing mild encephalopathic changes, but no overt epileptic phenomena. PLP was restarted (40 mg 3dd = 12 mg/kg/day) because of suspicion of a yet undetected pyridoxine/ PLP-responsive epilepsy, and again her clinical condition improved significantly. Levetiracetam was started at 20 mg/kg/day.

At 14 months of age she had an epileptic insult after sleep deprivation. The parents tried to reduce the PLP dose at 18 months of age, but she had another insult after that, so they restarted the medication. The girl has signs of pavor nocturnus from 20 months of age. She has had several epileptic insults that were mostly induced by viral infections/fever or sleep deprivation. At the age of 3 years and 10 months, her B6 therapy was switched to pyridoxine at 100 mg/day in one dose (= 5.9 mg/kg/day), because PN has less severe side effects on the long term. B6 vitamer conversion went smoothly and at the age of 4 years and 2 months,

levetiracetam was gradually discontinued. This did not seem to affect frequency of seizures. She had a seizure about once every two months at this time, more severe than on the PLP regimen. Seizures occurred mostly during illness. At the same age (4 years and 2 months), her pyridoxine dose was leveled up to 150 mg/day (100 mg in the morning and 50 mg in the evening, = 8.8 mg/kg/day) and her seizures became less frequent. The dose was adjusted to 100 mg 2dd (= 9.0 mg/kg/day) at the age of 5 years. Midazolam is used during seizure attacks. In addition, she is also taking omeprazol (10mg BID) and macrogol (4g daily) to control her GE reflux and constipation, respectively.

Her development currently at age of 5 years is profoundly delayed; she could walk independently at 35 months of age, but she is autistic and does not speak. She has strabismus. Physical examination at 3.2 years of age showed no overt dysmorphism except a slight upslant of the eyes and a slightly prominent forehead. Length at the 25th centile and head circumference at 2.5th centile / -2 SD. Neurologically, at 3 years and 8 months she hardly makes eye contact, follows her own lead. She has some stereotypic hand movements, and her hand motor skills are slightly clumsy, but not ataxic. She walks somewhat unstable with a wide based gait. The leg tonus seems slightly high, reflexes are vivid and no Babinski reflex.

Additional investigations included TORCH serology (negative). Metabolic screening of urine at day 3 before PLP therapy showed normal amino acid profile, a trace of sulfite, high lactate, and negative α-AASA. In blood, carnitines, acylcarnitines and methylmalonic acid levels were normal, and plasma amino acids showed elevated glycine 915 µmol/L (normal range 197-487 µmol/L) and ornithine (197 µmol/l, normal range 42-170 µmol/L).

Pre-treatment CSF screening at day 3 revealed normal total protein (670 mg/L, normal range: 450-1090 mg/L); high lactate 4.4 mmol/l (normal range: 1.1-2.4 mmol/L); high

pyruvate (0.23 mmol/L, normal range: 0.03-0.15 mmol/L) and normal glucose (4.2 mmol/L, normal range: 2.2-4.4 mmol/L). Amino acids showed slightly high values of glycine (25 µmol/L; normal range: 3-17 µmol/L), threonine, glutamine, and ornithine. Neurotransmitters and pterins were normal.

Chromosome micro-array showed a paternal 5p15.2 duplication of 433 kb (genes in the duplication interval are *ANKRD33B*, *DAP* and *CTNND2*) and a maternal 12q24.33 duplication of 370 kb (genes in the duplication interval are: *GPR133* and *LOC116437*). Both variants are likely benign. Whole-exome sequencing of the proband and both parents was performed as described (278), identifying a homozygous missense variant in the *PLPBP* gene: Chr8(GRCh37):g.37623143G>A; NM_007198.3:c.199G>A; p.(Glu67Lys).

Patient 6

This boy, now 4 years and 3 months old, was born to consanguineous parents (second cousins) from the UAE after a pregnancy complicated by possible fetal seizures in the late third trimester consisting of rapid movements. There is a family history of similar epileptic encephalopathy with infantile spasms in a sibling who died from pneumonia while being treated with steroids. He was born at term with birth weight of 2.8 kg. His head circumference measured at the age of 10 months was at the 10th percentile (44 cm) and has remained normocephalic. Apgar scores were not available but there were no reports of complications or need for resuscitation after delivery. He had irritability from the first day with possible seizures and clear diagnosis of seizures by day 4 of life. Initial seizures types were infantile spasms and rapid clonic seizures. Results of first EEG at 2 months are unknown. An EEG at 4 months showed multifocal epileptiform activity predominantly in the frontal and parietal regions. He

had transient response with 2 weeks seizure free on prednisolone then the effect waned. He had no response to levetiracetam or vigabatrin. Around 6 months of age, pyridoxine 50 mg BID (approximately 6 mg/kg/day) was given, then cutting back to 25 mg BID resulted in complete control of spasms and clonic seizures, and his EEG normalized. Within 1-2 months, however, he developed new seizures, generalized tonic-clonic seizures with illness or fever, lasting up to 30 minutes in duration every 1-3 months. He has had improvement in duration and frequency of seizures with oxcarbazepine and early treatment with diazepam. His longest seizure free interval was approximately 3 months. He had a brief withdrawal of PN for two days with recurrence of seizures and thus it was resumed at a dose of 50 mg BID. After PLPHP deficiency diagnosis was made, his PN dose was increased to 100 mg BID (12.8 mg/kg/day). He has been on this dose ongoing in addition to oxcarbazepine 420 mg BID (53.8 mg/kg/day).

Developmentally, he was severely delayed without achieving any milestones during the first 6 months prior to PN treatment; he was markedly hypotonic and made no eye contact. After treatment, he made excellent improvement in his development but still has mild motor delays and a diagnosis of ASD was made at 2 ½ years old. He sat independently by 12 months, walked by 2 years, and had a pincer on one hand by 2 ½ years. He repeats words but does not talk independently or communicate with gestures and his eye contact is limited. He has limited social reciprocity and joint attention. He has frequent stereotypies and self-stimulatory behaviors fitting the ASD.

At 2 years and 7 months of age, he was assessed on the Bayley Scales of Infant and Toddler Development, where his scores were: Cognitive Composite 70 (2^{nd} percentile), Language Composite 62 (1^{st} percentile), Motor Composite 85 (16^{th} percentile).

Patient 10

This girl, currently at 10 years and 6 months of age, was born from consanguineous (first cousins) parents of Kurdish descent. There is a family history of similar disease in the younger sister (patient 11). She was born at 38 weeks gestation via C-section due to fetal decelerations and meconium stained amniotic fluid. Ultrasound examination performed at 20 weeks of gestation was remarkable for cysts in the head, but these were not seen on repeat ultrasound at 28 weeks. Her APGAR scores were 8 and 9. After birth, she was irritable with a high-pitched cry, dysconjugate eye movements, and tonic posturing was seen early on.

Within the first day of life, she presented with seizures characterized by flexor spasms and eye deviations; oxygen desaturations were seen. She continued to exhibit irritability and seizure activity with segmental myoclonic jerks involving the upper trunk, eye deviation, crying, hiccupping and flexor spasms.

She was given a phenobarbital load during the first two days of life, with a mild response. An EEG after phenobarbital load showed discontinuous background rhythm with periods of quiescence, lasting up to 10 seconds, consistent with mild cerebral dysrhythmia. On day four of life, an overnight extended video EEG was pursued. At the beginning, near burst suppression pattern was seen, characterized by spike and slow wave and poly spike and slow wave complexes lasting up to 10 seconds. Relative periods of quiescence lasting up to 20 seconds were seen. During the burst of generalized paroxysmal discharges, she exhibited periodic episodes of high pitched cry, flexor spasms with arm extension, with and without hiccupping and with and without eye bobbing, lip smacking and emesis.

A 50 mg dose of PN was given twice over a short period of time. After 5 minutes, the periodic episodes of high pitched cry, flexor spasm, and hiccupping stopped and there was a

significant improvement in the EEG background rhythm. During wakefulness, the background rhythm was continuous with fair synchrony and symmetry for age. Background rhythm appeared to be discontinuous during quiet sleep. A moderate number of sharp waves were seen over the left central temporal and right temporal region. Phenobarbital and phenytoin were discontinued, and the child remained without seizures. She was discharged home at 11 days of age, was breast feeding well and taking 75 mg PN per day. Doses were given in the evening since the child became very sleepy as a result. At the age of 8 years and 2 months, the family took her off PN treatment for two weeks which led to uncontrollable seizures and was taken to the ED where her seizures could not be stopped until she was put back on PN.

In terms of her language development, she began babbling at approximately 12 months of age. She started to say "mama" and "dada" at 3 years of age. She currently has several hundred words, which tend to be more representative of objects, and can sometimes be difficult to recognize. She will string four or five words together to communicate. She can follow one-step, very familiar commands or one-step commands with gestures. She does know her body parts including more minor body parts such as teeth and elbows. She does identify many of her letters. She is able to play with other children mostly her siblings. She points when she wants something and is fully potty-trained.

A neurological exam found that she has hypotonia with joint laxity, mild dysmetria and is unable to balance on each foot for 3 seconds. She has a wide based gait with poor coordination but is able to navigate an iPad. She can walk up and down stairs by herself, hops on each leg independently. She can kick and throw a ball and ride a tricycle. She needs some help with dressing but can pull up pants and underpants on her own and can take off her coat. She needs some help with putting on a coat. She can use a spoon and a fork well but makes a

lot of mess. She holds a pen well. She does not yet write letters or numbers but can trace them or do so if her family is using hand over hand. She does not yet draw items that others recognize.

For her seizures she now takes 100 mg PN BID (4.7 mg/kg/day). She also requires lamotrigine 50 mg BID (3.5 mg/kg/day) and clobazam 10 mg BID (0.75 mg/kg/day) for optimal seizure control. During illness however, she can have breakthrough seizures.

Biochemical investigations included normal urine organic acids and purines; blood lactate, acylcarnitines, amino acids (both after PN therapy); and a normal CSF amino acids (except for a slight increase in alanine (43 nmol/ml)), folate/5MTHF, lactate, protein, glucose, BH4, neopterin, PLP, and neurotransmitter metabolites (5HIAA, HVA, 3-OMD).

Genetic investigations included normal 500Kb array CGH microarray, Prader-Willi/Angelman methylation studies, and Sanger analysis of *ALDH7A1* (heterozygous for non-pathogenic variant p.K411Q), and deletion/duplication analysis (negative), *CDKL5, SCN1A, SCN1B, GABRG2,* and *PCDH19* sequencing (all negative).

Patient 11

This girl, who is now 6 years and 10 months old, is the sister of patient 10. She was delivered via C-section after an unremarkable pregnancy. Her head circumference was in the 2nd percentile. On the first day of life, she had ophisthotonus, irritability, and eye deviation throughout the day (episodic, but up to 1 hour). This was not diagnosed as seizures until an EEG was performed at a few days of life. The EEG showed a discontinuous record with multifocal sharp waves (bilateral frontal/central/temporal). She was admitted to the NICA for two weeks due to meconium aspiration and seizures.

She was noted to have focal seizures (hemibody clonic activity with lateral eye deviation to either side) lasting 7 seconds to 5 minutes (average 2 minutes, 2-3 times a week), or generalized convulsions with whole body stiffening and neck extension, lasting more than 2 minutes, about twice a month. Her seizures typically occurred at night.

She had no initial response to AEDs. With initial PN administration, the EEG report describes persistence of sharp waves at moderate frequency, and her seizures did persist over several weeks and thus levetiracetam was added to her treatment. Subsequent additions of clobazam and lamotrigine have been helpful, but she still has seizures with fever. At the age of 4 years and 10 months, her PN dose was reduced to 50 mg BID and she suffered increase in frequency of seizures. She is currently on following medications: 100 mg PN BID (7.8 mg/kg/day), lamotrigine 37.5 mg BID (4.5 mg/kg/day) and clobazam 10 mg BID (1.25mg/kg/day).

Her neurological examination revealed mild dysmetria, and a wide based and ataxic gait. She is very hypotonic in the trunk, making mobility much more difficult. She continues to progress in gross and fine motor skills. Still cannot climb up or down stairs. She has separation anxiety and severe stranger anxiety. She knows a lot more words now than previously. She is interested in others, points at what she wants, but cries if approached by other children.

Biochemical investigations: A comprehensive metabolic panel (sodium, potassium, chloride, calcium, bicarbonates, glucose, BUN, creatinine, total protein, albumin, A/G ratio, total bilirubin, alkaline phosphatase, GOT/AST, GPT/ALT) was screened four times (first one at age of 15 months) and resulted normal profiles in all.

Genetic investigations: GeneDx Infantile Epilepsy Panel (all negative): sequencing and deletion/duplication analysis of the following genes: *ADSL, ALDH7A1, ARX, ATP6AP2, CDKL5, CLN3, CLN5, CLN6, CLN8, CNTNAP2, CTSD, FOXG1, GABRG2, GAMT, KCNQ2, KCNQ3, MECP2, MFSD8, NRXN1, PCDH19, PNKP, PNPO, POLG, PPT1, SCN1A, SCN2A, SCN1B, SLC25A22, SLC2A1, SLC9A6, SPTAN1, STXBP1, TCF4, TPP1, TSC1, TSC2, UBE3A* and *ZEB2*.

Clinical whole exome sequencing ultimately discovered the *PLPBP* variant in patients 10 and 11 after reanalysis as the original analysis did not classify the "*PROSC*" gene that had not yet been described.

Mild phenotypes

Patient 2

This boy of Omani descent currently aged 13 years and 10 months was born to consanguineous parents (first cousins) at term without antenatal or postnatal complications. There is family history of 2 siblings' deaths; both were due to intractable seizures (at the age of 2-4 months). He has 5 living siblings (3 males and 2 females) that are all healthy. His birth head circumference was at the 10th percentile.

At the age of 7 days, brief, frequent seizures were noted with behavioral arrest progressing to tonic-clonic movements. He was tried on different AEDs but no response until pyridoxine was administered and subsequently seizures were controlled before the age of 1 month. Infrequent seizures occurred mainly during febrile illnesses, the most recent one at the age of 7-8 years. EEG reports are not available.

He is currently on pyridoxine 80 mg BID (= 5 mg/kg/day), increased during febrile illness to 80mg TID. Physical examination revealed no dysmorphic features, anthropometric measurements on the 10th centile, no systemic abnormalities and no organomegaly. Development in all domains and cognition are normal for age; he attends a regular grade 6 at school and has average school performance. His motor neurological exam was reported as normal. Biochemical screening revealed no detectable α-AASA in urine and Sanger sequencing of *ALDH7A1* was negative. Given the striking response to pyridoxine, no other investigations were carried.

Patient 8

This boy of Arab descent, now 8 years and 1 month old, was born at term via spontaneous vaginal delivery to a primigravida mother with insulin dependent diabetes. The parents are consanguineous with a family history of pyridoxine-dependent epilepsy. The patient is 1st cousins with patient 9.

His APGAR scores were 7 & 9 at 1 & 5 minutes, respectively. At birth he weighed 2.98 kg (50th percentile), was 55 cm tall (90th percentile) and his head circumference was 35cm (50th percentile). He was feeding well and active until the age of 1 week when he started to have episodes of myoclonic movements of the upper and lower limbs lasting for few seconds in clusters. He continued to have daily episodes. He was irritable and crying with disturbed sleep. The seizures became very frequent with time and at the age of 3 weeks he was admitted for the control of seizures. His initial EEG at the age of 3 weeks showed burst suppression. He was initially loaded with phenobarbitone but there was no response. He was then started on midazolam infusion and IV levetiracetam but he continued to have frequent seizures. At age

of 25 days, a dose of 20 mg oral PN was tried and the seizures immediately stopped. He was sleepy for more than 10 hours for which he was shifted to PICU for observation. An EEG was repeated and it was normal. He was then gradually weaned off midazolam and levetiracetam. He was back to his normal activity. Phenobarbitone was also tapered and discontinued. He continued to be on PN only 40 mg BID with increasing the dose to TID during febrile illnesses. He remained seizure free since then except at the age of 5 years when he had a febrile illness and there was not enough PN at home to increase the dose. After that he had no more seizures. He is currently on pyridoxine 80 mg BD (6 mg/kg/day), increased during febrile illness to 80 mg TID = 8.8 mg/kg/day.

He achieved all his developmental milestones at an appropriate age. He is in grade 2 at school now with excellent performance. A physical examination found no dysmorphic features or neurocutaneous marks, no organomegally, and his motor neurological exam was normal (normal tone, power and DTR, planters are downgoing, normal cranial nerves examination, no cerebellar signs). His weight, height and head circumference are currently between the 50^{th} and 75^{th} percentiles.

Biochemical investigations found normal pipecolic acid levels and metabolic workup at the age of 3 weeks revealed raised blood lactate (4.5 & 3.4) but normal pH. Amino acids and acylcarnitines were unremarkable on tandem mass spectrometry in dried blood spots. Long-term EEG at the age of 4 years and 4 months resulted normal.

Patient 9

This boy of Arab descent, now 14 months old, was born at term by spontaneous vaginal delivery 37 weeks of gestation to a primigravida mother with no antenatal complications. The

parents were consanguineous with a family history of pyridoxine-dependent epilepsy, the patient is the cousin of patient 8. His APGAR scores were 9 and 10 at 1 and 5 minutes, respectively. His birth weight was 2.56kg (50^{th} percentile), he was 49cm tall (50^{th} percentile) and his head circumference was 33cm (50^{th} percentile). He was admitted to the SCBU soon after delivery with the impression of TTN (transient tachypnea of the newborn). He was in SCBU for 5 days during which he was treated for presumed sepsis and jaundice. After discharge on day 5 of life, the parents started to notice frequent episodes of tonic seizures. The episodes were brief and lasting for seconds only. He continued to be active and was feeding well. His first EEG at the age of 10 days showed burst suppression. He was started on PN at home by his uncle (father of patient 8). At hospital, he received 40 mg once and he became very sleepy but had no more seizures. Within 24 hours he became active and was again feeding well. He was discharged on oral PN. He had no other symptoms. He is currently on 20 mg PN BID (8.5 mg/kg/day), increased during febrile illness to 80 mg TID (= 12.5 mg/kg/day).

Physical examination revealed no dysmorphic features or neurocutaneous marks and his weight, height and head circumference are all now in the 10^{th}-50^{th} percentile. He has normal tone, power and cranial nerves examination but noted to have hyperreflexia in all limbs. Urinary aminoadipic semialdehyde was mildly elevated at 0.35 mmol/mol Creatinine (reference, 0-0.19). Urinary pipecolic acid concentration was normal at 0.12 mmol/mol Creatinine (reference, 0.01-1.54). Piperidine-6 carboxylic acid was normal at 0.37 mmol/mol Creatinine (reference 0-1.62). Amino acids and acylcarnitines were unremarkable on tandem mass spectrometry in dried blood spots. Repeat EEG at 10 months was normal.

Unclassified severity

Patient 12

This African American girl, now 5 months old, was born via spontaneous vaginal delivery at 35 weeks of gestation to a 17-year-old G1 P0 female after an uncomplicated pregnancy. The parents were consanguineous. Her APGAR scores were 7 at 1 minute and 9 at 5 minutes and birth head circumference was 31 cm which is at 22nd percentile. She presented shortly after birth with neonatal seizures. She started having repeated stereotyped episodes of extremity jerking and irregular respirations within the first few hours of life and evolved into super refractory neonatal seizures.

She did have initial period of seizure freedom after phenobarbital loading but relapsed within the first week of life. Her seizures failed multiple antiepileptic medications, including phenobarbital, phenytoin, topiramate, levetiracetam, clonazepam, vigabatrin, midazolam, lorazepam, leucovorin, and a single dose of PN (100 mg IV) given early in the course. The VEEG background had no noted improvement after the first PN dose. She had focal seizures and myoclonic jerks followed by tonic posturing and initial EEG showed a burst suppression pattern followed by very frequent multifocal motor seizures as well as bilateral synchronous tonic seizures and/or myoclonic seizures with generalized epileptiform activity. After failing multiple conventional anticonvulsants, dextromethorphan was tried without success. She was placed on a 3:1 ketogenic diet and serine supplementation for low CSF serine. PLP was started at one month of age resulting in seizure freedom, significant improvement in EEG background activity and improvement in her neurologic exam. EEG background became continuous and no electrographic or clinical seizures were after PLP was started. Focal interictal epileptiform activity continued to be present but overall there was much improvement after initiation of PLP.

For seizure control, she is now taking 40 mg/kg/day of PLP divided q12h and 9 mg/kg/day of phenobarbital. She has been weaned from the ketogenic diet. On exam at age 2 months, she was microcephalic (z score -4.4), non-dysmorphic and was feeding well by mouth. She had conjugate eye movements and emerging visual fixation. She had normal axial tone and localized pain to extremity. Her deep tendon reflexes were 3+. No myoclonus was seen. Upon most recent check at age of 4.5 months, her EEG has 4-4.5 Hz background of normal voltage with no epileptiform activity. She is developing relatively well, has mild hypotonia but intact visual fixation and is a good oral feeder. Mother reports possible rare brief seizures but none noted in 24 hour EEG. She appears to have cerebrotendinous xanthomatosis.

Her laboratory work-up revealed normal CBC, normal CMP, negative CRP, normal ammonia, initial elevated serum lactic acid which normalized within first 2 days, negative HSV PCR, negative TORCH titers, normal CSF lactic acid, normal CSF pyruvic acid, normal CSF glucose and normal CSF protein. Low CSF serine (30 nmol/mL, normal range: 44 - 136 nmol/mL) was noted, but other CSF amino acids were normal. Plasma amino acids checked at age of 6 days revealed elevated glycine (575 nmol/mL, reference range: 111 - 426 nmol/mL). Repeat plasma amino acids at 9 days of life showed normal glycine levels (370 nmol/mL). CSF glycine was normal at 3 weeks of age 23 nmol/ml (reference range: 5 - 115 nmol/mL). Acylcarnitine, urine organic acids and uric acid were all within reference intervals. Lymphocyte choriomeningitis AB IgG and IgM was negative. Pipecolic acid was 0.4 nmol/mL (normal range <6 nmol/mL). Urinary S-sulfocysteine was within limits. CSF neurotransmitters (5-hydroxyindoleacetic acid, HVA, 3-Omethyldopa) were all normal.

A microarray showed vast areas of homozygosity, totaling 20% of the genome. GeneDX Xome DxSlice on the proband revealed a pathogenic mutation in the gene *PLPBP*

which results in pyridoxine-dependent seizures, in addition to 3 additional heterozygous mutations of uncertain significance (c.1421G>A in *CYP27A1*, c.1429A>G in *DENND5A* and c.997C>T in *VPS53*, all typically associated with recessive disorders and here without second variants identified).

Supplemental methods

Whole-exome and Sanger sequencing and *in silico* analysis

Patients 1 and 2

Whole exome sequencing (WES) was performed on patients 1 and 2 using the SureSelectXT Library Prep Kit and Illumina HiSeq 4000 (Macrogen, Korea). The data was analyzed using a semi-automated bioinformatics pipeline (241). Illumina sequencing reads were aligned to the human reference genome version hg19 using Bowtie2 aligner (279) and local realignment was performed using Genome Analysis Toolkit (220), achieving mean coverage of 24x for both patients 1 and 2. Variants were called using SAMtools (223) and annotated using SnpEff (280). Rare variants were identified using public databases, such as exome variant server (EVS), dbSNP v138 (281) and the Exome Aggregation Consortium (ExAC) database (27), as well as our in-house database of more than 400 exomes and 40 genomes (UBC) and against an in-house database of 817 Saudi Arab exomes at Alfaisal University (Dr. Fowzan Alkuraya, personal communication). Manual inspection on variant quality was carried out with Integrative Genomics Viewer (IGV) (282).

Patient 3

Clinical child-parents whole-exome sequencing (trio-WES) was performed at the Department of Human Genetics at the Radboudumc (Nijmegen, The Netherlands), with examination of all known genes according to previously described WES methods (283, 284).

Patient 4

Whole-exome sequencing of the proband and both parents was performed as described (278).

Patient 5

Trio WES was performed using SureSelect Human All Exon Kit version 4 (Agilent) for target enrichment. The library was sequenced with 100bp paired-end reads on a HiSeq 2000 platform (Illumina), and bioinformatics analysis was carried out as described previously (278). Sanger sequencing showed the affected individual was homozygous for this variant, parents heterozygous.

Patients 6, 7, 10, 11 and 12

Using genomic DNA from the proband and parents if available, the exonic regions and flanking splice junctions of the genome were captured using the SureSelect Human All Exon V4 (50 Mb), the Clinical Research Exome kit (Agilent) or the IDT xGen Exome Research Panel v1.0. Massively parallel (NextGen) sequencing was done on an Illumina system with 100bp or greater paired-end reads. Reads were aligned to human genome build GRCh37/UCSC hg19 and analyzed for sequence variants using a custom-developed analysis tool. Additional sequencing technology and variant interpretation protocol has been previously described (285). The general assertion criteria for variant classification are publicly available

on the GeneDx ClinVar submission page (http://www.ncbi.nlm.nih.gov/clinvar/submitters/26957/). Given patient 11 is a sibling of patient 10, the variants were diagnosed through targeted Sanger sequencing.

Patients 8 and 9

The *PLPBP* mutation in these cousin patients was identified by targeted Sanger sequencing.

In silico assessment of variants

In silico variant effect predictions and scores from the 6 prediction algorithms (SIFT, Polyphen2 HDIV, MutationTaster, MutationAssessor, FATHMM MKL and PROVEAN) for all *PLPBP* single-nucleotide variants (SNVs) were retrieved from GenomeBrowse 2.1.2 (Golden Helix, USA) using its data track "dbNSFP Functional Predictions and Scores 3.0". The track curates and visualizes functional predictions and scores that are originally obtained from the dbNSFP database (286, 287). Only one tool (MutationTaster (191)) provided prediction for the 4bp deletion mutation in patients 5 and 12 (obtained manually from http://www.mutationtaster.org). CADD scores (30) were queried individually.

Primary skin fibroblast culture

For patient 5, a skin biopsy was taken from which a fibroblast cell line was established at the Centre for Applied Genomics (Toronto, Canada) and maintained in HyClone DMEM media (GE Healthcare Life Sciences) supplemented with 10% FBS, Penicillin-Streptomycin

(SV30010, GE Healthcare Life Sciences) and 2mm L-glutamine (SH3003401, Thermo Scientific).

Patient fibroblast protein analysis

Total protein from the patient and three control lines was extracted in RIPA buffer containing protease inhibitors (Sigma) and was run on SDS-PAGE (20µg) following standard protocols. Antibodies used were rabbit anti-PROSC (Proteintech, 25154-1-AP, 1:5000); anti-β-tubulin (Abcam, ab6046, 1:20 000) and anti-GAPDH (ImmunoChemical, 200-901-BJ4, 1:10 000) were used as loading controls. HRP-linked anti-rabbit or anti-mouse IgG (1:2000) was used as secondary, and the Clarity ECL WB Substrate kit (BioRad) was used for protein detection using a ChemiDoc Touch Imaging System (BioRad).

Analysis of mitochondrial function in fibroblasts

A sample of the patient 5 fibroblast line was sent to the Mitochondrial Disease Laboratory (SickKids, Toronto). Measurements performed were pyruvate dehydrogenase (PDH) in its native and dichloroacetate activated forms, pyruvate carboxylase (PC), cytochrome oxidase, succinate cytochrome c reductase, and the cellular lactate/pyruvate ratio.

Oxygen consumption rate (OCR) was measured in patient and control fibroblasts using a Seahorse XF-24 Extracellular Flux Analyzer and V7 PS cell culture microplates (Agilent). Cells were seeded 50 000/well 24 hours before the assay, which followed the standard protocols of the XF Cell Mito Stress Test (Agilent). Data were normalized to protein concentration.

PLPBP targeting in HEK293 cells

Two guide RNAs were designed in exon 2 of *PLPBP* (NM_007198) targeting the region downstream of the start codon using the CRISPR design website (http://crispr.mit.edu/). The guide RNA sequences were TTGCTGACCGCCACTAGCCG (Guide 1 on reverse strand; primers 1F 5' CACCGTTGCTGACCGCCACTAGCCG 3' and 1R 5' AAACCGGCTAGTGGCGGTCAGCAAC 3') and CATCCAGCCCCGGCTAGTGG (Guide 2 on forward strand; primers 2F 5' CACCGCATCCAGCCCCGGCTAGTGG 3' and 2R 5' AAACCCACTAGCCGGGGCTGGATG C 3'). Oligonucleotide guide sequences were cloned into the pSpCas9(BB)-2A-GFP plasmid (Addgene Plasmid 48138). The resulting plasmids were transfected into HEK293 cells and GFP positive cells were sorted two days after transfection. These cells were used for obtaining clonal cell lines. We obtained two clonal cell lines with predicted biallelic disease-causing mutations; Guide 1_B, homozygous for c.124_127delCTAG (L42Wfs*12) and Guide 2_C, homozygous for c.128_129ins131bp (A44Gfs*55).

PLPHP overexpression in HEK293 cells and sample preparation for immunofluorescence

HEK293 cells were seeded in 12-well plates containing coverslips and transfected with a plasmid encoding Myc-DDK-tagged *PLPBP* (Origene, RC200853, C-terminal) using TurboFect (Thermo Fisher) following manufacturer specifications. Cells were fixed in pre-warmed 4% paraformaldehyde in PBS at room temperature for 10 minutes. After washing with PBS, coverslips were blocked for one hour with 1% BSA in PBS/0.3% Triton-X100. Primary

antibodies (mouse anti-DDK monoclonal (Origene, TA50011, 1:100) and a rabbit polyclonal against human Tom20 (FL-145) (Santa Cruz sc-11415, 1:1000) were diluted in PBS containing 1% BSA and incubated for one hour. Secondary antibodies (Cy3-AffiniPure Goat anti-mouse IgG (H+L) (Jackson ImmunoResearch 115-165-003, 1:750) and Alexa Fluor 488 goat anti-rabbit IgG (H+L) (Life Sciences A11034, 1:750)) were diluted in PBS containing 1% BSA and incubated for one hour. Cover slips were stained for five minutes in DAPI. Microscopy was performed using AxioObserver Z1 LSM800 63x/1.4 (Zeiss).

Quantification of B6 vitamers in plasma, leucocytes and cultured cells

Plasma samples from patient 4 (prior to treatment with any form of vitamin B6) and patient 3 (during treatment with PLP) were collected, shed from light and stored at -80°C. B6 vitamers PLP, pyridoxal (PL), PN, pyridoxamine (PM) and the degradation product 4-pyridoxic acid (PA) were quantified by LC-MSMS as previously described (256, 288). Pyridoxine-5'-phosphate (PNP) was not quantified due to plasma-related technical limitations of the method (ion suppression) and pyridoxamine-5'-phosphate (PMP) was not quantified as it is known to be highly unstable in plasma.

Fibroblasts from patient 5 and four controls, and HEK293 cells were cultured in DMEM GlutaMAX-I (Gibco, cat # 31966) containing 10% fetal bovine serum and 1% penicillin-streptomycin. B6 vitamers were extracted with tricholracetic acid (50g/L) and quantified with UPLC-MS/MS in biological triplicates as described by (256).

Zebrafish genotyping

F1s were raised to adulthood and were fin-clipped for genotyping by HMA-PAGE. Fish with candidate variants causing frameshift mutations were backcrossed to WT fish to further reduce the chance of off-target effects, generating F2 heterozygotes. F3 larvae from the crossing of F2 heterozygotes were genotyped by extracting DNA from 3-4 days post-fertilization (dpf) larval fins and HMA-PAGE was used following previously described protocols (148, 149). Primers used: *plpbp-F 5'* GCACTCTGGCTATGTGGAGA 3'; *plpbp*-R 5' AGCTGTCACTCATCCCTCGT 3'. Because differentiating homozygous mutants and homozygous WT genotypes requires two rounds of HMA-PAGE, and since no suitable primers could be identified for a reliable multiplex PCR strategy that would clearly identify homozygous mutants, two separate F2 mutant lines were crossed to generate compound heterozygous F3 offspring which facilitated genotyping by HMA-PAGE in a high-throughput manner (Supplementary Figs. 4.5 and 4.6). A pilot study was performed to show no difference in phenotype or survival between the compound heterozygous and homozygous mutant lines (Supplementary Fig. 4.7).

Western blotting for zebrafish larvae

Pools of 4 larvae were collected at 11dpf and total soluble proteins were extracted following previously established protocols (149). 40µg of protein from each sample was separated by SDS-PAGE using BioRad 4-20% pre-cast stain-free gels and blotted on low fluorescence PVDF (BioRad). Antibodies used were rabbit Anti-PROSC (Proteintech, 25154-1-AP, 1:5000) and HRP-linked anti-rabbit IgG (1:2000) was used as secondary. The Clarity ECL WB Substrate kit (BioRad) was used for protein detection using a ChemiDoc Touch Imaging System (BioRad) and proteins were quantified against stain-free total protein.

Supplemental Figures and Tables

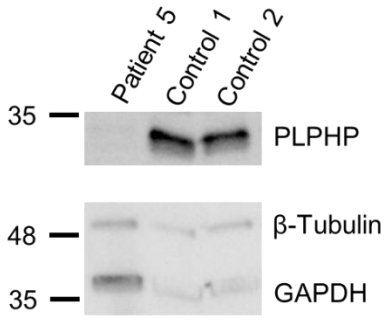

Supplementary Figure 4.1: Patient 5's fibroblasts do not express PLPHP.

Western blot of fibroblast lysates (20µg protein) showing that patient 5 is deficient for PLPHP.

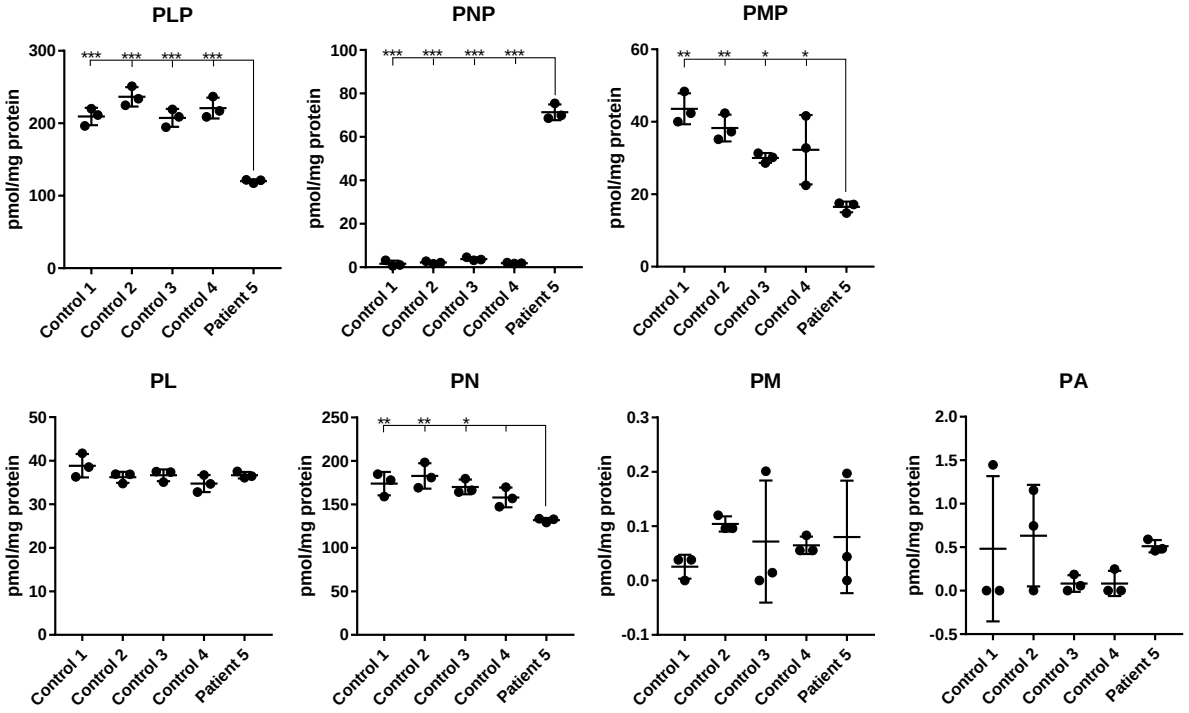
PLP
PNP
PMP
PL
PN
PM
PA
pmol/mg protein
Control 1
Control 2
Control 3
Control 4
Patient 5

Supplementary Figure 4.2: B6 vitamer profiles in cultured fibroblasts from four control subjects and patient 5.

Data are n=3 biological replicates per group. PA, pyridoxic acid; PL, pyridoxal; PLP, pyridoxal 5'-phosphate; PM, pyridoxamine; PMP, pyridoxamine 5'-phosphate; PN, pyridoxine; PNP, pyridoxine 5'-phosphate. ANOVA ***$p<0.001$, **$p<0.01$, *$p<0.05$.

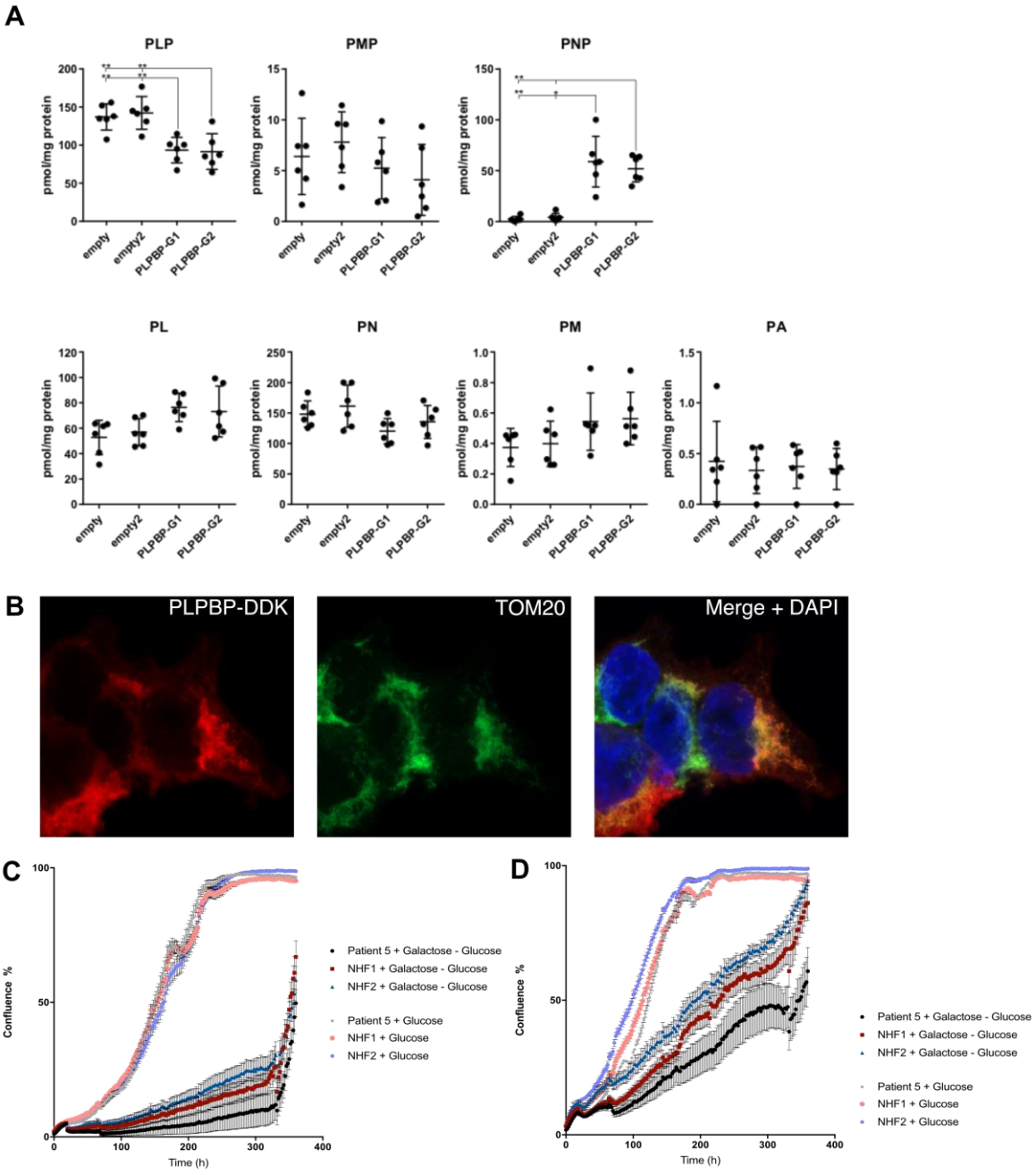
A
PLP
PMP
PNP
PL
PN
PM
PA
pmol/mg protein
empty
empty2
PLPBP-G1
PLPBP-G2
B
PLPBP-DDK
TOM20
Merge + DAPI
C
D
Confluence %
Time (h)
Patient 5 + Galactose - Glucose
NHF1 + Galactose - Glucose
NHF2 + Galactose - Glucose
Patient 5 + Glucose
NHF1 + Glucose
NHF2 + Glucose

Supplementary Figure 4.3: HEK293 cells deficient for PLPHP show altered B6 vitamer profiles and expression of DDK-tagged PLPHP shows mitochondrial localization.

(A) B6 vitamer profiles in control (WT+empty vector) nd PLPHP-deficient HEK293 cells (PLPHP-KO: PLPBP-G1 and PLPBP-G2). Data are from n=6 independent experiments (each consisting of 3 biological replicates per group), ±SD. (B) HEK293T cells overexpressing PLPHP with a C-terminal Myc-DDK tag shows co-localization of PLPHP with Tom20, a mitochondrial marker. Incucyte analysis of cell growth in 5mM galactose or 25mM glucose as carbon source seeded at 500 cells per well (C) or 1000 cells per well (D) in 96 well plates. DMEM no glucose + 1mM sodium pyruvate was used as base media for C and D. Abbreviations: PN, pyridoxine; PL, pyridoxal; PM, pyridoxamine; PNP, pyridoxine 5'-phosphate; PLP, pyridoxal 5'-phosphate; PMP, pyridoxamine 5'-phosphate; PA, pyridoxic acid. **$p<0.01$, *$p<0.05$.

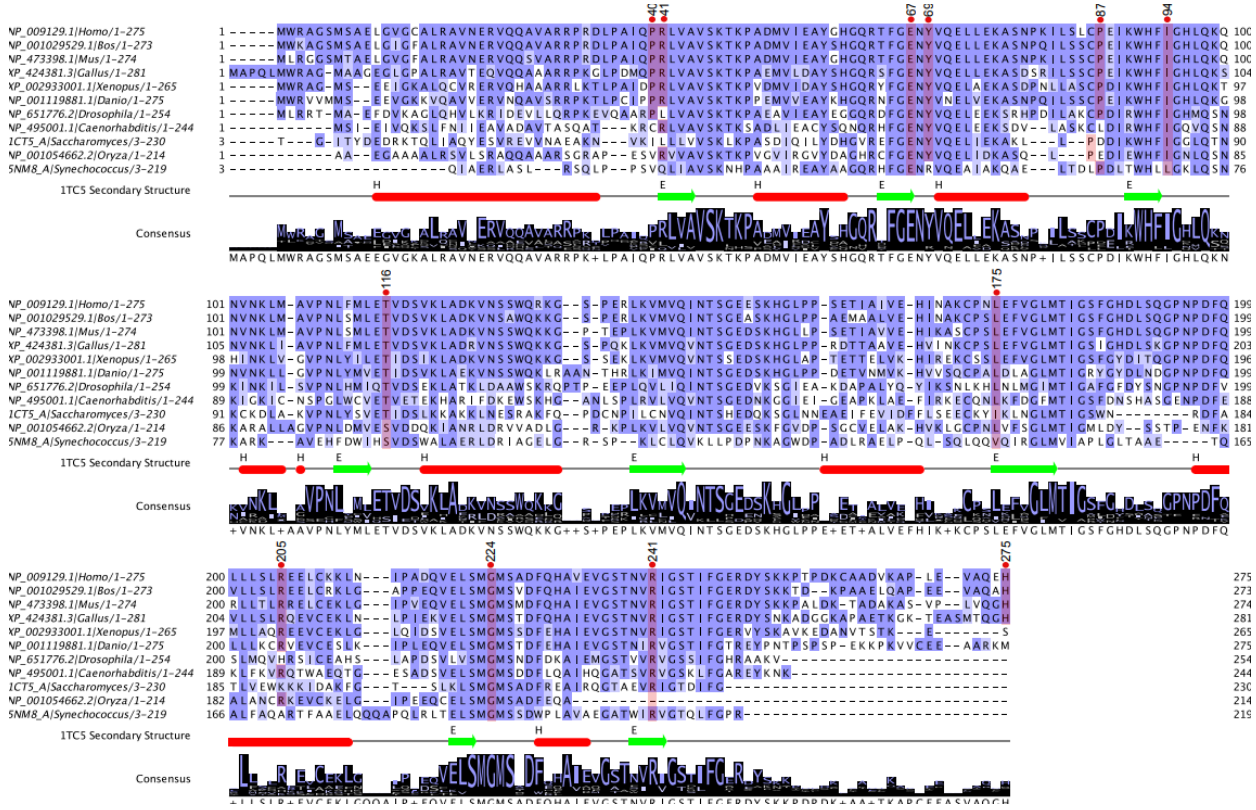
NP_009129.1|Homo/1-275
NP_001029529.1|Bos/1-273
NP_473398.1|Mus/1-274
XP_424381.3|Gallus/1-281
XP_002933001.1|Xenopus/1-265
NP_001119881.1|Danio/1-275
NP_651776.2|Drosophila/1-254
NP_495001.1|Caenorhabditis/1-244
1CT5_A|Saccharomyces/3-230
NP_001054662.2|Oryza/1-214
5NM8_A|Synechococcus/3-219
1TC5 Secondary Structure
Consensus
MAPQLMWRAGSMSAEEGVGKALRAVNERVQQAVARRPK+LPAIQPRLVAVSKTKPADMVIEAYSHGQRTFGENYVQELLEKASNP+ILSSCPDIKWHFIGHLQKN

Supplementary Figure 4.4: Protein sequence alignment of PLPHP orthologues from several species.

Residues found mutated in patients are highlighted in red (missense mutations). Secondary structure as in the yeast orthologue (PDB 1CT5) is shown under the alignment. Consensus sequence is also shown. Image produced using Jalview (289) . RefSeq identifiers shown in the sequence labels.

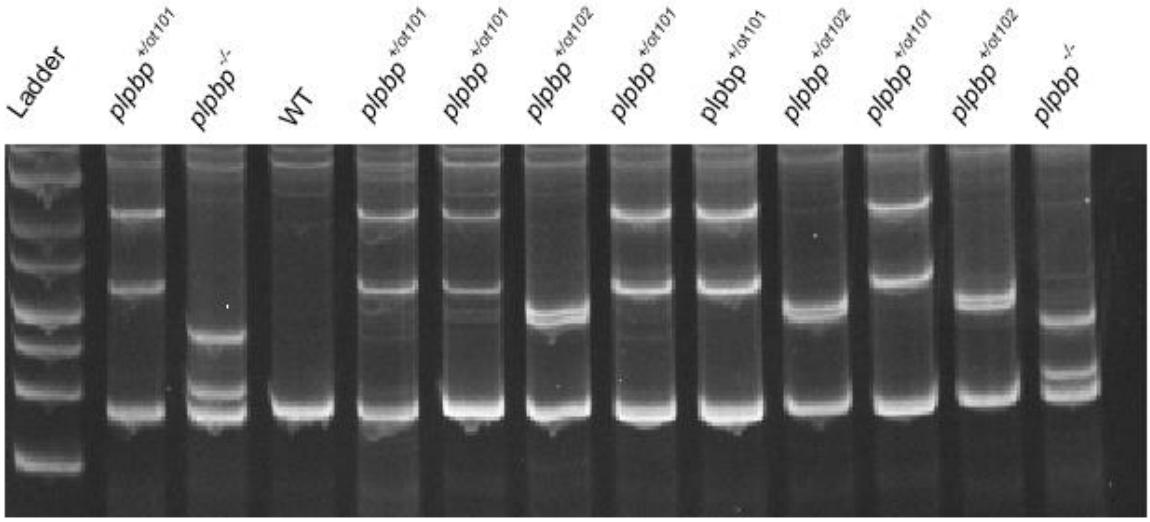
Ladder
plpbp +/at101
plpbp -/-
WT
plpbp +/at101
plpbp +/at101
plpbp +/at102
plpbp +/at101
plpbp +/at101
plpbp +/at102
plpbp +/at101
plpbp +/at102
plpbp -/-

Supplementary Figure 4.5: Example HMA-PAGE gel showing the four genotypes.

Each genotype can easily be distinguished from a single gel run by denaturing the PCR products and running on a PAGE gel, forming heteroduplexes in non-homozygous genotypes.

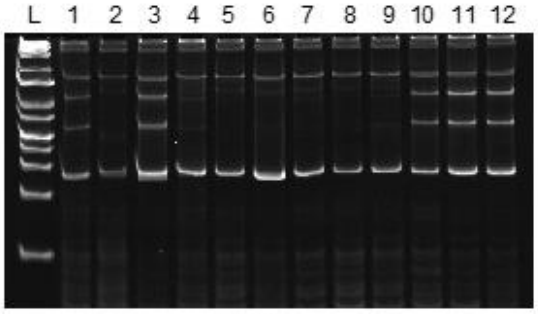

Gel 1

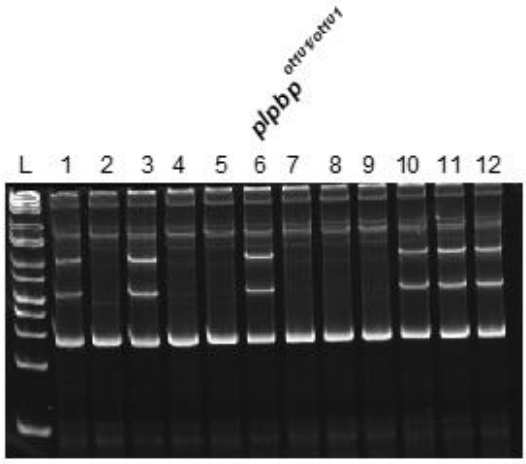

Gel 2: PCR product mixed with WT

Supplementary Figure 4.6: HMA-PAGE gels from a crossing of *plpbp*$^{+/ot101}$ heterozygous F2s.

Since homozygous mutant genotypes do not form heteroduplexes, a second round of HMA-PAGE must be run by mixing the PCR products with PCR products from known WT fish (right), to distinguish mutants from WT larvae. Given the need for rapid genotyping, a compound heterozygous mutant model was used for most experiments, however homozygous mutants were shown to have the same phenotype (see Supplementary Figure 7).

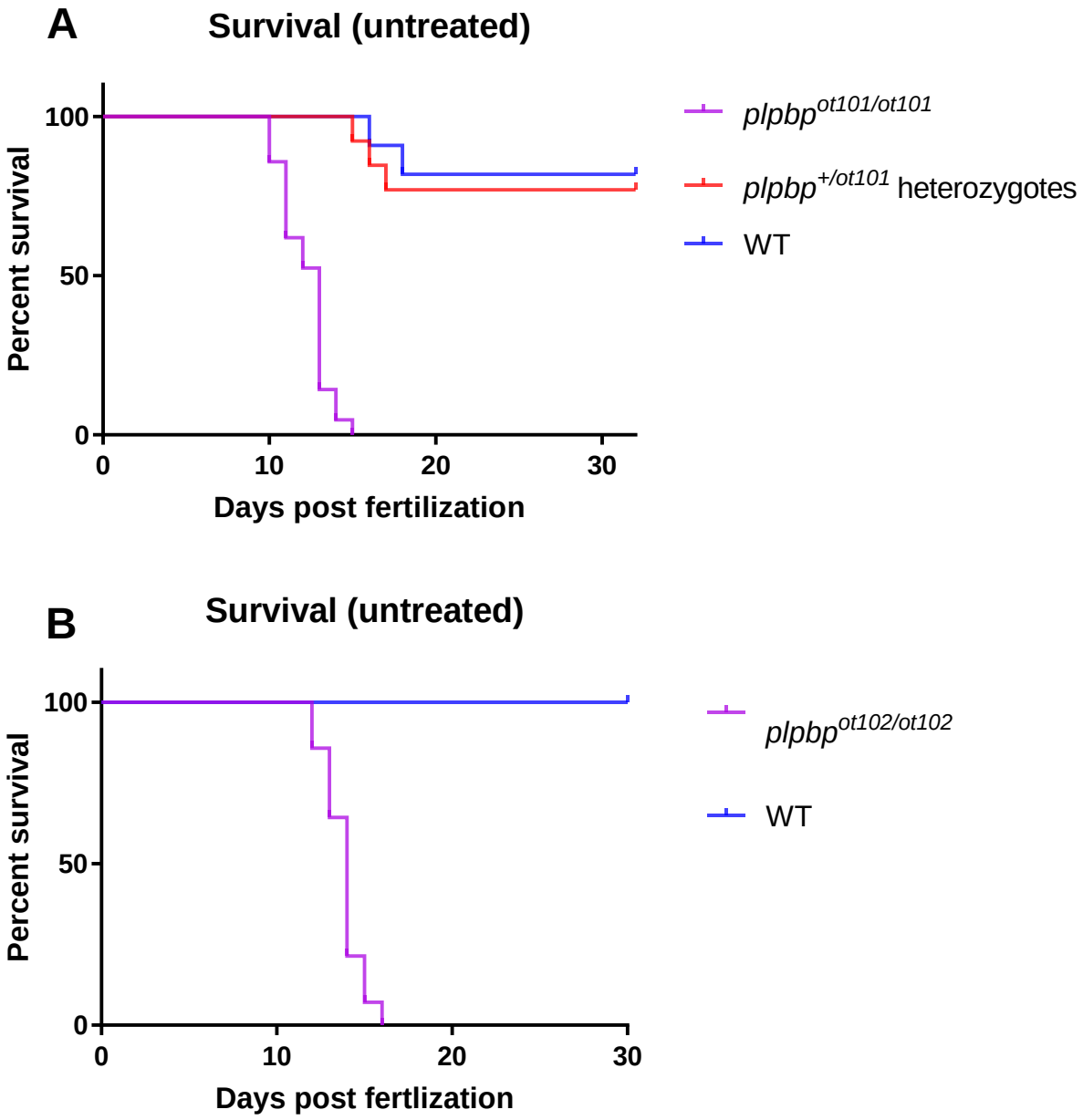
A
Survival (untreated)
Percent survival
100
50
0
0
10
20
30
Days post fertilization
plpbp ot101/ot101
plpbp +/ot101 heterozygotes
WT
B
Survival (untreated)
Percent survival
100
50
0
0
10
20
30
Days post fertlization
plpbp ot102/ot102
WT

Supplementary Figure 4.7: Comparison of survival between compound heterozygous and homozygous mutant zebrafish.

Mutant zebrafish larvae homozygous for either the 4bp (A) or 2bp (B) frameshift mutations show a similar survival pattern as the compound heterozygous larvae plpbp$^{ot101p/ot102}$ (Fig. 4C). Additionally, these larvae start seizing by 10dpf/11dpf. We thus did subsequent experiments with compound heterozygotes due to ease of genotyping (Supplementary Figures 4.5 and 4.6).

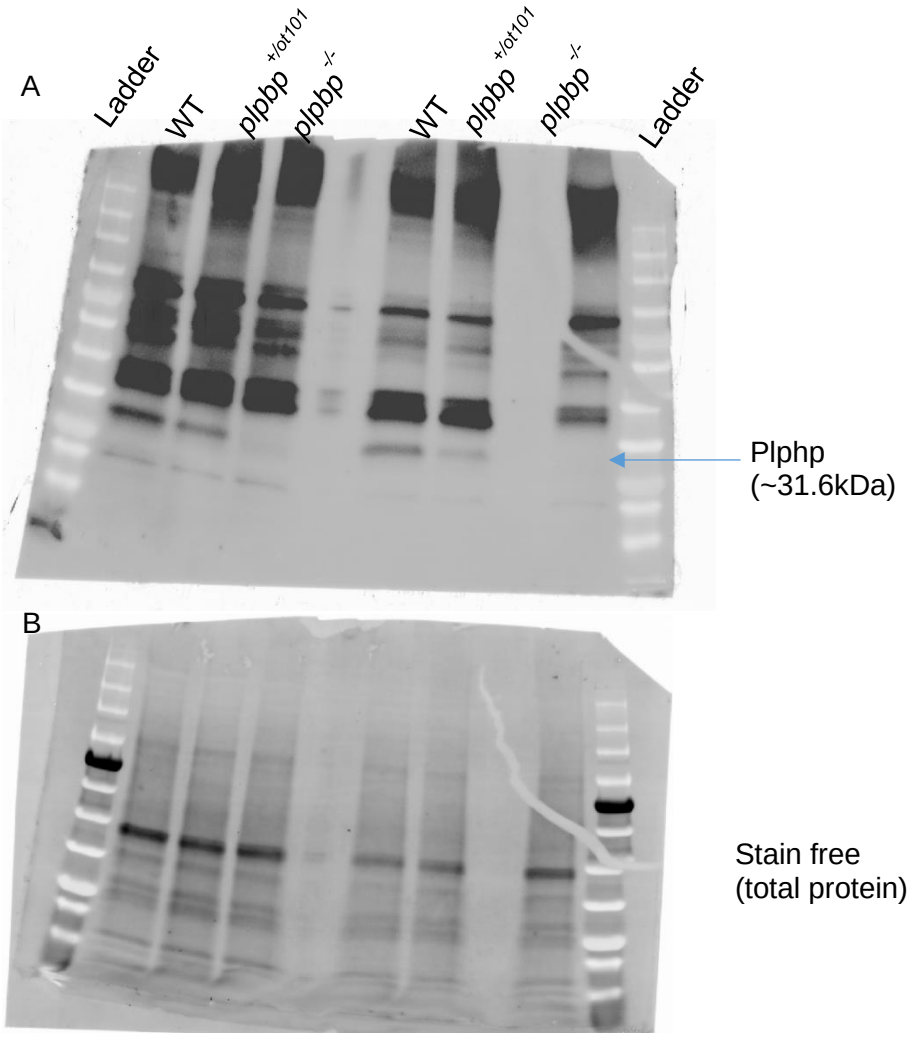
A
Ladder
WT
plpbp +/ot101
plpbp -/-
WT
plpbp +/ot101
plpbp -/-
Ladder
Plphp
(~31.6kDa)
B
Stain free
(total protein)

Supplementary Figure 4.8: Whole image of WB showing no Plphp protein detected in *plpb*$^{-/-}$ larvae.

The left three lanes represent pools of four larvae, whereas the lanes on the right are individual larvae. (A) chemiluminescent blot (B) stain free blot.

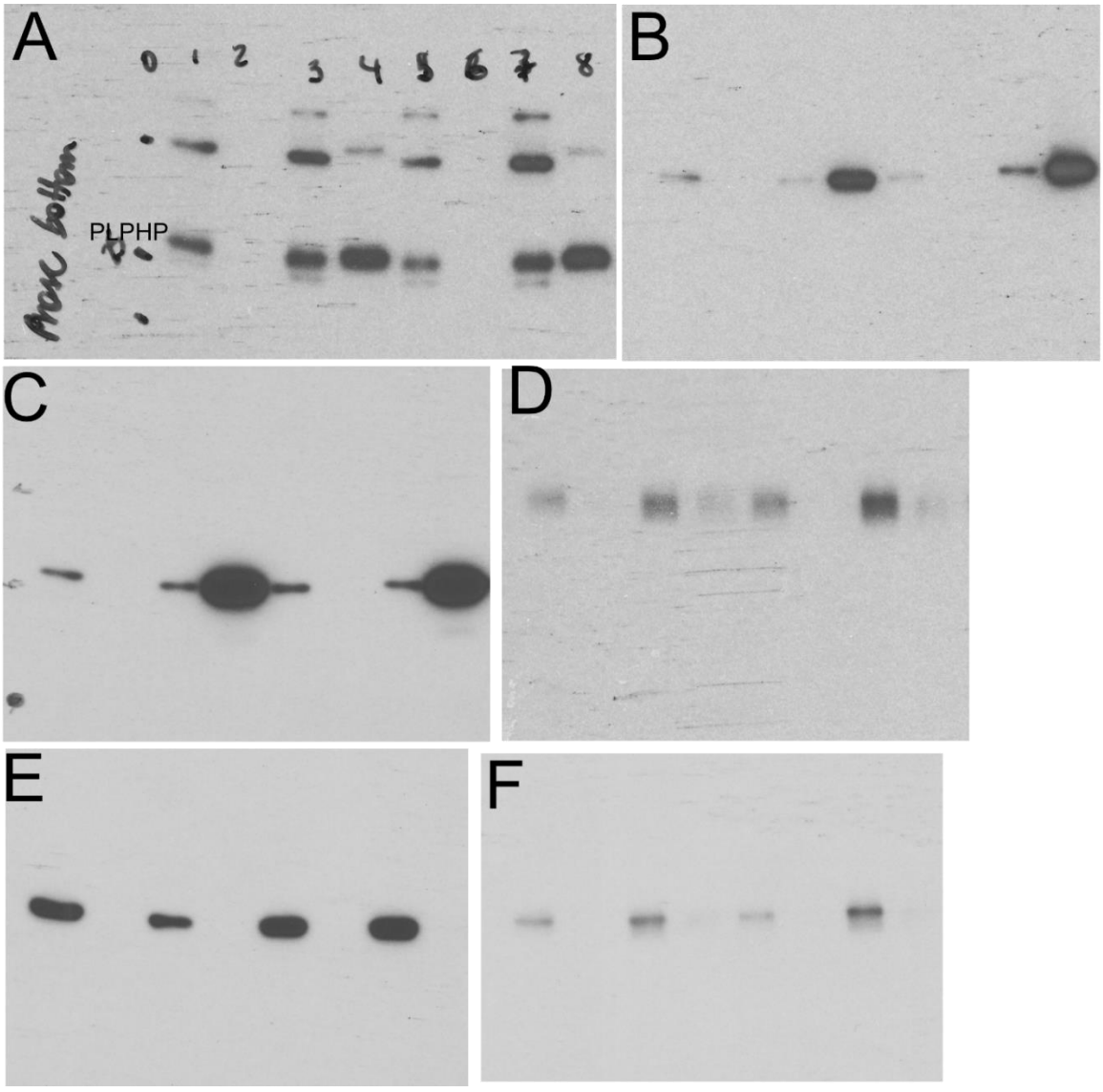
A
0 1 2 3 4 5 6 7 8
Acyc bottom
PLPHP
B
C
D
E
F

Supplementary Figure 4.9: Uncropped western blots of HeLa cells.

Wild type (lanes 1,2, 5,6) and HA-tagged mitochondria (lanes 3, 4, 7,8), ran as whole cell lysates (lanes 1, 3, 5, 7) or immunoprecipitated with anti-HA (lanes 2, 4, 6, 8). Blots show (A) PLPHP, (B) SHMT2, (C) VDAC, (D) LAMP2, (E) GAPDH, and (F) GOLGIN-97.

Supplementary Table 4.1: Detailed MRI findings for 12 *PLPBP* patients.

Patient ID	Patient 1	Patient 2	Patient 3	Patient 4	Patient 5	Patient 6	Patient 7	Patient 8	Patient 9	Patient 10	Patient 11	Patient 12
MRI age	6 weeks, 8.5 months, 3.5 y	Not performed	10 days	1 day	6 days	8 months	12 weeks, 3.5 months,	MRI not available for review	MRI not available for review	6 years	2 years	MRI not available for review
WM abnormalities	Very mild T2-hyperintense and T1-hypointense changes in periventricular WM at age 6 weeks		Yes, T2 hyperintense and T1 hypointense, swollen aspect	Yes, T2 hyperintense and T1 hypointense, swollen aspect, subcortical cystic degeneration	Yes, T2 hyperintense and T1 hypointense, swollen aspect, subcortical cystic degeneration	No	no			Mild T2-hyperintensity in the posterior periventricular white matter	Faint T2-hyperintensity in the posterior periventricular white matter	
Cortex abnormalities	no		Simplified gyral pattern	Simplified gyral pattern	Simplified gyral pattern	no	no			no	no	
Basal ganglia abnormalities	no		no	no	no	no	no			no	no	
Thalamus abnormalities	no		no	no	no	no	no			no	no	
Cerebellar involvement	no		no	T2-hyperintense signal of the hilus of the dentate nucleus	no	no	no			no	no	
Cysts anterior horn	no		++	++	+ (L>R)	no	no			no	no	
CC abnormalities	no		Thin CC	Thin CC		no	no			Pronounced isthmus	no	
Other abnormalities	Age 8 months: mild communicating hydrocephalus with prominent external CSF spaces. Age 3.5 y: normal MRI			Lactate doublet at MR spectroscopy (basal ganglia)	Cavum septi pellucidi; small lactate doublet at MR spectroscopy (basal ganglia)	MRI normal	MRI normal	MRI at age 4 weeks reported as normal.	MRI at age 10 months reported as normal.			MRI at ages of 2 days and 3 weeks: Diffuse broadening of the gyri in both cerebral hemispheres, mild dilatation of the lateral and third ventricles with multiple intraventricular septations. There are blood products in the left lateral ventricule.

Supplementary Table 4.2: List of PLPBP variants found in our cohort of 12 patients.

Variant annotation				Detailed *in silico* predictions [predicted effect (score)]						
Genomic (GRCh37)	**cDNA and protein**	**Variant frequency (gnomAD)**	**DUET Predicted Stability Change (ΔΔG):**	**SIFT**	**Polyphen2 HDIV**	**MutationTaster**	**MutationAssessor**	**FATHMM MKL**	**PROVEAN**	**CADD score**
chr8: g.37630300 C>T	NM_007198: c.347C>T; p.Thr116Ile	NR	0.123 Kcal/mol (Stabilizing)	Damaging (0.003)	Probably damaging (1)	Damaging (1)	Functional (high) (3.855)	Damaging (0.98019)	Damaging (-5.56)	29.20
chr8: g.37635617 C>G	NM_007198: c.823C>G; p.His275Asp	NR	Not modeled*	Damaging (0.017)	Benign (0.361)	Damaging (0.918861)	Non-functional (low) (1.1)	Damaging (0.96396)	Neutral (-0.71)	23.3
chr8: g.37623066 G>A	NM_007198: c.122G>A; p.Arg41Gln	$4.06*10^{-6}$	-0.265 Kcal/mol (Destabilizing)	Damaging (0.04)	Probably damaging (0.978)	Damaging (1)	Non-functional (low) (1.795)	Damaging (0.99714)	Damaging (-2.73)	28.7
Chr8: g.37623143 G>A	NM_007198.3: c.199G>A; p.Glu67Lys	$4.06*10^{-6}$	-2.127 Kcal/mol (Destabilizing)	Damaging (0)	Probably damaging (1)	Damaging (1)	Functional (high) (4.1)	Damaging (0.99824)	Damaging (-3.96)	35
Chr8: g.37630271 A>G	NM_007198.3: c.320-2A>G splicing	$1.08*10^{-5}$	-	NA	NA	Damaging (1)	NA	Damaging (0.99207)	NA	24.7
Chr8: g.37633509 G>C	NM_007198.3: c.671G>C; p.Gly224Ala	NR	-0.966 Kcal/mol (Destabilizing)	Damaging (0)	Probably damaging (0.999)	Damaging (1)	Functional (high) (4.07)	Damaging (0.99191)	Damaging (-5.69)	27.7
Chr8: g.37630323_37630326del	NM_007198: c.370_373del; (p.Asp124Lysfs*2)	NR	-	NA	NA	Damaging (1)	NA	NA	NA	NA
chr8: g.37623834 A>T	NM_007198: c.280A>T; p.Ile94Phe	NR	-1.398 Kcal/mol (Destabilizing)	Damaging (0.001)	Probably damaging (1)	Damaging (1)	Functional (high) (4.43)	Damaging (0.99692)	Damaging (-3.96)	29.6

All variants are expressed as found in PLPHP (NP_009129.1). Variant effect is predicted is based on 7 *in silico* prediction tools (SIFT, Polyphen2 HDIV, MutationTaster, MutationAssessor, FATHMM MKL, PROVEAN and CADD). DUET uses as input the structural model developed for the human PLPHP to predict if a given amino acid change is stabilizing or destabilizing (ΔΔG). * Not modelled due to lack of this residue in yeast model used as template. NA: not available; NR: not reported

Supplementary Table 4.3: Concentrations of B6 vitamers in plasma from 2 patients affected with PLPHP deficiency.
Concentrations are expressed in nM.

	PL	PM	PN	PA	PLP
Patient 4	39	<2.7	0,1	130	1,1
Patient 3, treated	276	<2.7	0,1	365	685
Reference interval, untreated (288)	6.6-54	<2.7	<1	6.7-84	16-269

Chapter 5 Discussion and Conclusions

The overall objective of my thesis was to use next-generation sequencing tools and model systems to understand novel disease mechanisms associated with early infantile epileptic encephalopathy.

Key findings

- Exome sequencing is a valuable tool for the discovery of single gene disorders
- Recessive mutations in *PIGP*, *PIGQ*, and *PLPBP* can cause early infantile epileptic encephalopathy, but clinical spectrums are broad
- Mutations in *PIGP* and *PIGQ* lead to impaired cell surface localization of GPI-anchored proteins
- Mutations in *PLPBP* impact the homeostasis of the B6 vitamers and significantly change the amino acid and neurotransmitter profile of cell lines, yeast, and zebrafish
- *plpbp*$^{-/-}$ zebrafish recapitulate features of the human disease, including B6-responsive seizures and reduced survival
- PLPHP is enriched in mitochondrial fractions, thus may play a function in mitochondrial metabolism

5.1 *PIGP* and *PIGQ*

In Chapters 2 and 3, I showed that, similarly to other IGDs, patients with mutations in *PIGP* (Chapter 2) and *PIGQ* (Chapter 3) present with early onset refractory seizures, as well as significant cognitive delays, hypotonia, congenital anomalies, and in many cases, early death. Given that there are no effective treatments for IGDs, more work is necessary to study the impact of the individual anticonvulsant therapies, as well as explore other therapeutic approaches. Indeed, as discussed in Chapters 2 and 3, the impact of IGDs on the ~150 GPI-APs suggests a plethora of possible mechanisms and pathways that could be responsible for disease phenotypes, either individually or synergistically. The development of model systems, such as the zebrafish model in Chapter 4 for PLPHP, may provide further opportunities to study the molecular underpinnings of IGDs. One such approach would be to investigate the effect of IGDs on neurotransmitters and amino acid profiles, using both patient cells and a model system.

Effective and readily available biomarkers for IGDs require further development. I highlighted the dichotomy of elevated ALP levels found in some IGDs in Chapter 3, but it remains unclear as to exactly what mechanism(s) causes this finding. Some of the patients with *PIGQ* variants had elevated or intermittently elevated ALP, while others did not. Based on the hypothesis that mutations early in the GPI biosynthesis cause ER-associated degradation, low ALP would be expected, which was not observed (177, 214). Others have also shown that hyper- and hypophosphatasia are variable, thus the utility of ALP for clinical classification remains limited (290), and there may be a need for alternative hypotheses about how mutations in this pathway affect ALP levels and the various GPI-APs.

5.1.1 *PIGP* is a novel gene associated with EIEE

Since the publication of my *PIGP* manuscript, two subsequent papers have published findings on a single patient (291), and four siblings (292), respectively, with substantial phenotypic overlap with the patients I describe in Chapter 2, and validating my novel gene discovery. In the discussion of Chapter 2, I touched on the effectiveness of levetiracetam for seizure control in one of the siblings with *PIGP* mutations. This was not consistently observed with subsequent patients but given the association between excess *PIGP* expression and levetiracetam resistance (196), there may yet be reason to investigate this relationship. A model organism will be helpful in further study of the disease mechanism. I would like to highlight that I did begin the development of a *pigp*$^{-/-}$ zebrafish, and while I did not observe seizures in the first generation, there was a survival phenotype. More work will be necessary to validate and further characterize this model to improve our understanding of disease pathogenesis.

5.1.2 The clinical spectrum of PIGQ-associated EIEE

In Chapter 3, I expanded the phenotypic spectrum of disease caused by mutations in *PIGQ*. With now 10 known patients with variants in *PIGQ*, we are starting to understand to clinical spectrum, but more patients and more research may help elucidate whether a genotype-phenotype correlation exists. There is a puzzling difference in phenotype between St1, who had a relatively mild phenotype for an IGD, and St6, who had a severe phenotype associated with early mortality despite having a genetic variant that in theory was more benign. I mentioned that St6's phenotype needs to be interpreted in the context of other regions of

homozygosity due to parental consanguinity, which is often the case in rare recessive diseases. This highlights the importance of having model systems so that the impact of the mutations in the gene of interest can be investigated in a relatively more controlled setting. Of course, model organisms are not without their limitations, zebrafish and mice are not human after all, and are themselves generally inbred. Nevertheless, model organisms have proven their value to research countless times, including in Chapter 4.

5.2 *PLPBP*

Chapter 4 highlights the usefulness of model organisms for understanding the molecular underpinning of disease. Using knockout and patient cell lines, yeast and zebrafish, this chapter helps us better understand the impact of *PLPBP* mutations on B6 vitamer homeostasis, and neurotransmitter and amino acid profiles. Furthermore, the suspicion of a mitochondrial encephalopathy is supported by the demonstration that PLPHP is enriched in mitochondrial fractions. The next question of course, is precisely what roles PLPHP is playing in the mitochondria, as well as outside it. Many research groups are tackling these questions, and for example, one group is already using a customized proteome of PLP-binding proteins, to study PLPHP and PLP homeostasis (293). Some early findings already show a possible dimeric assembly of PLPHP, and upregulation of cytoskeleton and cell division-associated proteins, with possible important roles in cell division and muscle function (294).

5.3 Possible overlap between IGDs and B6 dependent epilepsy

An interesting overlap exists between the IGDs and the vitamin B6 responsive epilepsies. As I mentioned in Chapter 3, there are reported cases of patients with mutations in *PIGO*, *PIGV*, and *PIGS* that show some responsiveness to Vitamin B6 therapy. Furthermore, seizures in children with infantile hypophosphatasia caused mutations in the gene *ALPL*, a GPI-AP, are pyridoxine responsive (295). Thus, future work should investigate to what extent there may be overlap between IGDs and the metabolic pathways impacted in the various vitamin B6 dependent epilepsies.

5.4 Deep phenotyping compliments the use of NGS

Key to understanding any rare disease and providing an early diagnosis is detailed, or deep, phenotyping. The phenotyping bottleneck remains a substantial challenge, and the rare disease clinical community must continue to work towards standardizing phenotyping, particularly in the context of hypothesis free genome-wide sequencing approaches. Facilitating the efforts for deep phenotyping, is the use of image recognition software. In one study, Knaus *et al* (290) were able to show the utility of facial image analysis to parse subtle differences between IGDs caused by mutations in different genes in this pathway. This is by no means a perfect solution, but as the number of reported cases of *PIGP*, *PIGQ*, and other IGDs increases, the power of such tools should become more precise, and perhaps one day in the future imaging solutions may be an important tool for the early diagnosis of these diseases.

5.5 Clinical characterization of rare diseases

For *PIGQ* and *PLPBP,* Chapters 3 and 4, respectively, represent the largest clinical cohorts to date. With such patient resources, it is important to ensure deep phenotyping to facilitate the clinical characterization of disease. For example, in Chapter 4 I was able to begin the development of a clinical phenotypic scoring system, based on a model used in PDE caused by mutations in *ALDH7A1* (248). The phenotypic heterogeneity of this disease highlights that there remains a substantial need to investigate the downstream effects of mutations in these pathways, so we can better understand the mechanisms behind the variability in clinical presentation and identify disease modifiers that might be possible drug targets.

5.6 Developmental and epileptic encephalopathy

Another perspective that needs to be considered for these patients is the dichotomy of epileptic encephalopathy versus developmental and epileptic encephalopathy. While some of the patients with IGDs or B6 dependent epilepsies have good seizure control, there can remain substantial cognitive and developmental delays. This suggests that the term ‘developmental and epileptic encephalopathy’ may be more fitting to describe the diseases in these pathways. It also highlights the need to pursue therapies for these disease beyond the clinical outcome of simply controlling seizure activity.

5.7 Future directions

Next generation sequencing technologies, particularly exome sequencing, have facilitated the discovery of a growing number of genes associated with refractory epilepsy, and its success suggests it may deserve to be used earlier in the 'diagnostic odyssey' (22). Despite the incredible progress in disease gene discovery over the past decade, there remains a significant need to continue identifying novel disease genes and variants as globally most patients with a rare disease are undiagnosed. Similarly, clinical characterization of these rare diseases must continue. Detailed clinical phenotyping and capture of standardized outcomes will facilitate best practices, establish clinical end-points for future drug trials, and may enable the identification of disease modifiers that are suitable drug targets.

Despite the high diagnostic utility of exome sequencing, the disease mechanism for some patients will be out of reach using this approach (10). To take the next step, there is increasing exploration of the next wave of 'omics' technologies to solve the unsolved rare disease patient (296). Whole genome sequencing is becoming more affordable, and with improved algorithms and pipelines for handling the larger datasets, having a better understanding of mutations in non-coding regions, as well as improved coverage in the coding regions, will likely lead to new discoveries in rare disease. RNA sequencing of whole transcriptomes is another approach, which has been used, for example, for the discovery of the role of *ASAH1* in SMA-PME (297). In summary, the rapidly expanding molecular toolkit is catalyzing future discovery.

As we move further towards the era of personalized and precision medicine, advancements in *in vitro* and *in vivo* disease modeling will also be critical. Beyond animal models, technology is moving towards using patient derived cells to perform drug screening

and therapeutic configuration. In one example, patient-derived neurons were used to identify a novel disease mechanism for a patient-specific *SCN1A* mutation causing Dravet syndrome (298). By coupling technologies such as induced pluripotent stem cells (iPSCs) and microelectrode arrays, customized high-throughput drug screening is possible (299). For the IGDs and B6 dependent epilepsies, there remains a significant challenge to unravel all the downstream effects of impaired GPI-anchoring and reduced efficiency of PLP-dependent enzymes. Coupling the use of modern technologies with improved disease-state phenotyping will hopefully lead us towards a future where better therapies are possible for these devastating conditions.

References

1. Baird PA, Anderson TW, Newcombe HB, Lowry RB. 1988. Genetic disorders in children and young adults: a population study. Am J Hum Genet 42:677-693.

2. Boycott KM, Vanstone MR, Bulman DE, MacKenzie AE. 2013. Rare-disease genetics in the era of next-generation sequencing: discovery to translation. Nat Rev Genet 14:681-691.

3. Carter CO. 1977. Monogenic disorders. J Med Genet 14:316-320.

4. Kaufmann P, Pariser AR, Austin C. 2018. From scientific discovery to treatments for rare diseases - the view from the National Center for Advancing Translational Sciences - Office of Rare Diseases Research. Orphanet J Rare Dis 13:196.

5. Dye DE, Brameld KJ, Maxwell S, Goldblatt J, Bower C, Leonard H, Bourke J, Glasson EJ, O'Leary P. 2011. The impact of single gene and chromosomal disorders on hospital admissions of children and adolescents: a population-based study. Public Health Genomics 14:153-161.

6. McCandless SE, Brunger JW, Cassidy SB. 2004. The burden of genetic disease on inpatient care in a children's hospital. Am J Hum Genet 74:121-127.

7. Yoon PW, Olney RS, Khoury MJ, Sappenfield WM, Chavez GF, Taylor D. 1997. Contribution of birth defects and genetic diseases to pediatric hospitalizations. A population-based study. Arch Pediatr Adolesc Med 151:1096-1103.

8. Ottman R, Hirose S, Jain S, Lerche H, Lopes-Cendes I, Noebels JL, Serratosa J, Zara F, Scheffer IE. 2010. Genetic testing in the epilepsies--report of the ILAE Genetics Commission. Epilepsia 51:655-670.

9. Bamshad MJ, Ng SB, Bigham AW, Tabor HK, Emond MJ, Nickerson DA, Shendure J. 2011. Exome sequencing as a tool for Mendelian disease gene discovery. Nat Rev Genet 12:745-755.

10. Myers KA, Johnstone DL, Dyment DA. 2019. Epilepsy genetics: Current knowledge, applications, and future directions. Clin Genet 95:95-111.

11. Kaiser J. 2010. Human genetics. Affordable 'exomes' fill gaps in a catalog of rare diseases. Science 330:903.

12. McKusick VA. 2007. Mendelian Inheritance in Man and its online version, OMIM. Am J Hum Genet 80:588-604.

13. Antonarakis SE, Beckmann JS. 2006. Mendelian disorders deserve more attention. Nat Rev Genet 7:277-282.

14. Metzker ML. 2010. Sequencing technologies - the next generation. Nat Rev Genet 11:31-46.

15. Adey A, Morrison HG, Asan, Xun X, Kitzman JO, Turner EH, Stackhouse B, MacKenzie AP, Caruccio NC, Zhang X, Shendure J. 2010. Rapid, low-input, low-bias construction of shotgun fragment libraries by high-density in vitro transposition. Genome Biol 11:R119.

16. Sawyer SL, Hartley T, Dyment DA, Beaulieu CL, Schwartzentruber J, Smith A, Bedford HM, Bernard G, Bernier FP, Brais B, Bulman DE, Warman Chardon J, Chitayat D, Deladoey J, Fernandez BA, Frosk P, Geraghty MT, Gerull B, Gibson W, Gow RM, Graham GE, Green JS, Heon E, Horvath G, Innes AM, Jabado N, Kim RH, Koenekoop RK, Khan A, Lehmann OJ, Mendoza-Londono R, Michaud JL, Nikkel SM, Penney LS, Polychronakos C, Richer J, Rouleau GA, Samuels ME, Siu VM, Suchowersky O, Tarnopolsky MA, Yoon G, Zahir FR, Consortium FC, Care4Rare Canada C, Majewski J, Boycott KM. 2016. Utility of whole-exome sequencing for those near the end of the diagnostic odyssey: time to address gaps in care. Clin Genet 89:275-284.

17. Yang Y, Muzny DM, Reid JG, Bainbridge MN, Willis A, Ward PA, Braxton A, Beuten J, Xia F, Niu Z, Hardison M, Person R, Bekheirnia MR, Leduc MS, Kirby A, Pham P, Scull J, Wang M, Ding Y, Plon SE, Lupski JR, Beaudet AL, Gibbs RA, Eng CM. 2013. Clinical whole-exome sequencing for the diagnosis of mendelian disorders. N Engl J Med 369:1502-1511.

18. Levy SE, Myers RM. 2016. Advancements in Next-Generation Sequencing. Annu Rev Genomics Hum Genet 17:95-115.

19. Helbig KL, Farwell Hagman KD, Shinde DN, Mroske C, Powis Z, Li S, Tang S, Helbig I. 2016. Diagnostic exome sequencing provides a molecular diagnosis for a significant proportion of patients with epilepsy. Genet Med 18:898-905.

20. Retterer K, Juusola J, Cho MT, Vitazka P, Millan F, Gibellini F, Vertino-Bell A, Smaoui N, Neidich J, Monaghan KG, McKnight D, Bai R, Suchy S, Friedman B, Tahiliani J, Pineda-Alvarez D, Richard G, Brandt T, Haverfield E, Chung WK, Bale S. 2016. Clinical application of whole-exome sequencing across clinical indications. Genet Med 18:696-704.

21. Palmer EE, Schofield D, Shrestha R, Kandula T, Macintosh R, Lawson JA, Andrews I, Sampaio H, Johnson AM, Farrar MA, Cardamone M, Mowat D, Elakis G, Lo W, Zhu Y, Ying K, Morris P, Tao J, Dias KR, Buckley M, Dinger ME, Cowley MJ, Roscioli T, Kirk EP, Bye A, Sachdev RK. 2018. Integrating exome sequencing into a diagnostic pathway for epileptic encephalopathy: Evidence of clinical utility and cost effectiveness. Mol Genet Genomic Med 6:186-199.

22. Stark Z, Schofield D, Alam K, Wilson W, Mupfeki N, Macciocca I, Shrestha R, White SM, Gaff C. 2017. Prospective comparison of the cost-effectiveness of clinical whole-exome sequencing with that of usual care overwhelmingly supports early use and reimbursement. Genet Med 19:867-874.

23. Willig LK, Petrikin JE, Smith LD, Saunders CJ, Thiffault I, Miller NA, Soden SE, Cakici JA, Herd SM, Twist G, Noll A, Creed M, Alba PM, Carpenter SL, Clements MA, Fischer RT, Hays JA, Kilbride H, McDonough RJ, Rosterman JL, Tsai SL, Zellmer L, Farrow EG, Kingsmore SF. 2015. Whole-genome sequencing for identification of Mendelian disorders in critically ill infants: a retrospective analysis of diagnostic and clinical findings. Lancet Respir Med 3:377-387.

24. Daoud H, Luco SM, Li R, Bareke E, Beaulieu C, Jarinova O, Carson N, Nikkel SM, Graham GE, Richer J, Armour C, Bulman DE, Chakraborty P, Geraghty M, Lines MA, Lacaze-Masmonteil T, Majewski J, Boycott KM, Dyment DA. 2016. Next-generation sequencing for diagnosis of rare diseases in the neonatal intensive care unit. CMAJ 188:E254-E260.

25. Krabbenborg L, Vissers LE, Schieving J, Kleefstra T, Kamsteeg EJ, Veltman JA, Willemsen MA, Van der Burg S. 2016. Understanding the Psychosocial Effects of WES Test Results on Parents of Children with Rare Diseases. J Genet Couns 25:1207-1214.

26. Genomes Project C, Abecasis GR, Auton A, Brooks LD, DePristo MA, Durbin RM, Handsaker RE, Kang HM, Marth GT, McVean GA. 2012. An integrated map of genetic variation from 1,092 human genomes. Nature 491:56-65.

27. Lek M, Karczewski KJ, Minikel EV, Samocha KE, Banks E, Fennell T, O'Donnell-Luria AH, Ware JS, Hill AJ, Cummings BB, Tukiainen T, Birnbaum DP, Kosmicki JA, Duncan LE, Estrada K, Zhao F, Zou J, Pierce-Hoffman E, Berghout J, Cooper DN, Deflaux N, DePristo M, Do R, Flannick J, Fromer M, Gauthier L, Goldstein J, Gupta N, Howrigan D, Kiezun A, Kurki MI, Moonshine AL, Natarajan P, Orozco L, Peloso GM, Poplin R, Rivas MA, Ruano-Rubio V, Rose SA, Ruderfer DM, Shakir K, Stenson PD, Stevens C, Thomas BP, Tiao G, Tusie-Luna MT, Weisburd B, Won HH, Yu D, Altshuler DM, et al. 2016. Analysis of protein-coding genetic variation in 60,706 humans. Nature 536:285-291.

28. Adzhubei I, Jordan DM, Sunyaev SR. 2013. Predicting functional effect of human missense mutations using PolyPhen-2. Curr Protoc Hum Genet Chapter 7:Unit7 20.

29. Kumar P, Henikoff S, Ng PC. 2009. Predicting the effects of coding non-synonymous variants on protein function using the SIFT algorithm. Nat Protoc 4:1073-1081.

30. Kircher M, Witten DM, Jain P, O'Roak BJ, Cooper GM, Shendure J. 2014. A general framework for estimating the relative pathogenicity of human genetic variants. Nat Genet 46:310-315.

31. WHO. February 2017 2017. Epilepsy. http://www.who.int/mediacentre/factsheets/fs999/en/. Accessed

32. Hirtz D, Thurman DJ, Gwinn-Hardy K, Mohamed M, Chaudhuri AR, Zalutsky R. 2007. How common are the "common" neurologic disorders? Neurology 68:326-337.

33. Myers CT, Mefford HC. 2015. Advancing epilepsy genetics in the genomic era. Genome Med 7:91.

34. Hildebrand MS, Dahl HH, Damiano JA, Smith RJ, Scheffer IE, Berkovic SF. 2013. Recent advances in the molecular genetics of epilepsy. J Med Genet 50:271-279.

35. Banerjee PN, Filippi D, Allen Hauser W. 2009. The descriptive epidemiology of epilepsy-a review. Epilepsy Res 85:31-45.

36. Fiest KM, Sauro KM, Wiebe S, Patten SB, Kwon CS, Dykeman J, Pringsheim T, Lorenzetti DL, Jette N. 2017. Prevalence and incidence of epilepsy: A systematic review and meta-analysis of international studies. Neurology 88:296-303.

37. Hesdorffer DC, Logroscino G, Benn EK, Katri N, Cascino G, Hauser WA. 2011. Estimating risk for developing epilepsy: a population-based study in Rochester, Minnesota. Neurology 76:23-27.

38. Thurman DJ, Hesdorffer DC, French JA. 2014. Sudden unexpected death in epilepsy: assessing the public health burden. Epilepsia 55:1479-1485.

39. Fisher RS, Acevedo C, Arzimanoglou A, Bogacz A, Cross JH, Elger CE, Engel J, Jr., Forsgren L, French JA, Glynn M, Hesdorffer DC, Lee BI, Mathern GW, Moshe SL, Perucca E, Scheffer IE, Tomson T, Watanabe M, Wiebe S. 2014. ILAE official report: a practical clinical definition of epilepsy. Epilepsia 55:475-482.

40. Berg AT, Berkovic SF, Brodie MJ, Buchhalter J, Cross JH, van Emde Boas W, Engel J, French J, Glauser TA, Mathern GW, Moshe SL, Nordli D, Plouin P, Scheffer IE. 2010. Revised terminology and concepts for organization of seizures and epilepsies: report of the ILAE Commission on Classification and Terminology, 2005-2009. Epilepsia 51:676-685.

41. Scheffer IE, Berkovic S, Capovilla G, Connolly MB, French J, Guilhoto L, Hirsch E, Jain S, Mathern GW, Moshe SL, Nordli DR, Perucca E, Tomson T, Wiebe S, Zhang YH, Zuberi SM. 2017. ILAE classification of the epilepsies: Position paper of the ILAE Commission for Classification and Terminology. Epilepsia 58:512-521.

42. Thomas RH, Berkovic SF. 2014. The hidden genetics of epilepsy-a clinically important new paradigm. Nat Rev Neurol 10:283-292.

43. Lennox WG. 1947. The genetics of epilepsy. Am J Psychiatry 103:457-462.

44. Annegers JF, Hauser WA, Anderson VE, Kurland LT. 1982. The risks of seizure disorders among relatives of patients with childhood onset epilepsy. Neurology 32:174-179.

45. Hemminki K, Li X, Johansson SE, Sundquist K, Sundquist J. 2006. Familial risks for epilepsy among siblings based on hospitalizations in Sweden. Neuroepidemiology 27:67-73.

46. Peljto AL, Barker-Cummings C, Vasoli VM, Leibson CL, Hauser WA, Buchhalter JR, Ottman R. 2014. Familial risk of epilepsy: a population-based study. Brain 137:795-805.

47. Berkovic SF, Howell RA, Hay DA, Hopper JL. 1998. Epilepsies in twins: genetics of the major epilepsy syndromes. Ann Neurol 43:435-445.

48. Kjeldsen MJ, Corey LA, Solaas MH, Friis ML, Harris JR, Kyvik KO, Christensen K, Pellock JM. 2005. Genetic factors in seizures: a population-based study of 47,626 US, Norwegian and Danish twin pairs. Twin Res Hum Genet 8:138-147.

49. Kjeldsen MJ, Kyvik KO, Christensen K, Friis ML. 2001. Genetic and environmental factors in epilepsy: a population-based study of 11900 Danish twin pairs. Epilepsy Res 44:167-178.

50. Vadlamudi L, Milne RL, Lawrence K, Heron SE, Eckhaus J, Keay D, Connellan M, Torn-Broers Y, Howell RA, Mulley JC, Scheffer IE, Dibbens LM, Hopper JL, Berkovic SF. 2014. Genetics of epilepsy: The testimony of twins in the molecular era. Neurology 83:1042-1048.

51. Chambers C, Jansen LA, Dhamija R. 2016. Review of Commercially Available Epilepsy Genetic Panels. J Genet Couns 25:213-217.

52. Wirrell E, Farrell K, Whiting S. 2005. The epileptic encephalopathies of infancy and childhood. Can J Neurol Sci 32:409-418.

53. McTague A, Howell KB, Cross JH, Kurian MA, Scheffer IE. 2016. The genetic landscape of the epileptic encephalopathies of infancy and childhood. Lancet Neurol 15:304-316.

54. Engel J, Jr., International League Against E. 2001. A proposed diagnostic scheme for people with epileptic seizures and with epilepsy: report of the ILAE Task Force on Classification and Terminology. Epilepsia 42:796-803.

55. Cowan LD, Hudson LS. 1991. The epidemiology and natural history of infantile spasms. J Child Neurol 6:355-364.

56. Bayat A, Hjalgrim H, Moller RS. 2015. The incidence of SCN1A-related Dravet syndrome in Denmark is 1:22,000: a population-based study from 2004 to 2009. Epilepsia 56:e36-39.

57. Hurst DL. 1990. Epidemiology of severe myoclonic epilepsy of infancy. Epilepsia 31:397-400.

58. Cone TE, Jr. 1970. On a peculiar form of infantile convulsions (hypsarrhythmia) as described in his own infant son by Dr. W.J. West in 1841. Pediatrics 46:603.

59. Gastaut H, Roger J, Ouahchi S, Timsit M, Broughton R. 1963. An electro-clinical study of generalized epileptic seizures of tonic expression. Epilepsia 4:15-44.

60. Landau WM, Kleffner FR. 1957. Syndrome of acquired aphasia with convulsive disorder in children. Neurology 7:523-530.

61. Trivisano M, Specchio N. 2020. What are the epileptic encephalopathies? Curr Opin Neurol 33:179-184.

62. Ohtahara S, Ishida T, Oka E, Yamatogi Y, Inoue H. 1976. On the Specific Age Dependent Epileptic Syndrome: The Early-Infantile Epileptic Encephalopathy with Suppression-Burst. NO TO HATATSU 8:270-280.

63. Yamatogi Y, Ohtahara S. 1981. Age-dependent epileptic encephalopathy: a longitudinal study. Folia Psychiatr Neurol Jpn 35:321-332.

64. Berg AT, Langfitt JT, Testa FM, Levy SR, DiMario F, Westerveld M, Kulas J. 2008. Global cognitive function in children with epilepsy: a community-based study. Epilepsia 49:608-614.

65. Shepherd C, Hosking G. 1989. Epilepsy in school children with intellectual impairments in Sheffield: the size and nature of the problem and the implications for service provision. J Ment Defic Res 33 (Pt 6):511-514.

66. Dravet C. 2011. The core Dravet syndrome phenotype. Epilepsia 52 Suppl 2:3-9.

67. Hamdan FF, Myers CT, Cossette P, Lemay P, Spiegelman D, Laporte AD, Nassif C, Diallo O, Monlong J, Cadieux-Dion M, Dobrzeniecka S, Meloche C, Retterer K, Cho MT, Rosenfeld JA, Bi W, Massicotte C, Miguet M, Brunga L, Regan BM, Mo K, Tam C, Schneider A, Hollingsworth G, Deciphering Developmental Disorders S, FitzPatrick DR, Donaldson A, Canham N, Blair E, Kerr B, Fry AE, Thomas RH, Shelagh J, Hurst JA, Brittain H, Blyth M, Lebel RR, Gerkes EH, Davis-Keppen L, Stein Q, Chung WK, Dorison SJ, Benke PJ, Fassi E, Corsten-Janssen N, Kamsteeg EJ, Mau-Them FT, Bruel AL, Verloes A, Ounap K, et al. 2017. High Rate of Recurrent De Novo Mutations in Developmental and Epileptic Encephalopathies. Am J Hum Genet 101:664-685.

68. Akman CI, Yu J, Alter A, Engelstad K, De Vivo DC. 2016. Diagnosing Glucose Transporter 1 Deficiency at Initial Presentation Facilitates Early Treatment. J Pediatr 171:220-226.

69. van Karnebeek CD, Tiebout SA, Niermeijer J, Poll-The BT, Ghani A, Coughlin CR, 2nd, Van Hove JL, Richter JW, Christen HJ, Gallagher R, Hartmann H, Stockler-Ipsiroglu S. 2016. Pyridoxine-Dependent Epilepsy: An Expanding Clinical Spectrum. Pediatr Neurol 59:6-12.

70. Chiron C, Dulac O. 2011. The pharmacologic treatment of Dravet syndrome. Epilepsia 52 Suppl 2:72-75.

71. Brunklaus A, Dorris L, Ellis R, Reavey E, Lee E, Forbes G, Appleton R, Cross JH, Ferrie C, Hughes I, Jollands A, King MD, Livingston J, Lynch B, Philip S, Scheffer IE, Williams R, Zuberi SM. 2013. The clinical utility of an SCN1A genetic diagnosis in infantile-onset epilepsy. Dev Med Child Neurol 55:154-161.

72. Catarino CB, Liu JY, Liagkouras I, Gibbons VS, Labrum RW, Ellis R, Woodward C, Davis MB, Smith SJ, Cross JH, Appleton RE, Yendle SC, McMahon JM, Bellows ST, Jacques TS, Zuberi SM, Koepp MJ, Martinian L, Scheffer IE, Thom M, Sisodiya SM. 2011. Dravet syndrome as epileptic encephalopathy: evidence from long-term course and neuropathology. Brain 134:2982-3010.

73. Brodie MJ, Barry SJ, Bamagous GA, Norrie JD, Kwan P. 2012. Patterns of treatment response in newly diagnosed epilepsy. Neurology 78:1548-1554.

74. Kwan P, Brodie MJ. 2000. Early identification of refractory epilepsy. N Engl J Med 342:314-319.

75. Kim JB. 2014. Channelopathies. Korean J Pediatr 57:1-18.

76. van Loo KMJ, Becker AJ. 2019. Transcriptional Regulation of Channelopathies in Genetic and Acquired Epilepsies. Front Cell Neurosci 13:587.

77. Bernard C. 2012. Alterations in synaptic function in epilepsy. *In* th, Noebels JL, Avoli M, Rogawski MA, Olsen RW, Delgado-Escueta AV (ed), Jasper's Basic Mechanisms of the Epilepsies, Bethesda (MD).

78. Brockmann K, Wang D, Korenke CG, von Moers A, Ho YY, Pascual JM, Kuang K, Yang H, Ma L, Kranz-Eble P, Fischbarg J, Hanefeld F, De Vivo DC. 2001. Autosomal dominant glut-1 deficiency syndrome and familial epilepsy. Ann Neurol 50:476-485.

79. Klepper J, Willemsen M, Verrips A, Guertsen E, Herrmann R, Kutzick C, Florcken A, Voit T. 2001. Autosomal dominant transmission of GLUT1 deficiency. Hum Mol Genet 10:63-68.

80. Hudson G, Deschauer M, Busse K, Zierz S, Chinnery PF. 2005. Sensory ataxic neuropathy due to a novel C10Orf2 mutation with probable germline mosaicism. Neurology 64:371-373.

81. Jarrett SG, Liang LP, Hellier JL, Staley KJ, Patel M. 2008. Mitochondrial DNA damage and impaired base excision repair during epileptogenesis. Neurobiol Dis 30:130-138.

82. Van Goethem G, Luoma P, Rantamaki M, Al Memar A, Kaakkola S, Hackman P, Krahe R, Lofgren A, Martin JJ, De Jonghe P, Suomalainen A, Udd B, Van Broeckhoven C. 2004. POLG mutations in neurodegenerative disorders with ataxia but no muscle involvement. Neurology 63:1251-1257.

83. Lamar KJ, Carvill GL. 2018. Chromatin Remodeling Proteins in Epilepsy: Lessons From CHD2-Associated Epilepsy. Front Mol Neurosci 11:208.

84. Ohtsuka Y, Ohmori I, Oka E. 1998. Long-term follow-up of childhood epilepsy associated with tuberous sclerosis. Epilepsia 39:1158-1163.

85. Yu JY, Pearl PL. 2013. Metabolic causes of epileptic encephalopathy. Epilepsy Res Treat 2013:124934.

86. Noebels J. 2015. Pathway-driven discovery of epilepsy genes. Nat Neurosci 18:344-350.

87. Oliver KL, Lukic V, Thorne NP, Berkovic SF, Scheffer IE, Bahlo M. 2014. Harnessing gene expression networks to prioritize candidate epileptic encephalopathy genes. PLoS One 9:e102079.

88. UniProt C. 2015. UniProt: a hub for protein information. Nucleic Acids Res 43:D204-212.

89. Ferguson MAJ, Hart GW, Kinoshita T. 2015. Glycosylphosphatidylinositol Anchors, p 137-150. *In* rd, Varki A, Cummings RD, Esko JD, Stanley P, Hart GW, Aebi M, Darvill AG, Kinoshita T, Packer NH, Prestegard JH, Schnaar RL, Seeberger PH (ed), Essentials of Glycobiology doi:10.1101/glycobiology.3e.012, Cold Spring Harbor (NY).

90. Kinoshita T, Fujita M. 2016. Biosynthesis of GPI-anchored proteins: special emphasis on GPI lipid remodeling. J Lipid Res 57:6-24.

91. Nozaki M, Ohishi K, Yamada N, Kinoshita T, Nagy A, Takeda J. 1999. Developmental abnormalities of glycosylphosphatidylinositol-anchor-deficient embryos revealed by Cre/loxP system. Lab Invest 79:293-299.

92. Tarutani M, Itami S, Okabe M, Ikawa M, Tezuka T, Yoshikawa K, Kinoshita T, Takeda J. 1997. Tissue-specific knockout of the mouse Pig-a gene reveals important roles for GPI-anchored proteins in skin development. Proc Natl Acad Sci U S A 94:7400-7405.

93. Park S, Lee C, Sabharwal P, Zhang M, Meyers CL, Sockanathan S. 2013. GDE2 promotes neurogenesis by glycosylphosphatidylinositol-anchor cleavage of RECK. Science 339:324-328.

94. McKean DM, Niswander L. 2012. Defects in GPI biosynthesis perturb Cripto signaling during forebrain development in two new mouse models of holoprosencephaly. Biol Open 1:874-883.

95. Kondoh G, Tojo H, Nakatani Y, Komazawa N, Murata C, Yamagata K, Maeda Y, Kinoshita T, Okabe M, Taguchi R, Takeda J. 2005. Angiotensin-converting enzyme

is a GPI-anchored protein releasing factor crucial for fertilization. Nat Med 11:160-166.

96. Alfieri JA, Martin AD, Takeda J, Kondoh G, Myles DG, Primakoff P. 2003. Infertility in female mice with an oocyte-specific knockout of GPI-anchored proteins. J Cell Sci 116:2149-2155.

97. Lopez-Cobo S, Campos-Silva C, Vales-Gomez M. 2016. Glycosyl-Phosphatidyl-Inositol (GPI)-Anchors and Metalloproteases: Their Roles in the Regulation of Exosome Composition and NKG2D-Mediated Immune Recognition. Front Cell Dev Biol 4:97.

98. Kinoshita T. 2016. Glycosylphosphatidylinositol (GPI) Anchors: Biochemistry and Cell Biology: Introduction to a Thematic Review Series. J Lipid Res 57:4-5.

99. Kinoshita T. 2014. Biosynthesis and deficiencies of glycosylphosphatidylinositol. Proc Jpn Acad Ser B Phys Biol Sci 90:130-143.

100. Murakami Y, Siripanyaphinyo U, Hong Y, Tashima Y, Maeda Y, Kinoshita T. 2005. The initial enzyme for glycosylphosphatidylinositol biosynthesis requires PIG-Y, a seventh component. Mol Biol Cell 16:5236-5246.

101. Watanabe R, Inoue N, Westfall B, Taron CH, Orlean P, Takeda J, Kinoshita T. 1998. The first step of glycosylphosphatidylinositol biosynthesis is mediated by a complex of PIG-A, PIG-H, PIG-C and GPI1. EMBO J 17:877-885.

102. Watanabe R, Murakami Y, Marmor MD, Inoue N, Maeda Y, Hino J, Kangawa K, Julius M, Kinoshita T. 2000. Initial enzyme for glycosylphosphatidylinositol biosynthesis requires PIG-P and is regulated by DPM2. EMBO J 19:4402-4411.

103. Orlean P, Menon AK. 2007. Thematic review series: lipid posttranslational modifications. GPI anchoring of protein in yeast and mammalian cells, or: how we learned to stop worrying and love glycophospholipids. J Lipid Res 48:993-1011.

104. Bellai-Dussault K, Nguyen TTM, Baratang NV, Jimenez-Cruz DA, Campeau PM. 2019. Clinical variability in inherited glycosylphosphatidylinositol deficiency disorders. Clinical Genetics 95:112-121.

105. Takeda J, Miyata T, Kawagoe K, Iida Y, Endo Y, Fujita T, Takahashi M, Kitani T, Kinoshita T. 1993. Deficiency of the GPI anchor caused by a somatic mutation of the PIG-A gene in paroxysmal nocturnal hemoglobinuria. Cell 73:703-711.

106. Brodsky RA. 2008. Advances in the diagnosis and therapy of paroxysmal nocturnal hemoglobinuria. Blood Rev 22:65-74.

107. Carmody LC, Blau H, Danis D, Zhang XA, Gourdine JP, Vasilevsky N, Krawitz P, Thompson MD, Robinson PN. 2020. Significantly different clinical phenotypes associated with mutations in synthesis and transamidase+remodeling

glycosylphosphatidylinositol (GPI)-anchor biosynthesis genes. Orphanet J Rare Dis 15:40.

108. Almeida AM, Murakami Y, Layton DM, Hillmen P, Sellick GS, Maeda Y, Richards S, Patterson S, Kotsianidis I, Mollica L, Crawford DH, Baker A, Ferguson M, Roberts I, Houlston R, Kinoshita T, Karadimitris A. 2006. Hypomorphic promoter mutation in PIGM causes inherited glycosylphosphatidylinositol deficiency. Nat Med 12:846-851.

109. Cole DE, Thompson MD. 2015. Neurogenetic Aspects of Hyperphosphatasia in Mabry Syndrome. Subcell Biochem 76:343-361.

110. Gomes WJ, Hunter JL. 1970. Mental retardation, cataracts, and unexplained hyperphosphatasia. Arch Dis Child 45:726-727.

111. Mabry CC, Bautista A, Kirk RF, Dubilier LD, Braunstein H, Koepke JA. 1970. Familial hyperphosphatase with mental retardation, seizures, and neurologic deficits. J Pediatr 77:74-85.

112. Krawitz PM, Schweiger MR, Rodelsperger C, Marcelis C, Kolsch U, Meisel C, Stephani F, Kinoshita T, Murakami Y, Bauer S, Isau M, Fischer A, Dahl A, Kerick M, Hecht J, Kohler S, Jager M, Grunhagen J, de Condor BJ, Doelken S, Brunner HG, Meinecke P, Passarge E, Thompson MD, Cole DE, Horn D, Roscioli T, Mundlos S, Robinson PN. 2010. Identity-by-descent filtering of exome sequence data identifies PIGV mutations in hyperphosphatasia mental retardation syndrome. Nat Genet 42:827-829.

113. Percudani R, Peracchi A. 2009. The B6 database: a tool for the description and classification of vitamin B6-dependent enzymatic activities and of the corresponding protein families. BMC Bioinformatics 10:273.

114. Magnusdottir S, Ravcheev D, de Crecy-Lagard V, Thiele I. 2015. Systematic genome assessment of B-vitamin biosynthesis suggests co-operation among gut microbes. Front Genet 6:148.

115. Wilson MP, Plecko B, Mills PB, Clayton PT. 2019. Disorders affecting vitamin B6 metabolism. J Inherit Metab Dis 42:629-646.

116. Eliot AC, Kirsch JF. 2004. Pyridoxal phosphate enzymes: mechanistic, structural, and evolutionary considerations. Annu Rev Biochem 73:383-415.

117. John RA. 1995. Pyridoxal phosphate-dependent enzymes. Biochim Biophys Acta 1248:81-96.

118. Percudani R, Peracchi A. 2003. A genomic overview of pyridoxal-phosphate-dependent enzymes. EMBO Rep 4:850-854.

119. Baxter P. 2001. Pyridoxine-dependent and pyridoxine-responsive seizures. Dev Med Child Neurol 43:416-420.

120. Clayton PT. 2006. B6-responsive disorders: a model of vitamin dependency. J Inherit Metab Dis 29:317-326.

121. Hunt AD, Jr., Stokes J, Jr., Mc CW, Stroud HH. 1954. Pyridoxine dependency: report of a case of intractable convulsions in an infant controlled by pyridoxine. Pediatrics 13:140-145.

122. Jr. GS. 2017 Apr 13 2017. Pyridoxine-Dependent Epilepsy, *on* University of Washington. https://www.ncbi.nlm.nih.gov/books/NBK1486/. Accessed

123. Mills PB, Surtees RA, Champion MP, Beesley CE, Dalton N, Scambler PJ, Heales SJ, Briddon A, Scheimberg I, Hoffmann GF, Zschocke J, Clayton PT. 2005. Neonatal epileptic encephalopathy caused by mutations in the PNPO gene encoding pyridox(am)ine 5'-phosphate oxidase. Hum Mol Genet 14:1077-1086.

124. Waymire KG, Mahuren JD, Jaje JM, Guilarte TR, Coburn SP, MacGregor GR. 1995. Mice lacking tissue non-specific alkaline phosphatase die from seizures due to defective metabolism of vitamin B-6. Nat Genet 11:45-51.

125. Mills PB, Struys E, Jakobs C, Plecko B, Baxter P, Baumgartner M, Willemsen MA, Omran H, Tacke U, Uhlenberg B, Weschke B, Clayton PT. 2006. Mutations in antiquitin in individuals with pyridoxine-dependent seizures. Nat Med 12:307-309.

126. De Wergifosse P, Jacques B, Jonniaux JL, Purnelle B, Skala J, Goffeau A. 1994. The sequence of a 22.4 kb DNA fragment from the left arm of yeast chromosome II reveals homologues to bacterial proline synthetase and murine alpha-adaptin, as well as a new permease and a DNA-binding protein. Yeast 10:1489-1496.

127. Ikegawa S, Isomura M, Koshizuka Y, Nakamura Y. 1999. Cloning and characterization of human and mouse PROSC (proline synthetase co-transcribed) genes. J Hum Genet 44:337-342.

128. Ito T, Iimori J, Takayama S, Moriyama A, Yamauchi A, Hemmi H, Yoshimura T. 2013. Conserved pyridoxal protein that regulates Ile and Val metabolism. J Bacteriol 195:5439-5449.

129. Prunetti L, El Yacoubi B, Schiavon CR, Kirkpatrick E, Huang L, Bailly M, ElBadawi-Sidhu M, Harrison K, Gregory JF, Fiehn O, Hanson AD, de Crecy-Lagard V. 2016. Evidence That COG0325 Proteins are involved in PLP Homeostasis. Microbiology 162:694-706.

130. Leonardi R, Zhang YM, Rock CO, Jackowski S. 2005. Coenzyme A: back in action. Prog Lipid Res 44:125-153.

131. Darin N, Reid E, Prunetti L, Samuelsson L, Husain RA, Wilson M, El Yacoubi B, Footitt E, Chong WK, Wilson LC, Prunty H, Pope S, Heales S, Lascelles K, Champion M, Wassmer E, Veggiotti P, de Crecy-Lagard V, Mills PB, Clayton PT. 2016. Mutations in PROSC Disrupt Cellular Pyridoxal Phosphate Homeostasis and Cause Vitamin-B6-Dependent Epilepsy. Am J Hum Genet 99:1325-1337.

132. Plecko B, Zweier M, Begemann A, Mathis D, Schmitt B, Striano P, Baethmann M, Vari MS, Beccaria F, Zara F, Crowther LM, Joset P, Sticht H, Papuc SM, Rauch A. 2017. Confirmation of mutations in PROSC as a novel cause of vitamin B 6 - dependent epilepsy. J Med Genet 54:809-814.

133. Gospe SM, Jr., Olin KL, Keen CL. 1994. Reduced GABA synthesis in pyridoxine-dependent seizures. Lancet 343:1133-1134.

134. Kurlemann G, Ziegler R, Gruneberg M, Bomelburg T, Ullrich K, Palm DG. 1992. Disturbance of GABA metabolism in pyridoxine-dependent seizures. Neuropediatrics 23:257-259.

135. Buske OJ, Girdea M, Dumitriu S, Gallinger B, Hartley T, Trang H, Misyura A, Friedman T, Beaulieu C, Bone WP, Links AE, Washington NL, Haendel MA, Robinson PN, Boerkoel CF, Adams D, Gahl WA, Boycott KM, Brudno M. 2015. PhenomeCentral: a portal for phenotypic and genotypic matchmaking of patients with rare genetic diseases. Hum Mutat 36:931-940.

136. Sobreira N, Schiettecatte F, Valle D, Hamosh A. 2015. GeneMatcher: a matching tool for connecting investigators with an interest in the same gene. Hum Mutat 36:928-930.

137. Philippakis AA, Azzariti DR, Beltran S, Brookes AJ, Brownstein CA, Brudno M, Brunner HG, Buske OJ, Carey K, Doll C, Dumitriu S, Dyke SO, den Dunnen JT, Firth HV, Gibbs RA, Girdea M, Gonzalez M, Haendel MA, Hamosh A, Holm IA, Huang L, Hurles ME, Hutton B, Krier JB, Misyura A, Mungall CJ, Paschall J, Paten B, Robinson PN, Schiettecatte F, Sobreira NL, Swaminathan GJ, Taschner PE, Terry SF, Washington NL, Zuchner S, Boycott KM, Rehm HL. 2015. The Matchmaker Exchange: a platform for rare disease gene discovery. Hum Mutat 36:915-921.

138. Boycott KM, Campeau PM, Howley HE, Pavlidis P, Rogic S, Oriel C, Berman JN, Hamilton RM, Hicks GG, Lipshitz HD, Masson JY, Shoubridge EA, Junker A, Leroux MR, McMaster CR, Michaud JL, Turvey SE, Dyment D, Innes AM, van Karnebeek CD, Lehman A, Cohn RD, MacDonald IM, Rachubinski RA, Frosk P, Vandersteen A, Wozniak RW, Pena IA, Wen XY, Lacaze-Masmonteil T, Rankin C, Hieter P. 2020. The Canadian Rare Diseases Models and Mechanisms (RDMM) Network: Connecting Understudied Genes to Model Organisms. Am J Hum Genet 106:143-152.

139. Cunliffe VT. 2016. Building a zebrafish toolkit for investigating the pathobiology of epilepsy and identifying new treatments for epileptic seizures. J Neurosci Methods 260:91-95.

140. Hortopan GA, Dinday MT, Baraban SC. 2010. Zebrafish as a model for studying genetic aspects of epilepsy. Dis Model Mech 3:144-148.

141. Cunliffe VT. 2015. Building a zebrafish toolkit for investigating the pathobiology of epilepsy and identifying new treatments for epileptic seizures. J Neurosci Methods doi:10.1016/j.jneumeth.2015.07.015.

142. Auer TO, Duroure K, Concordet JP, Del Bene F. 2014. CRISPR/Cas9-mediated conversion of eGFP- into Gal4-transgenic lines in zebrafish. Nat Protoc 9:2823-2840.

143. Nasevicius A, Ekker SC. 2000. Effective targeted gene 'knockdown' in zebrafish. Nat Genet 26:216-220.

144. Stewart AM, Desmond D, Kyzar E, Gaikwad S, Roth A, Riehl R, Collins C, Monnig L, Green J, Kalueff AV. 2012. Perspectives of zebrafish models of epilepsy: what, how and where next? Brain Res Bull 87:135-143.

145. Baraban SC, Dinday MT, Hortopan GA. 2013. Drug screening in Scn1a zebrafish mutant identifies clemizole as a potential Dravet syndrome treatment. Nat Commun 4:2410.

146. Zhang Y, Kecskes A, Copmans D, Langlois M, Crawford AD, Ceulemans B, Lagae L, de Witte PA, Esguerra CV. 2015. Pharmacological characterization of an antisense knockdown zebrafish model of Dravet syndrome: inhibition of epileptic seizures by the serotonin agonist fenfluramine. PLoS One 10:e0125898.

147. Griffin A, Hamling KR, Knupp K, Hong S, Lee LP, Baraban SC. 2017. Clemizole and modulators of serotonin signalling suppress seizures in Dravet syndrome. Brain 140:669-683.

148. Kosuta C, Daniel K, Johnstone DL, Mongeon K, Ban K, LeBlanc S, MacLeod S, Et-Tahiry K, Ekker M, MacKenzie A, Pena I. 2018. High-throughput DNA Extraction and Genotyping of 3dpf Zebrafish Larvae by Fin Clipping. J Vis Exp doi:10.3791/58024.

149. Pena IA, Roussel Y, Daniel K, Mongeon K, Johnstone D, Mendes HW, Bosma M, Saxena V, Lepage N, Chakraborty P, Dyment DA, van Karnebeek CDM, Verhoeven-Duif N, Bui TV, Boycott KM, Ekker M, MacKenzie A. 2017. Pyridoxine-Dependent Epilepsy in Zebrafish Caused by Aldh7a1 Deficiency. Genetics 207:1501-1518.

150. Kinoshita T, Fujita M, Maeda Y. 2008. Biosynthesis, remodelling and functions of mammalian GPI-anchored proteins: recent progress. J Biochem 144:287-294.

151. Fauth C, Steindl K, Toutain A, Farrell S, Witsch-Baumgartner M, Karall D, Joset P, Bohm S, Baumer A, Maier O, Zschocke J, Weksberg R, Marshall CR, Rauch A. 2016. A recurrent germline mutation in the PIGA gene causes Simpson-Golabi-Behmel syndrome type 2. Am J Med Genet A 170A:392-402.

152. Johnston JJ, Gropman AL, Sapp JC, Teer JK, Martin JM, Liu CF, Yuan X, Ye Z, Cheng L, Brodsky RA, Biesecker LG. 2012. The phenotype of a germline mutation in PIGA: the gene somatically mutated in paroxysmal nocturnal hemoglobinuria. Am J Hum Genet 90:295-300.

153. Kato M, Saitsu H, Murakami Y, Kikuchi K, Watanabe S, Iai M, Miya K, Matsuura R, Takayama R, Ohba C, Nakashima M, Tsurusaki Y, Miyake N, Hamano S, Osaka H, Hayasaka K, Kinoshita T, Matsumoto N. 2014. PIGA mutations cause early-onset epileptic encephalopathies and distinctive features. Neurology 82:1587-1596.

154. Martin HC, Kim GE, Pagnamenta AT, Murakami Y, Carvill GL, Meyer E, Copley RR, Rimmer A, Barcia G, Fleming MR, Kronengold J, Brown MR, Hudspith KA, Broxholme J, Kanapin A, Cazier JB, Kinoshita T, Nabbout R, Consortium WGS, Bentley D, McVean G, Heavin S, Zaiwalla Z, McShane T, Mefford HC, Shears D, Stewart H, Kurian MA, Scheffer IE, Blair E, Donnelly P, Kaczmarek LK, Taylor JC. 2014. Clinical whole-genome sequencing in severe early-onset epilepsy reveals new genes and improves molecular diagnosis. Hum Mol Genet 23:3200-3211.

155. Edvardson S, Murakami Y, Nguyen TTM, Shahrour M, St-Denis A, Shaag A, Damseh N, Le Deist F, Bryceson Y, Abu-Libdeh B, Campeau PM, Kinoshita T, Elpeleg O. 2016. Mutations in the phosphatidylinositol glycan C (PIGC) gene are associated with epilepsy and intellectual disability. J Med Genet.

156. Ilkovski B, Pagnamenta AT, O'Grady GL, Kinoshita T, Howard MF, Lek M, Thomas B, Turner A, Christodoulou J, Sillence D, Knight SJ, Popitsch N, Keays DA, Anzilotti C, Goriely A, Waddell LB, Brilot F, North KN, Kanzawa N, Macarthur DG, Taylor JC, Kini U, Murakami Y, Clarke NF. 2015. Mutations in PIGY: expanding the phenotype of inherited glycosylphosphatidylinositol deficiencies. Hum Mol Genet 24:6146-6159.

157. Barone R, Aiello C, Race V, Morava E, Foulquier F, Riemersma M, Passarelli C, Concolino D, Carella M, Santorelli F, Vleugels W, Mercuri E, Garozzo D, Sturiale L, Messina S, Jaeken J, Fiumara A, Wevers RA, Bertini E, Matthijs G, Lefeber DJ. 2012. DPM2-CDG: a muscular dystrophy-dystroglycanopathy syndrome with severe epilepsy. Ann Neurol 72:550-558.

158. Fujiwara I, Murakami Y, Niihori T, Kanno J, Hakoda A, Sakamoto O, Okamoto N, Funayama R, Nagashima T, Nakayama K, Kinoshita T, Kure S, Matsubara Y, Aoki Y. 2015. Mutations in PIGL in a patient with Mabry syndrome. Am J Med Genet A 167A:777-785.

159. Ng BG, Hackmann K, Jones MA, Eroshkin AM, He P, Wiliams R, Bhide S, Cantagrel V, Gleeson JG, Paller AS, Schnur RE, Tinschert S, Zunich J, Hegde MR, Freeze HH. 2012. Mutations in the glycosylphosphatidylinositol gene PIGL cause CHIME syndrome. Am J Hum Genet 90:685-688.

160. Chiyonobu T, Inoue N, Morimoto M, Kinoshita T, Murakami Y. 2014. Glycosylphosphatidylinositol (GPI) anchor deficiency caused by mutations in PIGW

is associated with West syndrome and hyperphosphatasia with mental retardation syndrome. J Med Genet 51:203-207.

161. Horn D, Krawitz P, Mannhardt A, Korenke GC, Meinecke P. 2011. Hyperphosphatasia-mental retardation syndrome due to PIGV mutations: expanded clinical spectrum. Am J Med Genet A 155A:1917-1922.

162. Thompson MD, Roscioli T, Marcelis C, Nezarati MM, Stolte-Dijkstra I, Sharom FJ, Lu P, Phillips JA, Sweeney E, Robinson PN, Krawitz P, Yntema HG, Andrade DM, Brunner HG, Cole DE. 2012. Phenotypic variability in hyperphosphatasia with seizures and neurologic deficit (Mabry syndrome). Am J Med Genet A 158A:553-558.

163. Xue J, Li H, Zhang Y, Yang Z. 2016. Clinical and genetic analysis of two Chinese infants with Mabry syndrome. Brain Dev 38:807-818.

164. Brady PD, Moerman P, De Catte L, Deprest J, Devriendt K, Vermeesch JR. 2014. Exome sequencing identifies a recessive PIGN splice site mutation as a cause of syndromic congenital diaphragmatic hernia. Eur J Med Genet 57:487-493.

165. Maydan G, Noyman I, Har-Zahav A, Neriah ZB, Pasmanik-Chor M, Yeheskel A, Albin-Kaplanski A, Maya I, Magal N, Birk E, Simon AJ, Halevy A, Rechavi G, Shohat M, Straussberg R, Basel-Vanagaite L. 2011. Multiple congenital anomalies-hypotonia-seizures syndrome is caused by a mutation in PIGN. J Med Genet 48:383-389.

166. McInerney-Leo AM, Harris JE, Gattas M, Peach EE, Sinnott S, Dudding-Byth T, Rajagopalan S, Barnett CP, Anderson LK, Wheeler L, Brown MA, Leo PJ, Wicking C, Duncan EL. 2016. Fryns Syndrome Associated with Recessive Mutations in PIGN in two Separate Families. Hum Mutat 37:695-702.

167. Ohba C, Okamoto N, Murakami Y, Suzuki Y, Tsurusaki Y, Nakashima M, Miyake N, Tanaka F, Kinoshita T, Matsumoto N, Saitsu H. 2014. PIGN mutations cause congenital anomalies, developmental delay, hypotonia, epilepsy, and progressive cerebellar atrophy. Neurogenetics 15:85-92.

168. Couser NL, Masood MM, Strande NT, Foreman AK, Crooks K, Weck KE, Lu M, Wilhelmsen KC, Roche M, Evans JP, Berg JS, Powell CM. 2015. The phenotype of multiple congenital anomalies-hypotonia-seizures syndrome 1: report and review. Am J Med Genet A 167A:2176-2181.

169. Fleming L, Lemmon M, Beck N, Johnson M, Mu W, Murdock D, Bodurtha J, Hoover-Fong J, Cohn R, Bosemani T, Baranano K, Hamosh A. 2016. Genotype-phenotype correlation of congenital anomalies in multiple congenital anomalies hypotonia seizures syndrome (MCAHS1)/PIGN-related epilepsy. Am J Med Genet A 170A:77-86.

170. Krawitz PM, Murakami Y, Hecht J, Kruger U, Holder SE, Mortier GR, Delle Chiaie B, De Baere E, Thompson MD, Roscioli T, Kielbasa S, Kinoshita T, Mundlos S, Robinson PN, Horn D. 2012. Mutations in PIGO, a member of the GPI-anchor-synthesis pathway, cause hyperphosphatasia with mental retardation. Am J Hum Genet 91:146-151.

171. Nakamura K, Osaka H, Murakami Y, Anzai R, Nishiyama K, Kodera H, Nakashima M, Tsurusaki Y, Miyake N, Kinoshita T, Matsumoto N, Saitsu H. 2014. PIGO mutations in intractable epilepsy and severe developmental delay with mild elevation of alkaline phosphatase levels. Epilepsia 55:e13-17.

172. Kuki I, Takahashi Y, Okazaki S, Kawawaki H, Ehara E, Inoue N, Kinoshita T, Murakami Y. 2013. Vitamin B6-responsive epilepsy due to inherited GPI deficiency. Neurology 81:1467-1469.

173. Makrythanasis P, Kato M, Zaki MS, Saitsu H, Nakamura K, Santoni FA, Miyatake S, Nakashima M, Issa MY, Guipponi M, Letourneau A, Logan CV, Roberts N, Parry DA, Johnson CA, Matsumoto N, Hamamy H, Sheridan E, Kinoshita T, Antonarakis SE, Murakami Y. 2016. Pathogenic Variants in PIGG Cause Intellectual Disability with Seizures and Hypotonia. Am J Hum Genet 98:615-626.

174. Kvarnung M, Nilsson D, Lindstrand A, Korenke GC, Chiang SC, Blennow E, Bergmann M, Stodberg T, Makitie O, Anderlid BM, Bryceson YT, Nordenskjold M, Nordgren A. 2013. A novel intellectual disability syndrome caused by GPI anchor deficiency due to homozygous mutations in PIGT. J Med Genet 50:521-528.

175. Nakashima M, Kashii H, Murakami Y, Kato M, Tsurusaki Y, Miyake N, Kubota M, Kinoshita T, Saitsu H, Matsumoto N. 2014. Novel compound heterozygous PIGT mutations caused multiple congenital anomalies-hypotonia-seizures syndrome 3. Neurogenetics 15:193-200.

176. Lam C, Golas GA, Davids M, Huizing M, Kane MS, Krasnewich DM, Malicdan MC, Adams DR, Markello TC, Zein WM, Gropman AL, Lodish MB, Stratakis CA, Maric I, Rosenzweig SD, Baker EH, Ferreira CR, Danylchuk NR, Kahler S, Garnica AD, Bradley Schaefer G, Boerkoel CF, Gahl WA, Wolfe LA. 2015. Expanding the clinical and molecular characteristics of PIGT-CDG, a disorder of glycosylphosphatidylinositol anchors. Mol Genet Metab 115:128-140.

177. Murakami Y, Tawamie H, Maeda Y, Buttner C, Buchert R, Radwan F, Schaffer S, Sticht H, Aigner M, Reis A, Kinoshita T, Jamra RA. 2014. Null mutation in PGAP1 impairing Gpi-anchor maturation in patients with intellectual disability and encephalopathy. PLoS Genet 10:e1004320.

178. Granzow M, Paramasivam N, Hinderhofer K, Fischer C, Chotewutmontri S, Kaufmann L, Evers C, Kotzaeridou U, Rohrschneider K, Schlesner M, Sturm M, Pinkert S, Eils R, Bartram CR, Bauer P, Moog U. 2015. Loss of function of PGAP1 as a cause of severe encephalopathy identified by Whole Exome Sequencing: Lessons of the bioinformatics pipeline. Mol Cell Probes 29:323-329.

179. Williams C, Jiang YH, Shashi V, Crimian R, Schoch K, Harper A, McHale D, Goldstein D, Petrovski S. 2015. Additional evidence that PGAP1 loss of function causes autosomal recessive global developmental delay and encephalopathy. Clin Genet 88:597-599.

180. Howard MF, Murakami Y, Pagnamenta AT, Daumer-Haas C, Fischer B, Hecht J, Keays DA, Knight SJ, Kolsch U, Kruger U, Leiz S, Maeda Y, Mitchell D, Mundlos S, Phillips JA, 3rd, Robinson PN, Kini U, Taylor JC, Horn D, Kinoshita T, Krawitz PM. 2014. Mutations in PGAP3 impair GPI-anchor maturation, causing a subtype of hyperphosphatasia with mental retardation. Am J Hum Genet 94:278-287.

181. Knaus A, Awaya T, Helbig I, Afawi Z, Pendziwiat M, Abu-Rachma J, Thompson MD, Cole DE, Skinner S, Annese F, Canham N, Schweiger MR, Robinson PN, Mundlos S, Kinoshita T, Munnich A, Murakami Y, Horn D, Krawitz PM. 2016. Rare Noncoding Mutations Extend the Mutational Spectrum in the PGAP3 Subtype of Hyperphosphatasia with Mental Retardation Syndrome. Hum Mutat 37:737-744.

182. Hansen L, Tawamie H, Murakami Y, Mang Y, ur Rehman S, Buchert R, Schaffer S, Muhammad S, Bak M, Nothen MM, Bennett EP, Maeda Y, Aigner M, Reis A, Kinoshita T, Tommerup N, Baig SM, Abou Jamra R. 2013. Hypomorphic mutations in PGAP2, encoding a GPI-anchor-remodeling protein, cause autosomal-recessive intellectual disability. Am J Hum Genet 92:575-583.

183. Krawitz PM, Murakami Y, Riess A, Hietala M, Kruger U, Zhu N, Kinoshita T, Mundlos S, Hecht J, Robinson PN, Horn D. 2013. PGAP2 mutations, affecting the GPI-anchor-synthesis pathway, cause hyperphosphatasia with mental retardation syndrome. Am J Hum Genet 92:584-589.

184. Jezela-Stanek A, Ciara E, Piekutowska-Abramczuk D, Trubicka J, Jurkiewicz E, Rokicki D, Mierzewska H, Spychalska J, Uhrynowska M, Szwarc-Bronikowska M, Buda P, Said AR, Jamroz E, Rydzanicz M, Ploski R, Krajewska-Walasek M, Pronicka E. 2016. Congenital disorder of glycosylphosphatidylinositol (GPI)-anchor biosynthesis--The phenotype of two patients with novel mutations in the PIGN and PGAP2 genes. Eur J Paediatr Neurol 20:462-473.

185. Beaulieu CL, Majewski J, Schwartzentruber J, Samuels ME, Fernandez BA, Bernier FP, Brudno M, Knoppers B, Marcadier J, Dyment D, Adam S, Bulman DE, Jones SJ, Avard D, Nguyen MT, Rousseau F, Marshall C, Wintle RF, Shen Y, Scherer SW, Consortium FC, Friedman JM, Michaud JL, Boycott KM. 2014. FORGE Canada Consortium: outcomes of a 2-year national rare-disease gene-discovery project. Am J Hum Genet 94:809-817.

186. Genomes Project C, Auton A, Brooks LD, Durbin RM, Garrison EP, Kang HM, Korbel JO, Marchini JL, McCarthy S, McVean GA, Abecasis GR. 2015. A global reference for human genetic variation. Nature 526:68-74.

187. Rong Y, Nakamura S, Hirata T, Motooka D, Liu YS, He ZA, Gao XD, Maeda Y, Kinoshita T, Fujita M. 2015. Genome-Wide Screening of Genes Required for Glycosylphosphatidylinositol Biosynthesis. PLoS One 10:e0138553.

188. Cooper GM, Stone EA, Asimenos G, Program NCS, Green ED, Batzoglou S, Sidow A. 2005. Distribution and intensity of constraint in mammalian genomic sequence. Genome Res 15:901-913.

189. Adzhubei IA, Schmidt S, Peshkin L, Ramensky VE, Gerasimova A, Bork P, Kondrashov AS, Sunyaev SR. 2010. A method and server for predicting damaging missense mutations. Nat Methods 7:248-249.

190. Ng PC, Henikoff S. 2001. Predicting deleterious amino acid substitutions. Genome Res 11:863-874.

191. Schwarz JM, Cooper DN, Schuelke M, Seelow D. 2014. MutationTaster2: mutation prediction for the deep-sequencing age. Nat Methods 11:361-362.

192. Mathe E, Olivier M, Kato S, Ishioka C, Hainaut P, Tavtigian SV. 2006. Computational approaches for predicting the biological effect of p53 missense mutations: a comparison of three sequence analysis based methods. Nucleic Acids Res 34:1317-1325.

193. Tavtigian SV, Deffenbaugh AM, Yin L, Judkins T, Scholl T, Samollow PB, de Silva D, Zharkikh A, Thomas A. 2006. Comprehensive statistical study of 452 BRCA1 missense substitutions with classification of eight recurrent substitutions as neutral. J Med Genet 43:295-305.

194. Fujita M, Kinoshita T. 2012. GPI-anchor remodeling: potential functions of GPI-anchors in intracellular trafficking and membrane dynamics. Biochim Biophys Acta 1821:1050-1058.

195. Ng BG, Freeze HH. 2015. Human genetic disorders involving glycosylphosphatidylinositol (GPI) anchors and glycosphingolipids (GSL). J Inherit Metab Dis 38:171-178.

196. Grimminger T, Pernhorst K, Surges R, Niehusmann P, Priebe L, von Lehe M, Hoffmann P, Cichon S, Schoch S, Becker AJ. 2013. Levetiracetam resistance: Synaptic signatures & corresponding promoter SNPs in epileptic hippocampi. Neurobiol Dis 60:115-125.

197. Steinfeld R, Grapp M, Kraetzner R, Dreha-Kulaczewski S, Helms G, Dechent P, Wevers R, Grosso S, Gartner J. 2009. Folate receptor alpha defect causes cerebral folate transport deficiency: a treatable neurodegenerative disorder associated with disturbed myelin metabolism. Am J Hum Genet 85:354-363.

198. Labasque M, Faivre-Sarrailh C. 2010. GPI-anchored proteins at the node of Ranvier. FEBS Lett 584:1787-1792.

199. Stogmann E, Reinthaler E, Eltawil S, El Etribi MA, Hemeda M, El Nahhas N, Gaber AM, Fouad A, Edris S, Benet-Pages A, Eck SH, Pataraia E, Mei D, Brice A, Lesage S, Guerrini R, Zimprich F, Strom TM, Zimprich A. 2013. Autosomal recessive cortical myoclonic tremor and epilepsy: association with a mutation in the potassium channel associated gene CNTN2. Brain 136:1155-1160.

200. Knaus A, Kortum F, Kleefstra T, Stray-Pedersen A, Dukic D, Murakami Y, Gerstner T, van Bokhoven H, Iqbal Z, Horn D, Kinoshita T, Hempel M, Krawitz PM. 2019. Mutations in PIGU Impair the Function of the GPI Transamidase Complex, Causing Severe Intellectual Disability, Epilepsy, and Brain Anomalies. Am J Hum Genet doi:10.1016/j.ajhg.2019.06.009.

201. Bayat A, Knaus A, Juul AW, Dukic D, Gardella E, Charzewska A, Clement E, Hjalgrim H, Hoffman-Zacharska D, Horn D, Horton R, Hurst JA, Josifova D, Larsen LHG, Lascelles K, Obersztyn E, Pagnamenta A, Pal DK, Pendziwiat M, Ryten M, Taylor J, Vogt J, Weber Y, Krawitz PM, Helbig I, Kini U, Moller RS, Group DDDS. 2019. PIGT-CDG, a disorder of the glycosylphosphatidylinositol anchor: description of 13 novel patients and expansion of the clinical characteristics. Genet Med doi:10.1038/s41436-019-0512-3.

202. Hong Y, Ohishi K, Watanabe R, Endo Y, Maeda Y, Kinoshita T. 1999. GPI1 stabilizes an enzyme essential in the first step of glycosylphosphatidylinositol biosynthesis. J Biol Chem 274:18582-18588.

203. Tiede A, Daniels RJ, Higgs DR, Mehrein Y, Schmidt RE, Schubert J. 2001. The human GPI1 gene is required for efficient glycosylphosphatidylinositol biosynthesis. Gene 271:247-254.

204. Hamosh A, Scott AF, Amberger JS, Bocchini CA, McKusick VA. 2005. Online Mendelian Inheritance in Man (OMIM), a knowledgebase of human genes and genetic disorders. Nucleic Acids Res 33:D514-517.

205. Alazami AM, Patel N, Shamseldin HE, Anazi S, Al-Dosari MS, Alzahrani F, Hijazi H, Alshammari M, Aldahmesh MA, Salih MA, Faqeih E, Alhashem A, Bashiri FA, Al-Owain M, Kentab AY, Sogaty S, Al Tala S, Temsah MH, Tulbah M, Aljelaify RF, Alshahwan SA, Seidahmed MZ, Alhadid AA, Aldhalaan H, AlQallaf F, Kurdi W, Alfadhel M, Babay Z, Alsogheer M, Kaya N, Al-Hassnan ZN, Abdel-Salam GM, Al-Sannaa N, Al Mutairi F, El Khashab HY, Bohlega S, Jia X, Nguyen HC, Hammami R, Adly N, Mohamed JY, Abdulwahab F, Ibrahim N, Naim EA, Al-Younes B, Meyer BF, Hashem M, Shaheen R, Xiong Y, Abouelhoda M, et al. 2015. Accelerating novel candidate gene discovery in neurogenetic disorders via whole-exome sequencing of prescreened multiplex consanguineous families. Cell Rep 10:148-161.

206. Starr LJ, Spranger JW, Rao VK, Lutz R, Yetman AT. 2019. PIGQ glycosylphosphatidylinositol-anchored protein deficiency: Characterizing the phenotype. Am J Med Genet A 179:1270-1275.

207. Johnstone DL, Nguyen TT, Murakami Y, Kernohan KD, Tetreault M, Goldsmith C, Doja A, Wagner JD, Huang L, Hartley T, St-Denis A, le Deist F, Majewski J, Bulman DE, Care4Rare Canada C, Kinoshita T, Dyment DA, Boycott KM, Campeau PM. 2017. Compound heterozygous mutations in the gene PIGP are associated with early infantile epileptic encephalopathy. Hum Mol Genet 26:1706-1715.

208. Coppola G, Plouin P, Chiron C, Robain O, Dulac O. 1995. Migrating partial seizures in infancy: a malignant disorder with developmental arrest. Epilepsia 36:1017-1024.

209. Burgess R, Wang S, McTague A, Boysen KE, Yang X, Zeng Q, Myers KA, Rochtus A, Trivisano M, Gill D, Consortium E, Sadleir LG, Specchio N, Guerrini R, Marini C, Zhang YH, Mefford HC, Kurian MA, Poduri AH, Scheffer IE. 2019. The Genetic Landscape of Epilepsy of Infancy with Migrating Focal Seizures. Ann Neurol 86:821-831.

210. Baratang NV, Jimenez Cruz DA, Ajeawung NF, Nguyen TTM, Pacheco-Cuellar G, Campeau PM. 2019. Inherited glycophosphatidylinositol deficiency variant database and analysis of pathogenic variants. Mol Genet Genomic Med 7:e00743.

211. Lam C, Golas GA, Davids M, Huizing M, Kane MS, Krasnewich DM, Malicdan MCV, Adams DR, Markello TC, Zein WM, Gropman AL, Lodish MB, Stratakis CA, Maric I, Rosenzweig SD, Baker EH, Ferreira CR, Danylchuk NR, Kahler S, Garnica AD, Bradley Schaefer G, Boerkoel CF, Gahl WA, Wolfe LA. 2015. Expanding the clinical and molecular characteristics of PIGT-CDG, a disorder of glycosylphosphatidylinositol anchors. Mol Genet Metab 115:128-140.

212. Skauli N, Wallace S, Chiang SC, Baroy T, Holmgren A, Stray-Pedersen A, Bryceson YT, Stromme P, Frengen E, Misceo D. 2016. Novel PIGT Variant in Two Brothers: Expansion of the Multiple Congenital Anomalies-Hypotonia Seizures Syndrome 3 Phenotype. Genes (Basel) 7.

213. Yang L, Peng J, Yin XM, Pang N, Chen C, Wu TH, Zou XM, Yin F. 2018. Homozygous PIGT Mutation Lead to Multiple Congenital Anomalies-Hypotonia Seizures Syndrome 3. Front Genet 9:153.

214. Murakami Y, Kanzawa N, Saito K, Krawitz PM, Mundlos S, Robinson PN, Karadimitris A, Maeda Y, Kinoshita T. 2012. Mechanism for release of alkaline phosphatase caused by glycosylphosphatidylinositol deficiency in patients with hyperphosphatasia mental retardation syndrome. J Biol Chem 287:6318-6325.

215. Almeida AM, Murakami Y, Baker A, Maeda Y, Roberts IA, Kinoshita T, Layton DM, Karadimitris A. 2007. Targeted therapy for inherited GPI deficiency. N Engl J Med 356:1641-1647.

216. Nguyen TTM, Murakami Y, Wigby KM, Baratang NV, Rousseau J, St-Denis A, Rosenfeld JA, Laniewski SC, Jones J, Iglesias AD, Jones MC, Masser-Frye D, Scheuerle AE, Perry DL, Taft RJ, Le Deist F, Thompson M, Kinoshita T, Campeau PM. 2018. Mutations in PIGS, Encoding a GPI Transamidase, Cause a Neurological

Syndrome Ranging from Fetal Akinesia to Epileptic Encephalopathy. The American Journal of Human Genetics 103:602-611.

217. Thompson MD, Killoran A, Percy ME, Nezarati M, Cole DE, Hwang PA. 2006. Hyperphosphatasia with neurologic deficit: a pyridoxine-responsive seizure disorder? Pediatr Neurol 34:303-307.

218. Pagnamenta AT, Murakami Y, Taylor JM, Anzilotti C, Howard MF, Miller V, Johnson DS, Tadros S, Mansour S, Temple IK, Firth R, Rosser E, Harrison RE, Kerr B, Popitsch N, Study DDD, Kinoshita T, Taylor JC, Kini U. 2017. Analysis of exome data for 4293 trios suggests GPI-anchor biogenesis defects are a rare cause of developmental disorders. Eur J Hum Genet 25:669-679.

219. Li H, Durbin R. 2009. Fast and accurate short read alignment with Burrows-Wheeler transform. Bioinformatics 25:1754-1760.

220. McKenna A, Hanna M, Banks E, Sivachenko A, Cibulskis K, Kernytsky A, Garimella K, Altshuler D, Gabriel S, Daly M, DePristo MA. 2010. The Genome Analysis Toolkit: a MapReduce framework for analyzing next-generation DNA sequencing data. Genome Res 20:1297-1303.

221. Wang K, Li M, Hakonarson H. 2010. ANNOVAR: functional annotation of genetic variants from high-throughput sequencing data. Nucleic Acids Res 38:e164.

222. Karczewski KJ, Weisburd B, Thomas B, Solomonson M, Ruderfer DM, Kavanagh D, Hamamsy T, Lek M, Samocha KE, Cummings BB, Birnbaum D, The Exome Aggregation C, Daly MJ, MacArthur DG. 2017. The ExAC browser: displaying reference data information from over 60 000 exomes. Nucleic Acids Res 45:D840-D845.

223. Li H, Handsaker B, Wysoker A, Fennell T, Ruan J, Homer N, Marth G, Abecasis G, Durbin R, Genome Project Data Processing S. 2009. The Sequence Alignment/Map format and SAMtools. Bioinformatics 25:2078-2079.

224. Rimmer A, Phan H, Mathieson I, Iqbal Z, Twigg SRF, Consortium WGS, Wilkie AOM, McVean G, Lunter G. 2014. Integrating mapping-, assembly- and haplotype-based approaches for calling variants in clinical sequencing applications. Nat Genet 46:912-918.

225. Van der Auwera GA, Carneiro MO, Hartl C, Poplin R, Del Angel G, Levy-Moonshine A, Jordan T, Shakir K, Roazen D, Thibault J, Banks E, Garimella KV, Altshuler D, Gabriel S, DePristo MA. 2013. From FastQ data to high confidence variant calls: the Genome Analysis Toolkit best practices pipeline. Curr Protoc Bioinformatics 43:11 10 11-11 10 33.

226. McLaren W, Gil L, Hunt SE, Riat HS, Ritchie GR, Thormann A, Flicek P, Cunningham F. 2016. The Ensembl Variant Effect Predictor. Genome Biol 17:122.

227. O'Leary NA, Wright MW, Brister JR, Ciufo S, Haddad D, McVeigh R, Rajput B, Robbertse B, Smith-White B, Ako-Adjei D, Astashyn A, Badretdin A, Bao Y, Blinkova O, Brover V, Chetvernin V, Choi J, Cox E, Ermolaeva O, Farrell CM, Goldfarb T, Gupta T, Haft D, Hatcher E, Hlavina W, Joardar VS, Kodali VK, Li W, Maglott D, Masterson P, McGarvey KM, Murphy MR, O'Neill K, Pujar S, Rangwala SH, Rausch D, Riddick LD, Schoch C, Shkeda A, Storz SS, Sun H, Thibaud-Nissen F, Tolstoy I, Tully RE, Vatsan AR, Wallin C, Webb D, Wu W, Landrum MJ, Kimchi A, et al. 2016. Reference sequence (RefSeq) database at NCBI: current status, taxonomic expansion, and functional annotation. Nucleic Acids Res 44:D733-745.

228. Paila U, Chapman BA, Kirchner R, Quinlan AR. 2013. GEMINI: integrative exploration of genetic variation and genome annotations. PLoS Comput Biol 9:e1003153.

229. Richards S, Aziz N, Bale S, Bick D, Das S, Gastier-Foster J, Grody WW, Hegde M, Lyon E, Spector E, Voelkerding K, Rehm HL, Committee ALQA. 2015. Standards and guidelines for the interpretation of sequence variants: a joint consensus recommendation of the American College of Medical Genetics and Genomics and the Association for Molecular Pathology. Genet Med 17:405-424.

230. Stranneheim H, Engvall M, Naess K, Lesko N, Larsson P, Dahlberg M, Andeer R, Wredenberg A, Freyer C, Barbaro M, Bruhn H, Emahazion T, Magnusson M, Wibom R, Zetterstrom RH, Wirta V, von Dobeln U, Wedell A. 2014. Rapid pulsed whole genome sequencing for comprehensive acute diagnostics of inborn errors of metabolism. BMC Genomics 15:1090.

231. Clayton PT. 2006. B6-responsive disorders: A model of vitamin dependency. Journal of Inherited Metabolic Disease 29:317-326.

232. Baumgartner-Sigl S, Haberlandt E, Mumm S, Scholl-Bürgi S, Sergi C, Ryan L, Ericson KL, Whyte MP, Högler W. 2007. Pyridoxine-responsive seizures as the first symptom of infantile hypophosphatasia caused by two novel missense mutations (c.677T>C, p.M226T; c.1112C>T, p.T371I) of the tissue-nonspecific alkaline phosphatase gene. Bone 40:1655-1661.

233. Basura GJ, Hagland SP, Wiltse AM, Gospe SM. 2009. Clinical features and the management of pyridoxine-dependent and pyridoxine-responsive seizures: review of 63 North American cases submitted to a patient registry. European Journal of Pediatrics 168:697-704.

234. Surtees R, Mills P, Clayton P. 2006. Inborn errors affecting vitamin B6 metabolism. Future Neurology Future Neurology 1:615-620.

235. Walker V, Mills GA, Peters SA, Merton WL. 2000. Fits, pyridoxine, and hyperprolinaemia type II. Arch Dis Child 82:236-237.

236. Stockler S, Plecko B, Gospe SM, Jr., Coulter-Mackie M, Connolly M, van Karnebeek C, Mercimek-Mahmutoglu S, Hartmann H, Scharer G, Struijs E, Tein I, Jakobs C,

Clayton P, Van Hove JL. 2011. Pyridoxine dependent epilepsy and antiquitin deficiency: clinical and molecular characteristics and recommendations for diagnosis, treatment and follow-up. Mol Genet Metab 104:48-60.

237. Gospe SJ. 2017 Apr 13 2017. Pyridoxine-Dependent Epilepsy, *on* University of Washington. https://www.ncbi.nlm.nih.gov/books/NBK1486/. Accessed

238. Eswaramoorthy S, Gerchman S, Graziano V, Kycia H, Studier FW, Swaminathan S. 2003. Structure of a yeast hypothetical protein selected by a structural genomics approach. Acta Crystallogr D Biol Crystallogr 59:127-135.

239. Tremino L, Forcada-Nadal A, Rubio V. 2018. Insight into vitamin B6 -dependent epilepsy due to PLPBP (previously PROSC) missense mutations. Hum Mutat 39:1002-1013.

240. Tremino L, Forcada-Nadal A, Contreras A, Rubio V. 2017. Studies on cyanobacterial protein PipY shed light on structure, potential functions, and vitamin B6 -dependent epilepsy. FEBS Lett 591:3431-3442.

241. Tarailo-Graovac M, Shyr C, Ross CJ, Horvath GA, Salvarinova R, Ye XC, Zhang LH, Bhavsar AP, Lee JJ, Drogemoller BI, Abdelsayed M, Alfadhel M, Armstrong L, Baumgartner MR, Burda P, Connolly MB, Cameron J, Demos M, Dewan T, Dionne J, Evans AM, Friedman JM, Garber I, Lewis S, Ling J, Mandal R, Mattman A, McKinnon M, Michoulas A, Metzger D, Ogunbayo OA, Rakic B, Rozmus J, Ruben P, Sayson B, Santra S, Schultz KR, Selby K, Shekel P, Sirrs S, Skrypnyk C, Superti-Furga A, Turvey SE, Van Allen MI, Wishart D, Wu J, Wu J, Zafeiriou D, Kluijtmans L, Wevers RA, et al. 2016. Exome Sequencing and the Management of Neurometabolic Disorders. N Engl J Med 374:2246-2255.

242. Webb B, Sali A. 2014. Comparative Protein Structure Modeling Using MODELLER. Curr Protoc Bioinformatics 47:5 6 1-32.

243. Emsley P, Lohkamp B, Scott WG, Cowtan K. 2010. Features and development of Coot. Acta Crystallogr D Biol Crystallogr 66:486-501.

244. Wiederstein M, Sippl MJ. 2007. ProSA-web: interactive web service for the recognition of errors in three-dimensional structures of proteins. Nucleic Acids Res 35:W407-410.

245. Schrodinger, LLC. 2015. The PyMOL Molecular Graphics System, Version 1.8.

246. Jubb HC, Higueruelo AP, Ochoa-Montano B, Pitt WR, Ascher DB, Blundell TL. 2017. Arpeggio: a web server for calculating and visualising interatomic interactions in protein structures. J Mol Biol 429:365-371.

247. Pires DE, Ascher DB, Blundell TL. 2014. DUET: a server for predicting effects of mutations on protein stability using an integrated computational approach. Nucleic Acids Res 42:W314-319.

248. Al Teneiji A, Bruun TU, Cordeiro D, Patel J, Inbar-Feigenberg M, Weiss S, Struys E, Mercimek-Mahmutoglu S. 2017. Phenotype, biochemical features, genotype and treatment outcome of pyridoxine-dependent epilepsy. Metab Brain Dis 32:443-451.

249. Chen WW, Freinkman E, Sabatini DM. 2017. Rapid immunopurification of mitochondria for metabolite profiling and absolute quantification of matrix metabolites. Nat Protoc 12:2215-2231.

250. Westerfield M. 1993. The zebrafish book : a guide for the laboratory use of zebrafish (Brachydanio rerio). M. Westerfield, Eugene, OR.

251. Kilkenny C, Browne WJ, Cuthill IC, Emerson M, Altman DG. 2012. Improving bioscience research reporting: the ARRIVE guidelines for reporting animal research. Osteoarthritis Cartilage 20:256-260.

252. Hwang WY, Fu Y, Reyon D, Maeder ML, Tsai SQ, Sander JD, Peterson RT, Yeh JR, Joung JK. 2013. Efficient genome editing in zebrafish using a CRISPR-Cas system. Nat Biotechnol 31:227-229.

253. Sander JD, Maeder ML, Reyon D, Voytas DF, Joung JK, Dobbs D. 2010. ZiFiT (Zinc Finger Targeter): an updated zinc finger engineering tool. Nucleic Acids Res 38:W462-468.

254. Zhu X, Xu Y, Yu S, Lu L, Ding M, Cheng J, Song G, Gao X, Yao L, Fan D, Meng S, Zhang X, Hu S, Tian Y. 2014. An efficient genotyping method for genome-modified animals and human cells generated with CRISPR/Cas9 system. Sci Rep 4:6420.

255. Baraban SC, Taylor MR, Castro PA, Baier H. 2005. Pentylenetetrazole induced changes in zebrafish behavior, neural activity and c-fos expression. Neuroscience 131:759-768.

256. van der Ham M, Albersen M, de Koning TJ, Visser G, Middendorp A, Bosma M, Verhoeven-Duif NM, de Sain-van der Velden MG. 2012. Quantification of vitamin B6 vitamers in human cerebrospinal fluid by ultra performance liquid chromatography-tandem mass spectrometry. Anal Chim Acta 712:108-114.

257. van Vliet D, Bruinenberg VM, Mazzola PN, van Faassen MH, de Blaauw P, Kema IP, Heiner-Fokkema MR, van Anholt RD, van der Zee EA, van Spronsen FJ. 2015. Large Neutral Amino Acid Supplementation Exerts Its Effect through Three Synergistic Mechanisms: Proof of Principle in Phenylketonuria Mice. PLoS One 10:e0143833.

258. Nagano N, Orengo CA, Thornton JM. 2002. One fold with many functions: the evolutionary relationships between TIM barrel families based on their sequences, structures and functions. J Mol Biol 321:741-765.

259. Dias-Lopes C, Neshich IA, Neshich G, Ortega JM, Granier C, Chavez-Olortegui C, Molina F, Felicori L. 2013. Identification of new sphingomyelinases D in pathogenic fungi and other pathogenic organisms. PLoS One 8:e79240.

260. Wierenga RK. 2001. The TIM-barrel fold: a versatile framework for efficient enzymes. FEBS Lett 492:193-198.

261. Uhlen M, Fagerberg L, Hallstrom BM, Lindskog C, Oksvold P, Mardinoglu A, Sivertsson A, Kampf C, Sjostedt E, Asplund A, Olsson I, Edlund K, Lundberg E, Navani S, Szigyarto CA, Odeberg J, Djureinovic D, Takanen JO, Hober S, Alm T, Edqvist PH, Berling H, Tegel H, Mulder J, Rockberg J, Nilsson P, Schwenk JM, Hamsten M, von Feilitzen K, Forsberg M, Persson L, Johansson F, Zwahlen M, von Heijne G, Nielsen J, Ponten F. 2015. Proteomics. Tissue-based map of the human proteome. Science 347:1260419.

262. Pagliarini DJ, Calvo SE, Chang B, Sheth SA, Vafai SB, Ong SE, Walford GA, Sugiana C, Boneh A, Chen WK, Hill DE, Vidal M, Evans JG, Thorburn DR, Carr SA, Mootha VK. 2008. A mitochondrial protein compendium elucidates complex I disease biology. Cell 134:112-123.

263. Calvo SE, Clauser KR, Mootha VK. 2016. MitoCarta2.0: an updated inventory of mammalian mitochondrial proteins. Nucleic Acids Res 44:D1251-1257.

264. Smith AC, Robinson AJ. 2016. MitoMiner v3.1, an update on the mitochondrial proteomics database. Nucleic Acids Res 44:D1258-1261.

265. Soiferma D, Saada A. 2015. The Use of Fibroblasts from Patients with Inherited Mitochondrial Disorders for Pathomechanistic Studies and Evaluation of Therapies, p 378-398, The Functions, Disease-Related Dysfunctions, and Therapeutic Targeting of Neuronal Mitochondria doi:doi:10.1002/9781119017127.ch18.

266. Lasserre JP, Dautant A, Aiyar RS, Kucharczyk R, Glatigny A, Tribouillard-Tanvier D, Rytka J, Blondel M, Skoczen N, Reynier P, Pitayu L, Rotig A, Delahodde A, Steinmetz LM, Dujardin G, Procaccio V, di Rago JP. 2015. Yeast as a system for modeling mitochondrial disease mechanisms and discovering therapies. Dis Model Mech 8:509-526.

267. Barrientos A. 2003. Yeast models of human mitochondrial diseases. IUBMB Life 55:83-95.

268. Teng Y, Xie X, Walker S, Rempala G, Kozlowski DJ, Mumm JS, Cowell JK. 2010. Knockdown of zebrafish Lgi1a results in abnormal development, brain defects and a seizure-like behavioral phenotype. Hum Mol Genet 19:4409-4420.

269. Brun L, Ngu LH, Keng WT, Ch'ng GS, Choy YS, Hwu WL, Lee WT, Willemsen MA, Verbeek MM, Wassenberg T, Regal L, Orcesi S, Tonduti D, Accorsi P, Testard H, Abdenur JE, Tay S, Allen GF, Heales S, Kern I, Kato M, Burlina A, Manegold C,

Hoffmann GF, Blau N. 2010. Clinical and biochemical features of aromatic L-amino acid decarboxylase deficiency. Neurology 75:64-71.

270. Giardina G, Brunotti P, Fiascarelli A, Cicalini A, Costa MG, Buckle AM, di Salvo ML, Giorgi A, Marani M, Paone A, Rinaldo S, Paiardini A, Contestabile R, Cutruzzola F. 2015. How pyridoxal 5'-phosphate differentially regulates human cytosolic and mitochondrial serine hydroxymethyltransferase oligomeric state. FEBS J 282:1225-1241.

271. Kikuchi G, Motokawa Y, Yoshida T, Hiraga K. 2008. Glycine cleavage system: reaction mechanism, physiological significance, and hyperglycinemia. Proc Jpn Acad Ser B Phys Biol Sci 84:246-263.

272. Shi H, Enriquez A, Rapadas M, Martin E, Wang R, Moreau J, Lim CK, Szot JO, Ip E, Hughes JN, Sugimoto K, Humphreys DT, McInerney-Leo AM, Leo PJ, Maghzal GJ, Halliday J, Smith J, Colley A, Mark PR, Collins F, Sillence DO, Winlaw DS, Ho JWK, Guillemin GJ, Brown MA, Kikuchi K, Thomas PQ, Stocker R, Giannoulatou E, Chapman G, Duncan EL, Sparrow DB, Dunwoodie SL. 2017. NAD Deficiency, Congenital Malformations, and Niacin Supplementation. N Engl J Med 377:544-552.

273. Rios-Avila L, Nijhout HF, Reed MC, Sitren HS, Gregory JF, 3rd. 2013. A mathematical model of tryptophan metabolism via the kynurenine pathway provides insights into the effects of vitamin B-6 deficiency, tryptophan loading, and induction of tryptophan 2,3-dioxygenase on tryptophan metabolites. J Nutr 143:1509-1519.

274. Wassenberg T, Willemsen MA, Geurtz PB, Lammens M, Verrijp K, Wilmer M, Lee WT, Wevers RA, Verbeek MM. 2010. Urinary dopamine in aromatic L-amino acid decarboxylase deficiency: the unsolved paradox. Mol Genet Metab 101:349-356.

275. Prasad C, Rupar T, Prasad AN. 2011. Pyruvate dehydrogenase deficiency and epilepsy. Brain Dev 33:856-865.

276. Hamilton A, Tetreault M, Dyment DA, Zou R, Kernohan K, Geraghty MT, Consortium FC, Care4Rare Canada C, Hartley T, Boycott KM. 2016. Concordance between whole-exome sequencing and clinical Sanger sequencing: implications for patient care. Mol Genet Genomic Med 4:504-512.

277. Azzopardi D. 2015. Clinical applications of cerebral function monitoring in neonates. Semin Fetal Neonatal Med 20:154-163.

278. Dyment DA, Smith AC, Alcantara D, Schwartzentruber JA, Basel-Vanagaite L, Curry CJ, Temple IK, Reardon W, Mansour S, Haq MR, Gilbert R, Lehmann OJ, Vanstone MR, Beaulieu CL, Consortium FC, Majewski J, Bulman DE, O'Driscoll M, Boycott KM, Innes AM. 2013. Mutations in PIK3R1 cause SHORT syndrome. Am J Hum Genet 93:158-166.

279. Langmead B, Salzberg SL. 2012. Fast gapped-read alignment with Bowtie 2. Nat Methods 9:357-359.

280. Cingolani P, Platts A, Wang le L, Coon M, Nguyen T, Wang L, Land SJ, Lu X, Ruden DM. 2012. A program for annotating and predicting the effects of single nucleotide polymorphisms, SnpEff: SNPs in the genome of Drosophila melanogaster strain w1118; iso-2; iso-3. Fly (Austin) 6:80-92.

281. Sherry ST, Ward MH, Kholodov M, Baker J, Phan L, Smigielski EM, Sirotkin K. 2001. dbSNP: the NCBI database of genetic variation. Nucleic Acids Res 29:308-311.

282. Robinson JT, Thorvaldsdottir H, Winckler W, Guttman M, Lander ES, Getz G, Mesirov JP. 2011. Integrative genomics viewer. Nat Biotechnol 29:24-26.

283. de Ligt J, Willemsen MH, van Bon BW, Kleefstra T, Yntema HG, Kroes T, Vulto-van Silfhout AT, Koolen DA, de Vries P, Gilissen C, del Rosario M, Hoischen A, Scheffer H, de Vries BB, Brunner HG, Veltman JA, Vissers LE. 2012. Diagnostic exome sequencing in persons with severe intellectual disability. N Engl J Med 367:1921-1929.

284. Lelieveld SH, Reijnders MR, Pfundt R, Yntema HG, Kamsteeg EJ, de Vries P, de Vries BB, Willemsen MH, Kleefstra T, Lohner K, Vreeburg M, Stevens SJ, van der Burgt I, Bongers EM, Stegmann AP, Rump P, Rinne T, Nelen MR, Veltman JA, Vissers LE, Brunner HG, Gilissen C. 2016. Meta-analysis of 2,104 trios provides support for 10 new genes for intellectual disability. Nat Neurosci 19:1194-1196.

285. Tanaka AJ, Cho MT, Millan F, Juusola J, Retterer K, Joshi C, Niyazov D, Garnica A, Gratz E, Deardorff M, Wilkins A, Ortiz-Gonzalez X, Mathews K, Panzer K, Brilstra E, van Gassen KL, Volker-Touw CM, van Binsbergen E, Sobreira N, Hamosh A, McKnight D, Monaghan KG, Chung WK. 2015. Mutations in SPATA5 Are Associated with Microcephaly, Intellectual Disability, Seizures, and Hearing Loss. Am J Hum Genet 97:457-464.

286. Liu X, Jian X, Boerwinkle E. 2011. dbNSFP: a lightweight database of human nonsynonymous SNPs and their functional predictions. Hum Mutat 32:894-899.

287. Liu X, Jian X, Boerwinkle E. 2013. dbNSFP v2.0: a database of human non-synonymous SNVs and their functional predictions and annotations. Hum Mutat 34:E2393-2402.

288. Mathis D, Abela L, Albersen M, Burer C, Crowther L, Beese K, Hartmann H, Bok LA, Struys E, Papuc SM, Rauch A, Hersberger M, Verhoeven-Duif NM, Plecko B. 2016. The value of plasma vitamin B6 profiles in early onset epileptic encephalopathies. J Inherit Metab Dis 39:733-741.

289. Waterhouse AM, Procter JB, Martin DM, Clamp M, Barton GJ. 2009. Jalview Version 2--a multiple sequence alignment editor and analysis workbench. Bioinformatics 25:1189-1191.

290. Knaus A, Pantel JT, Pendziwiat M, Hajjir N, Zhao M, Hsieh TC, Schubach M, Gurovich Y, Fleischer N, Jager M, Kohler S, Muhle H, Korff C, Moller RS, Bayat A, Calvas P, Chassaing N, Warren H, Skinner S, Louie R, Evers C, Bohn M, Christen HJ, van den Born M, Obersztyn E, Charzewska A, Endziniene M, Kortum F, Brown N, Robinson PN, Schelhaas HJ, Weber Y, Helbig I, Mundlos S, Horn D, Krawitz PM. 2018. Characterization of glycosylphosphatidylinositol biosynthesis defects by clinical features, flow cytometry, and automated image analysis. Genome Med 10:3.

291. Krenn M, Knaus A, Westphal DS, Wortmann SB, Polster T, Woermann FG, Karenfort M, Mayatepek E, Meitinger T, Wagner M, Distelmaier F. 2019. Biallelic mutations in PIGP cause developmental and epileptic encephalopathy. Ann Clin Transl Neurol 6:968-973.

292. Vetro A, Pisano T, Chiaro S, Procopio E, Guerra A, Parrini E, Mei D, Virdo S, Mangone G, Azzari C, Guerrini R. 2020. Early infantile epileptic-dyskinetic encephalopathy due to biallelic PIGP mutations. Neurol Genet 6:e387.

293. Fux A, Pfanzelt M, Kirsch VC, Hoegl A, Sieber SA. 2019. Customizing Functionalized Cofactor Mimics to Study the Human Pyridoxal 5'-Phosphate-Binding Proteome. Cell Chem Biol 26:1461-1468 e1467.

294. Fux A, Sieber SA. 2020. Biochemical and Proteomic Studies of Human Pyridoxal 5'-Phosphate-Binding Protein (PLPBP). ACS Chem Biol 15:254-261.

295. Ishida Y, Komaru K, Oda K. 2011. Molecular characterization of tissue-nonspecific alkaline phosphatase with an Ala to Thr substitution at position 116 associated with dominantly inherited hypophosphatasia. Biochim Biophys Acta 1812:326-332.

296. Boycott KM, Hartley T, Biesecker LG, Gibbs RA, Innes AM, Riess O, Belmont J, Dunwoodie SL, Jojic N, Lassmann T, Mackay D, Temple IK, Visel A, Baynam G. 2019. A Diagnosis for All Rare Genetic Diseases: The Horizon and the Next Frontiers. Cell 177:32-37.

297. Kernohan KD, Fresard L, Zappala Z, Hartley T, Smith KS, Wagner J, Xu H, McBride A, Bourque PR, Consortium CRC, Bennett SAL, Dyment DA, Boycott KM, Montgomery SB, Warman Chardon J. 2017. Whole-transcriptome sequencing in blood provides a diagnosis of spinal muscular atrophy with progressive myoclonic epilepsy. Hum Mutat 38:611-614.

298. Liu Y, Lopez-Santiago LF, Yuan Y, Jones JM, Zhang H, O'Malley HA, Patino GA, O'Brien JE, Rusconi R, Gupta A, Thompson RC, Natowicz MR, Meisler MH, Isom LL, Parent JM. 2013. Dravet syndrome patient-derived neurons suggest a novel epilepsy mechanism. Ann Neurol 74:128-139.

299. Odawara A, Katoh H, Matsuda N, Suzuki I. 2016. Physiological maturation and drug responses of human induced pluripotent stem cell-derived cortical neuronal networks in long-term culture. Sci Rep 6:26181.

Contribution of collaborators

Devon L Johnstone
I wrote all manuscripts (Chapters 2-4) and contributed to all experiments, with the following exceptions: I did not perform exome library preparations myself (I analysed the results), I did not develop the HAP1 cells or perform the HAP1 experiments used in Chapter 2, and in Chapter 4, I did not develop the structural model, perform the yeast experiments, or mass spectrometry, however I did analyse all results.

Kym M. Boycott
Thesis supervisor. Experimental planning for all chapters, and critical assessment of manuscripts and thesis

David A. Dyment
Chapters 2 and 4: Patient identification and exome analysis, funding support for zebrafish, guidance, critical assessment of manuscripts

Philippe Campeau
Chapters 2 and 3: Co-senior author, critical assessment of manuscripts

Kristin Kernohan
Chapters 2-4: guidance and assistance with experimental designs, critical assessment of manuscripts

Thi-Tuyet-Mai Nguyen
Chapters 2 and 3: flow cytometry experiments on blood samples, flow cytometry experiments and experimental planning for lentivirus rescue experiments on fibroblasts, co-first author for Chapter 2, editing of chapter 3

Yoshiko Murakami
Chapter 2: HAP1 experiments, editing of manuscript

Martine Tétreault
Chapter 2: exome analysis, editing of manuscript

Claire Goldsmith
Chapter 2: clinical description, editing of manuscript

Asif Doja
Chapter 2: clinical description, editing of manuscript

Justin D. Wagner
Chapter 2: assistance with genotyping, editing of manuscript

Lijia Huang
Chapter 2: exome analysis, editing of manuscript

Taila Hartley
Chapters 2 and 3: exome analysis, editing of manuscript

Anik St-Denis
Chapters 2 and 3: assistance with flow cytometry, editing of manuscript

Françoise le Deist
Chapter 2: assistance with flow cytometry, editing of manuscript

Jacek Majewski
Chapters 2-4: Exome analysis and pipeline development, editing of manuscripts

Dennis E. Bulman
Chapter 2: guidance for experimental planning, editing of manuscript

Taroh Kinoshita
HAP1 experiments, editing of manuscript

Jessica Zambonin
Chapter 3: collection and analysis of patient data, revision of supplemental clinical data summaries

Nissan V. Baratang
Chapter 3: assistance with flow cytometry, editing of manuscript

Michael T. Geraghty
Chapter 3: Collection and analysis of patient data, editing of manuscript

Julie Richer
Chapter 3: Collection and analysis of patient data, editing of manuscript

Eric Bareke
Chapter 3: Exome analysis and pipeline, editing of manuscript

Andrea Guerin
Chapter 3: Collection and analysis of patient data, editing of manuscript

Manuela Pendziwiat
Chapter 3: Collection and analysis of patient data, editing of manuscript

Loren D.M. Pena
Chapter 3: Collection and analysis of patient data, editing of manuscript

Hilde M.H. Braakman
Chapter 3: Collection and analysis of patient data, editing of manuscript

Karen W. Gripp
Chapter 3: Collection and analysis of patient data, editing of manuscript

Andrew C. Edmondson
Chapter 3: Collection and analysis of patient data, functional data for patient 2, editing of manuscript

Miao He
Chapter 3: cell culture and flow cytometry for patient 2

Rebecca C. Spillmann
Chapter 3: Collection and analysis of patient data, editing of manuscript

Erik A. Eklund
Chapter 3: Collection and analysis of patient data, editing of manuscript

Allan Bayat
Chapter 3: Collection and analysis of patient data, editing of manuscript

Hugh J. McMillan
Chapter 3: Collection and analysis of patient data, MRI analysis, editing of manuscript

Hilal H. Al-Shekaili
Chapter 4: Co-first author (contributed to introduction, clinical description sections), editing of manuscript

Maja Tarailo-Graovac
Chapter 4: Analysis of genetic data, help with in silico analysis of pathogenicity, critical assessment of manuscript

Nicole I. Wolf
Chapter 4: analysis of patient MRIs, critical assessment of manuscript

Autumn S. Ivy
Chapter 4: Provided clinical details for a patient, clinical assessment of clinical phenotype scoring, critical assessment of manuscript

Scott Demarest
Chapter 4: Provided clinical details for a patient, critical assessment of manuscript

Yann Roussel
Chapter 4: Performed optic tectum electrophysiology experiments on zebrafish, critical assessment of manuscript

Jolita Ciapaite
Chapter 4: Cultured cells, mass spec experiments and analysis for patient fibroblasts, HEK293 cells, zebrafish (for B6 vitamers only), editing of manuscript

Carlo W.T. van Roermund
Chapter 4: Yeast experiments, critical assessment of manuscript

Ceres Kosuta
Chapter 4: Assistance with zebrafish experiments (fin clipping, genotyping, survival experiments)

Kevin Ban
Chapter 4: Assistance with zebrafish experiments (fin clipping, genotyping, survival experiments)

Yoko Ito
Chapter 4: Guidance for staining for microscopy, critical assessment of manuscript

Skye McBride
Chapter 4: Assistance with microscopy, critical assessment of manuscript

Khalid Al-Thihli
Chapter 4: Provided clinical details for a patient, critical assessment of manuscript

Rana A. Abdelrahim
Chapter 4: Provided clinical details for a patient, critical assessment of manuscript

Roshan Koul
Chapter 4: Provided clinical details for a patient, critical assessment of manuscript

Amna Al Futaisi
Chapter 4: Provided clinical details for a patient, critical assessment of manuscript

CharlotteA. Haaxma
Chapter 4: Provided clinical details for a patient, critical assessment of manuscript

Heather Olson
Chapter 4: Provided clinical details for a patient, critical assessment of manuscript

Laufey Yr. Sigurdardottir
Chapter 4: Provided clinical details for a patient, critical assessment of manuscript

Georgianne L. Arnold
Chapter 4: Provided clinical details for a patient, critical assessment of manuscript

Erica H. Gerkes
Chapter 4: Provided clinical details for a patient, critical assessment of manuscript

M. Boon
Chapter 4: Provided clinical details for a patient, critical assessment of manuscript

M. Rebecca Heiner-Fokkema
Chapter 4: Collected and analyzed metabolic data for Patient 3, critical assessment of manuscript

Sandra Noble
Chapter 4: Help with the design and development of guides for Cas9 in zebrafish, early help with fish work, editing of manuscript

Marjolein Bosma
Chapter 4: Analyzed HEK 293 cells, plasma samples, leucocytes, yeast and zebrafish for B6 vitamers, editing of manuscript

Judith Jans
Chapter 4: Experimental design and data interpretation for mass spec experiments (fibroblasts, HEK293, zebrafish) for B6 vitamers, editing of manuscript

David A. Koolen
Chapter 4: Provided clinical details for a patient, data analysis, critical assessment of manuscript

Erik-Jan Kamsteeg
Chapter 4: Provided clinical details for a patient, data analysis, critical assessment of manuscript

Britt Drögemöller
Chapter 4: Genomic analysis, critical assessment of manuscript

Colin J. Ross
Chapter 4: Genomic analysis, critical assessment of manuscript

Megan T. Cho
Chapter 4, exome analysis, critical assessment of manuscript

Amber Begtrup
Chapter 4, exome analysis, critical assessment of manuscript

Wyeth W. Wasserman
Chapter 4: Bioinformatics contributions for genomic analysis

Tuan Bui
Chapter 4: Zebrafish electrophysiology facilities and equipment, critique of manuscript

Elise Brimble
Chapter 4: Provided clinical details for a patient, critical assessment of manuscript

Sara Violante
Chapter 4: Immunofluorescence and CRISPR KO experiments for HEK293 cells, critical assessment of manuscript

Sander M. Houten
Chapter 4: Immunofluorescence and CRISPR KO experiments for HEK293 cells, critical assessment of manuscript

Ron A. Wevers
Chapter 4: Analysis of data, critical assessment of manuscript

Martijn van Faassen
Chapter 4: Mass spec for neurotransmitters, critical assessment of manuscript

Ido P. Kema
Chpater 4: Mass spec for neurotransmitters, critical assessment of manuscript

Nathalie Lepage
Chapter 4: Assistance with mass spec for amino acid panel of zebrafish

Matthew A. Lines
Chapter 4: clinical details and identification of *PROSC* for patient 5, guidance, critical assessment of manuscript

Ronald J.A. Wanders
Chapter 4: yeast experiment, critical assessment of manuscript

Nanda Verhoeven-Duif
Chapter 4: Mass spec experiments and analysis for patient fibroblasts, HEK293 cells, zebrafish (for B6 vitamers only), editing of manuscript

Marc Ekker
Chapter 4: Supervision of zebrafish work (development, survival and drug experiments), critical assessment of manuscript

Jan M. Friedman
Chapter 4: Co-supervisor of Hilal Al-Shekaili, significant editing contribution to manuscript throughout development

Izabella A. Pena
Chapter 4: Co-senior author. 2-D and 3-D modeling of PLPHP protein, mass spec of amino acid panel for zebrafish, assistance with fish experiments (design and execution), significant contribution to manuscript throughout development

Clara D.M. van Karnebeek
Chapter 4: Co-senior author and co-supervisor of Hilal Al-Shekaili, significant contribution to manuscript throughout development